Flt1 determines neuronal regeneration by titrating Vegf levels and innate immune response at the neurovascular interface

Zur Erlangung des akademischen Grades einer

DOKTORIN DER NATURWISSENSCHAFTEN

(Dr. rer. nat.)

von der KIT-Fakultät für Chemie und Biowissenschaften

des Karlsruher Instituts für Technologie (KIT)

genehmigte

DISSERTATION

von

Andria Michael

1. Referent/Referentin: Prof. Dr. Ferdinand le Noble

2. Referent/Referentin: Prof. Dr. Martin Bastmeyer

Tag der mündlichen Prüfung: 20.07.2020

Erklärung

Ich versichere hiermit, dass ich diese Arbeit selbstständig verfasst habe und keine anderen, als die angegebenen Quellen und Hinweise benutzt habe. Wörtlich oder inhaltlich übernommene Stellen sind als solche gekennzeichnet und die Satzung des Karlsruher Instituts für Technologie (KIT) zur Sicherung guter wissenschaftlicher Praxis habe ich in der gültigen Fassung beachtet. Ich versichere außerdem, dass die beigelegte, elektronische Version der Arbeit mit der schriftlichen übereinstimmt und dass die Abgabe und Archivierung der Primärdaten gemäß Abs. A (6) der Regeln zur Sicherung guter wissenschaftlicher Praxis des KIT beim Institut gesichert ist.

Andria Michael   Karlsruhe, den 10.06.2020

Acknowledgments

I would foremost like to thank Prof. Dr. Ferdinand le Noble for taking me in his lab and believing in me, even when I lost faith. His guidance through my PhD journey was of immense importance as he urged me to develop my own ideas, and guided me to become the researcher I am today. I would also like to thank Dr. Dietmar Gradl for being a huge support, either in regards to supervising students or stepping up last minute providing me with useful insights into fulfilling this thesis.

Many thanks go to my past and present colleagues for all their emotional support during this journey. Special thanks to our little 'GGC' group, for sharing laughter, worries and whenever necessary brainstorming ideas. Without say, I owe a huge thank you to Esther Fuchs, without whom I would be literally lost. She was a great support to my journey since day one.

I am also very grateful to all my students, bachelor and master as I both taught and learned a lot from them in return. Special thanks go to Jakov and Sven for their passion and energy who filled my days working with them with joy. Many thanks also go to my past student and current colleague Julia Hammer, who was the first person to teach me more about Germany and welcomed me into her life as if she always knew me. I would also like to thank my current student and past Hiwi, Anna Lischke for her support not only with experiments but also emotionally.

I would like to thank my parents for their patience and support throughout this journey, and my little sister for always believing in me. Many thanks to all my friends who cheered me on in reaching the 'finish-line'. I would like to also thank my 'Yoga Instructor' for providing me with some moments of calm while going through the writing process. Last but not least, I would like to thank my best friend for his endless patience and guidance through this journey.

Table of contents

5

1   Abstract

Neuronal degeneration is one of the key contributors in the severity of ALS, Alzheimer's and Parkinson's disease. Spinal cord injuries due to external traumas also lead to neuronal degeneration and life- long paralysis. This is due to the humans limited ability to regenerate their neurons. On the contrary, zebrafish are capable of regenerating their central nervous system throughout their lifetime and are thus used in identifying novel mediators of regeneration. Regeneration of the zebrafish central nervous system is proposed to be mediated by a precise orchestration of neurovascular cross-talk and innate immune processes, which may involve the Vascular endothelial growth factor receptor 1; Flt1. Flt1 has two isoforms, formed via alternative splicing; the soluble Flt1 (sFlt1) and the membrane bound Flt1 (mFlt1). The soluble Flt1 has no signalling properties, but functions as a Vegfa (Vascular endothelial growth factor a) scavenger, negatively regulating neuronal vascularization by trapping Vegfa at the neurovascular interface. Membrane bound Flt1 has signalling properties and could induce macrophage recruitment via binding to the Plgf (placental growth factor) ligand. Macrophages are also key contributors in neuronal and tissue regeneration in zebrafish models. We thus hypothesized that Flt1 and its ligands, Vegfa, Vegfb and Plgf could play a role in axonal regeneration post injury.

This study shows that axonal and glia connectivity are completely abolished in *flt1*$^{-/-}$ but intact in the *mflt1*$^{-/-}$. This provides new insights into the role of sFlt1 in neuronal regeneration, independent of the mFlt1's tyrosine kinase activity. Loss of *flt1* results in a Vegfa gain of function (GOF) scenario and accordingly reducing Vegfa levels in *flt1*$^{-/-}$ restores axonal regeneration. Regeneration defects varied in other Vegfa GOF scenarios, like *von hippel landau* mutants (*vhl*$^{-/-}$), where initial axonal regeneration was unaffected, but collateral formation was impaired. Flt1 not only binds to Vegfa but also to Plgf and Vegfb according to a ligand competition model, as excess Plgf or Vegfb displace Vegfa from Flt1, predicting further Vegfa GOF scenarios. Similar to the *vhl*$^{-/-}$, *plgf* and *vegfba* GOF scenarios also impaired functional (collateral) recovery. In *vivo* imaging of macrophage migration and immune stainings showed a reduced macrophage recruitment to the lesion site in *flt1* loss of function and other Vegfa GOF

scenarios. Re-introducing WT macrophages back into the *flt1⁻/⁻*, using parabiosis, partially restored neuronal regeneration and axonal connectivity in *flt1⁻/⁻* mutants.

Altogether, we show that neuronal repair involved stem cell differentiation and macrophage recruitment, both of which require precise titration of neuronal Vegf levels through sFlt1.

2   Zusammenfassung

Degeneration von Motorneuronen ist eine der Hauptursachen für schwere Verläufe neurodegenerativer Krankheiten, wie ALS-, Alzheimer- und Parkinson. Die eingeschränkte Fähigkeit von Menschen, neuronale Verletzungen des Rückenmarks, aufgrund äußerer Traumata, zu regenerieren, führt häufig zu lebenslangen Lähmungen. Im Gegensatz zum Menschen ist es dem Zebrafisch möglich, Verletzungen seines zentralen Nervensystems über die gesamte Lebenspanne hinweg zu regenerieren. Deshalb wird er in der Grundlagenforschung dazu verwendet neue Komponenten des Regenerationsprozesses zu identifizieren. Einer gängigen Theorie zur Regeneration des Zentralnervensystems von Zebrafischen zufolge, wird diese durch eine präzise Feinabstimmung neurovaskulärer Interaktionen und des angeborenen Immunsystems reguliert. Hierbei soll Flt1, ein Rezeptor für Wachstumsfaktoren der VEGF-Familie, eine entscheidende Rolle spielen. Durch alternatives Spleißen kann Flt1 in zwei Isoformen vorkommen: das lösliche Flt1 (sFlt1) und das membrangebundene Flt1 (mFlt1). Der löslichen Variante des Rezeptors (sFlt1) konnte bisher keine Signaleigenschaft zugeschrieben werden. Jedoch ist der Rezeptor dazu in der Lage Vegfa (Vaskulärer endothelialer Wachstumsfaktor a) von seinem angiogenetisch aktiven Rezeptor Kdrl abzufangen und dadurch die biologische Verfügbarkeit von Vegfa zu senken. Dies wiederum beeinflusst die neuronale Vaskularisierung negativ. Membrangebundenes Flt1 weist Signaleigenschaften auf und es wird spekuliert, dass der Rezeptor über Bindung an den Ligand Plgf (Plazenta Wachstumsfaktor) Makrophagen rekrutiert. Makrophagen tragen ebenfalls maßgeblich zur Regeneration von Neuronen und Geweben in Zebrafischmodellen bei. Daher stellen wir die Hypothese auf, dass Flt1 und seine Liganden Vegfa, Vegfb und Plgf an der Regeneration der Axone nach einer Verletzung beteiligt sind.

Diese Studie zeigt, dass Verbindungen zwischen Axonen und Gliazellen in *flt1$^{-/-}$* vollständig aufgehoben sind, in *mflt $^{-/-}$* jedoch intakt bleiben. Dies liefert neue Einblicke in die Rolle von sFlt1 in der neuronalen Regeneration, unabhängig der Tyrosinkinaseaktivität von mFlt1. Der Verlust von *flt1* führt zu einer erhöhten Konzentration von Vegfa, welches für Kdrl verfügbar ist. Im englischen wird dieses Szenario als Funktionsgewinn bezeichnet (GOF, gain of function). Dementsprechend

resultiert eine Verringerung der Vegf-Spiegel in *flt1⁻ᐟ⁻* in axonaler Regeneration. Regenerationsdefekte variierten in anderen Vegfa GOF-Szenarien, wie von Hippel Landau-Mutanten (*vhl⁻ᐟ⁻*), bei denen die anfängliche axonale Regeneration nicht beeinflusst wurde, die Quervernetzung jedoch beeinträchtigt war. Flt1 bindet nicht nur an Vegfa, sondern auch an Plgf und Vegfb. Gemäß einem Modell in dem die Liganden in einem Wettbewerb um den Rezeptor stehen, können weitere Vegfa-GOF Szenarien angewendet werden. So verdrängt beispielsweise überschüssiges Plgf oder Vegfb den Liganden Vegfa von Flt1 und erhöhen so dessen Bioverfügbarkeit. Ähnlich wie in den *vhl⁻ᐟ⁻*, konnte in den *plgf*- und *vegfba*-GOF-Szenarien beeinträchtigte funktionale Regeneration der Neuronen beobachtet werden. *In vivo* Mikroskopie der Makrophagenmigration und Immunfärbung zeigte eine verringerte Rekrutierung von Makrophagen zur Verletzung in Fischen mit flt1-Funktionsverlust und anderen Vegfa-GOF-Szenarien. Wiedereinführung von WT-Makrophagen in *flt1⁻ᐟ⁻* unter Verwendung von Parabiose stellte die neuronale Regeneration und die axonale Quervernetzung in *flt1⁻ᐟ⁻* Mutanten teilweise wieder her.

Insgesamt zeigen wir, dass neuronale Regeneration die Differenzierung neuronaler Stammzellen und Rekrutierung von Makrophagen umfasst. Beide Prozesse erfordern eine genaue Titration der neuronalen Vegf-Spiegel durch sFlt1.

3   Introduction

3.1   General Introduction – opening remarks

Our neuronal system is critical for the physiology of almost any organ as well as the control of whole-body homeostasis. The neuronal system determines cardiac activity, organ perfusion, skeletal muscle contraction and body movement (Ng, Brack and Coote, 2001; P Ko, 2001; Hanna *et al.*, 2017). More specialized functions allow us to sense light, taste and critically determines our food intake in combination with the hormonal system (Chambers, Sandoval and Seeley, 2013). Specialized structures like the limbic system contribute to the regulation of emotions, memory, and arousal (Rolls, 2015). It is therefore not surprising that dysfunctions in this complex system sometimes result in devastating, life-threatening diseases. Some examples involve dementia (-with the ever-increasing life-expectations), amyotrophic lateral sclerosis; ALS (recently known by the ice-bucket challenge), Alzheimer's and Parkinson disease (Dugger and Dickson, 2017). While these diseases have been linked to genetic components, other neuronal diseases are inflicted by external traumas as occurs in the complex regional pain syndrome and spinal cord lesions, which severely affect patient's ability to control behaviour of their extremities (Oaklander and Horowitz, 2015). While it is recognized that there is a great need for a personalized medicine approach to curing neuronal and neurodegenerative diseases, our basic lack of understanding of the nervous system including aspects of the ontogenesis, plasticity, and regenerative capacity, hampered the design of rational therapeutic approaches into these important areas of medicine. In this thesis we addressed the regeneration of the spinal cord with special emphasis on the Vegf-Flt1-Kdr signalling pathway in the neurovascular cross-talk, activation of the innate immune response, and control of neuronal stem cell differentiation.

3.2   Regeneration

3.2.1 Importance in targeting neuronal regeneration

Neuronal regeneration is of vital importance for the restoration of damaged neurons during spinal cord injuries or neurodegenerative diseases. The brain, as well as the

spinal cord, are prone to acute or chronic type of injuries. Unlike, tissues such as the skin, liver or the intestines, mammalian brain tissue is highly limited in its regenerative capacity (Jessberger, 2016). As a result, the brain is unable to heal any damaged areas resulting from ischemic stroke or traumatic brain injuries (Péron and Berninger, 2015; Jessberger, 2016). Worldwide, stroke is considered to be the main cause of morbidity and mortality and although the mortalities are declining, the number of new cases and disease burden keeps accumulating over the years (de Jong *et al.*, 2020). Another ever-increasing challenge in the medical field is treating patients with spinal cord injuries. The World Health Organization has reported that every year, around 250 000 – 500 000 people will have a spinal cord injury worldwide (World Health Organization 2003). Due to our inability to heal such wounds, these injuries may lead to incomplete or complete paraplegia. Spinal cord injuries are characterized by a primary and secondary phase. In the primary phase, the spinal cord is injured due to physical forces which may include compression, shearing and acute distraction. These are important determinants in the later severity of the injury. After the initial phase, a cascade of events will lead up to a second phase of injury which involves the expansion of the neuronal tissue damage area and worsens the neurological deficits and disease's resolution. During this second phase, the injury will start releasing proinflammatory cytokines, followed by the formation of an astroglial-fibrous scars as the lesion matures into the chronic phage, thus impeding any chance for regeneration (Ahuja *et al.*, 2017).

3.2.2 Other organs with regenerative impairment

Other tissues which fail to regenerate include the heart and skeletal muscles. Cardiovascular diseases are indeed the number one cause of death worldwide, as more people die from it than from any other disease or cause (Roth *et al.*, 2017; World Health Organization 2017). Once a cardiac injury occurs, there is a loss of cardiomyocytes and fibrotic scar formation. All these will eventually lead to cardiac dilation, myocardial ischemic damage and overall cardiac malfunction leading to a heart failure (Cohn, Ferrari and Sharpe, 2000). At that point the only available solution is heart transplantations. This is necessary as the adult human heart has a very limited regenerative ability (Hashimoto, Olson and Bassel-Duby, 2018). Therefore, the need for new treatments in the regenerative field is of fundamental importance.

3.2.3 Stem cells as possible therapeutic target

One such approach that scientists have tried in promoting regeneration is the regenerative or stem cell-based therapies. In these approaches, they either transplant cells to directly dock to the injury site and eventually differentiate in hope of enhancing the organ functionality or indirectly via transplantation of cytokines to induce an innate immune response from the local stem cells (Behfar *et al.*, 2014). Initial approaches involved transplanting of bone marrow mononuclear cells (BM-MNCs) after a myocardial infarction, as this could be done without any serious complications and could also result in a decrease in infarct size. This caused a new wave of enthusiasm in the scientific community as it demonstrated the benefits of stem cell therapies. However, BM-MNCs are a heterogeneous cell population, composed with only 1% or less hematopoietic stem cells (Rehman, 2013; Behfar *et al.*, 2014). Another approach, involved the injection of pluripotent stem cells into the myocardium. However, this approach is accompanied with a lot of unaddressed issues, such as their lack of properly integrating in the host tissue and insufficient nutrient delivery (Yeung *et al.*, 2019). This is where tissue engineering comes to play. Human induced pluripotent stem cell-derived cardiomyocytes (hiPSC-CMs) were used to make a bio-absorbable patch, which was then transplanted to the infarcted tissue of the heart. Even though results in rats showed enhanced electrical conductivity in the heart, there is still a long way before such approaches become commercially available (Lancaster *et al.*, 2019).

3.2.4 Stem cells, resident stem cells and stem cell niche

Stem cells are vital in tissue maintenance and repair, as they are a source of self-renewing cells with the ability to differentiate into any specific tissue. In embryos, these cells can differentiate to any functional organ while in adult tissues somatic stem cells are present, which can differentiate into specific tissues during repair processes (Pennings, Liu and Qian, 2018). Adult stem cells or otherwise known as resident stem cells, are self-renewing cells that stay throughout the whole adult life. They are multipotent and can differentiate to give rise to multiple cell types of a specific organ, to maintain tissue remodelling and repair. Their potency and plasticity however decline with age, thus impairing their regenerative capacity. Some of these resident stem cells include hematopoietic and neural stem cells (Raveh-Amit *et al.*, 2013). As we age, the haematopoietic stem cell population increases in the bone marrow, the lymphoid

lineage turns to a more myeloid one and the bone marrow niche is altered. These alterations may lead to an enhanced risk of getting leukaemia with increasing age (Henry, Marusyk and DeGregori, 2011). As regards the neural stem cells, their proliferative and regenerative rate reduces with age. This decrease in neurogenesis may in turn lead to neurodegenerative diseases. The cell signalling in the neuronal stem cell niche is also altered with age (Artegiani and Calegari, 2012; Raveh-Amit *et al.*, 2013). Indeed, stem cell fate is dependent on their microenvironment, stem cell niche, where they receive and integrate extrinsic signals to influence their behaviour (Ferraro and Lo Celso, 2010).

One such niche is the bone marrow, where haematopoietic stem cells reside. Osteoblastic cells were recently identified to be regulating these cells through Notch activation (Calvi *et al.*, 2003). Furthermore, murine bone marrow was shown to also be in close proximity to blood vessels (Sipkins *et al.*, 2005).

3.2.5 Neuronal stem cell niches

In the adult mammalian nervous system, neural stem cells (NSCs) are found in the subventricular zone (SVZ) of the brain (Doetsch *et al.*, 1999) and in the subgranule cell layer, subgranular zone (SGZ), of the dentrate gyrus in the hippocampus (Palmer, Takahashi and Gage, 1997). The SVG region is made of migrating neuroblasts, immature precursors, astrocytes and ependymal cells. Neuroblasts migrate to the olfactory bulb to form local interneurons, while astrocytes are precursors of newly formed neurons in the brain (Doetsch *et al.*, 1999). Both of these stem cell populations are found to be in close proximity to blood vessels, capillaries, as they need to receive enough oxygen and nutrients to support their high metabolic needs. However, that is not their sole purpose, as blood vessels were also shown to regulate stem cell properties (Karakatsani, Shah and Ruiz de Almodovar, 2019).

3.2.6 Endothelial cells modulate neuronal stem cell activity

Interestingly, NSC proliferation and differentiation into neurons was shown, *in vitro*, to be regulated by the surrounding endothelial cells (ECs) (Wurmser, Palmer and Gage, 2004). The ECs found in these capillaries have the Vascular Endothelial Growth Factor Receptor 2 (VEGFR2) and the vascular endothelial (VE)-cadherin (Rafii, Butler and Ding, 2016). This could suggest that ECs secrete certain signalling molecules to induce NSCs proliferation and differentiation (Wurmser, Palmer and Gage, 2004). These signalling molecules are a set of growth factors, known as angiocrine factors, which are responsible for organ repair, maintaining homeostasis and metabolism (Rafii, Butler and Ding, 2016). For instance, mouse brain capillary ECs were shown to activate Notch signalling in order to induce NSCs self-renewal and neurogenesis (Shen *et al.*, 2004). Furthermore, angiocrine expression of EphrinB2 and Jagged-1 are important in maintaining the quiescence state of NSCs (Rafii, Butler and Ding, 2016). A ligand of Vascular Endothelial Growth Factor Receptor 1 (VEGFR1); placental growth factor 2 (PLGF-2) has also been observed to induce NSCs proliferation in the SVZ region (Crouch *et al.*, 2015). Another paper published that Neuropilin 1 (NRP1) positively regulates the neuronal progenitor cell (NPCs) mitotic behaviour in mouse embryo hindbrains, as ablation of NRP1 in the endothelial cells, led to a premature cell cycle exit of NPCs, thus leading to incomplete neuronal differentiation (Tata *et al.*, 2016). Therefore, ECs are important components in the regulation of NSC niche.
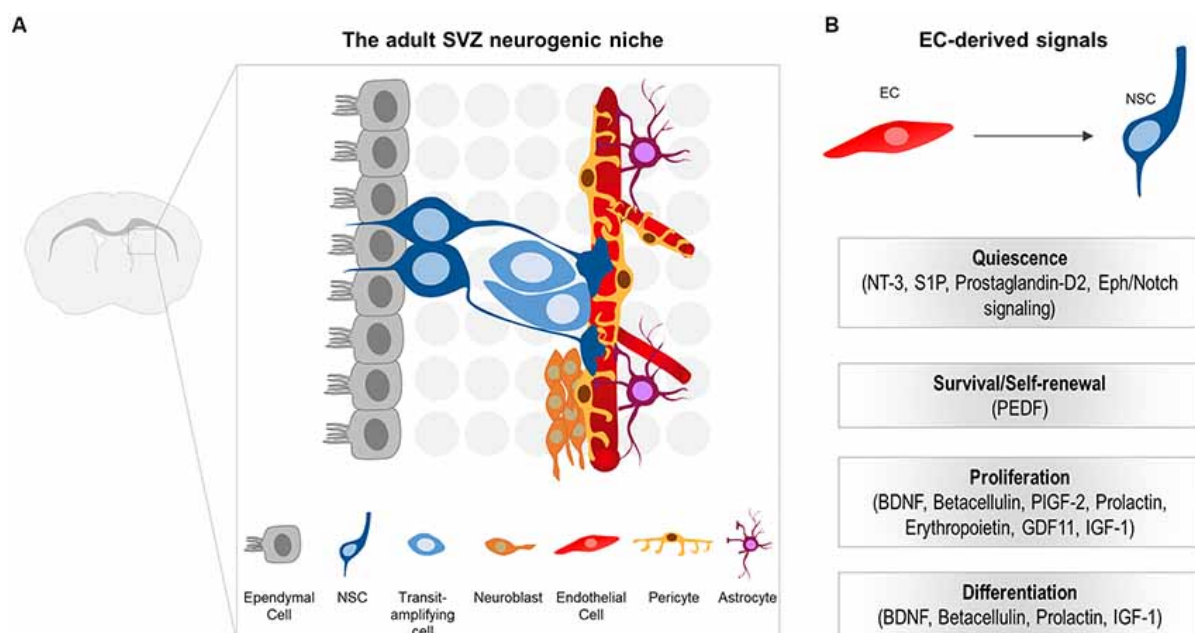
Figure 3. 1: Schematic representation of the SVZ niche in the adult mouse brain.

(A) NSCs create transit-amplifying cells, which then give rise to the migrating neuroblasts. NSCs are docked below the ependymal cell layer. The main function of NSCs involve the ECs of the blood vessels. It is of note that pericytes and astrocytes wrap around the blood vessels. **(B)** EC-derived signals that guide quiescence, survival, proliferation and differentiation of NSCs in adult central nervous system; CNS (Karakatsani, Shah and Ruiz de Almodovar, 2019).

3.2.7 Stem cells in a Petri-Dish: An Organoid story

The mammalian skin has some regenerative capacity. However, when you have burns so severe that skin grafts received from donors are not enough to cover the wound, new approaches are bound to be found. In 1980s two siblings, 5 and 6 years of age, received burns that covered more than 95% of their whole skin surface. Dr Green and his team developed cultured human epidermal cells to create coherent epithelial sheets, enough to cover the whole surface, thus restoring half or more of the body's surface (Gallico *et al.*, 1984). Another lab also tried to grow ocular surface epithelial cells in cultures to be used as grafts (Lindberg *et al.*, 1993). They then went on to use cultivated limbal stem cells, obtained from the healthy eye of the patients, to make grafts for applying to the injured eye, on 112 patients suffering from corneal blindness. This resulted in permanent restoration in 76.6% of the cases (Rama *et al.*, 2010). These two pioneer studies were the first to successfully reconstruct 3D tissues obtained from cultured human stem cells, setting the foundation of a whole new wave of research on 'organoids'. Organoids are now developed from stem cells and comprise of organ-specific cell types that self-organize into 3D structures. In general, they can derive either from pluripotent embryonic stem (ES) cells and their pluripotent stem (iPS) cells or from more restricted adult stem cells (aSCs) (Clevers, 2016).

3.2.8 Importance of a functional vasculature in organoids survival

Besides their promising potential, they also come with a lot of limitations as they lack structure and tissue size. As *in vivo* tissues requires a complex vasculature to exchange oxygen and nutrients, but also growth factors to aid in their development, maybe this is the missing piece in improving organoid development (Grebenyuk and Ranga, 2019). Indeed, human cortical organoids (hCOs) are missing microvasculature, thus less oxygen and nutrients could reach the inner-most part of the organoid. This lack of vasculature eventually leads to apoptotic cell death at their

inner-most part and failure in neuronal progenitor differentiation. Therefore, Cakir et al. developed human embryonic stem cells expressing the human ETS variant 2 (ETV2), which in turn contributed in a vascular-like network in the hCOs. This enhanced their maturation, created some blood-brain-barrier characteristics and aided in the formation of perfused vasculature (Cakir *et al.*, 2019). One step further, Wimmer et al. used iPS and ES cells to develop self-organized 3D human blood vessel organoids. When transplanted into mice, these organoids form perfused vasculature and were found to mimic the microvascular changes observed in diabetic patients when exposed to hyperglycaemia and inflammatory cytokines (Wimmer *et al.*, 2019).

3.2.9 Metabolic changes during stem cell differentiation

One should also note that the metabolic programming of stem cells is very different to the one of proliferating cells. During high multipotency, pluripotent stem cells (PSCs) maintain an open euchromatic state to maintain their epigenetic status and self-renewal (Gaspar-Maia *et al.*, 2011). They are also high in glycolysis and fatty acid oxidation. However, reactive oxygen levels (ROS) stay low and there is a general hypoxic environment maintained. In times of proliferation, oxygen levels and glycolysis go up, ROS signalling gets activated and mitochondrial oxidation rises. Any further differentiation will decrease the level of glycolysis and further enhance mitochondrial oxidation (Shyh-Chang and Ng, 2017).
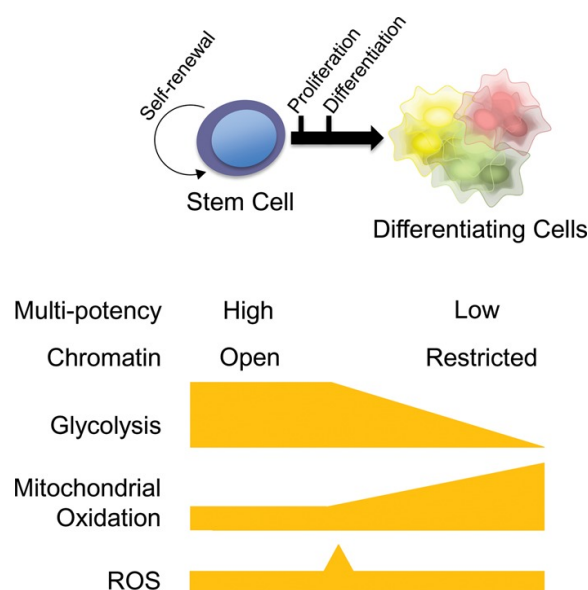
Figure 3. 2: Common metabolic changes seen during both PSCs and adult stem cell differentiation.

When the multipotency is high, the cells maintain a relatively open chromatin state, a highly glycolytic status. They still retain mitochondrial oxidation, but the levels of ROS are typically low in a hypoxic environment. During proliferation, glycolysis is still high, accompanied by a burst of ROS, rise in oxygen levels and mitochondrial oxidation. Further differentiation will lead to a decrease in glycolysis and an increase in mitochondrial oxidation (Shyh-Chang and Ng, 2017).

Therefore, understanding how the microenvironments are being formed and the changes in metabolism during proliferation will aid our ability to reprogram pluripotent stem cells and have more targeted tissue-specific stem cell regenerative therapies in the future (Pennings, Liu and Qian, 2018).

3.3 Neurodegenerative diseases and external trauma

3.3.1 A clinical overview on spinal cord lesions

3.3.1.1 A short history of spinal cord injuries

The first description of spinal cord injuries or incidences date all the way back to the Edwin Smith Papyrus, around 5000 years ago. The first attempts in treating spinal cord injuries were carried out by Hippocrates, who tried to treat the wound using huge amounts of liquids, including donkey milk mixed with honey and Egyptian white wine. He even used a traction table to place patients in such a way to avoid any further injuries from occurring. It was not until the 20th century when science began to show advancements, that spinal cord injuries could be investigated further. New pharmacological treatments and the hype of stem cell research has given some hope to this grim debilitating disease (Harkey *et al.*, 2003).
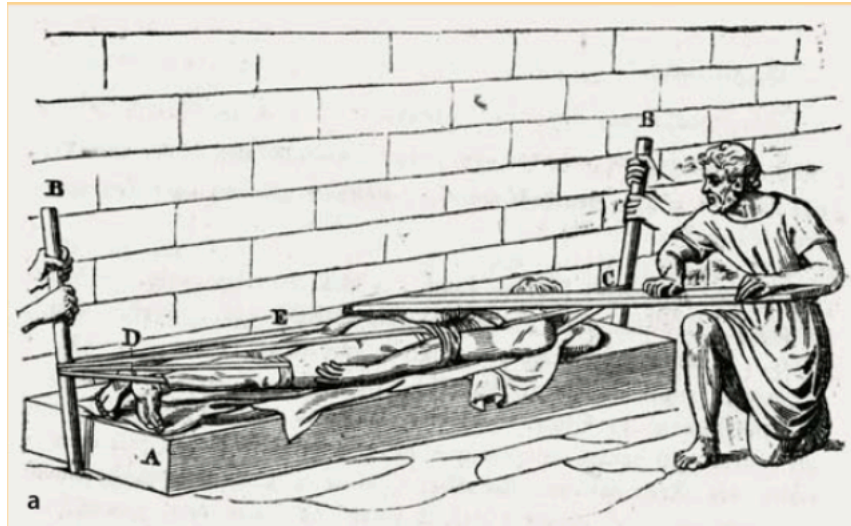
Figure 3. 3: Hippocrate's traction table.

As illustrated by E. Littré who published all of Hippocrates work in the 19th Century (Modified from Boos and Aebi, 2008).

3.3.1.2 Anatomy of the spinal cord

To tackle and resolve these injuries, one should first understand the spinal cord anatomy. The spinal cord starts from the brainstem and extends all the way down to the lower extremities. It is a soft delicate structure enclosed in the meninges, where cerebrospinal fluid is flowing to provide it with nutrients and cushion it from fractures. It is then further protected by a surrounding bony structure, ligaments, cartilage, muscle and intervertebral discs. Therefore, any injury occurring at any of these structures may in fact lead to a spinal cord injury (Harkey *et al.*, 2003). This is particularly evident in elderly individuals, where osteoporosis or arthritis may weaken this vertebral structure, thus even a small fall may easily lead to spinal cord injuries.

In general, spinal cord injuries can be classified in two generic types depending on the location of the deficit; the upper motor neuron (UMN) and the lower motor neuron (LMN) lesions. UMNs are responsible for sending signals down to the lower motor neurons to initiate movement, while LMNs regulate muscle contraction and relaxation (Lohia and McKenzie, 2019).
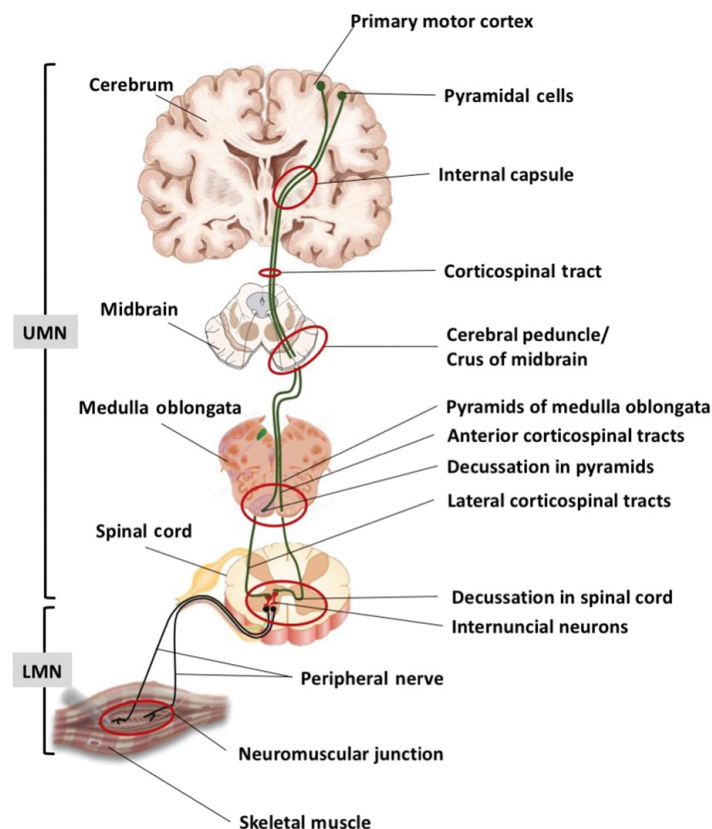
Figure 3. 4: Illustration of the motor tract.

The UMNs initiate from the pyramidal cells of the cerebellar cortex and pass down through the internal capsule to enter the midbrain, then through the pons and medulla to eventually reach the spinal cord. At the spinal cord level, the UMNs axons form synapses with interneurons and LMNs. The LMNs project their axons outside of the spinal cord to induce muscle movement. UMNs are shown in green and LMNs in black (Yeager and Miller, 2014).

The UMN lesions occur when an injury occurs on a supraspinal site, such as the motor cortex. This will in turn, through its extending axons, affect the spinal cord. Symptoms of UMN lesions involve the weakening of not just one but a group of muscles, hypertonia (muscle tightness) and hyperreflexia (overresponsive reflexes and spastic tendencies). The LMN lesions involve injuries to the spinal cord grey matter, whose axons directly interact with the skeletal muscles. Symptoms of LMN lesions involve involuntary muscle twitching and weakening, hypotonia (reduced muscle strength) and hyporeflexia (absence of reflexes) (Harkey *et al.*, 2003).

3.3.1.3 Classification of spinal cord injuries

In accordance to the American Spinal Injury Association, spinal cord injury outcomes are classified in two big generic groups; tetraplegia and paraplegia. Tetraplegia involves motor and/or sensory neuronal defects occurring in the cervical segments. As the name suggests, it leads to paralysis on all four extremities (arms, trunk, legs and pelvic organs) and involves lesions specifically to the neural canal. Paraplegia involves motor and/or sensory neuronal defects occurring in the thoracic, lumbar or sacral regions of the spinal cord. In this type of injuries, the arms functionality is unaffected, but impairment can occur to the other three extremities. The level of severity then depends on the area where the injury occurred (Kirshblum *et al.*, 2011). The injury is further identified as complete (lack of all motor neuron or sensory functions below the level of injury) or incomplete (if some motor neuron or sensory functions are still observed below the level of injury) (Harkey *et al.*, 2003). Lastly, a light touch or pin prick sensation test will be performed to the patient, which will be subsequently compared to a scale to quantify the extend of motor or sensory damage (Harkey *et al.*, 2003; Kirshblum *et al.*, 2011).
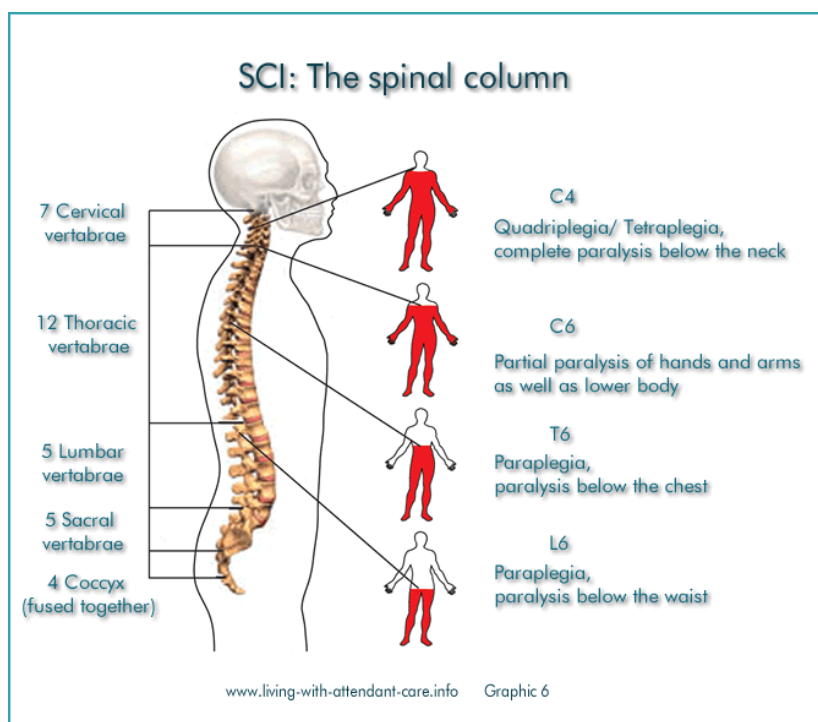
Figure 3. 5: Illustration of the spinal cord injury induced paralysis.

The spinal cord is consistent of 33 vertebrae. Each of these vertebrae is classified based on its location and number. For instance, there are 7 cervical vertebrae (C1-C7), 12 thoracic vertebrae (T1-12) and 5 lumbar vertebrae (L1-5). Depending on the location of the injury, the respective body area is impaired.

For example, an injury at the C4 vertebrae will lead to tetraplegia, while an injury at the L6 vertebrae will lead to paraplegia (*Living with Attendant Care: Spinal Cord injury : Understanding spinal cord injury*, no date).

3.3.1.4 Pathophysiology of spinal cord injuries

A spinal cord lesion is usually the outcome of a mechanical lesion, causing direct neuronal damage, neuronal cell death, and vascular injury evolving into local bleeding and hypoperfusion. This decrease in blood vessel number and function, impede perfusion and lead to a lack in oxygen availability. Consequently the hypoperfusion can progress into ischemic necrosis (Bareyre and Schwab, 2003). This necrotic side contains large number of apoptotic or necrotic neurons and glia. Further metabolic disturbances involve an increase in the intra-neuronal Ca^{2+} levels and an increase in the extracellular K^+, which as a result leads to an impairment in the neuronal function (Bareyre and Schwab, 2003) . Progression of this primary injury to the surrounding tissue over the following weeks is known as a secondary injury. Several mechanisms lead to this secondary injury involving hypoxia, free radicals and inflammatory responses. Inflammatory responses include the invasion of neutrophils (6-24 hours post injury), activation of resident microglia and invasion of peripheral macrophages (24hours to 2 weeks post injury) and T cells (Bareyre and Schwab, 2003; Beck *et al.*, 2010; Burnside and Bradbury, 2014). Astrocytes get activated, oligodendrocyte die via apoptosis and Wallerian degeneration (WD) occurs (Hausmann, 2003). In the chronic phase, which can take days up to years after the initial injury, oligodendrocyte apoptosis continues and channel and receptor functions are impeded. There is tissue scaring, demyelination and WD (Bareyre and Schwab, 2003). WD is a complicated phenomenon which occurs at a distal location from the initial injured nerves, as they change their morphology after being lesioned. This occurs both in central and peripheral axons (Waller, 1850; Vargas and Barres, 2007; Mietto, Mostacada and Martinez, 2015).
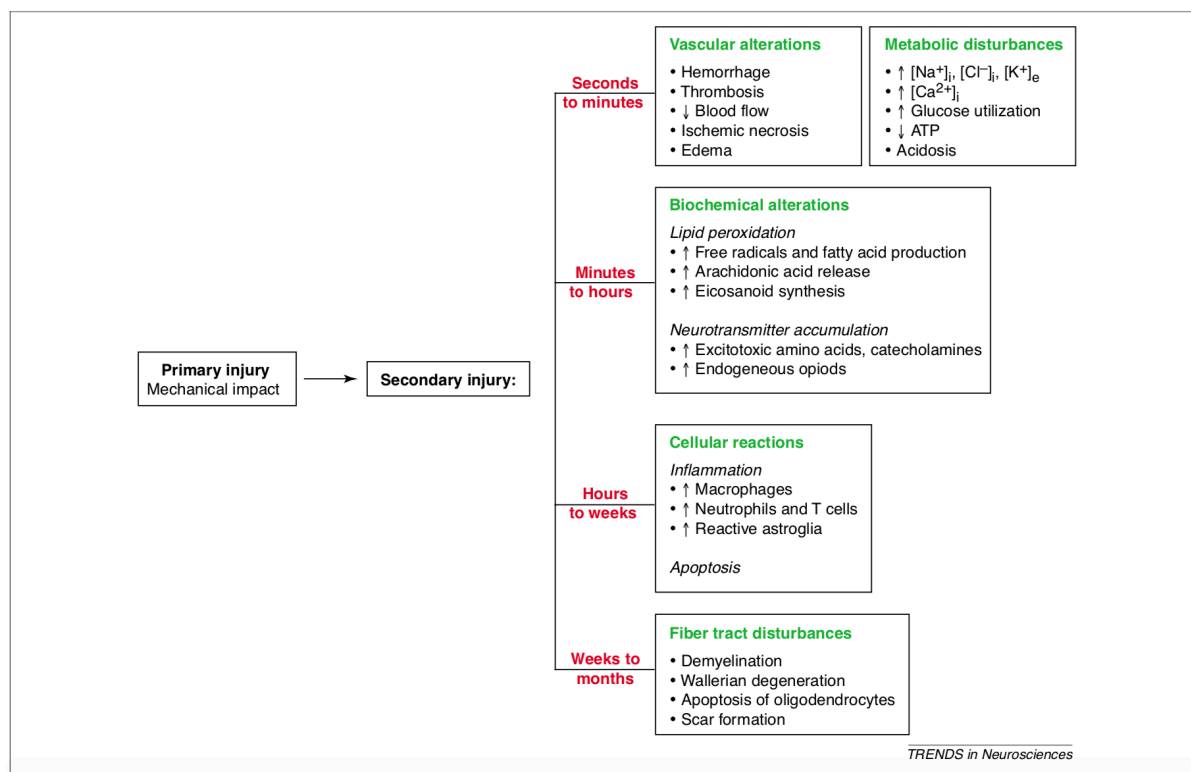
Figure 3. 6: Pathophysiology after a spinal cord injury (Bareyre and Schwab, 2003).

3.3.2 Peripheral nervous system (PNS) – a better take in regeneration potential

3.3.2.1 WD is slow in CNS

WD is initiated with axonal degeneration and is followed by an increase in the permeability of the blood brain barrier (BBB) and the breakdown of myelin sheaths. In the PNS, this event triggers a macrophage influx which clears the myelin debris located distal to the site of axonal damage. Even though in mammalian PNS, this process takes between 7-14 days, it is significantly slower in the CNS, as it takes months to years for it to be able to successfully clear this myelin debris (Vargas and Barres, 2007). The clearance of myelin debris is fundamental for successful regeneration as the debris contains various inhibitors which can imped axonal regeneration (He and Koprivica, 2004). One of the key elements involved in WD in PNS is Schwann cells, as they are able to break down and clear myelin sheaths and debris respectively. Schwann cells have also been considered to be a source for the vascular endothelial growth factor; VEGF-A (Mukouyama *et al.*, 2002). In the CNS, the cellular counterparts of Schwann cells are the oligodendrocytes. In contrast to Schwann cells,

oligodendrocytes have very limited ability in clearing myelin debris. Oligodendrocytes are also dependant on axonal contact for their survival and development. Thus, after an injury, oligodendrocytes undergo apoptosis due to loss of the axon during WD, they fail to divide and are unable to clear myelin debris (Vargas and Barres, 2007).

3.3.2.2 Peripheral nervous system anatomy, function and regeneration

The adult mammalian CNS has been shown to have limited regenerative abilities due to changes in the microenvironment and strong immune response following an injury. The PNS, on the other hand, has shown some degree of regeneration after injury. This could be attributed to the activation of Schwann cells and macrophages (Mietto, Mostacada and Martinez, 2015). The PNS is made of neurons whose cell bodies are either in the CNS or in the periphery and their axons extend outside of the brain and spinal cord. Their primary function is the initiation of voluntary and involuntary movements, and behavioural responses. For example, when touching a hot plate or scratching to remove irritants off the skin. Apart from their signal transmission to the CNS, they could also sense alarms present in the surrounding environment and thus send signals to the immune system to release neuropeptides or growth factors (Basso *et al.*, 2019). Under normal physiological conditions, the peripheral nerves are made of resident macrophages, fibroblasts, Schwann cells and the PNS-wrapping glia. One possible contributor to their more effective regenerative ability could be the large proportion of Schwann cells present, outnumbering macrophages, as their close contact to the axons may prove as first line of defence after axonal injury. As soon as the Schwann cells detect a nerve injury, they release a massive wave of inflammatory response which occurs before any damage happens to the distal axons. Probably due to their close contact to the axons they may also be able to sense any minor changes in the nerve homeostasis and set an inflammatory response in time for repair (Mietto, Mostacada and Martinez, 2015).

3.3.2.3 WD and Schwann cells role in regeneration of the PNS

During the first steps of WD in PNS, Schwann cells detach from axons and start cleaning up any myelin or axonal debris from the wound. This process is further accompanied by the infiltration of macrophages (Narciso *et al.*, 2009). Peripheral nerve glia was indeed shown to release tumour necrosis factor alpha; tnfa, a pro-

inflammatory cytokine produced by Schwann cells, after a compression injury (Wagner and Myers, 1996). This release of pro-inflammatory cytokines is partly triggered by Toll-like receptor signalling. This includes an accumulation of macrophages and enhanced myelin sheath degradation. Schwann cells further upregulate a galactose-specific lectin, galectin-3 (Gal-3), shown to affect the efficacy by which Schwann cells and macrophages phagocytose myelin (Narciso *et al.*, 2009). Gal-3 is inhibitory for Schwann cell proliferation in sciatic nerves (Gustavsson *et al.*, 2007). Thus, Gal-3 knockout mice were used to study sciatic nerve regeneration. In these mice, the absence of Gal-3 led to a faster axonal regeneration, due to boosted inflammatory response and increased phagocytic abilities of Schwann and macrophages (Narciso *et al.*, 2009; Mietto *et al.*, 2013).

3.3.3 Neurodegenerative diseases

3.3.3.1 Axon degeneration in Neurodegenerative diseases

Axon degeneration or Wallerian-like degeneration (WLD) is an asset of many neurodegenerative diseases, such as ALS, Alzheimer's, Parkinson's disease, where the affected neurons show similar characteristics as axons undergoing trauma induced WD (Conforti, Gilley and Coleman, 2014; Mietto, Mostacada and Martinez, 2015). Unlike WD, where the site and timing of the lesion are known, it is much harder to study this in neurodegenerative diseases, as the axonal degeneration occurs both gradually and is heterogeneous, in regards to the axonal population. Furthermore, the onset of pathogenesis is largely unknown. Therefore, using WD models could be an excellent way to tackle at least one of the many factors leading to axonal degeneration (Conforti, Gilley and Coleman, 2014). To investigate this further, a slow Wallerian degeneration (*Wld^S*) mutant mouse was developed by spontaneous mutation, where WD seems to be delayed by 10-fold. Genetic analysis has shown a mutation on chromosome 4, encoding an in-frame fusion of the N-terminus of the ubiquitination factor E4B (Ube4b) fused to nicotinamide mononucleotide adenyltransferase 1 (Nmnat1) and the ability to express a novel chimeric protein (Wld^S) in the nuclei of neurons (Mack *et al.*, 2001; Coleman and Perry, 2002; Beirowski *et al.*, 2005). *Wld^S* mice are shown to delay axonal degeneration in different disorders and are thus valuable models to study neurodegenerative disorders (Coleman and Perry, 2002).

Nature Reviews | Neuroscience
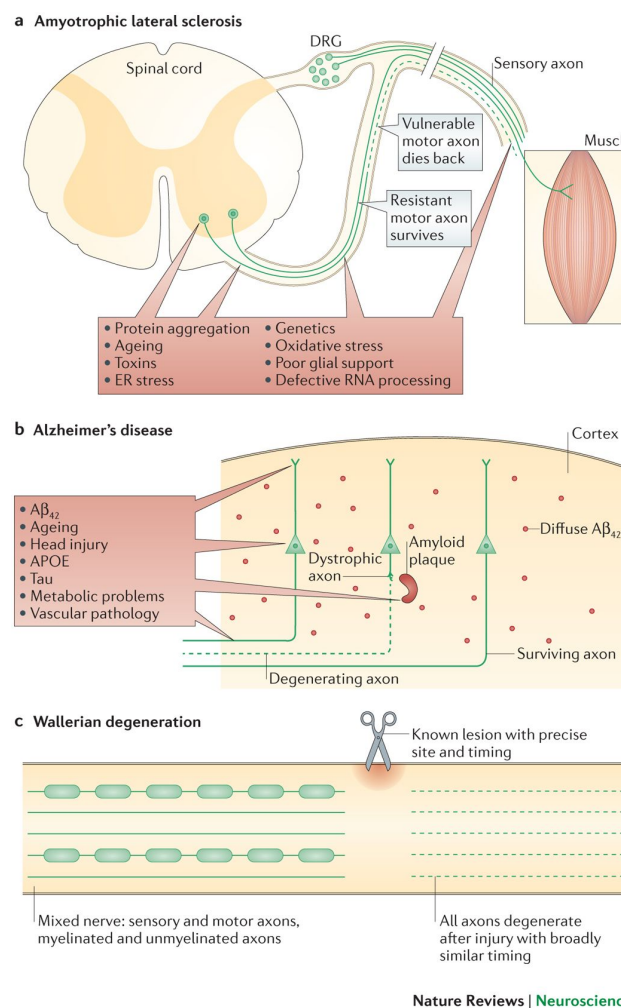
Figure 3. 7: Systems for studying axon degeneration.

The scheme shows the causes and effects of axonal degeneration in ALS, Alzheimer's disease and WD model systems. **(a)** In ALS, vulnerable spinal motor neurons are susceptible to axonal degeneration, as a result of various causative factors. This degeneration results in the loss of connectivity between the muscles and the spinal cord, thus subsequently leading to the death of these affected neurons. There is though, a population of 'resistant motor axons' who are immune to these stressors and are thus not degenerating. **(b)** In Alzheimer's disease a combination of causative factors leads to axonal dystrophy in vulnerable neurons, while other neurons experience less of these pathogenic factors and are thus not degenerated. **(c)** In contrast, in WD, the site and timing of the injury is well known and degeneration occurs in all axons of the nerve shortly after injury (Conforti, Gilley and Coleman, 2014).

3.3.3.2 Amyotrophic lateral sclerosis (ALS)

Amyotrophic lateral sclerosis (ALS) is the most common motor neuron (MN) disease in humans. It involves selective death of MNs, which eventually leads to progressive paralysis. It has a prevalence of 2-3 cases per 100 000 people and it leads to mortality

within 1-5 years of onset. It has claimed many lives such as famous baseball player Lou Gehrig and Nobel-prize winner, astrophysicist Stephen Hawking, who suffered from an unusually slow progression form of the disease. In his case, he had almost complete paralysis but no cognitive impairment, indicating the selectivity in neuronal loss of this disease (Cleveland and Rothstein, 2001). Interestingly, for cases such as Lou Gehrig, the disease's causative factor, could well be associated to traumas of the CNS experienced in collision sports (Abel, 2007; Mckee *et al.*, 2010). In 90-95% of all cases, the onset of disease is largely unknown; sporadic ALS, yet for the rest 5-10% of the cases there are some identified hereditary factors linked to the disease; familial ALS. The hallmarks for both cases are progressive loss of muscle strength, atrophy and spasticity, which indicate the degeneration of both UMN and LMNs in the CNS. One of the now known genetic mutations is a missense mutation in the ubiquitously expressed enzyme copper/zinc superoxide dismutase (SOD1) (Cleveland and Rothstein, 2001; Velde *et al.*, 2004). To study this, Wld^S mice were used, and even though the axonal degeneration was delayed, it was insufficient to slow the disease's onset in SOD1 mutants. However, they did detect defects in retrograde transport (transport of molecules from the axon termini towards the cell body) as a result of the SOD1-mutation (Velde *et al.*, 2004). In another study, using a different SOD1 mutant mice, showed that the Wld^S gene could extend survival rate and was also able to delay the denervation at the neuromuscular junction (Fischer *et al.*, 2005). Using the mouse model for motoneuron disease (progressive motor neuropathy; *pmn*) to study ALS, they crossed it to the Wld^S mice and showed that the Wld^S gene could rescue the MN size and number and also delay the retrograde transport defect, suggesting new therapeutic options in studying WLD to treat ALS (Ferri *et al.*, 2003).

3.3.3.3 Alzheimer's disease (AD)

Alzheimer's disease (AD) is the most prevalent cause of dementia and affects around 30 million people worldwide. It is the most common form of dementia, hallmarks of which include decline in memory and other cognitive abilities. The disease starts with lack in concentration of the individual, followed by language impairment, visual difficulties and even changes in personality traits. Even though the individuals can be independent over the first stages of disease, later progression requires special assistant by caretakers. With a prevalence rate of 1 in 8 over the age of 65 and a

mortality rate of 7-10 years, patients suffering from AD need extensive care over long periods of time, thus burdening the global public health system (Holtzman, Morris and Goate, 2011). Primary markers of AD include the overexpression of tau (a microtubule-stabilizing factor) forming intraneuronal neurofibrillary tangles and extracellular plagues of β-amyloid (Coleman and Perry, 2002; Nussbaum *et al.*, 2012). Recent studies have shown that the neuronal defects observed in AD are depicting a 'dying-back' pattern of degeneration. This involves defects in synaptic morphology, decreased number of synapses and abnormal connectivity of axons long before the somatic cells die (Kanaan *et al.*, 2013). Another common feature of AD is the microstructural abnormalities in the white matter, which could reflect a WLD as a secondary outcome (Alves *et al.*, 2015).These axonal abnormalities and degeneration, as well as reduced myelination in the brain, are key components of AD pathophysiology (Kanaan *et al.*, 2013). *Wld^S* mice are shown to be neuroprotective and were thus used to test if they can also offer synapse protection during aging. Results of the study showed that protection in the CNS happened independent of age, and was rather dose dependent to the *Wld^S* gene. Thus this gene may offer some therapeutic properties on the synaptic protection over aging (Wright *et al.*, 2010).

3.3.3.4 Parkinson's disease (PD)

Parkinson's disease is the second highest cause of neurodegenerative diseases, after AD, with an incidence rate of 1 in 200 individuals. The hallmarks of the disease include cardiac motor symptoms of resting tremor, rigidity and bradykinesia. Defects include a deficiency in dopamine neurons and the presence of Lewy Bodies (abnormal protein aggregations) in the rest of the neurons. Unfortunately, even though some treatments are able to alleviate the symptoms of the disease, there is no current known drug able to slow down its progression (Thobois, Delamarre-Damier and Derkinderen, 2005; Hasbani and O'Malley, 2006). One possible reason for this, is that the symptoms appear after about 70-80% of the striatal dopamine gets depleted, and around 50% of nigral dopamine-producing cells have already died. Thus, dopamine depletion determines the disease's level of severity. Studies in PD patients show that this cell death could be attributed to apoptosis. However, since post-mortem studies are not precise in studying the events leading up to apoptosis, mouse models were used instead. To mimic the disease, mice were treated with neurotoxic compounds such as

the 1-methyl-4-phenyl-1,2,3,6-tetrahydropyridine (MPTP) (Blum *et al.*, 2001). This method has suggested that the mechanism by which nigral neurons degenerate is in a 'dying back' fashion, similarly to AD, where degeneration initiates at the distal part of the axon and moves over time towards the cell body. Thus, by delaying this degeneration might also delay the onset of disease. As the MPTP treated mouse has shown to cause degeneration through inhibition of the mitochondria and mitochondrial deficiencies have been liked to WD, they decided to use Wld^S mice treated with MPTP to study PD. Results showed that the Wld^S gene was able to prevent axonal degeneration, increase survival rate, but were unable to save the cell bodies (Hasbani and O'Malley, 2006). Using another neurotoxin to mimic PD, 6-hydroxydopamine (6-OHDA) was injected in Wld^S mice. This showed dopamine fibre protection and protection against anterograde (or WD) but not retrograde degeneration (Sajadi, Schneider and Aebischer, 2004; Cheng and Burke, 2010). Thus, studying axonal degeneration using WD models is of fundamental importance in deciphering the pathogenesis and resolution of neurodegenerative diseases.

3.4   Neurovascular interface

3.4.1 Neurons and blood vessels – similarities and interactions

Microvascular defects are linked to neurodegeneration and neurodegenerative diseases of the brain (Zlokovic, 2014). Preventing vascular dysfunction is therefore considered at the basis of novel targeted therapies. In particular, research should aim at how vessels influence nerves, and how nerves communicate with blood vessels to sustain neuronal functions. Interestingly, the nervous and vascular systems share many similarities: they are both highly branched, they consist of an afferent and efferent system (arteries-veins; sensory-motor neurons), they use common growth factors (like VEGF and nerve growth factor; NGF), guidance factors and have functional similar cell types – tip cells/axonal growth cone, that can sense these cues to establish correct connectivity and wiring. In fact, it is believed that during evolution the vascular system has co-opted growth principles from the nervous system (Quaegebeur, Lange and Carmeliet, 2011). The similarities between both systems were already noticed all the way back to the middle ages. It was all the way back to

the 1543, when Andreas Vesalius first characterised this model, showing parallel alignment of arteries and nerves, thus laying down the foundation for the neurovascular concept (Carmeliet and Tessier-Lavigne, 2005; Wälchli *et al.*, 2015). Both systems are vital for transferring information. Afferent neurons; sensory neurons, pass sensory stimuli from the skin to the brain via electrical signals, while veins bring deoxygenated blood from the surrounding tissues back to the heart. Similarly, efferent neurons; motor neurons, control muscle movement by transferring electrical signals from the CNS to the muscles, while arteries transport oxygen-rich blood away from the heart to all parts of the body (Wälchli *et al.*, 2015). In the PNS, arterial smooth muscle cells release Netrin-1 to control sympathetic arterial innervation via autonomic sympathetic nerves to regulate vascular tone and blood supply to the organs (Brunet *et al.*, 2014). On the other hand, CNS requires a highly specialized blood vessel network, for its proper formation and function. Interestingly the CNS maturation and blood vessel growth happen in a concomitant way, as different neural cell types develop. Thus angiogenesis of the CNS occurs in parallel to the neurogenesis and tissue expansion in the spinal cord, as neural tissue expansion relies on oxygen and nutrient delivery to supply their high metabolic needs (Paredes, Himmels and Ruiz de Almodovar, 2018). Thus correct patterning and guidance are fundamentally important for their development and function (Wälchli *et al.*, 2015).

3.4.2 Wiring of the neuronal axons and blood vessels

The vasculature is arranged in highly branched structures, similarly to the nervous system (Adams and Eichmann, 2010). Neurons use axons to elongate over long distances to reach their destination target. The elongated axon is guided through the 'growth cone', a motile sensory structure found at the tip of the axon. The growth cone can move and explore the surrounding environment through extension and retraction of the filopodia extensions. Once the target location is reached, the axon arborizes (forms branches) to innervate (stimulate with electrical signals) the target cells (Carmeliet and Tessier-Lavigne, 2005; Lowery and Vactor, 2009). On the other hand, vessels, during initial stages of vasculogenesis (*de novo* blood formation), using an assembly of locally proliferating ECs, form a primitive labyrinth of similarly sized vessels. Later on, during the development, new blood vessels emerge from pre-existing vessels. This process is known as angiogenesis. Unlike axonal cellular

extensions, angiogenesis involves vessel sprouting through ECs migration which will eventually anastomose to another sprout to form a lumenized network (Fantin *et al.*, 2010). This elongation is driven by the endothelial 'tip' cell, which is located at the tip of the elongated vessel and its function is similar to that of the axonal 'growth cone'. These 'tip' cells are followed by 'stalk' ECs, which in turn proliferate to accommodate the formation of the extending vessel. The vessel sprouts are also directed using extension and retraction of the filopodia (Carmeliet and Tessier-Lavigne, 2005; Jakobsson *et al.*, 2010; Wälchli *et al.*, 2015). Even though, the nervous wiring is different to the one observed in the vascular system, they both share some common cues and receptors which control both axonal guidance and vascular patterning (Carmeliet and Tessier-Lavigne, 2005).

3.4.3 Growth factors directing angiogenic and axonal sprouting

In both cases, sprouting is directed by the gradients of certain growth factors. In case of the vasculature, hypoxia (low levels of oxygen) trigger vessel growth through hypoxia-inducible transcription factors (HIFs), which in turn upregulate various angiogenic genes including induction of the vascular endothelial growth factor A (VEGF-A). The VEGF-A levels will eventually get downregulated when sufficient oxygen reaches the target tissue (Oosthuyse *et al.*, 2001). In regards to axonal terminals, cells with no synaptic input release growth factors, such as the nerve growth factor (NGF) to initiate innervation and are downregulated as soon as sufficient electrical stimuli reaches the target cells (Carmeliet and Tessier-Lavigne, 2005). Thus, formation of vascular capillary networks and axonal terminal arborization are guided by the metabolic and electrical needs of the target cells, respectively. Furthermore, sprouting requires not only the presence but also appropriate gradients of these factors (Carmeliet and Tessier-Lavigne, 2005).

3.4.3.1 VEGF – key regulator of angiogenesis

VEGF-A is stimulating physiological but also pathological angiogenesis, through a dose-dependent manner. Its functions include, initiating ECs division and migration and is essential during blood vessel's development (Carmeliet and Tessier-Lavigne, 2005). VEGF-A is the principle dancer of angiogenesis, as its levels need to be well titrated as both too much and too little VEGF/VEGF-A are lethal. The *Vegf* full mutant

mouse dies due to failure in generating endothelial cells. Mice haploinsufiiccient for *Vegf* also die during the early embryonic development (Carmeliet *et al.*, 1996; Oosthuyse *et al.*, 2001). VEGF-A is thus essential for early vascular development in a dose-dependent manner, as even haploinsufficiency leads to premature death. A downstream regulator of VEGF, delta-like 4 ligand (Dll4) which is specifically expressed in arteries was also identified to be important in vascular development, as even Dll4 heterozygous deficient mice showed severe vascular defects and were lethal in the embryonic stages (Gale *et al.*, 2004). Two-three fold overexpression of the VEGF also led to severe heart defects and embryonic lethality (Miquerol, Langille and Nagy, 2000) . VEGF is thus important for the normal vascular development and its levels have to be well titrated. Accumulating evidence also show that many pathologies relate to either too much VEGF (for instance, tumour growth and angiogenesis) or too little VEGF (as in ischemic cardiovascular diseases). Tumour growth is dependent on their ability to attract new blood vessels, as they cannot grow beyond 1-2mm without nutrient and oxygen supply. Thus, the tumour produces VEGF to induce an 'angiogenic switch' to aid its exponential growth (Carmeliet, 2005). Loss of VEGF leads to vessel rarefaction which hampers oxygen delivery to metabolic active tissue like heart muscle or neurons. Capillary drop-out in the heart, is a risk factor for developing a heart infarct, whereas vessel rarefaction in the brain has been linked to neurodegenerative diseases (Oosthuyse *et al.*, 2001; Sweeney *et al.*, 2018; Gogiraju, Bochenek and Schäfer, 2019).

3.4.3.2 VEGF-A gradient

One particular aspect regulated by VEGF-A is the guidance of angiogenic sprouts. VEGF-A, through its agonistic activity to the VEGF receptor 2 (VEGFR2), has been shown to regulate angiogenic sprouting by guiding the tip cell migration and the proliferative response of the stalk cells. Tip cell migration, unlike stalk cell proliferation which is VEGF-A concentration dependent, is guided through a VEGF-A gradient (Gerhardt *et al.*, 2003). VEGF-A has many different isoforms such as; $VEGF_{121}$ which is diffusible, $VEGF_{189}$ which can bind to the extracellular matrix (ECM) and $VEGF_{165}$ which has some intermediate characteristics. Thus, due to their special affinities they are able to produce a gradient, with $VEGF_{120}$ able to act over a long range and $VEGF_{188}$ acting at a shorter range. In fact, in $VEGF_{120}$ mutant mice (engineered to express the

VEGF$_{120}$ isoform), vessels are enlarged with reduced branching, as the tip cell loses its guidance cue. This occurs because of high levels of the diffusible VEGF$_{120}$ replacing the normal VEGF-A gradient. In contrast, VEGF$_{188}$ mutant mice (engineered to express the VEGFR$_{188}$ isoform), have a shortage of the diffusible VEGF-A and are thus high in branches but at the cost of lumen enlargement (Carmeliet and Tessier-Lavigne, 2005). Furthermore, VEGF$_{164}$ was shown to be able to bind to Neuropilin 1 (NRP1), an axonal guidance receptor, which in turn enhances VEGFR2 signalling in ECs (Gerhardt *et al.*, 2003).
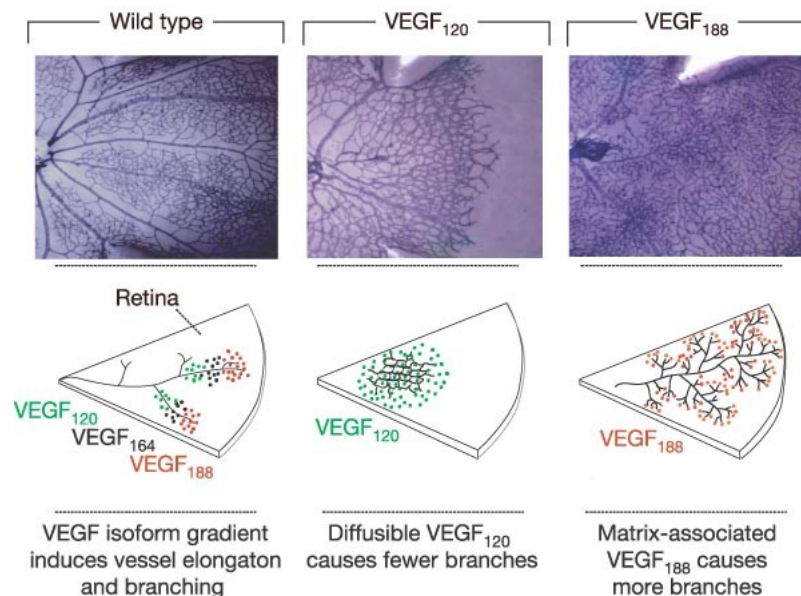
Figure 3. 8: VEGF gradients. VEGF isoforms guide blood vessels pathfinding in neonatal mouse retina.

In the upper section, the vascular network of the retina of wild type mice, VEGF$_{120}$ and VEGF$_{188}$ are shown from left to right. In wild type where a normal VEGF gradient is present, leads to proper vessel elongation and branching, with the VEGF$_{188}$ (shown in red) found close to the VEGF producing cell, the VEGF$_{120}$ (shown in green) in a more distal location and the VEGF$_{164}$ (shown n black) to be intermediately spatially distributed. In the diffusible VEGF$_{120}$ mice, vessels become enlarged at the cost of vessel branches. In the matrix-associated VEGF$_{188}$ mice there is a higher branch number at the expense of smaller blood vessels (Modified from Carmeliet and Tessier-Lavigne, 2005).

3.4.4 Angioneurins in physiological and pathophysiological conditions

3.4.4.1 Hypoxia controls axonal and blood vessel guidance

With the evolution of more complex organisms such as vertebrates, oxygen transfer by diffusion was insufficient. Therefore, the need for a more elaborate network for transferring oxygen led to the evolutionary development of endothelium-lined blood vessels; known as the vasculature. As the vasculature developed, it might have also incorporated some of the developmental mechanisms involved in neurogenesis (Zacchigna, Lambrechts and Carmeliet, 2008). During normoxia (normal oxygen levels) the hypoxia-induced transcription factor; HIF-1α gets hydroxylated by oxygen-dependent prolyl hydroxylases (PHDs) and is then degraded by the proteasome. However, in hypoxic conditions, the PHDs fail to efficiently hydroxylase HIF1-α. HIF1-α will then form heterodimers with HIF1-β and translocate to the nucleus. Once in the nucleus they bind to the hypoxia responsive elements (HREs) to activate transcription of their target genes, including the pro-angiogenic factor VEGF-A (Segura *et al.*, 2009; Van Rooijen *et al.*, 2010). Interestingly, hypoxia (low oxygen availability) was also shown to negatively regulate axonal pathfinding in *C. elegans* model, which lacks vasculature (Pocock and Hobert, 2008). Thus, suggesting that there are certain types of molecules that might have both vascular and angiogenic functions. These are now defined as angioneurins (Zacchigna, Lambrechts and Carmeliet, 2008; Segura *et al.*, 2009). Angioneurins involve molecules which contribute in angiogenesis, blood vessel perfusion, have neuroprotective and neuroregenerative functions and are also involved in the neuronal plasticity (Zacchigna, Lambrechts and Carmeliet, 2008).

3.4.4.2 Axonal guidance cues

Axonal and EC guidance is driven by certain common molecular cues; known as axonal guidance cues. These guidance cues are divided intro attractants (guide them through the tissue) and repellents (prevent them from innervating the tissue) and can either act over a short or longer range. In general, there are four well known families of axon guidance cues; netrins, semaphorins, ephrins and Slits and their respective receptors. These are further accompanied by a certain range of growth factors, including neurotrophins acting as attractants and morphogens, including Hedgehog

and Wnt acting both as attractants and repellents. How axons respond to these guidance cues indicates their plasticity and flexibility. As axons need to cover long distances, there need to be some intermediate targets to guide them towards their desired location. These intermediate targets then need to release both attractive cues, to attract the axons and repulsive cues, to redirect them towards their final destination (Carmeliet and Tessier-Lavigne, 2005; Stoeckli, 2018). Netrins are chemoattractants and guide axons to the midline of the brain by binding to the DCC (deleted in colorectal carcinoma) receptors. To silence this activity, Slit proteins bind to the roundabout receptors to form a complex with the DCC and thus dispel this attractant cue to let neurons move further along towards their target (Carmeliet and Tessier-Lavigne, 2005). Netrin-1 is also pro-angiogenic and is thus involved in sprouting angiogenesis and blood vessel guidance through its EC receptor; Unc5b. As in its axonal guidance function, it could either release repulsive cues in the vasculature through endothelial Unc5b or release attractive cues through an unknown pathway. On the other hand, Netrin-4 could either be anti-angiogenic through down-regulation of VEGF-A signalling or pro-angiogenic to induce proliferation and migration of non-CNS EC sprouts. Semaphorins are usually inhibitory, as they inhibit both axonal guidance and angiogenesis (Wälchli *et al.*, 2015). Indeed, semaphorins impair axonal pathfinding by interfering with the migration of plexin-expressing neuronal growth cones. Plexin-D1 receptor was also found on ECs. Using zebrafish models, they indicated that plexin is not only essential for axonal pathfinding but also for the vascular pathfinding (Torres-Vázquez *et al.*, 2004). Semaphorins have, apart from plexin, another receptor; neuropilin (NRP). NRP1 has been shown to induce axon growth cone collapse and to be also involved in vascular morphogenesis (Pan *et al.*, 2007). Two axonal guidance cues could also work together; 'synergistically', to induce repulsive cues. For example, interactions between the Netrin's receptor; Unc5c and ephrin receptor 2; EphB2 regulate lateral motor column axonal guidance. Furthermore Netrin-1 and ephrin interaction is also involved in the development of blood vessels (Poliak *et al.*, 2015).
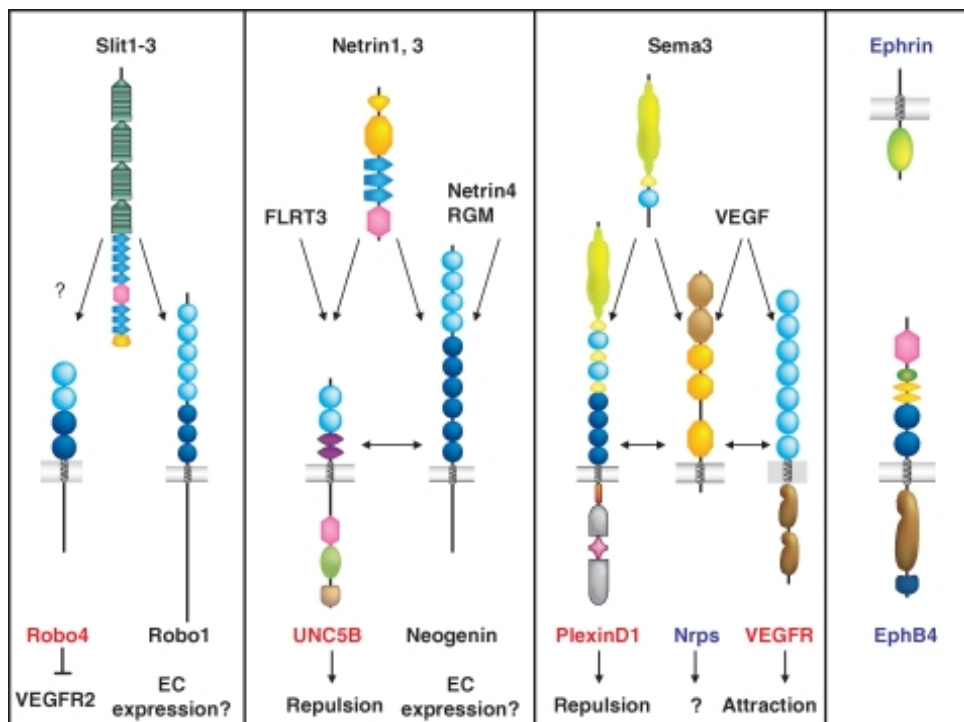
Figure 3. 9: Axonal guidance cues on ECs.

Illustrations of the four main axonal guidance cues and their respective receptors. Receptors mainly acting on ECs are labelled in red, while receptors with both neuronal and vascular functions are labelled in blue. Receptors with unknown functions in the vasculature are shown in black colour (Adams and Eichmann, 2010).

I would now start to focus on factors that were originally discovered as angiogenic factors, with accumulating amounts of evidence showing a function in the nervous system. These angiogenic factors include, VEGF-A and vascular endothelial growth factor 1; VEGFR1 or Flt1, as well as the placental growth factor (PlGF) and VEGF-B.

3.4.4.3 Angiogenic factors

3.4.4.3.1 VEGF-A – key regulator of angiogenesis and neurogenesis

To address molecules that have a function in both angiogenesis and neurogenesis, the term angioneurins was introduced. The most common example of angioneurin is VEGF-A. VEGF-A can regulate both angiogenic sprouting and axonal guidance (Zacchigna, Lambrechts and Carmeliet, 2008). As the absence of the *VEGF* allele is lethal, the hypoxic regulation of *Vegf* was investigated instead. Using the Cre/*loxP*

recombination system, the hypoxia-response element of the *Vegf* promoter was deleted (*Vegf*$^{\delta/\delta}$ mice). Interestingly, insufficient *Vegf* levels resulted in MN degeneration, proving Vegf for the first time, as an important neuroprotective factor (Oosthuyse *et al.*, 2001). Furthermore, VEGF-A was also identified to act via VEGFR2 in the floor plate to attract axons and could thus guide them towards their final destination (Ruiz de Almodovar *et al.*, 2011). VEGF-A additionally guides axonal pathfinding at the optic chiasm, via signalling through its NRP1 receptor (Erskine *et al.*, 2011). Moreover, It was shown to be involved in the neuronal migration in the CNS and axonal outgrowth of cortical neurons (De Almodovar *et al.*, 2009). Through the reactive oxygen species and focal adhesion mechanisms, VEGF-A was also suggested to induce oligodendrocyte precursor cells migration (Hayakawa *et al.*, 2011). It is also neuroprotective for neuronal cells under toxicity or ischemic insults (Nishijima *et al.*, 2007).

3.4.4.3.2 VEGF-A – a bimodal regulator of neurogenesis

In a twin-double publication, the effect of VEGF-A, VEGFR2 and Ephrins on rodent hippocampal pyramidal cells were investigated. Results indicated that loss of VEGFR2 led to increased immature filopodia extensions in dendrites, which could be rescued by VEGF-A. They then identified that EphrinB2 is regulating VEGFR2 internalization, activating downstream pathways to induce spine maturation, dendrite development and synaptic plasticity (Harde *et al.*, 2019). On the axonal end, VEGFR2 internalization is also important for axonal response to VEGF-A, but axonal branching was independent of EphrinB2 and Nrp1. Thus, dendritogenesis and axonal branching have distinct molecular mechanisms in regards to VEGF-A/VEGFR2 signalling. In axonal branches, VEGF-A stimulation leads to increased axon branching and promotes the branches growth. Furthermore, loss of VEGFR2 led to non-functional immature branches. This contradicts dendrite functions, as less VEGFR2 led to a decreased branched network. Thus, VEGF-A/VEGFR2 signalling is a rather bimodal regulator. This is in line with other axon guidance cues such as Sema3a (semaphorin 3a) which has a positive effect on dendritogenesis and an inhibitory one on axonal growth (Luck *et al.*, 2019).
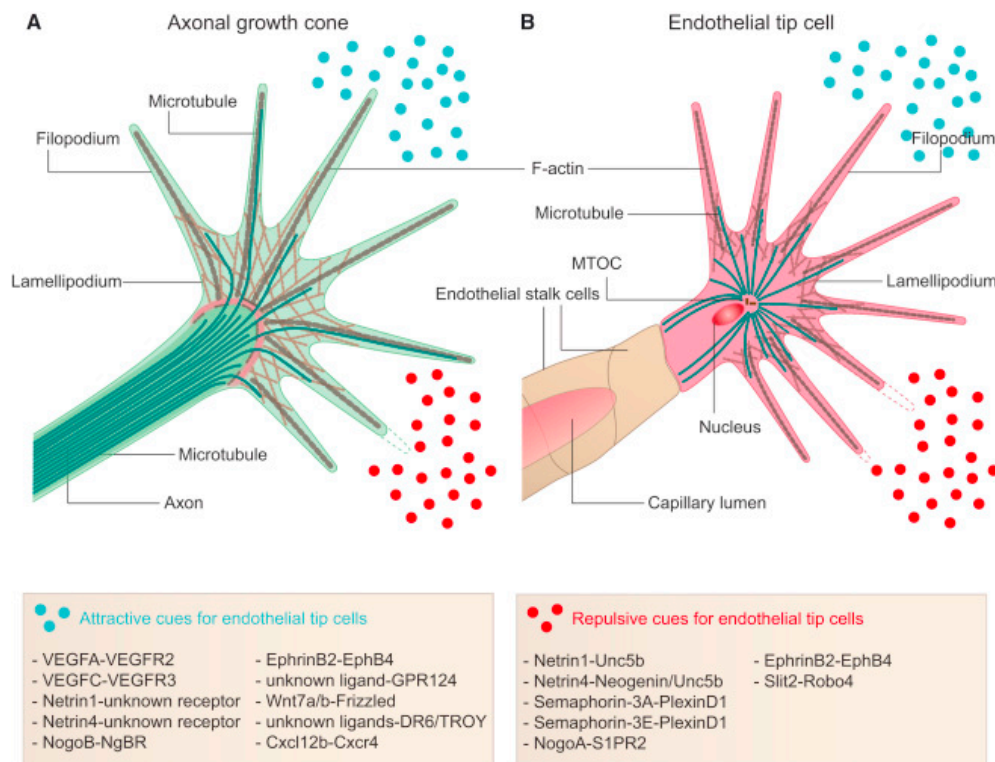
Figure 3. 10: Common guidance cues between neuronal growth cone and the endothelial tip cell.

Both sense guidance cues through their filopodia extensions. Despite their morphological differences, they are functional analogues as they share common attractive and repulsive cues. **(A)** Axonal growth cone at the tip of the extended neuron. It uses actin-based structures (brown) to guide it though attractive (blue) and repulsive (red) cues. **(B)** Endothelial top cell at the tip of sprouting vessel is followed by stalk cells. They too use actin-based structures (brown) to sense pro-angiogenic (blue) and anti-angiogenic (red) cues (Modified from Wälchli *et al.*, 2015).

While, VEGF-A's interaction with VEGFR2 has already been shown to induce angiogenesis, have neurotrophic and neuroprotective effects, VEGF-A's interaction to vascular endothelial growth factor 1; VEGFR1 has also been linked to astrocyte responses. Indeed, VEGFR1 activation via VEGF-A led to the astrocyte activation and proliferation and through the MAP kinase and PI3 kinase pathways led to glial growth and differentiation (Mani *et al.*, 2005).

3.4.4.3.3 VEGF-B and VEGF-C stimulate neurogenesis

VEGF family, also has other ligands such as VEGF-B, VEGF-C and the sub-family member; placental growth factor (PlGF). VEGF-B and VEGF-C can both stimulate neurogenesis in the brain (Carmeliet and De Almodovar, 2013). VEGF-B shares homology to VEGF-A and PlGF, but unlike them, it seems to have only a very limited

effect on angiogenesis. VEGF-B was identified as a potent apoptosis inhibitor acting through the VEGFR1 to supress apoptotic related genes in the retina and brain, thus rescuing neurons from degeneration without interfering with the angiogenesis process (Li *et al.*, 2008). Moreover, VEGF-B was also identified to have neuroprotective properties as it prevents degeneration of cultured primary MNs (Poesen *et al.*, 2008). VEGF-C is mainly known for its role in lymphangiogenesis. VEGF-C acts through the vascular endothelial receptor 3; VEGFR3 to form new lymphatic vessels from the pre-existing ones. However, VEGF-C and VEGFR3 were also detected in neural progenitor cells of tadpoles and mice embryos (Le Bras *et al.*, 2006). Interestingly, unlike Schwann cells whose proliferation is induced via VEGF-A, oligodendrocyte depend on VEGF-C for proliferation (Sondell, Lundborg and Kanje, 1999; Le Bras *et al.*, 2006).

3.4.4.4 Angioneurins in pathophysiological conditions

3.4.4.4.1 Pain and cancer

Pain is one of the most common side effects of cancer, and has huge implications on the patient's quality of life. As the sensory nerves and blood vessels are found in close proximity to each other in tumours, they decided to solve this by looking into angiogenic molecules such as VEGF-A. Both VEGF-A, PlGF-2 and VEGF-B induced pain by acting through their receptor; VEGFR1 located in the sensory neurons. They showed that VEGFR1 was indeed augmented in tumours and that loss of VEGFR1 from these sensory neurons led to pain attenuation and stopped the nerves from remodelling, a process initially induced by the tumour (Selvaraj *et al.*, 2015).

One of the most common malignant brain tumours in children is medulloblastoma. Current therapies involve surgery followed by radiotherapy and chemotherapy, which are highly toxic and increase the morbidity rate. Even though some therapies involve targeting the genetic onset of the tumour, the tumours are still able to develop resistant mutations against it and keep proliferating. Thus, there is a need for alternative targeted therapies to treat these tumours. PlGF is involved in many tumours, in some promoting the tumour progression and in other cases inhibiting its proliferation. They then went on to identify that PlGF was essential for medulloblastoma growth, regardless of the genetic background, and that it was made in the cerebellar stroma

by the Shh ligand derived from the tumour. They also identified that PlGF acts through the Nrp1 receptor, and not via the VEGFR1, to induce tumour growth and survival. Thus, targeting PlGF/Nrp1 interactions may provide an alternative therapy for treating medulloblastomas (Snuderl *et al.*, 2013).

3.4.4.4.2 VEGF-A and neurodegenerative diseases

VEGF-A is both a neuroprotective and neurotrophic factor. In a meta-analysis study of Swedish, Belgian and English population, they found that individuals with lower circulating VEGF-A levels, had a 1.8 times greater chance of getting ALS (Lambrechts, Storkebaum, Morimoto, Del-favero, *et al.*, 2003). Using a *Vegfa* mutant mouse (*Vegf$^{\partial/\partial}$* mice), Oosthuyse et al. identified that loss of *Vegfa* contributed to the progressive MN degeneration, and other neurodegenerative defects, reminiscent of the human ALS phenotype (Oosthuyse *et al.*, 2001; Lambrechts, Storkebaum, Morimoto, Del-Favero, *et al.*, 2003). Moreover, crossing the *Vegf$^{\partial/\partial}$* mouse with the *SOD1^{G93A}* mouse model of ALS, led to significant MN degeneration and early death. When Vegfa was re-introduced to the system, it led to neuroprotective effects against ischemic MN death. Thus Vegfa could be used as a possible therapeutic tool against MN degeneration (Lambrechts, Storkebaum, Morimoto, Del-Favero, *et al.*, 2003). However, VEGF-A is also a potent angiogenic factor, and can also affect vascular permeability, EC proliferation and migration. Thus, a less potent ligand, such as VEGF-B could be used instead. Indeed, loss of VEGF-B did not cause any vascular defects, such as blood-brain barrier leakage. Even though VEGF-B was dispensable under physiological conditions, its effect was only evident under neurodegenerative conditions, as it was shown to augment the severity of MN degeneration in SOD1 mice. VEGF-B$_{186}$ exerted its effects by acting through its receptor; VEGFR1 found in MNs. When VEGF-B$_{168}$ was administered to the SOD1 mutant rats, it acted as a neuroprotective factor and prolonged their survival rate (Poesen *et al.*, 2008).

Abnormal VEGF levels have also been observed in AD patients. *In vitro* studies have shown that Aβ bind to VEGFR2 and thus prevent it from interacting with VEGF-A, leading to EC migration defects. Therefore, this staling of VEGF-A in Aβ plaques could prevent it from exerting its neuroprotective and angiogenic properties. Re-introducing VEGF-A in AD mice, has been shown to alleviate some of the cognitive defects

observed in AD patients (Carmeliet and De Almodovar, 2013). On the contrary, VEGF could also be upregulated to compensate hypoperfusion, as AD patients and mice show leaky hypervascularization at the Aβ plaques. These leaky vessel could further interfere with the normal neuronal homeostasis and even be neurotoxic (Lange *et al.*, 2016).

In PD, the level of VEGF expressed by astrocytes increases, leading to increased abnormal microvasculature and leaky blood brain barrier, which boost a pro-inflammatory response and compromises the dopaminergic neuronal survival. A dose-dependent administration of VEGF in the 6-OHDA PD model could alleviate these symptoms as it promotes dopaminergic neurons survival, glia proliferation and improve vessel perfusion (Lange *et al.*, 2016).
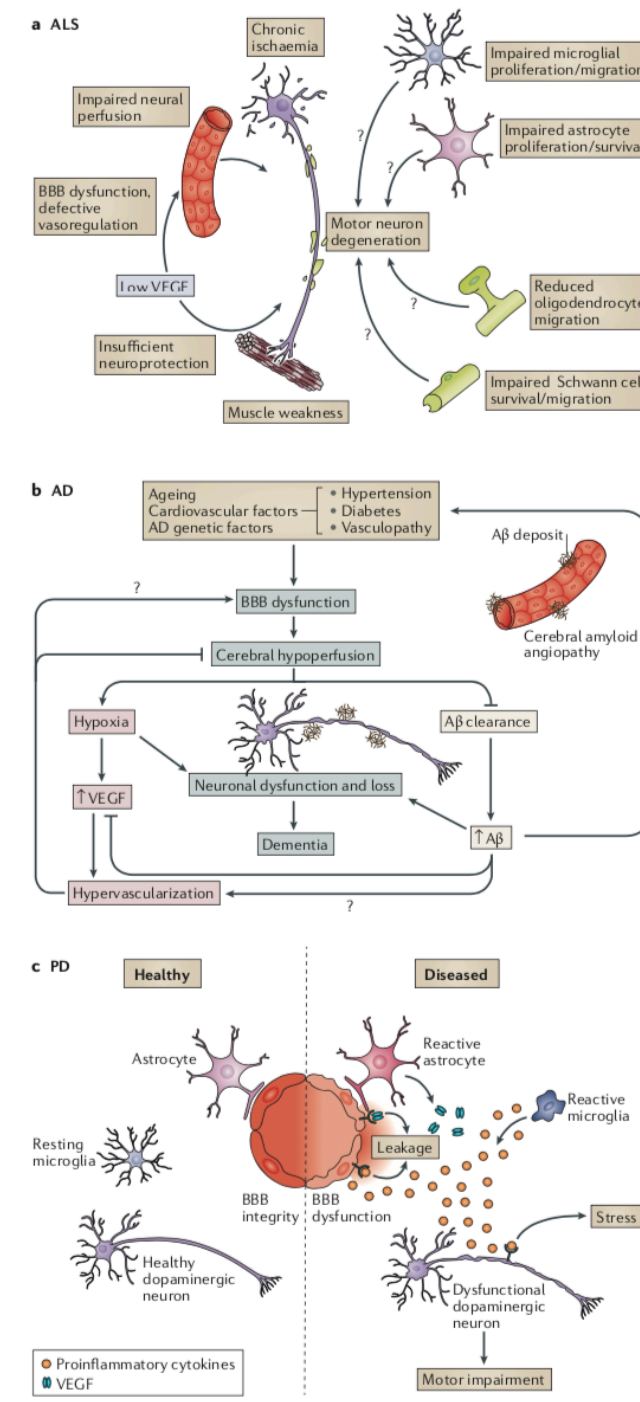
Figure 3. 11: VEGF effect in neurodegenerative diseases.

(a) ALS – low levels of VEGF lead to MN degeneration. Other neuronal cells are also impaired and could thus further contribute in MN degeneration. **(b)** AD – VEGF levels are enhanced by hypoxia leading to leaky hypervascularization, while Aβ accumulation inhibits VEGF signaling. **(c)** PD – promotes reactive gliosis, VEGF is released and astrocytes and microglia activate pro-inflammatory cytokines, thus promoting dopaminergic neuron defects and death (Lange *et al.*, 2016).

3.5   VEGF family, receptors and the vasculature

3.5.1 The VEGF family and receptors

VEGF or VEGF-A is the key member of the VEGF family and has important functions in both angiogenesis and neuroprotection. Other members in mammals include VEGF-B, VEGF-C, VEGF-D and PlGF and their receptor tyrosine kinases (RTKs). These include VEGFR1, VEGFR2 and VEGFR3 and co-receptors such as neuropilins (NRPs) (Olsson *et al.*, 2006). VEGF binds to receptors; VEGFR1, VEGFR2, NRP1 and NRP2. VEGF-B binds to VEGFR1 and NRP1. VEGF-C binds to VEGFR3, VEGFR2 and NRP1 (Lange *et al.*, 2016). While VEGFR2 binds to VEGF-A, the VEGFR1 binds both to VEGF-A and PlGF. Interestingly, VEGFR1 binding to PlGF results in intermolecular transphosphorylation of VEGR2, thus enhancing the VEGF-A driven angiogenesis (Autiero *et al.*, 2003). VEGF-A binding to the VEGFR2 (KDR/FLK) drives angiogenesis, as it regulates EC proliferation and sprouting. VEGFR1 (Flt1) acts as a VEGF-A scavenger receptor and has a higher affinity for VEGF-A binding than VEGFR2. (Adams and Alitalo, 2007; Wild *et al.*, 2017). VEGF-C acts through VEGFR3 to promote lymphangiogenesis (Leppänen *et al.*, 2013).
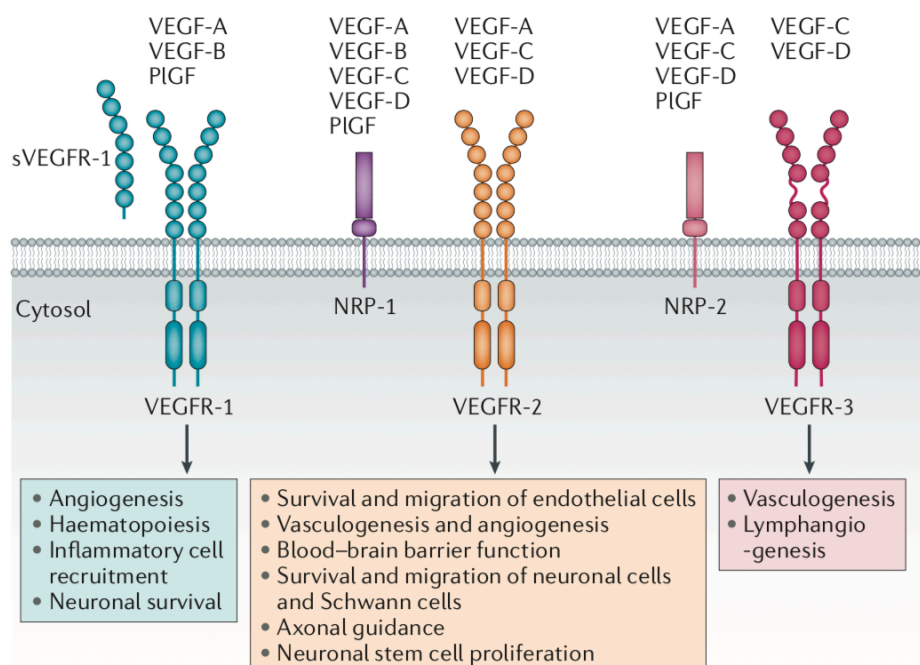

Figure 3. 12: VEGF family and receptors.

Illustration of the VEGF ligands binding to their RTKs and co-receptors. Coloured boxes are indicating their effect on the vasculature and CNS (Lange *et al.*, 2016).

3.5.2 The VEGFRs expression and regulation

Even though the VEGFRs were initially discovered as vascular targets, recent data has also identified them in some neuronal populations (Fong *et al.*, 1995; Shalaby *et al.*, 1995; Selvaraj *et al.*, 2015; Wild *et al.*, 2017). VEGFR2 is mainly found in the ECs and the lymphatic system in mouse models, while in zebrafish it is mainly expressed in the vascular ECs (Adams and Alitalo, 2007). VEGFR1 is an arterial marker, as it is mainly expressed in arteries and is barely detected in veins in zebrafish models (Hogan *et al.*, 2009; Krueger *et al.*, 2011; Cui *et al.*, 2015). It is also expressed in myeloid cells and in zebrafish neurons (Sawano *et al.*, 2001; Stefater III *et al.*, 2011; Wild *et al.*, 2017). While Vegfr3 or Flt4 is expressed both in arteries and veins during early embryonic development, at later developmental stages it is mainly detected in the venous ECs and the lymphatic system (Adams and Alitalo, 2007; Siekmann and Lawson, 2007; Hogan *et al.*, 2009). This study will mainly be focused on VEGFR1 (Flt1).

3.5.3 VEGFR1 splicing

VEGFR1 (Flt1) was first identified as a fms-like kinase gene (Shibuya *et al.*, 1990). It has a weak-tyrosine kinase activity and binds to VEGF, PlGF and VEGF-B with high affinity (Autiero *et al.*, 2003; Olsson *et al.*, 2006). In vertebrates there are two isoforms formed by alternative splicing; a membrane-bound form (mFlt1) and a shorter soluble one (sFlt1) (Krueger *et al.*, 2011). The Flt1 alternative splicing is regulated by the Jumonji domain-containing protein 6 (jmjd6) (Boeckel *et al.*, 2011). During normoxia, jmjd6 hydroxylates U2 small nuclear ribonucleoprotein auxiliary factor 65-kilodalton subunit (U2AF65) to splice Flt1, shifting the sFlt1/mFlt1 equilibrium towards mFlt1 production. However, in cases of hypoxia, the equilibrium shifts towards sFlt1 production in human umbilical vein ECs; HUVECs (Webby *et al.*, 2009; Boeckel *et al.*, 2011). In contrast, research on human microvascular endothelial cells (HMVECs) showed that sFlt1 is downregulated in these cells to aid in the formation of new blood vessels during hypoxic conditions (Ikeda *et al.*, 2011). Even though these results may seem inconsistent, it could indicate that different cell types are able to regulate Flt1 in a different manner.

3.5.4 VEGFR1 functions

3.5.4.1 VEGFR1 and angiogenesis

Contradictory data suggest VEGFR1 (Flt1) as either a positive or negative angiogenic regulator. Flt1 acting as a positive regulator was suggested as loss of Flt1 led to a reduction in vessel branching, increased sprout initiation and vessel collapse due to unproductive angiogenesis (Kearney *et al.*, 2004; Chappell *et al.*, 2016). However, the majority of studies are showing Flt1 as a negative regulator (Fong *et al.*, 1995; Chappell *et al.*, 2016). Fong et al. showed that FLT1 is not essential for vascular growth but rather to negatively control hemangioblast formation. To further test that, chimaeric embryos were analysed containing both wild type and *flt1*$^{-/-}$ cells. Chimaeras showed normal vasculature thus suggesting that Flt1 acts in a cell non-autonomous manner (Fong *et al.*, 1999). Other papers are showing an important function of FLT1 in angiogenesis in the mouse retinal plexus, as VEGFR1 (Flt1) deficiency led to tip cell initiation and EC proliferation, thus facilitating angiogenesis and was also protective against myocardial infarction (Ho *et al.*, 2012). Further zebrafish research also showed that loss of *flt1* led to increased vascular sprouting (Wild *et al.*, 2017). Vessel tone is regulated by VEGF-A through nitric oxide (NO) production depending on the endothelial nitric oxide synthase (eNOS) (Cudmore *et al.*, 2012). VEGFR1 signalling was identified to activate eNOS, mediated by the PlGF activation of PI3K, to induce NO-driven angiogenesis *in vitro* (Ahmad *et al.*, 2006). To further investigate this, VEGFR1 and VEGFR2 heterodimers were used (VEGFR$_{1-2}$). This dimer is composed of the VEGFR2 monomer (VEGF-E) and the VEGFR1 monomer (PlGF-1). Endothelial activation of this dimer also results in eNOS phosphorylation and NO release, thus regulating EC homeostasis (Cudmore *et al.*, 2012).

3.5.4.2 VEGFR1 and contractile cells

Heart and vasculature systems co-operate to compensate their hemodynamic needs in vertebrate models. Data showed that VEGF acts through the Flt1 receptor upstream of phospholipase C (PLCγ) to modulate cardiac contractility via regulating calcium cycling (Rottbauer *et al.*, 2005). Thus, placing Flt1 as a contractility cell modulator. Other contractile cells include mural cells, composed of vascular smooth muscle cells

(vSMCs) and pericytes which wrap themselves around capillary ECs and are essential for blood vessel formation and stability. Recent data showed that pericytes induce EC sprouting in mice postnatal retina via modulation of local VEGF signalling through expression of VEGFR1 (Eilken *et al.*, 2017). VEGF-A$_{165}$ was also identified to lead human aortic smooth muscle cells (hAOSMCs) migration in conjunction with a cross-talk between NRP1 and VEGFR1 expression and phosphoinositide 3-kinase/Akt kinase activation (Banerjee *et al.*, 2008). Another combined NRP1 and FLT1 function was also observed in lacteal chylomicron uptake (lymphatic vessels absorbing lipids) where they collaborate as a double decoy receptor of VEGF-A signalling. When both receptors were genetically ablated, VEGF-A was more freely available to find to bind to VEGFR2 and protect against diet-induced obesity (Zhang *et al.*, 2018).

3.5.4.3 VEGFR1 and macrophages

Macrophages were recently found to be associated with EC tip cells in the process of angiogenesis and during vessel anastomosis (fusion). While VEGF is essential for sprouting, macrophages aid in the anastomosis process (Fantin *et al.*, 2010). Using human monocytes, VEGF$_{165}$, VEGF$_{121}$ and PlGF$_{152}$ were all identified to be able to induce monocyte migration in a dose-dependent manner. VEGF chemotactic response on monocytes was mediated via the VEGFR1 (Barleon *et al.*, 1996). Interestingly, further data revealed that VEGFR1 (Flt1) and not KDR, is a monocyte/macrophage cell marker (Sawano *et al.*, 2001). Additionally, PlGF was shown to activate and recruit macrophages via releasing angiogenic and lymphangiogenic factors (Dewerchin and Carmeliet, 2012). This was further verified as VEGF- and PlGF-dependent peritoneal macrophage migration was impaired in Flt1 tyrosine kinase (mFlt1) deficient mice; Flt1 TK$^{-/-}$ (Muramatsu *et al.*, 2010). As these mutants were only targeted against the tyrosine kinase component of the receptor (mFlt1), they fail to address the effect of sFlt1 on macrophage migration.

3.5.4.4 VEGFR-1 and neurons

In zebrafish embryos, *flt1* was not only detected in the aorta, arterial intersegmental vessels (ISVs) and partly in the venous ISVs but also in spinal cord neurons. Additionally neuronal sFlt1 seems to be relevant for spinal cord vascularization via titrating Vegfa at the neurovascular interface (Wild *et al.*, 2017). Moreover, Flt1 has

also been shown in motor neurons (MNs), sensory neurons and the dorsal root ganglia and in most but not all astrocytes (Mani *et al.*, 2005; Storkebaum *et al.*, 2005; Poesen *et al.*, 2008; Dhondt *et al.*, 2011; Selvaraj *et al.*, 2015). mFlt1 is present in MNs and acts as a neuroprotective agent against degeneration via signalling down its tyrosine kinase domain (Poesen *et al.*, 2008). While VEGF is neuroprotective via the VEGFR2 on MNs, VEGF-B does so via Flt1 (Dhondt *et al.*, 2011). However, this does not hold true for astrocytes, as the neuroprotective effect is not mediated through the mFlt1 tyrosine kinase activity. Thus, Flt1 upregulation in astrocytes after an injury is still elusive on whether it is neuroprotective or not (Poesen *et al.*, 2008). Further investigation on sFlt1 could offer complimentary data and decipher new Flt1 neuroprotective functions. VEGF was also found to induce nociceptive sensitization in the PNS via VEGFR1 (Flt1). Cancer models show that Flt1 is overexpressed in sensory neurons and that by blocking Flt1, attenuates the cancer pain (Selvaraj *et al.*, 2015).

3.5.5 Studying VEGF and its receptors using mouse models

Studying the effects of VEGF-A and its receptors; VEGFR1 and VEGFR2 in the vasculature, is complicated as *Vegf* full mutant and even haploinsufficient mice die due to failure in blood vessel formation (Carmeliet *et al.*, 1996; Oosthuyse *et al.*, 2001). *Flk1* (*Vegfr2*) homozygous mutant mice are also lethal between E8.5 to E9.5 due to defective in haematopoietic and ECs differentiation (Shalaby, Rossant, *et al.*, 1995). In addition, overexpression of VEGF also led to severe heart defects and embryonic lethality (Miquerol, Langille and Nagy, 2000). Thus, VEGF needs to be tightly regulated at a protein level, which is achieved via VEGFR1 (Flt1). Unlike, Flk1, Flt1 is not essential for EC differentiation but is rather important in the organization of the vasculature in embryonic mice. *Flt1* homozygous mutant mice were also lethal *in utero* due to disorganized EC vasculature (Fong *et al.*, 1995).

3.5.6 Studying VEGF ligands and receptors using zebrafish models

3.5.6.1 Zebrafish – an alternative take on studying angiogenesis

An alternative approach was carried out using morpholinos to induce a *vegfa* knock-down in zebrafish models to induce vascular defects. (Nasevicius, Larson and Ekker, 2000). Zebrafish are great models in studying vascular development, as due to their small size they can receive oxygen by passive diffusion for several days post fertilization (dpf), even in the absence of vasculature (Isogai, Horiguchi and Weinstein, 2001). Another great advantage is their high fecundity and optical clarity which allows for direct visualization of the vascular development and defects *in vivo* (Isogai, Horiguchi and Weinstein, 2001; Payne and Look, 2009). They develop externally thus the developmental stages, including the heart rate and blood circulation can be easily observed under a stereomicroscope (Patton and Zon, 2001). Important genes for the regulation and formation of the cardiovascular system were indeed identified using forward genetics in zebrafish models (Stainier *et al.*, 1996). Development of transgenic lines further revolutionised the cardiovascular field as large scale forward genetics could be performed to detect the effect of various mutations *in vivo* (Lawson and Weinstein, 2002). Thus, arose the need for reverse genetic approaches to identify specific gene functions.

3.5.6.2 Zebrafish – morpholinos to mutants

Morpholinos were the first approach to block translation or splicing of the gene of interest to induce a gene knockdown (F. O. Kok *et al.*, 2015). As in the work of Nasevicius et al. a *vegfa* morpholino was injected in zebrafish embryos, which in turn displayed an enlarged pericardium and vascular defects. Initial axial vascular patterning was independent of *vegfa* levels, in contrast to intersegmental vessels which were nearly completely absent in the *vegfa* morphant embryos (Nasevicius, Larson and Ekker, 2000). One important factor to take into account is that due to genome duplication, zebrafish have more *vegf* isoforms than mammals (Glasauer and Neuhauss, 2014). These include; *vegfaa, vegfab, vegfba, vegfbb, vegfc, vegfd* and *plgf* (Jensen *et al.*, 2012, 2015; Rossi *et al.*, 2016; Wild *et al.*, 2017). *Vegfaa* encodes for the 2 Vegfa isoforms; Vegfaa-121 and Vegfa-165, while the *vegfab* for Vegfab-171 and

Vegfab-210 (Rossi *et al.*, 2016). Furthermore, in zebrafish the Kdr receptor is not orthologous to the mammalian KDR, while the kdr-like (kdrl) receptor is the major regulator of Vegf (Covassin *et al.*, 2009). Nrp1 is also composed of two paralogs; *nrp1a* and *nrp1b* (Martyn and Schulfe-Merker, 2004). On the other hand, *Flt1* and *Plgf* have only one paralog in zebrafish. Interestingly, morpholino work has shown that knocking down *vegfba* led to high embryonic lethality with embryos exhibiting developmental heart defects and head oedemas, while *vegfbb* knockdown led to a normal phenotype. Thus, for zebrafish, *vegfba* and not *vegfbb* is crucial for embryonic development. However, unlike the *vegfaa* knockdown embryos, *vegfba* deficient embryos had only modest defects in the intersegmental vessels (Jensen *et al.*, 2015). Despite the early promising morpholino data, morpholinos were recently identified to have off-target effects due to their ability to induce p53-dependent apoptosis (F. O. Kok *et al.*, 2015). New reverse genetic approaches were thus needed to induce targeted gene deletions. Such techniques now include Transcription activator-like effector nucleases (TALENs) and the RNA-guided clustered regularly interspaced shirt palindromic repeats (CRISPR) – Cas9 nuclease system to induce double strand breaks at the locus of the gene of interest (Ran *et al.*, 2013; F. O. Kok *et al.*, 2015). Using TALENs and CRISPRs, *vegfaa* and *vegfab* mutants were generated. Similarly, to the mouse data, *vegfaa* mutants experienced severe vascular defects, incompatible with life and could be rescued via *vegfaa* mRNA injections (Rossi *et al.*, 2016). Unpublished data have shown that overexpression of *vegfaa* also impairs MN patterning in zebrafish larvae. Furthermore, even though *plgf* was detected in MNs (Wild *et al.*, 2017), *plgf* zebrafish mutants showed no impact on MN patterning nor on the neurovascular interface. Overexpression of *plgf* and *vegfba* displayed an increase in the intersegmental vessel's (ISV) diameter but showed no defects in MN patterning (Alina Klems, unpublished).

3.5.6.3 Tertiary sprouting – a novel form of sprouting that regulates SC vascularization

De novo blood vessel formation of primary vascular plexus, dorsal aorta (DA), posterior cardinal vein (PCV) and the vascular surrounding the CNS are formed by a process known as vasculogenesis (Risau and Flamme, 1995; Herbert and Stainier, 2011). This study's focus however will be on angiogenesis, the formation of new vessels from pre-existing ones, a dynamic process of EC behavioural changes to induce sprouts (Carmeliet and Tessier-Lavigne, 2005; Fantin *et al.*, 2010; Wild *et al.*, 2017). These sprouting events in zebrafish are labelled as primary (arterial) and secondary (venous) sprouting (Wild *et al.*, 2017). Primary sprouting is dependent on the Vegfaa-Kdrl signalling and regulated by Notch (Siekmann and Lawson, 2007; Covassin *et al.*, 2009). This process involves the formation of the arterial intersegmental vessels (aISVs) from the DA. After the primary sprouting is completed, secondary veins grow out of the PCV to form venous intersegmental vessels (vISVs). This process is dependent on Vegfc-Flt4 signalling (Hogan *et al.*, 2009; Villefranc *et al.*, 2013).
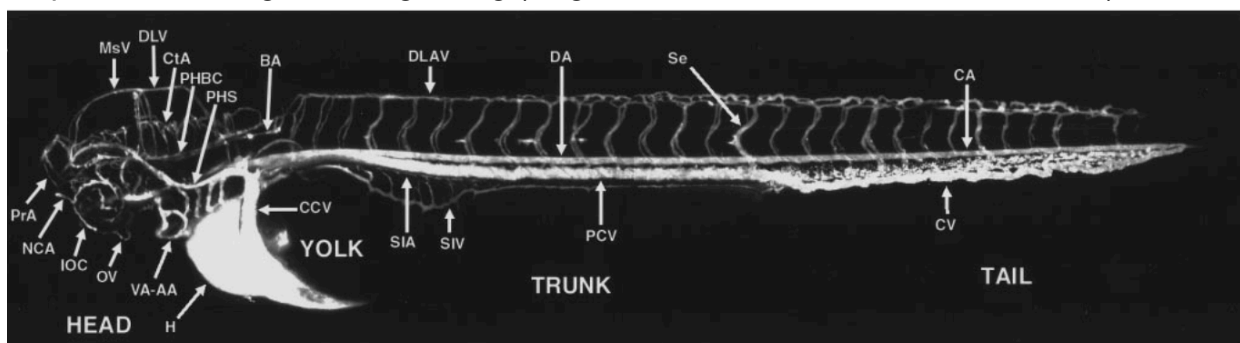

Figure 3. 13: Angiogram showing blood circulation in a 3-3.5 days post fertilization (dpf) zebrafish larvae.

H: heart; VA: ventral aorta; OV: Optic vein; IOC: Inner optic circle; NCA: nasal ciliary artery; PrA: Prosencephalic artery; MsV: mesencephalic vein; DLV: dorsal longitudinal vein; CtA: central artery; PHBC: primordial hindbrain channel; PHS: primary head sinus; BA: basilar artery; DLAV: dorsal longitudinal anastomotic vessel; DA: dorsal aorta; Se: intersegmental vessel; CA: causal artery; CV: caudal vein; PCV: posterior cardinal vein; SIV: subintestinal vein; SIA: supraintestinal artery; CCV: common cardinal vein (Modified from Isogai, Horiguchi and Weinstein, 2001).

A novel form of sprouting was recently described by Wild et al. termed as tertiary sprouting. Using CRISPR/Cas9 approaches, both *flt1* isoforms; *mflt1* and *sflt1* were targeted to obtain a full *flt1* mutant (*flt1ka601*, *flt1ka602* and *flt1ka603*). Furthermore, an *mflt1*-specific mutant was also generated (*flt1ka605*). Interestingly, a hyperbranching phenotype was observed at 2.5-3dpf around the neural tube in *flt1* mutants but not in the single *mflt1* mutants, suggesting that this effect is likely driven by the soluble Flt1. These ectopic sprouts emerged from the vISVs and are orchestrated by neuronal sFlt1 and Vegfaa (Wild *et al.*, 2017).
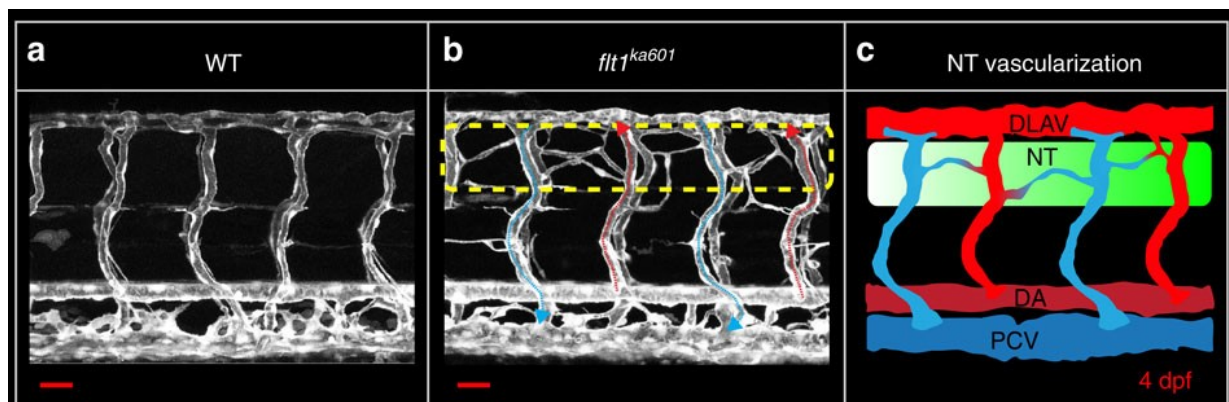

Figure 3. 14: *Flt1* mutant induces a hyperbranched network around the neural tube (spinal cord) at 4dpf.

(a) Wild type and **(b)** *flt1ka601* vasculature using a vascular transgenic line *Tg(kdrl:EGFP)s843*. Yellow dotted box indicates the area of the neural tube. Red arrows indicate perfused aISVs and the blue vISVs. **(c)** Illustration of the *flt1ka601* sprouting. aISVs are coloured in red and vISVs are in blue. DLAV: dorsal longitudinal anastomotic vessel; NT: neural tube; DA: dorsal aorta; PCV: posterior cardinal vein; dpf: days post fertilization. Scale bar, 50 μm (Modified from Wild *et al.*, 2017).

3.5.6.4 *vegfa* gain and loss-of-function scenarios

When *flt1* gets downregulated, more *vegfaa* is available to bind to *kdrl* and induce angiogenesis. *flt1* mutants thus mimic a *vegfaa*-gain-of-function (GOF) scenario. It would thus be interesting to further investigate this *vegfaa* overexpression scenario using other *vegfaa* GOF models. One model of triggering Vegfa expression, independent of *flt1*, is through manipulation of the hypoxia inducible factor system (Oosthuyse *et al.*, 2001; Pugh and Ratcliffe, 2003). During normoxic conditions; the hypoxia-induced transcription factor α (HIF-α) gets hydroxylated by the prolyl hydroxylases (PHD1-3) and is in turn targeted by the von Hippel-Lindau (VHL) protein for proteasomal degradation by the E3 ubiquitin ligase complex. However, during

hypoxic conditions, HIF-1α is able to form dimers with HIF-1β and can then translocate to the nucleus to induce transcriptional activation of angiogenic growth factors including VEGF-A (Pugh and Ratcliffe, 2003; Van Rooijen *et al.*, 2010). One way to induce this is by creating a *vhl* mutant. While *Vhlh* knockout mice are lethal at E11.5-12.5, zebrafish *vhl* mutants (*vhl^{hu2114}*) are viable until 8-11dpf (Van Rooijen *et al.*, 2009). In a similar manner to the *flt1* mutants, *vhl* mutants also display hyperbranching emanating from vISVs at the level of the neural tube (Van Rooijen *et al.*, 2010; Wild *et al.*, 2017). Thus, loss of *flt1* or *vhl* leads to an accumulation of the Vegfaa expression. Double *flt1^{ka601}*; *vhl^{hu2114}* mutants developed more ectopic sprouts than each mutant individually with many of the branches invading through the neural tube. One should note that in wild type, the spinal cord vascularization occurs at around 13dpf, unlike in the *vegfaa* gain-of-function (GOF) scenarios where this is observed as early as 3-4dpf (Wild *et al.*, 2017). To further investigate if the hyperbranching is induced by neuronal *Vegfaa*, *vegfaa165* and *vegfaa121* were individually overexpressed in neurons in a time dependent manner and also showed hyperbranching at the level of the neural tube as observed in *flt1* mutants. Thus neurons may be utilizing sFlt1-Vegfaa to form new blood vessels depending on their developmental needs (Wild *et al.*, 2017). As Flt1 was identified to bind both to PLGF and VEGF-B, and *plgf* mRNA was overexpressed in *flt1* mutants, these were further investigated as an alternative approaches to investigate *Vegfaa* overexpression (Wild *et al.*, 2017). This could be achieved by *plgf* or *vegfba* overexpression to compete *vegfaa* away from binding to *flt1*. Both *plgf* and *vegfba* overexpression models showed an increase in ISV diameter (diminishes at around 73 hours post fertilization; hpf), with *plgf* GOF phenocopying the *flt1* mutant phenotype, as hyperbranching was also observed around the level of the neural tube. In contrast, in *plgf* mutants, the vessel diameter was thinner than wild type (WT) which could suggest a *plgf* acts on the Vegfaa-Kdrl signalling (Alina Klems, unpublished).

3.5.6.5 VEGF-A macrophages and angiogenesis

Tissue macrophages were recently shown to interact with tip cells and promote vascular anastomosis, downstream of VEGF-mediated tip cell initiation (Fantin et al., 2010). Moreover, embryonic zebrafish tumour xenograft showed a decreased vascularisation in the absence of macrophages, suggesting a direct association between macrophages and migrating tip cells during tumour angiogenesis.

Furthermore, xenografts which overexpressed *vegfaa* showed a macrophage-dependent vascularisation, which could suggest a macrophages mediated Vegfa-driven tumour angiogenesis (Britto *et al.*, 2018). As both VEGF- and PlGF- mediated macrophage migration was impaired in Flt1 TK$^{-/-}$ (Muramatsu *et al.*, 2010), macrophage distribution was further investigated in *flt1* and *plgf* zebrafish mutants using the *leucocyte-specific plastin* (*l-plastin*) in-situ marker (Herbomel, Thisse and Thisse, 1999; Tsarouchas *et al.*, 2018). As *flt1* and *plgf* are usually detected at 2dpf around the aorta and hypochord respectively, in the mutant scenarios, macrophages dispersed out of that area and moved towards the trunk and tail (Krueger *et al.*, 2011; Alina Klems, unpublished).

3.6 Regeneration models

3.6.1 Macrophages and vessel remodelling

Macrophages are not only involved in vessel anastomosis but are also key players in wound healing (Petrie *et al.*, 2015; Gurevich *et al.*, 2018; Tsarouchas *et al.*, 2018). Recent data showed that macrophages migrate to the wound area to aid in blood vessel repair (Gurevich *et al.*, 2018). While neutrophils are only temporarily drawn to the damaged vessels, macrophages linger throughout the whole duration of repair and anastomosis (Gurevich *et al.*, 2018). Neutrophils are important during the initial stages of wound resolution. However, data on spinal cord lesions indicated that it is indeed the macrophages and not the neutrophils or microglia who are essential in wound repair (Tsarouchas *et al.*, 2018). Macrophages can be classified in two subpopulations, the pro-inflammatory M1 and the anti-inflammatory M2 macrophages, even though this classification is debatable (Petrie *et al.*, 2015). The first influx of macrophages to the wound is pro-inflammatory and express *vegfaa* to aid in the early vessel sprouting. These need to be subsequently transitioned into an anti-inflammatory state to aid during the later stages of vessel remodelling (Gurevich *et al.*, 2018).

3.6.2 Medaka – a broken heart story

Heart failure is the outcome of myocardial infarction (MI) as the adult human heart cannot replenish the damaged tissue and is thus unable to resolve the scar formation

(Kikuchi and Poss, 2012; Lai *et al.*, 2017). Even though, neonatal mammals have some regenerative capacities, these seem to be lost as we age (Seifert and Voss, 2013; Lavine *et al.*, 2014). Research showed that neonatal mice recruit an embryonic-derived resident cardiac macrophage population, which aid in cardiac regeneration by diminishing excessive inflammation, promoting cardiomyocyte proliferation and angiogenesis. Interestingly, in adult mice, these embryonic-derived macrophages are replaced by monocyte-derived ones which lack the regenerative properties found in the embryonic macrophages (Lavine *et al.*, 2014). Zebrafish, on the other hand, retain their ability to regenerate their cardiac tissue all the way to adulthood (Seifert and Voss, 2013; Vivien, Hudson and Porrello, 2016). Upon a cardiac injury, zebrafish endocardial and epicardial cells release factors to stimulate the proliferation of cardiomyocytes (Kikuchi and Poss, 2012). Despite this new hype in using fish models to study heart regeneration, not all fish retain the same regenerative capacities. Another water teleost fish, medaka (*Oryzias latipes*) is for example not able to regenerate its cardiac tissue upon injury. In contrast to zebrafish models, the injured heart experiences an excessive fibrotic response and its cardiomyocytes fail to proliferate (Ito *et al.*, 2014). Even though the two fish share the same living environment, they are evolutionary distinct making them ideal genetic models in deciphering regenerative mechanisms (Furutani-Seiki and Wittbrodt, 2004). To investigate this, a detailed comparative transcriptomic analysis was carried out on both species after a cardiac injury. Results showed that medaka had a delayed macrophage response upon injury when compared to zebrafish (Lai *et al.*, 2017). Inhibiting the inflammatory response in zebrafish, significantly impaired the cardiac regeneration and led to elevated collagen deposition (Huang *et al.*, 2013). Furthermore, delaying the macrophage migration to the cardiac injury led to defective neovascularization, less cardiomyocyte proliferation and scar formation (Lai *et al.*, 2017). Surprisingly, re-activating the inflammatory response in medaka fish boosted neovascularization, induced cardiomyocyte proliferation and alleviated the scaring (Lai *et al.*, 2017). Thus, the immune system response is of vital importance in initiating a regenerative response.

3.6.3 A tail story

As mammals have only a limited regenerative ability, high regenerative models such as axolotls and zebrafish have been employed to study analogous appendage regeneration (Petrie *et al.*, 2015; Baddar, Clithrala and Voss, 2019). Partial amputation of the adult zebrafish caudal fin takes around 2-4 weeks to be completely resolved (Wehner *et al.*, 2014; Pfefferli and Jaźwińska, 2015). Inflammatory responses observed in adult caudal fin injuries were similar to those observed in mammals. This involve the initial migration of neutrophils to the wound, followed by a macrophage accumulation (Petrie *et al.*, 2015; Wynn and Vannella, 2016). Similar to mammalian models where dermal healing was unaffected by neutrophil depletion (Dovi, He and Dipietro, 2002), in adult zebrafish, neutrophil inhibition also had no effect in the caudal fin regeneration rate (Petrie *et al.*, 2015). On the other hand, macrophages seem to be essential for epimorphic regeneration in mouse models (Simkin, Gawriluk, *et al.*, 2017; Simkin, Sammarco, *et al.*, 2017), and for caudal fin regeneration in zebrafish (Petrie *et al.*, 2015). Therefore, it seems that regeneration efficiency is rather macrophage than neutrophil dependent. Leukocyte migration to the wound was found to be mediated by elevated concentration of hydrogen peroxide, a reactive oxygen species (ROS), present at the wound margin (Niethammer *et al.*, 2009). ROS activation, in response to injury, to provide instructive cues for tail regeneration was not only detected in zebrafish larvae (Niethammer *et al.*, 2009) but also in axolotl embryos (Baddar, Clithrala and Voss, 2019). Therefore, ROS are also important in initiating a successful inflammatory response.

3.6.4 Regenerating the spinal cord – an ongoing research

The adult mammalian spinal cord is incapable of regenerating, thus leading to tetraplegia or paraplegia with high morbidity rates, and a huge emotional toll on the patients (Harkey *et al.*, 2003; Kirshblum *et al.*, 2011). This is attributed to the mammalian's limited ability to induce neurogenesis post CNS injury (Jessberger, 2016). It also holds true for a lot of neurodegenerative diseases and stroke as the neuronal loss is never recapitulated by neurogenesis (Becker and Becker, 2015). On the contrary, fish and salamanders are able to regenerate their spinal cord and brain all the way to adulthood (Seifert and Voss, 2013).
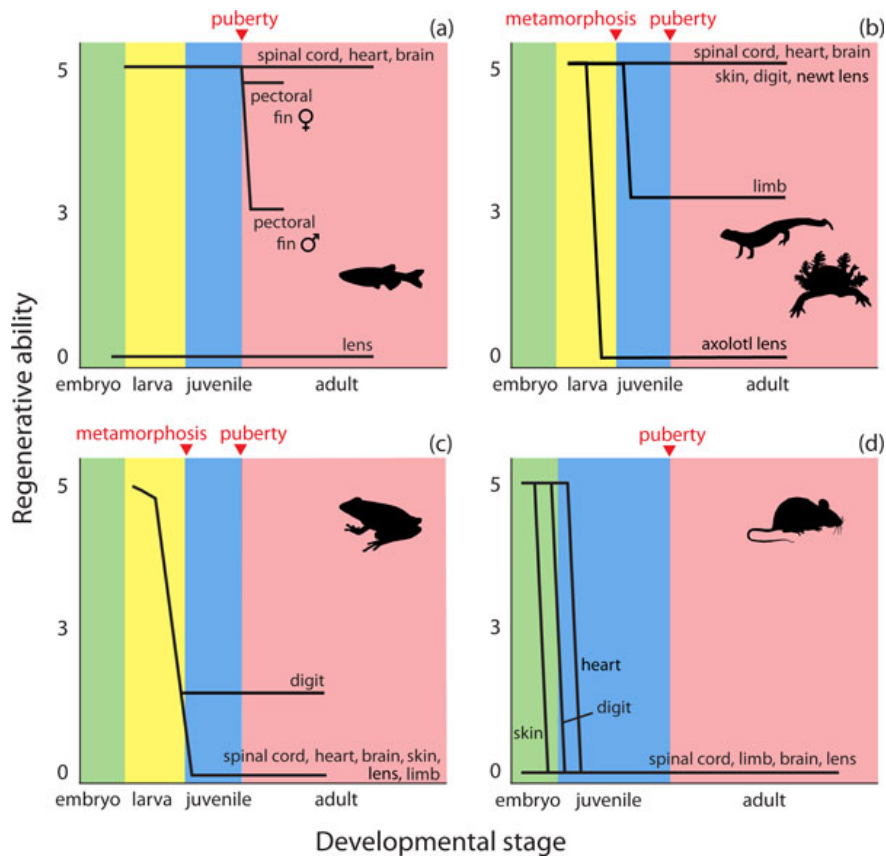
Figure 3. 15: Regenerative capacity of vertebrate models over the different developmental stages.

Regenerative ability scale 0 to 5, where 0 stands for no regeneration and 5 for proper regeneration. Developmental stages are indicated as embryo, larva, juvenile and adult stages. **(a)** Zebrafish are good models for studying cardiac and spinal cord regeneration as they maintain their regenerative ability all the way to adulthood. **(b)** Salamanders and newts also retain cardiac and CNS regeneration all the way to adulthood. **(c)** Even though frogs have some regenerative capacities as larvae, they lose this potential as they become adults. **(d)** Mammals have some regenerative abilities when in embryonic stages but lose this before or shortly after birth (Seifert and Voss, 2013).

In this study, three ways will be investigated to tackle spinal cord injuries; investigate effect of the immune system, the extracellular matrix (ECM) and neurogenesis/stem cell renewal in respect to angiogenesis.

3.6.4.1 Spinal cord regeneration and the immune system

To tackle the first and most studied topic; Kigerl et al used spinal cord injury mouse models. Her group observed a strong prolonged M1 macrophage response after injury which overwhelmed the small number of M2 macrophages migrating to the wound. M1 macrophages seem to be neurotoxic as compared to the M2 macrophages which have been shown to promote axonal regeneration in sensory neurons (Kigerl *et al.*, 2009). In fact, macrophages can have dual functions, promoting axonal regeneration in the CNS but also neurotoxic properties. Indeed, activation of macrophages led to initial axonal growth but prolonged exposure led to cell death and neurodegeneration (Gensel *et al.*, 2009). Similar results were also shown in zebrafish larvae spinal cord injury models, as pro-inflammatory cytokines are essential for initiating inflammation, promoting axonal bridging over the gap but detrimental if they prologue during the later phases of regeneration (Tsarouchas *et al.*, 2018). Thus, there needs to be an M1/M2 switch for successful tissue and neuronal regeneration.

3.6.4.2 Spinal cord regeneration and the ECM

Another defect in mammalian CNS is the decreased ability to remodel its neuronal coding to form functional neuronal connections post injury and thus leading to a defective plasticity (Fawcett *et al.*, 2012; Burnside and Bradbury, 2014). Even though the ECM offers a protective infrastructure for the CNS neurons, it can also restrict the CNS plasticity after injury (Burnside and Bradbury, 2014). After a spinal cord injury, astrocytes cover the wound (glial scar formation) in order to block the excessive inflammatory response from reaching the wound. It is thus also acting as a physical barrier for axons to be able to grow across (Goldshmit *et al.*, 2012). On the contrary, the zebrafish ECM allows sufficient axonal growth, post injury, to recapitulate movement. Interestingly, Collagen XII has recently been identified to promote axonal regeneration after spinal cord injuries in zebrafish larvae. It does so by forming 'bridges' across the wound-gap to aid axonal migration through the non-neural lesioned environment and recapitulate the lost neuronal connectivity (Wehner *et al.*, 2017). Therefore, the ECM should also be considered when investigating spinal cord regeneration.

3.6.4.3 Spinal cord regeneration and neurons/stem cell renewal

One other component responsible for making bridges across a spinal cord injury for the axons to grow across are the glia. In zebrafish models, glia are activated by fibroblast growth factor (FGF) to form 'bridges' across the gap over which axons can migrate to close the wound (Goldshmit *et al.*, 2012). One further much investigated aspect of regenerative medicine is the ability to redeploy mechanisms which were active during development; such as cell proliferation and cell death (Cardozo *et al.*, 2017). The vertebrate neural patterning is based on the idea that the neural tube is composed of two orthogonal axes; the anterior-posterior (AP) axis and the dorsal-ventral (DV) axis. Signalling gradients act along these axes to activate transcription of neuronal progenitors to give rise to different neuronal populations (Gouti, Metzis and Briscoe, 2015). For instance Fgf, Wnt and RA (retinoic acid) gradients signal to induce the AP patterning of the neural ectoderm during zebrafish embryogenesis (Kudoh, Wilson and Dawid, 2002). In zebrafish, these gradients get redeployed after a spinal cord injury to serve as axonal guidance cues to guide axonal regeneration along the AP axis (Cardozo *et al.*, 2017; Rasmussen and Sagasti, 2017). Pattering of the neural tube at the DV axis is controlled by Hh (Hedgehog), Wnt and BMP (bone morphogenic protein) gradients (Le Dréau and Martí, 2012). Wnt pathway was suggested to have a role in controlling neurogenesis (Vergara, Arsenijevic and Del Rio-Tsonis, 2005). Sonic Hh (Shh) is involved in modulating the early developmental CNS polarity, while BMP can induce neuronal proliferation and differentiation (Vergara, Arsenijevic and Del Rio-Tsonis, 2005). These gradients are all enhanced in response to injury (Cardozo *et al.*, 2017).
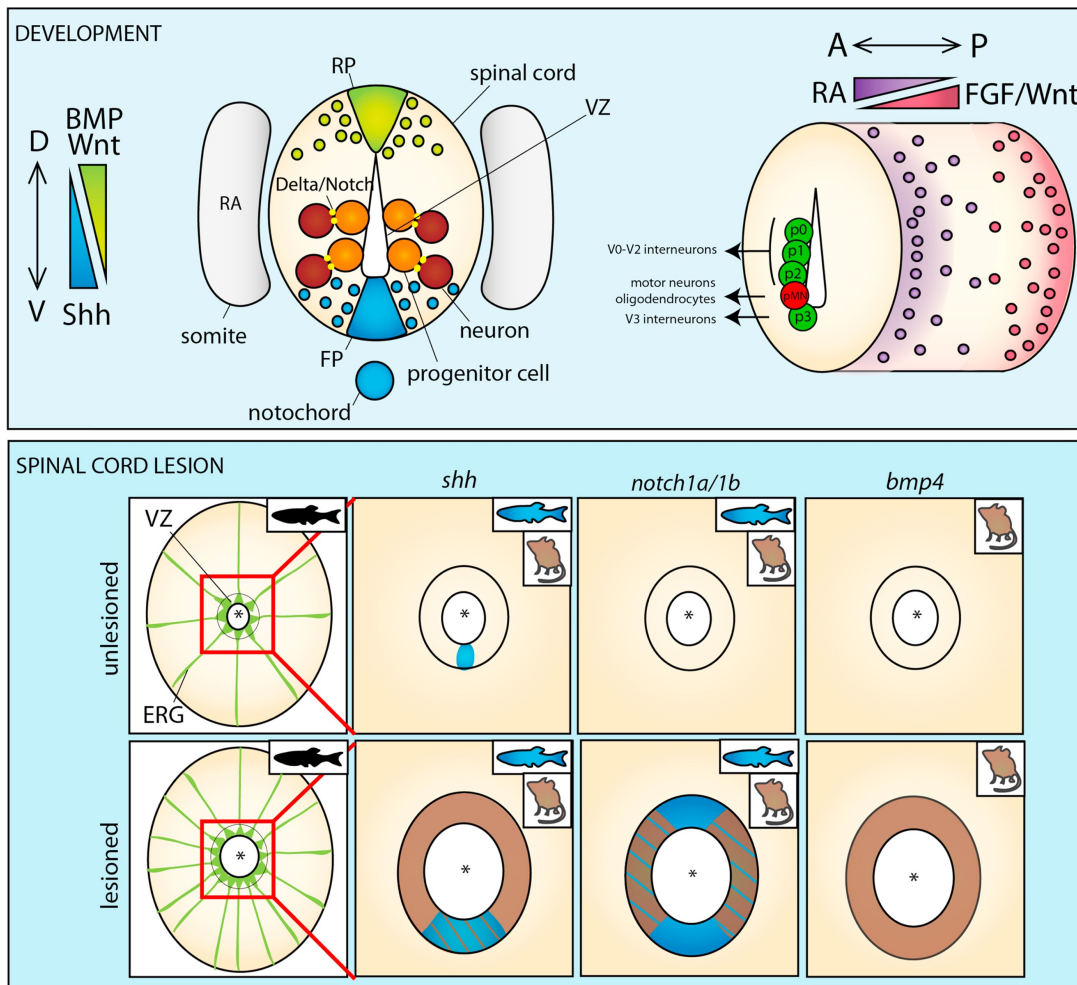
Figure 3. 16: Graphical illustration of the signalling pathways involved during normal spinal cord development and their re-activation during regeneration.
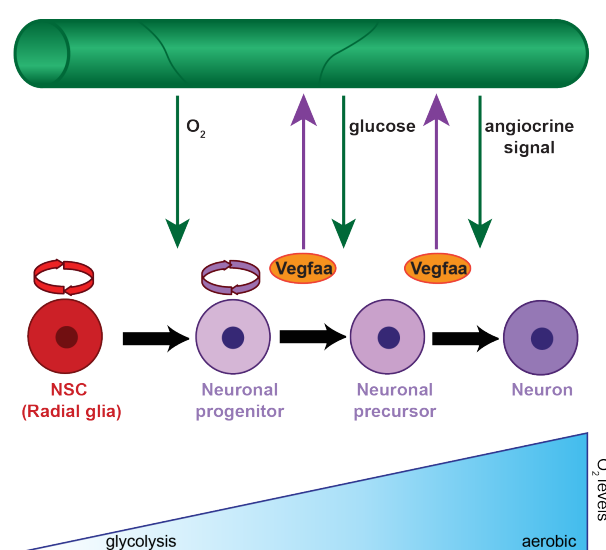
Development panel: Shh (blue) is present at the notochord and floor plate (FP) and diffuses through a ventral-dorsal gradient. BMP and Wnt (green) are found in the roof plate (RP) and diffuse through a dorsal-ventral gradient. At the VZ (ventricular zone) cells expressing Notch (orange) retain their proliferative status, while cells expressing Delta/Serrate differentiate into mature neurons (brown). On the right panel, distal ventral progenitor zones are indicated in green and progenitor MNs in red. Spinal cord patterning across the AP axis is mediated by the high anterior expression of RA (purple) opposed by the high posterior expression of FGF and Wnt (pink). Regeneration panel: In the unlesioned scenario, the VZ is surrounded by ependymo-radial glia (ERGs) with little to no activity. However, upon a spinal cord lesion, ERGs start proliferating, expanding the diameter of the central canal and upregulate genes such as *shh*, *notch1a/1b* and *bmp4.* Model organisms used to obtain these data are indicated on the top right; zebrafish (blue) and mouse (brown) (Cardozo *et al.*, 2017).

3.6.4.4 Spinal cord regeneration and angiogenesis

Despite the fact that blood vessels are important factors in the NSC niche, nourishing them and promoting neurogenesis, little is known on the molecular cross-talk between neuronal progenitor cells and blood vessels (Tata and Ruhrberg, 2018). The importance of angiogenesis after a spinal cord injury was investigated in rat models, showing that VEGF administration resulted in a higher number of blood vessel at the lesion area, less apoptosis and could also have possible effect glia cells and neuronal populations (Widenfalk *et al.*, 2003). Furthermore, local VEGF administration restored some of the spinal cord plasticity (Des Rieux *et al.*, 2014). Administrating angiogenic microspheres encapsulating VEGF, angiopoietin-1 and FGF at the site of injury also stimulated angiogenesis and enhance neurogenesis, thus speeding up the rat's recovery (Yu *et al.*, 2016). This is consistent with Oosthuyse et al data, where *Vegfa* was identified to have neuroprotective functions (Oosthuyse *et al.*, 2001). However, one should also note that VEGF-A enhancement led to increased axonal branching and growth, while VEGFR2 loss resulted in non-functional axonal branches. Thus VEGF-A/VEGFR2 need to tightly regulated for proper axonal development and regeneration (Luck *et al.*, 2019). Further investigation in this topic is thus vital to aid our understanding on neurogenesis and aid in deciphering novel treatments to treat neurodegenerative diseases and spinal cord injuries (Tata and Ruhrberg, 2018).

3.7 Aim of the study

VEGF has been implied in the regulation of vascular development and neuronal development. Vegf levels at the neurovascular interface have to be tightly regulated, and Flt1 plays a key-role herein. Neurons produce both Vegf and Flt1, and critically determine spinal cord vascularisation. In addition, neurons expressed VEGFR2 and Flt1, and VEGF, PlGF, VEGF-B, and mFlt1 signalling have been linked to neurotrophic effects in ischemic conditions, especially of MNs. Vegf and Flt1 thereby appear to play a dual role in neurons. On the one hand determining vascularisation, relevant for differentiation, and on other hand Flt1 signalling in neurons, exerting neurotrophic effects. Flt1/VEGFR2 heterodimers, or Nrp1 could directly act on the neurons themselves while exerting indirect effects via changes in vasculature of Vegf and Flt1. This study's focus is centred around the role of Flt1, and the Flt1 ligands, Vegf, Vegfb and Plgf, in spinal cord regeneration in the zebrafish larvae. To systematically address the role of Flt1 and Flt1 ligands, a genetic approach was used, substantiated by detailed *in vivo* imaging, immunohistochemistry, morpholinos, inhibitor treatments and parabiosis (fusing two embryos together) in zebrafish larvae. Previously generated mutants for the Flt1 specific ligands; Vegfb and Plgf, and additional tissue specific *vegfba* and *plgf* gain of function models were implemented. Furthermore, *flt1* mutants, neuronal tissue specific *flt1* loss of function and inducible *sflt1* tissue specific gain of function transgenics were also investigated. As *nrp1* has also been suggested to bind *plgf* of *vegfb*, *nrp1a*, *nrp1b* and *nrp1a/b* double mutants were also used. Zebrafish larva's spinal cord was lesioned at 3dpf and the regeneration capacity was investigated at 4dpf and 5dpf. The effects on neurogenesis and neuronal cell apoptosis were quantified using proliferative and apoptotic assays. Furthermore, the effect of macrophages and collagens were also considered in this study.

Figure 3. 17: Hypothetical representation of the neurovascular interface in regards to oxygen availability, neuronal proliferation and angiocrine signalling

4 Results

This study will focus on the role of *flt1* and its ligands during neuronal regeneration. The following questions will thus be addressed. Which *ftl1* is the important contributor in regeneration? To solve this, we carried out neuronal specific *flt1* loss-of-function mutants to decipher the neuronal *flt1* component and *mflt1* loss and *sflt1* gain-of function models to decipher which of the two isoforms is implicated in neuroregeneration. We then wanted to identify which pathway is involved in neuronal regeneration and how this regeneration is executed. Possible contributors to axonal regeneration are the glia, collagens and macrophages. All of these are responsible is setting the 'path' over which axons can grow across and 'bridge' the wound. These three components will also be addressed in this study. Furthermore, various *vegfaa* gain-of function lines were also employed to investigate the effect of *vegfaa* on glia formation and macrophage migration.

4.1 Loss of Flt1 impairs axonal regeneration

4.1.1 Flt1 loss of function (LOF) impairs neuronal but not tissue regeneration

Flt1 homozygous mutant mice show vascular plexus disarray and are lethal during early developmental stages (Fong *et al.*, 1995). As a first approach, *flt1*-ATG morpholino (MO) was injected in zebrafish embryos at one-cell-stage to induce a *flt1* knockdown. Three different regimes of injuries were then performed at 3dpf. They were then analysed at 1day post lesion (1dpl) and 2dpl. In muscle injury (Figure 4.1a-b') and fin clip injuries (Figure 4.1c-d', g-g') the morphants did not show muscular or tissue defects in regeneration. However, injuries to the spinal cord led to impaired neuronal regeneration (Figure 4.1e-f', h-h'). To further investigate the morpholino phenotype, *flt1* mutants were used to study the neuronal regeneration.
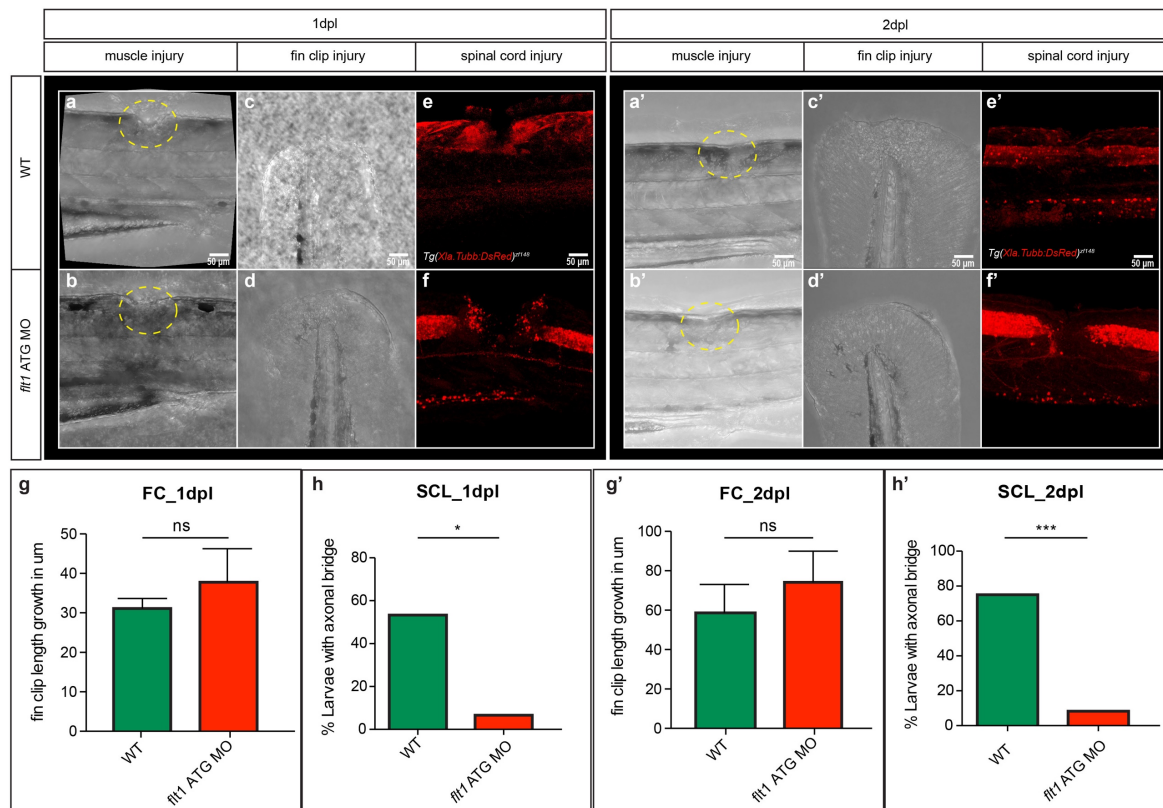
Figure 4. 1: *flt1* LOF fail to regenerate neurons after a spinal cord injury.

(a, a', b, b') Bright field images of the muscle injury in WT larvae at 1dpl (a) and 2dpl (a') and *flt1*-ATG MO injected larvae at 1dpl (b) and 2dpl (b') show no difference in regenerative capacity. **(c, c', d, d')** Bright field images of the fin clip injury in WT larvae at 1dpl (c) and 2dpl (c') and *flt1*-ATG MO injected larvae at 1dpl (d) and 2dpl (d') show comparable fin growth. **(e, e', f, f')** Transgenic larvae *Tg(Xla.Tubb:DsRed)^{zf148}* show that mature neurons (red) start showing axonal projections in WT at 1dpl (e) and completely regenerate by 2dpl (e'). Contrary *flt1*-ATG MO injected larvae fail to regenerate at both 1dpl (f) and 2dpl (f'). **(g)** Statistical analysis of the fin clip length growth (in μm) at 1dpl. Mann-Whitney test ± s.e.m, n(WT)=3, n(*flt1*-ATG MO)=4; n.s.=non-significant. **(g')** Statistical analysis of the fin clip length growth (in μm) at 2dpl. Mann-Whitney test ± s.e.m, n(WT)=6, n(*flt1*-ATG MO)=5;n.s.=non-significant. **(h)** Quantitative analysis shows the percentage of larvae with axonal bridge at 1dpl. Fisher's exact test n(WT)=15, n(*flt1*-ATG MO)=15; *P<0.05. **(h')** Quantitative analysis shows the percentage of larvae with axonal bridge at 2dpl. Fisher's exact test n(WT)=20, n(*flt1*-ATG MO)=12; ***P<0.001. WT=wild-type; MO=Morpholino; FC=Fin clip; SCL=Spinal cord lesion; dpl=days post lesion; n.s.= non-significant. Scale bar 50μm.

4.1.2 Generation of the Flt1 mutant lines

In order to study the effect of Flt1 during neuronal regeneration, we used the zebrafish model since neurovascular interactions can be observed using transgenic vascular and neuronal reporter lines. Furthermore, it has robust axonal regeneration capacities

which persist all the way to adulthood (Isogai, Horiguchi and Weinstein, 2001; Payne and Look, 2009; Wehner *et al.*, 2017). Using CRISPR/Cas, two *flt1* mutants were previously generated. The full mutant targets both the soluble and membrane Flt1 isoforms, the mFlt1 mutant targets only the membrane tethered form (Ran *et al.*, 2013; F. O. Kok *et al.*, 2015; Wild *et al.*, 2017). To generate the full *flt1* mutant, *flt1* exon 3 was targeted with small guide RNA which led to an early premature stop codon. The truncated protein lacks the Ig2 domain necessary for VEGF-binding. To obtain the *mflt1* single mutant exon 11b, necessary for *mflt1* transcription was targeted. This research will focus on *flt1* full mutants; *flt1*^{ka601}(-1nt) and *flt1*^{ka604}(-14nt) and *mflt1* single mutant; *flt1*^{ka605}(+28nt). Both *flt1*^{ka601} and *flt1*^{ka605} mutants showed no non-sense mediated decay (Wild *et al.*, 2017).

4.1.3 Time-lapse analysis of *flt1*^{ka604} regeneration

To verify the morpholino data, spinal cord lesions were done at 3dpf in WT and *flt1*^{ka604}. As axonal bridging after spinal cord injury in zebrafish larvae occurs between 12hpl-18hpl (Wehner *et al.*, 2017), the progression of wound healing in *flt1*^{ka604} was observed by time-lapse. Consistent with the morpholino data, *flt1*^{ka604} fail to regenerate their axonal connections post injury (Figure 4.2c). Not only are there no axonal connections but also the wound gap-size is increasing over time (Figure 4.2d).
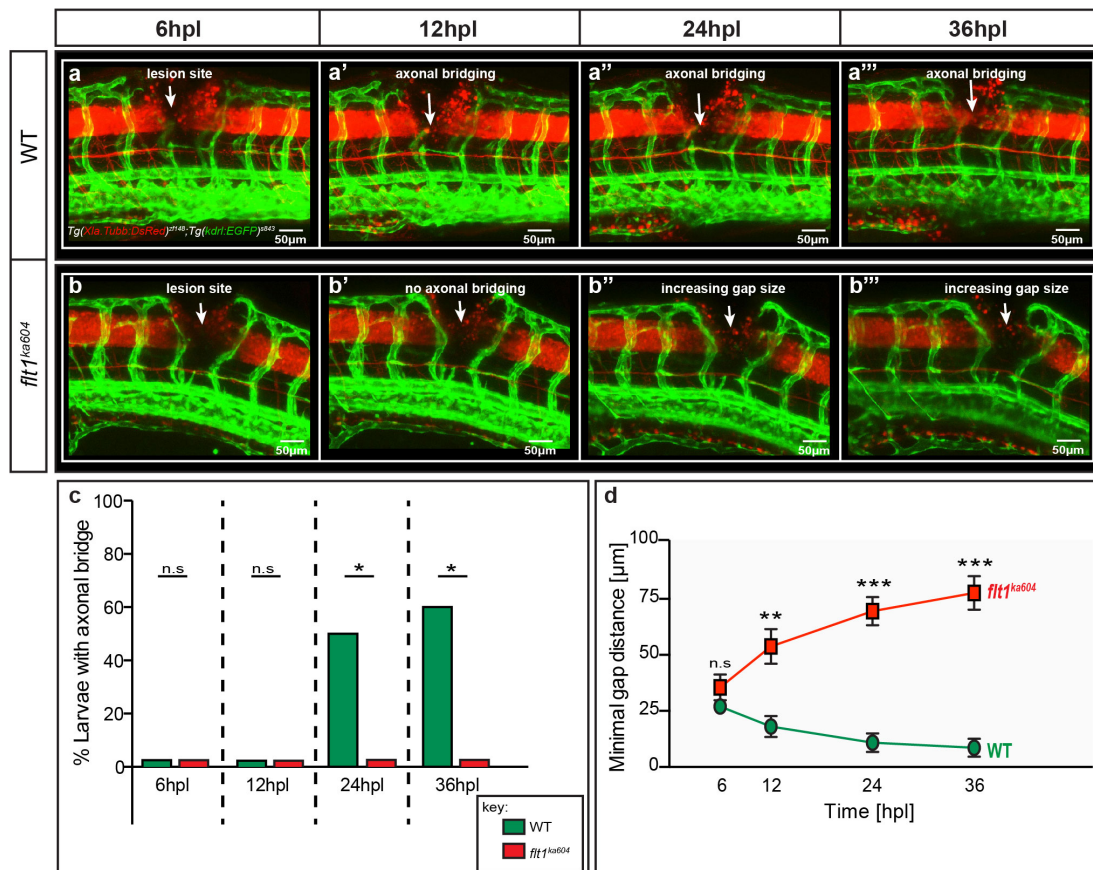
Figure 4. 2: *flt1^{ka604}* fail to regenerate neurons after a spinal cord injury.

(a-a''') Double transgenic larvae WT *Tg(Xla.Tubb:DsRed)^{zf148}; Tg(kdrl:EGFP)^{s843}* imaged from 6hpl until 36hpl show vessels (green) and neurons (red). At 12hpl (a') the first axons bridge across the wound. By 36hpl (a''') the axonal connections are almost back to uninjured scenario. **(b-b''')** Double transgenic larvae *flt1^{ka604} Tg(Xla.Tubb:DsRed)^{zf148}; Tg(kdrl:EGFP)^{s843}* imaged from 6hpl until 36hpl show vessels (green) and neurons (red). The white arrow indicates the lesion. Unlike in WT, axons do not bridge across the gap (b') and the gap size increases over time (b''-b''') **(c)** Quantitative analysis shows the percentage of larvae with axonal bridge at the different stages post injury. Fisher's exact test n(WT)=10, n(*flt1^{ka604}*)=10; *P<0.05. **(d)** Visual analysis of the minimal gap distance (in μm) within the lesion over the different stages. Mann-Whitney test ± s.e.m, n(WT)=10; n(*flt1^{ka604}*)=10; *P<0.05; ***P<0.001. WT=wild-type; hpl=hours post lesion, n.s.=non-significant; Scale bar 50μm.

4.1.4 Neuronal *flt1* determines the axonal bridging

Spinal cord vasculature is dependent on the neuronal sFlt1 and Vegfaa. To decipher if this is also the case in regenerating axons, a neuronal tissue specific *flt1* mutant (*flt1^{ΔNC}*) was generated (Ablain *et al.*, 2016; Wild *et al.*, 2017). The pan-neuronal promoter *xla.tubb* was used to specifically express *Cas9* in the neurons, driving Gal4-VP16 to induce the expression of UAS:Cas9-t2A-eGFP, thus, knockout cells are

visualised by GFP. The sgRNA formerly used to generate the *flt1^{ka601}* (*sgRNA^{flt1E3}*) was expressed under the ubiquitous promoter; U6 (Ablain *et al.*, 2016; Wild *et al.*, 2017). To increase the efficiency of the construct, *flt1^{ka604/+}* heterozygous mutants were injected at one-cell stage. Mosaic expression of *Cas9* and *sgRNA^{flt1E3}* led to the same axonal growth impairment as in *flt1^{ka604}*, suggesting that the neuronal Flt1 is essential for proper axonal bridging across a wound (Figure 4.3). This is phenotype, even though mosaic (roughly around 20% of the neurons were affected, see white arrows; Figure 4.3), had dramatic effects on neuronal regeneration. This suggests that deleting only some of the neuronal *flt1* is sufficient to impair axonal regeneration.
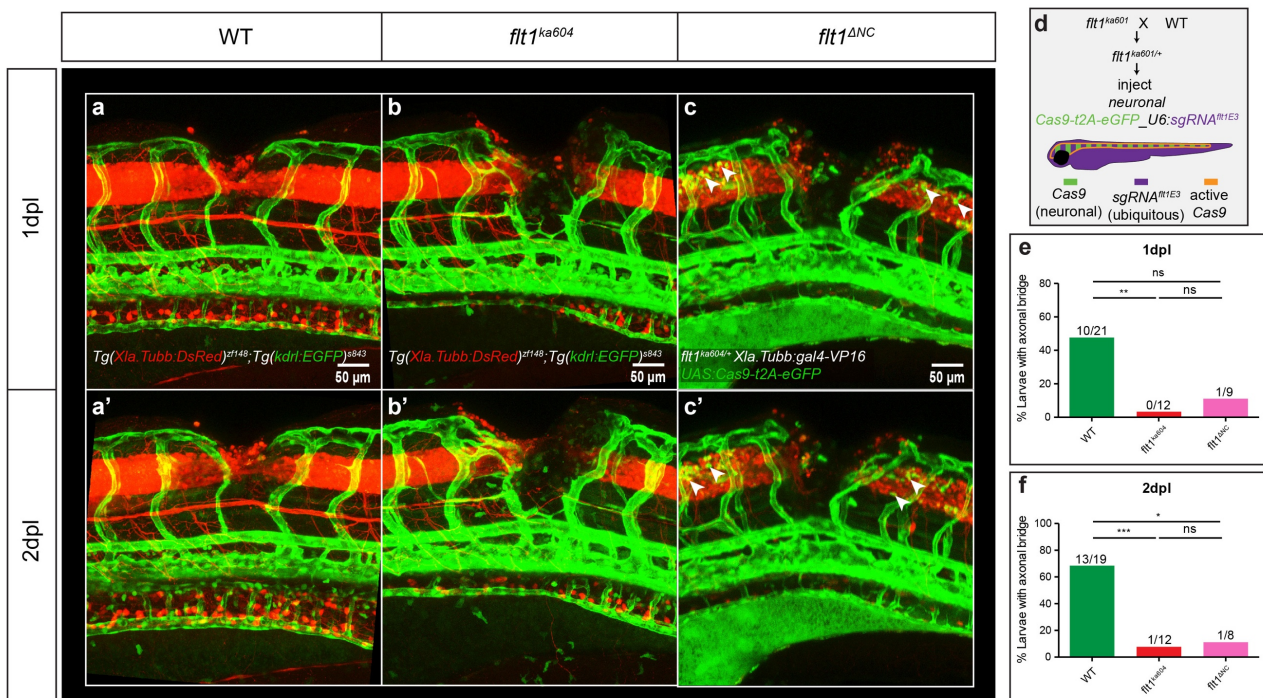

Figure 4. 3: Loss of neuronal *flt1* impairs axonal bridging.

(a-c') Double transgenic larvae WT (a-a'), *flt1^{ka604}* (b-b'), *flt1^{ΔNC}* (c-c') *Tg(Xla.Tubb:DsRed)^{zf148}; Tg(kdrl:EGFP)^{s843}* imaged at 1dpl and 2dpl show vessels (green) and neurons (red). Neuronal specific *flt1* mutants (*flt1^{ΔNC}*) indicate similar ectopic sprouting and failure in axonal regeneration as observed in *flt1^{ka604}*. Knockout neuronal cells (green) are indicated by white arrowheads. **(d)** Illustration of the neuronal tissue specific *flt1* mutant. Cas9 was expressed under the *Xla.Tubb* neuronal promoter, while the sgRNA was ubiquitously expressed, thus Cas9 activity was only in the neurons (shown in orange). To increase the efficiency, heterozygous *flt1^{ka604/+}* were used. **(e-f)** Quantitative analysis shows the percentage of larvae with axonal bridge at 1dpl (e) and 2dpl (f). Fisher's exact test; Fractions show how many larvae regenerated per sample group. n.s.=non-significant; *P<0.05; **P<0.01; ***P<0.001. WT=wild-type; dpl=days post lesion, n.s.=non-significant; Scale bar 50μm.

4.1.5 *flt1^{ka605}* (*mflt1*) show no axonal regeneration defects

To investigate whether axonal regeneration is driven by the membrane bound or the soluble Flt1, the regeneration capacity of *mflt1* mutant (*flt1^{ka605}*) was compared with *flt1^{ka604}*. Interestingly, the *flt1^{ka605}* (*mflt1*) mutants regenerate their axons much more efficiently that *flt1^{ka604}* and are comparable to the WT fish (Figure 4.4c-e). This could indicate that membrane tethering and the tyrosine kinase domain are not responsible for axonal regeneration and that regeneration is rather guided by sFlt1.
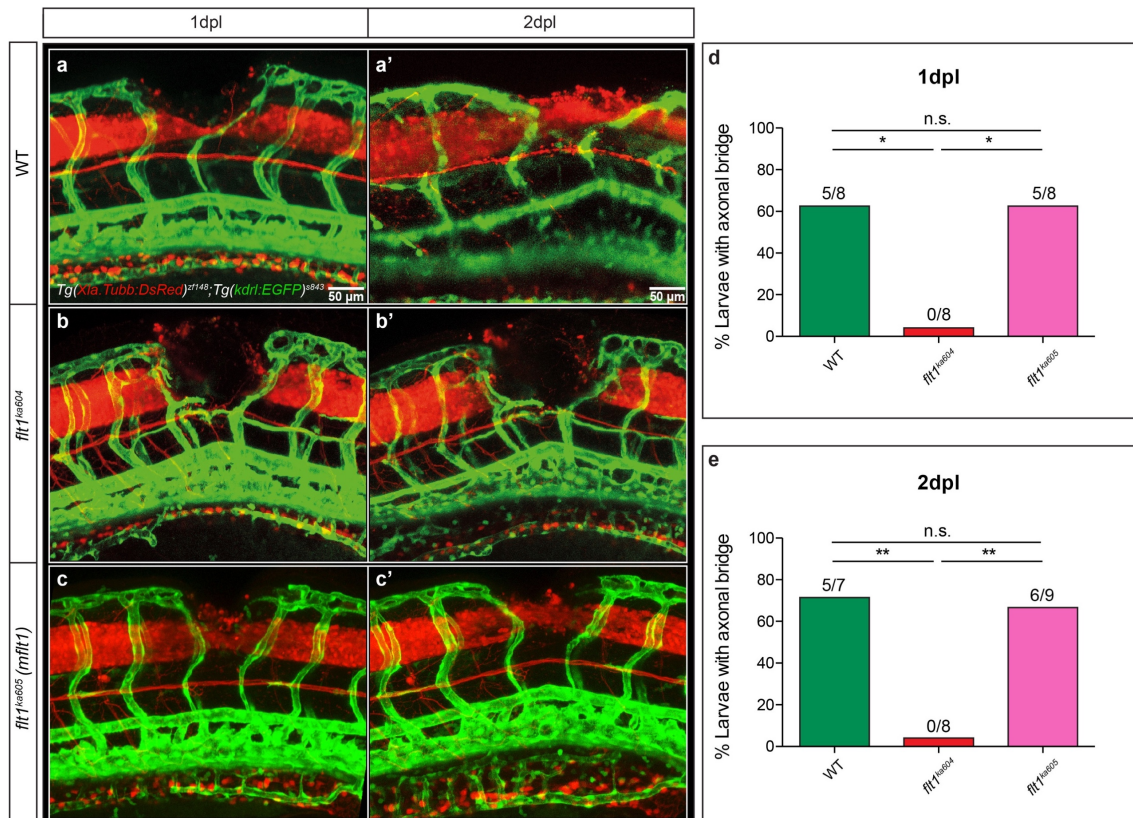

Figure 4. 4: *flt1^{ka605}* (*mflt1*) regenerates neurons after a spinal cord injury.

(a-c') Double transgenic larvae (a-a') WT, (b-b') *flt1^{ka604}* and (c-c') *flt1^{ka605}* (*mflt1*) *Tg(Xla.Tubb:DsRed)^{zf148}; Tg(kdrl:EGFP)^{s843}* imaged at 1dpl and 2dpl show vessels (green) and neurons (red). Note that *flt1*^{ka605} (*mflt1*) have axonal bridges similar to WT. **(d-e)** Quantitative analysis shows the percentage of larvae with axonal bridge at 1dpl (d) and 2dpl (e). Fisher's exact test; Fractions show how many larvae regenerated per sample group. n.s.=non-significant; *P<0.05; **P<0.01. WT=wild-type; dpl=days post lesion, n.s.=non-significant; Scale bar 50µm.

4.1.6 Neuronal soluble Flt1 controls spinal cord axonal regeneration

To examine if the neuronal *sflt1* is sufficient to induce axonal bridging, *sflt1* was overexpressed in the neurons of *flt1^{ka604}* fish using the neuronal specific *elavl* promoter. This was achieved using an inducible construct, where Gal4 was fused to the ligand binding domain of the oestrogen receptor (ERt2) and expressed under the neuronal promoter, *elavl*. The construct was then activated upon endoxifen administration at 52hpf (Figure 4.5d). Indeed, overexpression of even a few neuronal *sflt1* expressing spinal cord neurons during spinal cord regeneration were sufficient to rescued the axonal bridging and led to successful axonal regeneration (Figure 4.5). This experiment demonstrates that even trace amounts of neuronal sFlt1 are sufficient for inducing axonal regeneration.
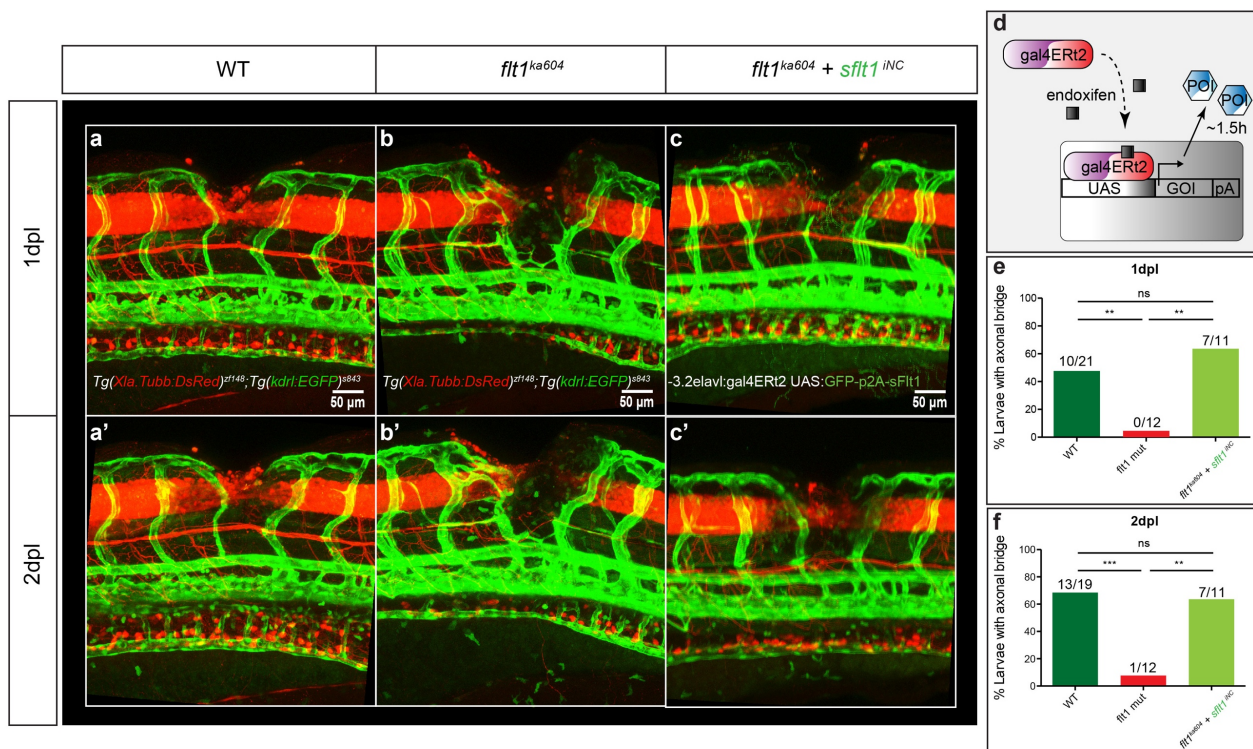

Figure 4. 5: Neuronal sFlt1 GOF rescues *flt1^{ka604}* axonal bridging.

(a-c') Double transgenic larvae WT (a-a'), *flt1^{ka604}* (b-b'), *flt1^{ka604}+sflt1^{iNC}* (c-c') *Tg(Xla.Tubb:DsRed)^{zf148}; Tg(kdrl:EGFP)^{s843}* imaged at 1dpl and 2dpl show vessels (green) and neurons (red). Endoxifen inducible neuronal specific *sflt1* GOF (*flt1^{ka604}+sflt1^{iNC}*) rescues the ectopic sprouting and recapitulates in axonal regeneration similar to WT levels. **(d)** Illustration of the endoxifen inducible *sflt1* GOF approach. Gal4, fused to the ligand binding domain of the oestrogen receptor (ERt2), is expressed under the neuronal promoter; *elavl*. **(e-f)** Quantitative analysis shows the percentage of larvae with axonal bridge at 1dpl (e) and 2dpl (f). Fisher's exact test; Fractions show how many larvae regenerated per sample group. n.s.=non-significant; **P<0.01; ***P<0.001. WT=wild-type; dpl=days post lesion, n.s.=non-significant; Scale bar 50µm.

The first set of data suggest an important function of Flt1 in neuronal regeneration processes. Experiments show that this activity is driven via the neuronal Flt1 and that the key player in axonal regeneration is the sFlt1. This is contradictory to previous publications where regeneration was linked to the mFlt1 signalling (Poesen *et al.*, 2008; Dhondt *et al.*, 2011). Here we show that axonal regeneration is independent of the mFlt1 signalling. To further investigate how regeneration is executed, we decided to look into different neuronal populations and how their proliferation and apoptotic rates are influenced in *flt1* mutants.

4.1.7 Loss of Flt1 also impairs other neuronal populations

Wound healing at the site of injury does not only mean that axons in the spinal cord need to regenerate, but also more ventrally locates sensory and motor neurons (MNs) need to repopulate the tissue depleted from its connection to the CNS.

First, we tested how motor neurons regenerate using the *Tg(mnx1:mCherry)* line, kindly donated to us by Dr Panakova. *flt1^{ka604}* showed an impaired MN regeneration as only 11% (2/17) compared to around 47% (7/15) of WT were able to form axonal bridges across the wound at 1dpl. This was not increased at 2dpl, as not more than 11% (2/17) showed axonal bridging, in comparison to WT who increased their regenerative capacity to 56% (9/16; Figure 4.6a-c). In order to find out how MNs are impaired, the proliferation and apoptotic rate of MNs was further analysed. For proliferation, EdU incorporation was counted in neurons at 1dpl. Apoptosis was determined with the TUNEL reaction kit. Surprisingly, the proliferation rate was significantly decreased in *flt1^{ka604}* (Figure 4.6d-f) whereas the apoptotic rate remained unchanged (Figure 4.6g-i).
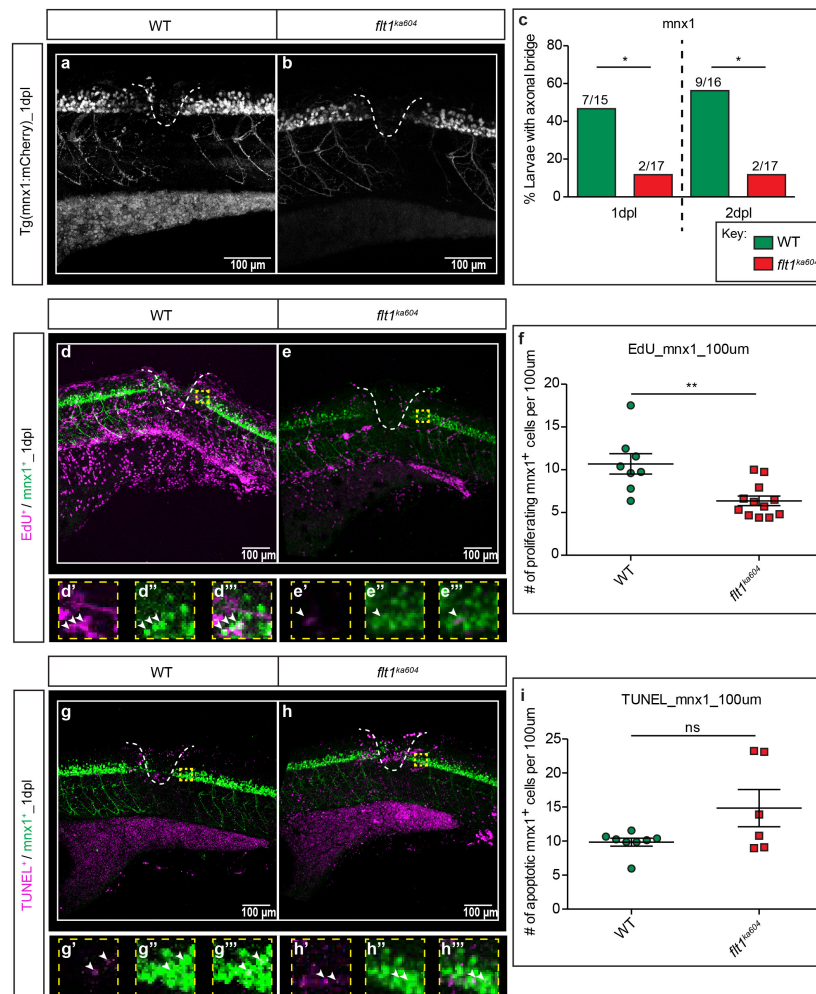
Figure 4. 6: Flt1 is important for motor neuron proliferation during spinal cord regeneration.

(a-b) Single transgenic larvae WT(a) and *flt1^ka604* (b) *Tg(mnx1:mCherry)* imaged at 1dpl.**(c)** Quantitative analysis shows the percentage of larvae with axonal bridge at 1dpl and 2dpl. Fisher's exact test; Fractions show how many larvae regenerated per sample group; *P<0.05. **(d-e''')** The lesion area is outlined with double-labelled mnx1+/EdU+ neurons. White dotted line indicates the lesion area. A lesion leads to a significant decrease in the number of mnx1+/EdU+ double labelled MNs in *flt1^ka604* compared to WT (compare d and e). d' to e''' show a higher magnification of the areas boxed in d and e (yellow dotted box), respectively, in single optical sections indicating double labelling. **(f)** Quantitative analysis of the number of EdU-labelled MNs per 100µm rostral and caudal to the spinal cord lesion at 1dpl. Unpaired t-test ± s.e.m, n(WT)=8; n(*flt1^ka604*)=12; **P<0.01. **(g-h''')** The lesion area is outlined with double-labelled mnx1+/TUNEL+ neurons. White dotted line indicates the lesion area. A lesion leads to a non-significant change in the number of mnx1+/TUNEL+ double labelled MNs in WT and *flt1^ka604* (compare g and h). g' to h''' show a higher magnification of the areas boxed in g and h (yellow dotted box), respectively, in single optical sections indicating double labelling. **(f)** Quantitative analysis of the number of TUNEL-labelled MNs per 100µm rostral and caudal to the spinal cord lesion at 1dpl. Mann-Whitney test ± s.e.m, n(WT)=8; n(*flt1^ka604*)=6; n.s.=non-significant. dpl=days post lesion; MNs=motor neurons; #=number; n.s.=non-significant; Scale bar 100µm.

71

Checking for sensory neuron reporter line; *Tg(-3.1neurog1:GFP)^{sb2}*, we found that the sensory neuronal regeneration is delayed in comparison to MN regeneration. In WT only 20% (3/15; Figure 4.7c) recapitulated sensory neuronal connections compared to 47% of the MNs (7/15; Figure 4.6c) at 1dpl. At 2dpl, WT recapitulated the lost sensory connections to 50% (8/16; Figure 4.7c), while *flt1^{ka604}* remained as low as approximately 12% (2/17; Figure 4.7a-c). Thus, also sensory neuronal regeneration depends on the presence of Flt1. Surprisingly the proliferation remained unaffected in these neurons (Figure 4.7d-f), instead apoptotic rate increased (Figure 4.7g-i). Thus, for sensory neurons, Flt1 should be considered as neuroprotective molecule, while for MNs, Flt1 acts as a growth factor.
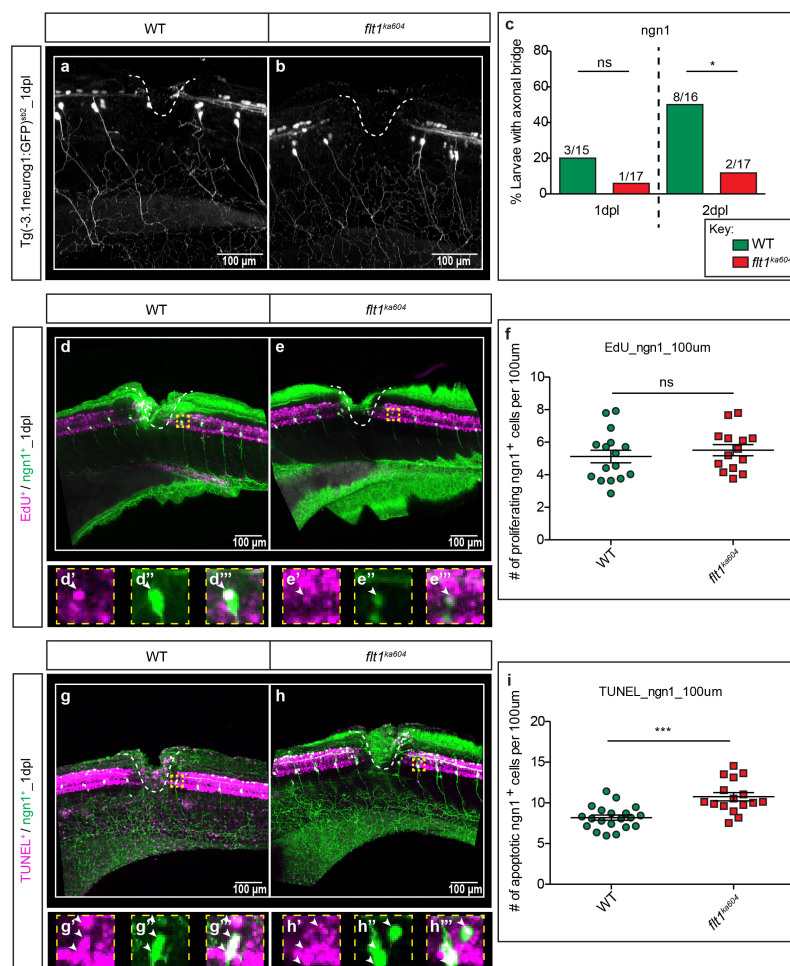

Figure 4. 7: Flt1 is neuroprotective against sensory neuron apoptosis.

(a-b) Single transgenic larvae WT(a) and *flt1^{ka604}* (b) *Tg(-3.1neurog1:GFP)^{sb2}* imaged at 1dpl.**(c)** Quantitative analysis shows the percentage of larvae with axonal bridge at 1dpl and 2dpl. Fisher's exact test; Fractions show how many larvae regenerated per sample group; n.s.=non-significant; *P<0.05. **(d-e''')** The lesion area is outlined with double-labelled ngn1+/EdU+ neurons. White dotted line indicates the lesion area. A lesion leads to a non-significant change in the number of ngn1+/EdU+ double labelled

sensory neurons in WT and *flt1^ka604^* (compare d and e). d' to e''' show a higher magnification of the areas boxed in d and e (yellow dotted box), respectively, in single optical sections indicating double labelling. **(f)** Quantitative analysis of the number of EdU-labelled sensory neurons detected per 100μm rostral and caudal to the spinal cord lesion at 1dpl. Unpaired t-test ± s.e.m, n(WT)=16; n(*flt1^ka604^*)=14; n.s.=non-significant. **(g-h''')** The lesion area is outlined with double-labelled ngn1+/TUNEL+ neurons. White dotted line indicates the lesion area. A lesion leads to a significant increase in the number of ngn1+/TUNEL+ double labelled sensory neurons in *flt1^ka604^* (compare g and h). g' to h''' show a higher magnification of the areas boxed in g and h (yellow dotted box), respectively, in single optical sections indicating double labelling. **(f)** Quantitative analysis of the number of TUNEL-labelled sensory neurons per 100μm rostral and caudal to the spinal cord lesion at 1dpl. Unpaired t-test ± s.e.m, n(WT)=20; n(*flt1^ka604^*)=16; ***P<0.001; n.s.=non-significant. dpl=days post lesion; #=number; n.s.=non-significant; Scale bar 100μm.

Both, sensory and MNs generate from common neuronal precursor cells. To check whether Flt1 effects only differentiated neurons or if also neuronal precursor cells use Flt1 as a neuroprotector or growth factor, we made use of the *Tg(huC:egfp)* transgenic zebrafish line. The zebrafish *elav/HuC* is present in neuronal precursor cells immediately after gastrulation. It is thus the earliest neuronal zebrafish marker (Kim *et al.*, 1996). Interestingly, using the *Tg(huC:egfp)* transgenic zebrafish line showed neuronal immunolabeling with Flt1, including MN, interneuron and sensory nerve domains. Further knockdown of *flt1* using *flt1*-ATG MO in the *Tg(huC:egfp)* showed some neuronal loss (Krueger *et al.*, 2011).

First, we checked whether *elavl* expression is regulated by *flt1*. Results showed a decrease in the *elavl* expression fold change in *flt1^ka604^* compared to WT (Figure 4.8c), suggesting that *elavl* is downregulated in *flt1^ka604^* at 1dpl. Further analysis on the *flt1^ka604^* HuC/D+ neurons showed a decrease in their proliferative rate (Figure 4.8a-b''',d) but not in the rate of apoptosis (Figure 4.8e-g''') compared to WT larvae at 1dpl. Thus, for neuronal precursor cells Flt1 acts as a growth factor but not as a neuroprotective molecule.
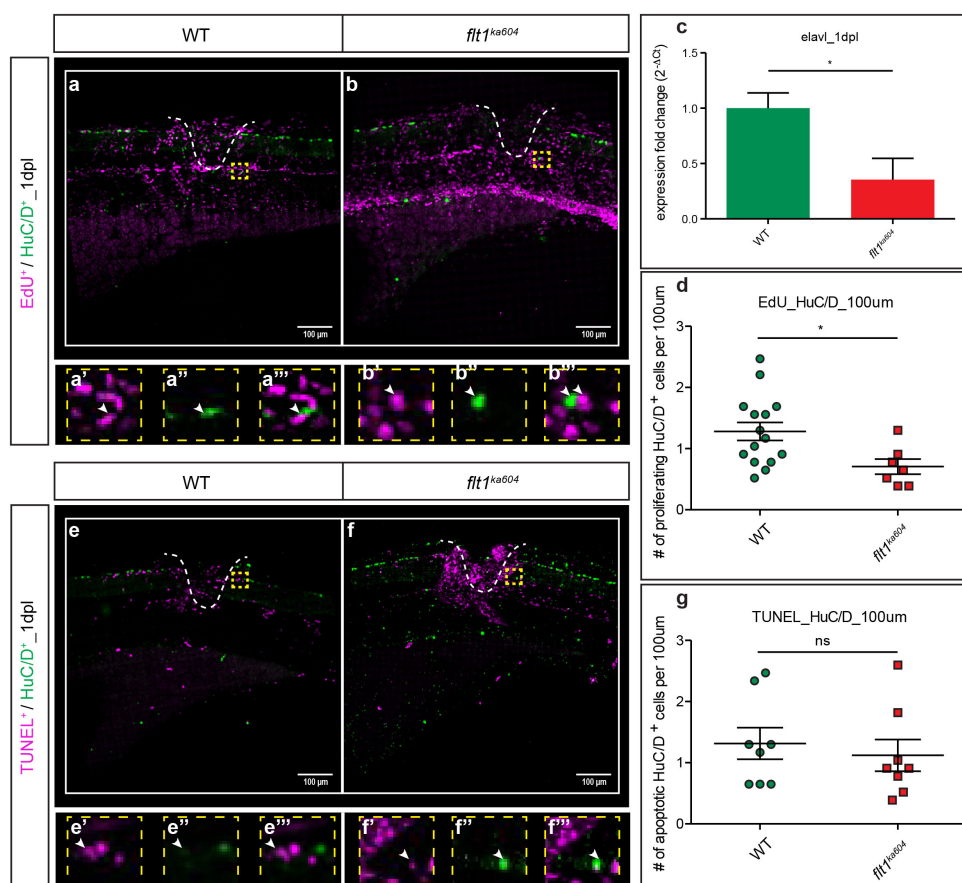
Figure 4. 8: Flt1 is important in early neuronal proliferation.

(a-b''') The lesion area is outlined with double-labelled HuC/D+/EdU+ neurons. White dotted line indicates the lesion area. A lesion leads to a decrease in the number of HuC/D+/EdU+ double labelled neurons in *flt1^ka604* compared to WT (compare a and b). a' to b''' show a higher magnification of the areas boxed in a and b (yellow dotted box), respectively, in single optical sections indicating double labelling. **(c)** qPCR analysis 1dpl show a decreased in *elavl* expression fold change in *flt1^ka604*. Unpaired t-test ± s.e.m; n(WT)=8; n(*flt1^ka604*)=5; *P<0.05 **(d)** Quantitative analysis of the number of EdU-labelled HuC/D+ neuros per 100μm rostral and caudal to the spinal cord lesion at 1dpl. Mann-Whitney test ± s.e.m, n(WT)=15; n(*flt1^ka604*)=7; *P<0.05. **(e-f'')** The lesion area is outlined with double-labelled HuC/D+/TUNEL+ neurons. White dotted line indicates the lesion area. A lesion leads to non-significant change in the number of HuC/D+/TUNEL+ double labelled neurons in WT and *flt1^ka604* (compare e and f). e' to f''' show a higher magnification of the areas boxed in e and f (yellow dotted box), respectively, in single optical sections indicating double labelling. **(f)** Quantitative analysis of the number of TUNEL-labelled HuC/D+ neurons per 100μm rostral and caudal to the spinal cord lesion at 1dpl. Mann-Whitney test ± s.e.m, n(WT)=8; n(*flt1^ka604*)=8; n.s.=non-significant. dpl=days post lesion; #=number; n.s.=non-significant; Scale bar 100μm.

Overall, proliferation and apoptotic assays identify Flt1 as an important MN and neuronal precursor growth factor, while acting as a neuroprotective factor in sensory neurons. As the sFlt1 and not the membrane bound isoform (mFlt1) was previously shown to influence axonal regeneration, we hypothesize that the molecular pathway guiding these processes is the Vegfa/Kdrl pathway. Vegfa is a neuroprotective factor (Oosthuyse *et al.*, 2001) which induces axonal pathfinding either through its VEGFR2/Kdrl receptor (Ruiz de Almodovar *et al.*, 2011) or via Nrp1 (Erskine *et al.*, 2011).

4.2 Vegfa/Kdrl is the key pathway in modulating neuroregeneration

4.2.1 Decreasing *vegfa* levels in the *flt1^ka604^* rescues axonal bridging

Flt1 is not only involved in neuronal proliferation but also acts as a decoy receptor in the vasculature. Indeed, when *flt1* gets downregulated, more *vegfaa* is available to bind to *kdrl* and induce angiogenesis. This is clearly observed in our *flt1* mutants, as hyperbranching occurred around the neural tube in *flt1* but not in *mflt1* single mutants, suggesting that the neuronal sFlt1 and Vegfaa are responsible for the spinal cord vascularization (Wild *et al.*, 2017). Therefore, the *flt1* mutants serve as a *vegfaa*-GOF scenario. If *vegfa* levels are over-enhanced in the *flt1^ka604^*, we would expect both a vascular and neuronal rescue when we lower the *vegfa* availability. To do so, two methods were employed; decreasing *vegfa* levels using a *vegfaa* morpholino and pharmacological inhibition of the kdrl receptor with the VEGFR2 Kinase inhibitor; ki8751 (Sigma-Aldrich).

As the *vegfa^-/-^* is homozygous lethal, we decided to knockdown *vegfaa* by morpholino injection. *Vegfaa* morpholino was injected at one-cell stage embryos and spinal cord lesions were performed at 3dpf. As expected, the hypersprouting of the *vegfaa* MO injected *flt1^ka604^* were rescued back to almost WT (See Appendix; Supplementary Figure 1). This would thus verify that the *vegfa* level is decreased after MO injection. Interestingly, the regeneration rate in *flt1^ka604^* larvae jumped from 0% (0/7; Figure 4.9e-e') to 75% (3/4; Figure 4.9e-e') at both 1dpl (Figure 4.9e) and 2dpl (Figure 4.9e'). This

could suggest that the failure of *flt1* mutants to regenerate might be caused by the ever-accumulated *vegfa* levels.
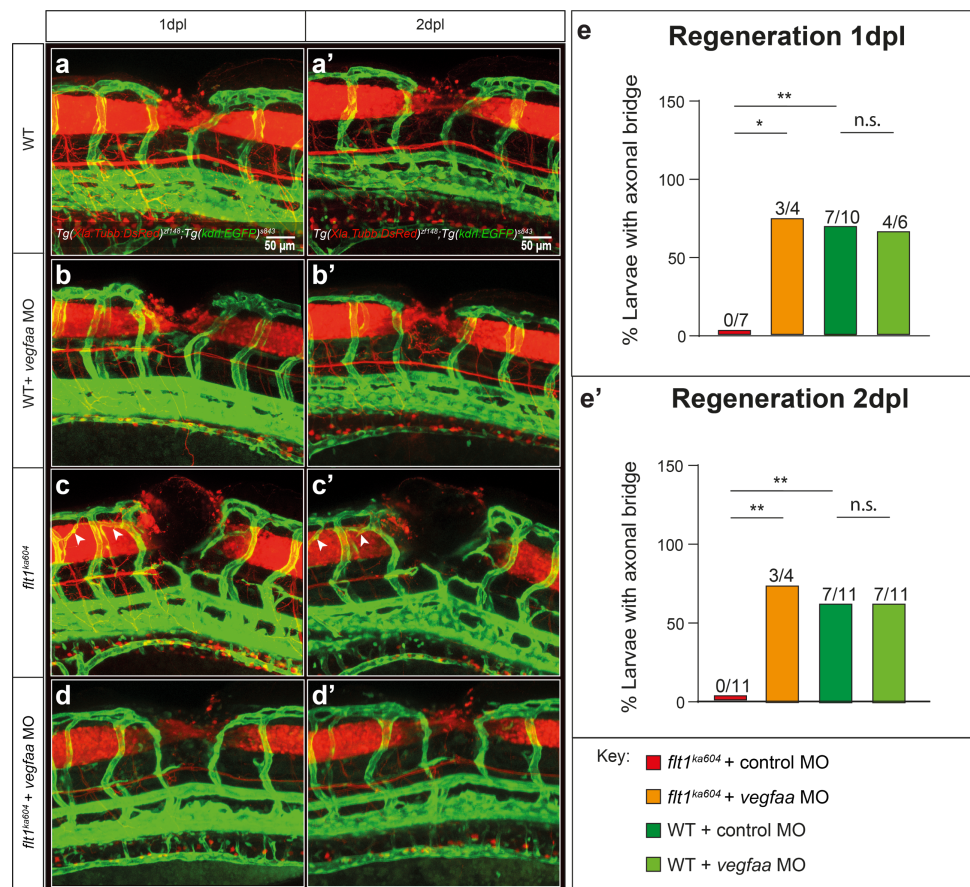

Figure 4. 9: *vegfaa* downregulation in *flt1^{ka604}* rescues the axonal connections.

(a-a') WT *Tg(Xla.Tubb:DsRed)^{zf148}; Tg(kdrl:EGFP)^{s843}* larvae injected with a control morpholino display axonal bridging at both 1dpl (a) and 2dpl (a'). Neurons are shown in red and vessels in green. **(b-b')** WT *Tg(Xla.Tubb:DsRed)^{zf148}; Tg(kdrl:EGFP)^{s843}* larvae injected with *vegfaa* MO are still able to form axonal bridges both at 1dpl (b) and 2dpl (b'). **(c-c')** *flt1^{ka604} Tg(Xla.Tubb:DsRed)^{zf148}; Tg(kdrl:EGFP)^{s843}* mutants injected with the control morpholino show impaired axonal bridging at both 1dpl (c) and 2dpl (c'). Neurons are shown in red and vessels in green. White arrowheads indicate the hypersprouts. **(d-d')** *flt1^{ka604} Tg(Xla.Tubb:DsRed)^{zf148}; Tg(kdrl:EGFP)^{s843}* mutants injected with *vegfaa* MO impair the ectopic sprout formation and enhances their regenerative capacity at both 1dpl (d) and 2dpl (d'). **(e)** Quantitative analysis shows the percentage of larvae with axonal bridges at 1dpl. Fisher's exact test; Fractions show how many larvae regenerated per sample group; n.s.=non-significant; *P<0.05; **P<0.01. **(e')** Quantitative analysis shows the percentage of larvae with axonal bridges at 2dpl. Fisher's exact test; Fractions show how many larvae regenerated per sample group; n.s.=non-significant; **P<0.01. WT=wild-type; MO=morpholino; ISVs=Intersegmental vessels; dpl=days post lesion; n.s.=non-significant; Scale bar 50μm.

To restrict downregulation of Vegfa/Kdrl signalling to the time of regeneration, the VEGFR2 Kinase inhibitor; ki8751 was added at the time of injury (3dpf). Pioneer experiments revealed that adding the inhibitor 12 hours before injury (60hpf) was embryonic lethal. Similarly, to the *vegfaa* MO injected *flt1^ka604^*, VEGFR2 inhibitor treatment also rescued the hypersprouting phenotype (Figure 4.10d-d') observed in the *flt1^ka604^* (Figure 4.10c-c'). Axonal bridging was not significantly impaired in WT larvae after VEGFR2 inhibition at both 1dpl (Figure 4.10e) and 2dpl (Figure 4.10e'), which was compatible to the *vegfa* MO data (Figure 4.9e-e'). Regeneration in *flt1^ka604^* was partially restored upon VEGFR2 inhibition (Figure 4.10e-e'), which was also in line with the *vegfaa* MO data (Figure 4.9e-e').
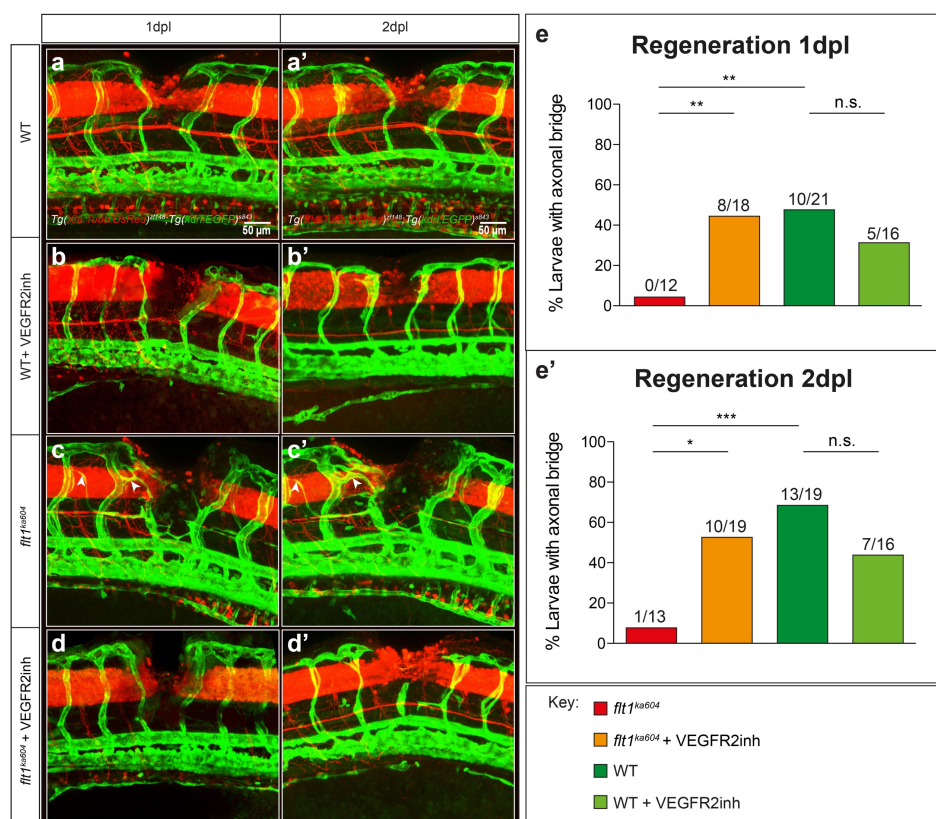

Figure 4. 10: VEGFR2 inhibitor rescues axonal bridging in *flt1^ka604^*.

(a-a') Untreated WT *Tg(Xla.Tubb:DsRed)^zf148^; Tg(kdrl:EGFP)^s843^* larvae display axonal bridging at 1dpl (a) and 2dpl (a'). Neurons are shown in red and vessels in green. **(b-b')** WT larvae treated with the VEGFR2 inhibitor at the point of injury **(c-c')** Untreated *flt1^ka604^ Tg(Xla.Tubb:DsRed)^zf148^; Tg(kdrl:EGFP)^s843^* mutants show impaired axonal bridging at 1dpl (c) and 2dpl (c'). Neurons are shown in red and vessels in green. White arrowheads indicate the hypersprouts. **(c-c')** *flt1^ka604^* mutants larvae treated with the VEGFR2 inhibitor at the point of injury, show some axonal connections at 1dpl (d) and 2dpl (d'). **(e)** Quantitative analysis shows the percentage of larvae with axonal bridges at 1dpl. Fisher's exact test; Fractions show how many larvae regenerated per sample group; n.s.=non-significant;

P<0.01. **(e') Quantitative analysis shows the percentage of larvae with axonal bridges at 2dpl. Fisher's exact test; Fractions show how many larvae regenerated per sample group; n.s.=non-significant; *P<0.05; ***P<0.001.WT=wild-type; hpf=hours post fertilization; dpl=days post lesion; VEGFR2inh=VEGFR2 inhibitor; n.s.=non-significant; Scale bar 50µm.

4.2.2 Neuropilin1 – an alternative receptor

VEGF-A, VEGF-B and PlGF not only bind to VEGFR-1 (Flt1) but also to the Neuropilin 1 (Nrp1) receptor (Lange *et al.*, 2016). NRP1 is expressed both in neurons and blood vessels (Erskine *et al.*, 2017). In neurons, NRP1 acts as a receptor for both VEGF-A and Semaphorin 3; Sema3. When VEGF-A binds to NRP1 it can induce migration, axonal pathfinding and neuronal survival (Cariboni *et al.*, 2011; Erskine *et al.*, 2011, 2017). Retinal ganglion cells were found to express NRP1 in order to sense VEGF-A signals, which are vital for contralateral axonal growth in the optic chiasm (Erskine *et al.*, 2011). Thus loss of NRP1 or of its VEGF-A binding site resulted in an increased number of retinal ganglion cells projecting their axons ipsilaterally but at the expense of contralateral projections (Erskine *et al.*, 2017). To study this model using our spinal cord lesion, we investigated axonal regeneration and collateral formation in the zebrafish larvae. Zebrafish have two paralogues; *nrp1a* and *nrp1b. nrp1a* is mainly expressed in the MNs, while *nrp1b* is expressed in the DA (Bovenkamp *et al.*, 2004). To exclude any compensation, both *nrp1a, nrp1b* and *nrp1a/b* double mutants were used.

Despite the neuronal component of Nrp1, a spinal cord lesion led to no axonal defects in *nrp1* single nor in double mutants both at 1dpl and 2dpl (Figure 4.11a-f'). This could be attributed as Vegfa exerts most of its neuroprotective properties via its VEGFR2/Kdrl receptor (Dhondt *et al.*, 2011). Furthermore, axonal branching was also found to be independent of Nrp1 (Luck *et al.*, 2019). We then decided to look at the collaterals and see if the regeneration was enough to recapitulate movement. No significant change in collateral numbers was observed between the *nrp1* mutants and WT control at 1dpl (Figure 4.11e). However, this changed at 2dpl, where *nrp1a* but not *nrp1b* or the double mutant, showed a significant decrease in the number of collateral formations (Figure 4.11e'). This is not surprising as *nrp1a* is mainly expressed in MNs, unlike the more 'vascular' *nrp1b* paralogue, and was possibly compensated in the

double mutant. This could suggest that *nrp1a* forms axonal bridging at the expense of collaterals, offering initial but not fully functional recovery.
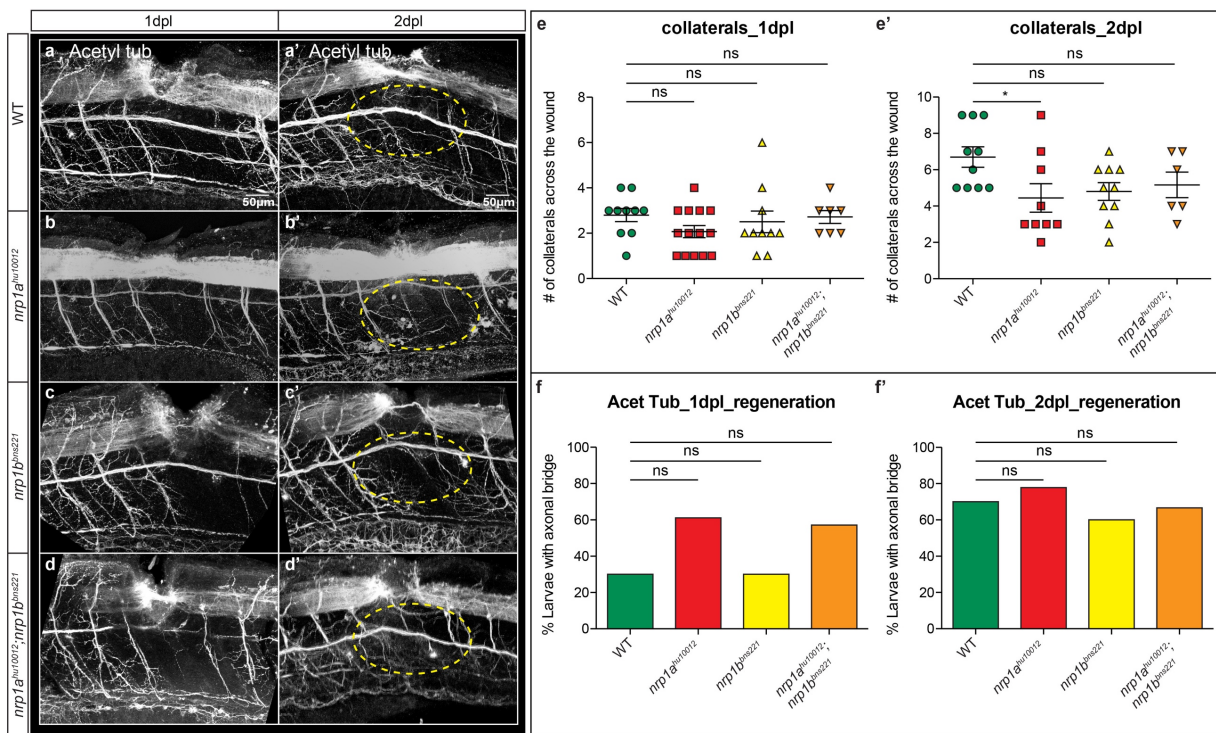

Figure 4. 11: *nrp1a* is important for collateral but not axonal regeneration.

(a-d') Acetylated tubulin single stained (a-a') WT, (b-b') *nrp1a^hu10012^*, (c-c') *nrp1b^bns221^* (d-d') *nrp1a^hu10012^*; *nrp1b^bns221^* larvae at 1 and 2dpl. Collaterals are indicated by a yellow dotted circle. **(e-e')** Quantitative analysis of collaterals innervating the area below the spinal cord lesion at 1dpl (e) and 2dpl (e'). Kruskal-Wallis test ± s.e.m, n(WT_1dpl)=10; n(*nrp1a^hu10012^*_1dpl)=14; n(*nrp1b^bns221^*_1dpl)=10; n(*nrp1a^hu10012^*; *nrp1b^bns221^*_1dpl)=7; n(WT_2dpl)=10; n(*nrp1a^hu10012^*_2dpl)=9; n(*nrp1b^bns221^*_2dpl)=10; n(*nrp1a^hu10012^*; *nrp1b^bns221^*_2dpl)=6; n.s.=non-significant; *P<0.05. **(f-f')** Quantitative analysis shows the percentage of larvae with axonal bridges at 1dpl (f) and 2dpl (f'), respectively. Fisher's exact test; Fractions show how many larvae regenerated per sample group; n.s.=non-significant. WT=wild-type; Anti-acet. Tubulin= Anti-Acetylated tubulin; #=number; dpl=days post lesion; n.s.=non-significant; Scale bar 50μm.

Nrp1 data were not as severe as the ones observed in *flt1^ka604^*, as axons could still regenerate across the wound, independent to Nrp1 (single and double mutants). This suggests that Flt1 loss of function influences neuroregeneration via the Vegfa/Kdrl pathways. We then focused on how modulating Vegfa levels could influence neuroregeneration using different *vegfaa* GOF lines.

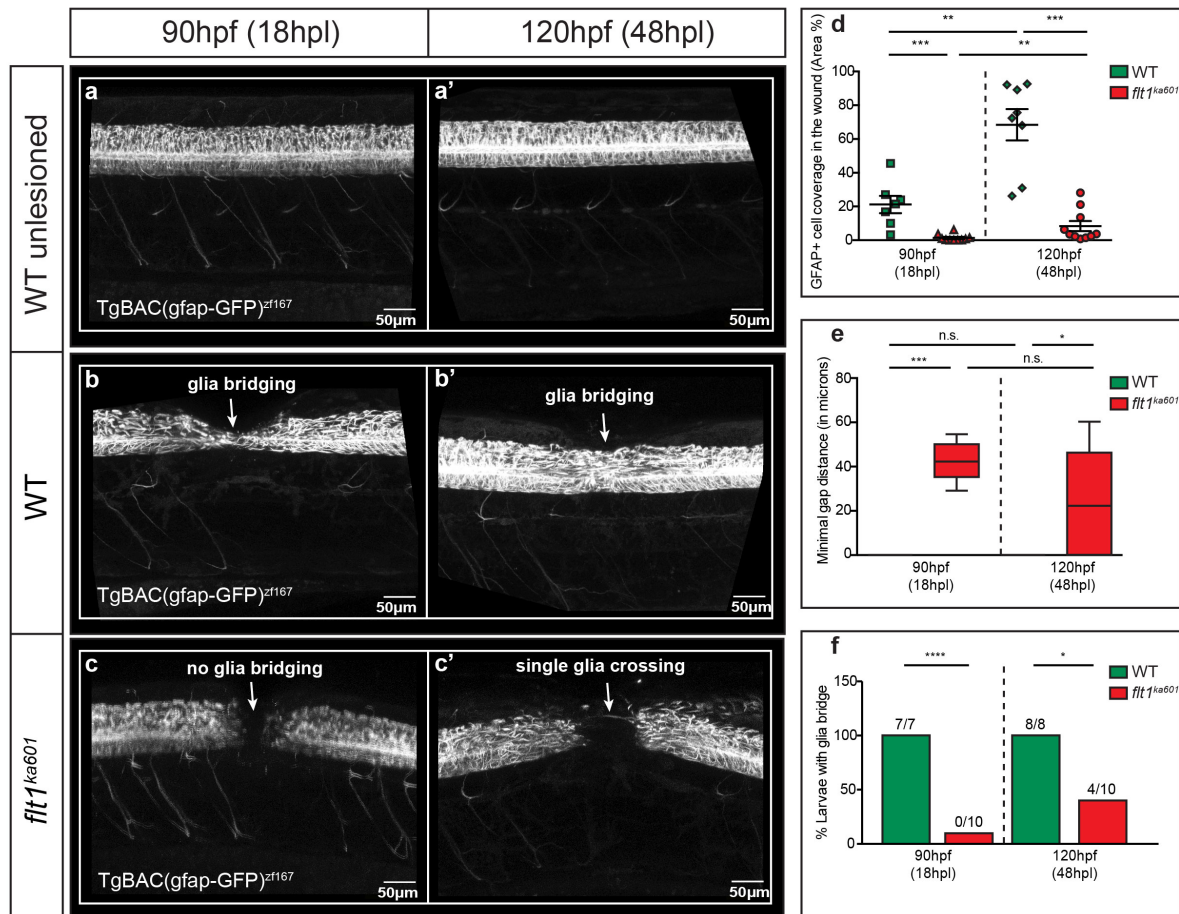## 4.3   Neuroregeneration – a complex interplay between different factors

Spinal cord regeneration is guided by multiple components. The most extensively studied ones are the influence of glia as guidance molecules, components of the ECM and more extensively macrophage migration to the wound. While glia were suggested to be essential for axonal guidance across the wound (Goldshmit *et al.*, 2012), other papers suggest that axons can grow independent of glia processes by utilising components of the ECM, such as collagens (Wehner *et al.*, 2017). On the other hand, macrophages were shown in multiple regeneration assays to play key roles in cardiac, tail and spinal cord regeneration (Petrie *et al.*, 2015; Lai *et al.*, 2017; Tsarouchas *et al.*, 2018). In this study we thus focused how axonal regeneration is executed under these three parameters in respect to Vegfa levels.

4.3.1 Glia bridging is impaired in *flt1* mutants

After a spinal cord lesion, axons need to be guided across the gap in order to close the wound. One component that has been suggested to form such 'bridges' are the glia (Goldshmit *et al.*, 2012). Even though *flt1* acts as a decoy receptor in the vasculature, it has also been suggested to be strongly associated with astroglia growth and reactivity. Mani et al. (2005) showed that Flt1was detected in most but not all astrocytes. However, Kdrl, despite being present in neurons and blood vessels, was not detected in astrocytes. The research further showed that inhibition of *flt1* by antisense-oligonucleotides (AS-ODNs) decreased glia immunoreactivity, while AS-ODNs inhibition of *kdrl* had no effect on astroglia growth and maturation. The study also concluded that VEGF activate the astrocytic *flt1* which leads to MAPK and PI-3 kinase downstream pathways in order to induce astrocyte proliferation, differentiation and maturation (Mani *et al.*, 2005). Ablation of radial glia in zebrafish models also led to hypersprouting around the neural tube, the effect of which was contributed to sFlt1 (Matsuoka *et al.*, 2016). Thus, we hypothesized that failure of axonal regeneration in *flt1*^{ka604} was due to mis-regulated glia processes.

The effect of *flt1* on glia was investigated in the glia transgenic line; TgBAC*(gfap:gfap-GFP)*^{zf167} which expresses GFP under the control of the glia-specific *gfap* promoter (Figure 4.12a-c'). Indeed, glia coverage around the wound was decreased in *flt1*^{ka601} in comparison to WT (Figure 4.12d) whereas the gap size increased (Figure 4.12e).

Thus, reduced axonal regeneration in *flt1* mutants might be, indeed, caused by mis-regulated glia. The effect of glia on *flt1* was tested using two different *flt1* mutants; *flt1^ka601* (Figure 4.12) and *flt1^ka604* (Figure 4.13). This was to verify that the glia deficiency is not linked to a certain mutation but is rather a general defect in *flt1* mutants.

Figure 4. 12: *flt1^ka601* fail to regenerate the glia connections.

(a-a') Single transgenic larvae WT TgBAC*(gfap:gfap-GFP)^zf167* imaged at 90hpf and 120hpf show intact glia at the spinal cord area **(b-c')** Single transgenic larvae WT(b-b') and *flt1^ka601* (c-c') TgBAC*(gfap:gfap-GFP)^zf167* imaged at 18hpl and 48hpl show glia bridging in WT but not in the *flt1^ka601*. **(d)** Quantitative analysis shows the total glia cell coverage (% Area) at 18hpl and 48 hpl. Mann-Whitney test ± s.e.m, n(WT_18hpl)=7; n(*flt1^ka601*_18hpl)=10; n(WT_48hpl)=8; n(*flt1^ka601*_48hpl)=10; **P<0.01; ***P<0.001. **(e)** Minimal gap distance (in μm) within the lesion at 18hpl and 48hpl. Mann-Whitney test ± s.e.m, n(WT_18hpl)=7; n(*flt1^ka601*_18hpl)=10; n(WT_48hpl)=8; n(*flt1^ka601*_48hpl)=10; n.s.=non-significant; *P<0.05; ***P<0.001. **(f)** Quantitative analysis shows the percentage of larvae with glia bridge at 1dpl and 2dpl. Fisher's exact test; Fractions show how many larvae regenerated per sample group; *P<0.05; ***P<0.001. WT=wild-type; hpf=hours post fertilization, hpl=hours post lesion, n.s.=non-significant; Scale bar 50μm.

To decipher how glia may affect axonal branching we decided to use immunohistochemical staining as published by Wehner et al. Axonal regeneration was initially investigated using the neuronal Acetylated tubulin staining. Axonal regeneration was impaired in *flt1*^{ka604} (full mutants) and unaffected in *flt1*^{ka605} (*mflt1* single mutant) both at 1dpl and 2dpl (Figure 4.13k,l). These results further support our earlier findings (Figure 4.4), that sFlt1, and not mFlt1, is important for axonal regeneration.

Another aspect to have a look at, is the formation of collaterals from surviving motor neurons (intact after spinal cord injury), whose axonal terminals (axonal sprouts) extend to the denervated muscles in order to reinnervate the muscle fibres and restore their function. This might improve voluntary control of the muscles after a spinal cord injury and improve the quality of life of the patient (Hagg, 2006). To investigate this, Acetylated tubulin stained larvae were used to quantify the number of axonal sprouts or collaterals below the level of injury (Figure 4.13g-j'). Even though collateral numbers were unaffected at 1dpl (Figure 4.13j), there was a significant decrease in collateral formation in *flt1*^{ka604} at 2dpl, suggesting a possible defect in the larvae's motility post injury (Figure 4.13j'). Thus, sFlt1 is not only important for axonal bridging (initial regeneration) but could also affect functional recovery (collaterals).

To test how these axonal bridges are guided across the wound, we decided to look how astroglia-like processes might aid axonal bridging through the wound. Transgenic experiments showed that the *flt1*^{ka601} have less to no glia bridging after a spinal cord lesion (Figure 4.12). Analyses of immunohistochemical markers for both neuronal (Acetylated tubulin staining) and glia (GFAP staining) processes in fixed lesioned larvae revealed that at 1dpl, around 66% (4/6) of the WT larvae (Figure 4.13a-a'', k'), 100% in *flt1*^{ka605} (*mflt1*) mutants (10/10; Figure 4.13e-e'', k') but only around 15% of the *flt1*^{ka604} (2/13; Figure 4.13c-c'', k') had started to cover the wound with both glia and axons. These differences remained at 2dpl where 90% in WT (9/10; Figure 4.13b-b'', l'), 100% in *flt1*^{ka605} (*mflt1*) mutants (10/10; Figure 4.13f-f'', l') and in 10% in *flt1*^{ka604}(1/10; Figure 4.13d-d'', l') covered the wound. Note that some axons were able to bridge over the gap even without a glia bridge (1dpl, WT 82% formed axonal bridges, but only 66% glia bridges were made). This could suggest other components

responsible for axonal bridging such as the ECM (see later on; Figure 4.17). However, infiltration of the wound by astroglia seems to depend on sFlt1 and goes hand in hand with axonal bridging.
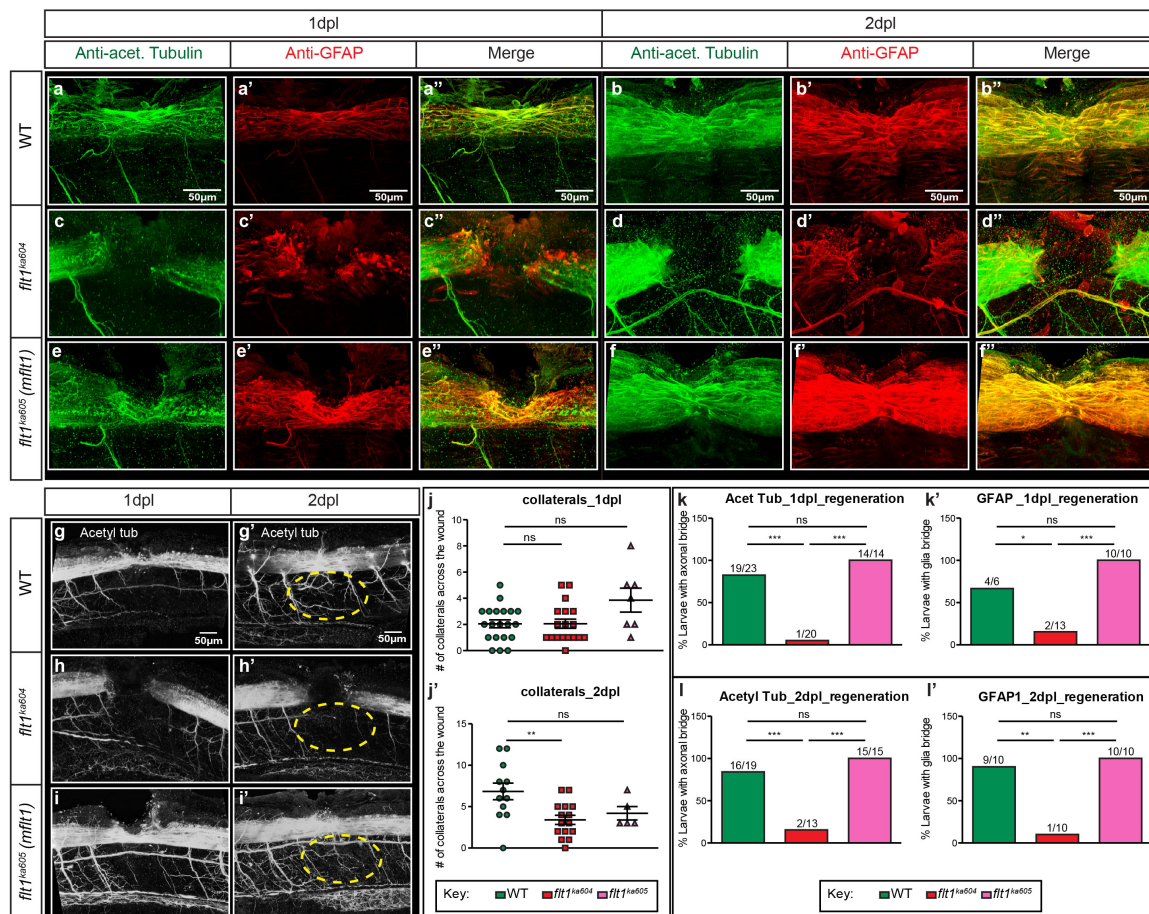

Figure 4. 13: *flt1^ka604* **fail to form glia bridges and collaterals post injury.**

(a-f'') Double immunohistochemically stained larvae for Acetylated tubulin (mature axons in green) and GFAP (glia in red). Merged channels showing axonal and glia overlapping are indicated in yellow. **(a-b'')** WT injured larvae seem to regenerate their axonal and glia connections at 1dpl (a-a'') and 2dpl (b-b''). **(c-d'')** On the contrary, *flt1^ka604* are unable to regenerate either their axonal or glia bridges both at 1dpl (c-c'') and 2dpl (d-d''). **(e-f'')** In a similar manner to WT, *flt1^ka605* (*mflt1*) are able to form axonal and glia bridges across the injured area. **(g-i')** Acetylated tubulin single stained (g-g') WT, (h-h') *flt1^ka604*, **(i-i')** *flt1^ka605* (*mflt1*) larvae at 1 and 2dpl. Collaterals are indicated by a yellow dotted circle. **(j-j')** Quantitative analysis of collaterals innervating the area below the spinal cord lesion at 1dpl (j) and 2dpl (j'). Kruskal-Wallis test ± s.e.m, n(WT_1dpl)=20; n(*flt1^ka604*_1dpl)=18; n(*flt1^ka605*_1dpl)=7; n(WT_2dpl)=12; n(*flt1^ka604*_2dpl)=15; n(*flt1^ka605*_2dpl)=5; n.s.=non-significant; **P<0.01. **(k-l')** Quantitative analysis shows the percentage of larvae with axonal (k,l) glia (k',l') bridges at 1dpl and 2dpl, respectively. Fisher's exact test; Fractions show how many larvae regenerated per sample group; n.s.=non-significant; *P<0.05; **P<0.01; ***P<0.001. WT=wild-type; Anti-acet. Tubulin= Anti-Acetylated tubulin; #=number; dpl=days post lesion; n.s.=non-significant; Scale bar 50μm.

4.3.2 Vegfa overexpression impacts regeneration

Having shown that reduced regeneration capacity in *flt1* mutants is due to accelerated Vegfa/kdrl signalling, we asked if alternative mechanisms to increase the Vegfa/kdrl signalling might also impair neuronal regeneration.

One way to do so is to target VHL, a protein initiating HIF-α for degradation. In *vhl* mutants, HIF1-α can translocate to the nucleus and induce transcriptional activation of Vegfa (Oosthuyse *et al.*, 2001; Pugh and Ratcliffe, 2003; Van Rooijen *et al.*, 2010). Similarly to the *flt1^{ka601}*, *vhl* mutants (*vhl^{hu2114}*) also display a hyperbranching phenotype at the level of the neural tube (Van Rooijen *et al.*, 2009; Wild *et al.*, 2017). In a comparable manner to the *flt1^{ka604}*, we decided to test for axonal and glia bridging in the *vhl^{hu2114}* and check their regenerative capacity using immunohistochemical staining.

As both *flt1^{ka604}* and *vhl^{hu2114}* induce a *vegfaa* GOF scenario, we initially wanted to investigate if the *vhl^{hu2114}* experience similar axonal bridging impairments as the ones observed in the *flt1^{ka604}* mutants. Surprisingly, *vhl^{hu2114}* exhibit no axonal bridging impairments as the ones observed in the *flt1^{ka604}* mutants. This result suggests a weaker effect in the *vhl^{hu2114}* mutant in comparison to the *flt1^{ka604}*. One important contributing factor could be that in *vhl^{hu2114}* mutants triggers a hypoxia response and hence the transcriptional activation of not only Vegfa but also of other angiogenic growth factors such as angiopoietin-2, platelet-derived growth factor and CXC chemokine receptor 4 (Van Rooijen *et al.*, 2010). Another parameter to consider for functional recovery is the collateral formation below the injury, as collaterals were previously shown to be affected in the *flt1^{ka604}* (Figure 4.13). At 2dpl, even though collateral numbers were unaffected at 1dpl (Figure 4.14g), there was a significant decrease in collateral formation in *vhl^{hu2114}* (Figure 4.14g'), similar to the one observed in the *flt1^{ka604}* (Figure 4.13j').

We then went on to investigate how these axonal bridging is mediated in *vhl^{hu2114}*, by looking into glia bridging post injury. At 1dpl, around 66% of the WT larvae (4/6; Figure 4.14a-a'', h') and 25% of the *vhl^{hu2114}* (Figure 4.14c-c'', h') had both axonal and glia bridges, which was still higher when compared to 15% in the *flt1^{ka604}* (2/13; Figure

4.13c-c'', k'). These further increased at 2dpl to 90% in WT (9/10; Figure 4.14b-b'', i') and to 36% in *vhl^hu2114* (4/11; Figure 4.14d-d'', i'). This is significantly lower than WT, yet three-times higher than what was observed in *flt1^ka604* at 2dpl (1/10; Figure 4.13d-d'', l'). This might also partly explain why more *vhl^hu2114* are able to form axonal bridges (3/4; 75% at 1dpl and 9/11; 81% Figure 4.14h,l, respectively) than *flt1^ka604* (1/20; 5% at 1dpl and 2/13; 15% Figure 4.13k,l, respectively).
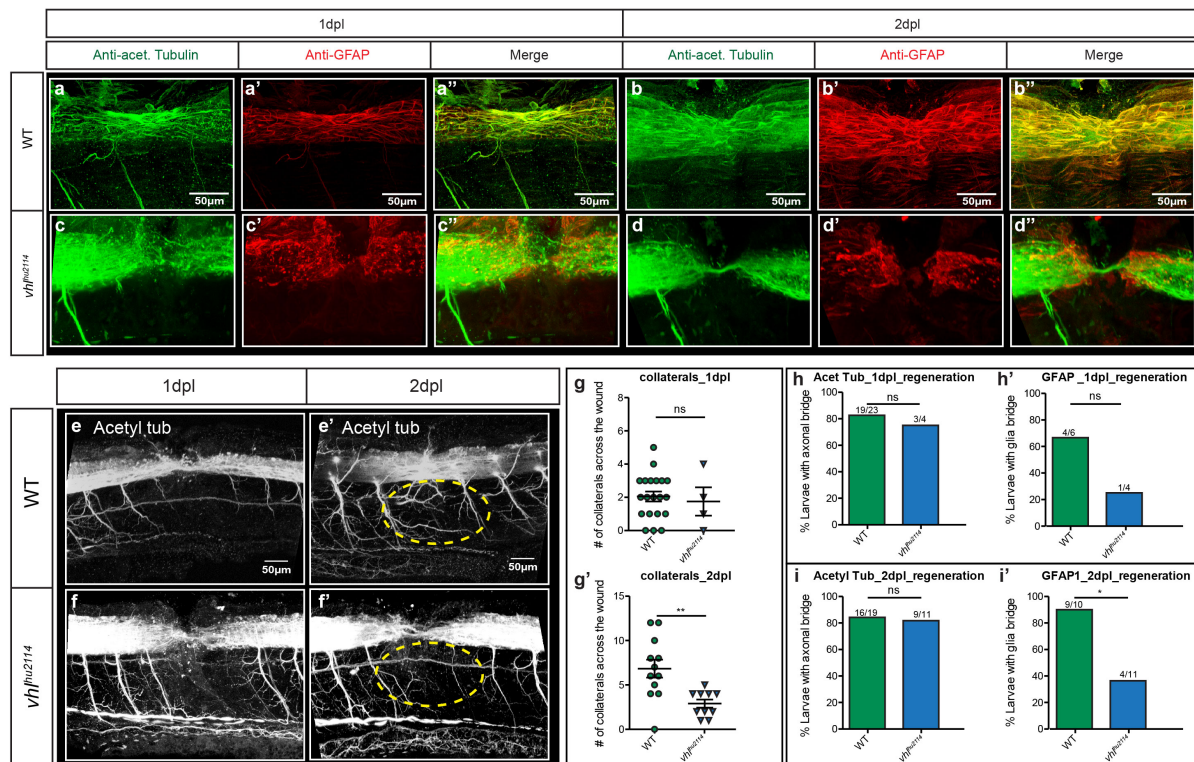

Figure 4. 14: *vhl^hu2114* **regenerate axonal bridging but not collateral formation.**

(a-d'') Double immunohistochemically stained larvae for Acetylated tubulin (mature axons in green) and GFAP (glia in red). Merged channels showing axonal and glia overlapping are indicated in yellow. **(a-b'')** WT injured larvae seem to regenerate their axonal and glia connections at 1dpl (a-a'') and 2dpl (b-b''). **(c-d'')** *vhl^hu2114* are also able to weakly regenerate either their axonal or glia bridges both at 1dpl (c-c'') and 2dpl (d-d''). **(e-f')** Acetylated tubulin single stained (e-e') WT and (f-f') *vhl^hu2114* larvae at 1 and 2dpl. Collaterals are indicated by a yellow dotted circle. **(g-g')** Quantitative analysis of collaterals innervating the area below the spinal cord lesion at 1dpl (g) and 2dpl (g'). Mann-Whitney test ± s.e.m, n(WT_1dpl)=20; n(*vhl^hu2114*_1dpl)=4; n(WT_2dpl)=12; n(*vhl^hu2114*_2dpl)=10; n.s.=non-significant; **P<0.01. **(h-i')** Quantitative analysis shows the percentage of larvae with axonal (h,i) glia (h',i') bridges at 1dpl and 2dpl, respectively. Fisher's exact test; Fractions show how many larvae regenerated per sample group; n.s.=non-significant; *P<0.05. WT=wild-type; Anti-acet. Tubulin= Anti-Acetylated tubulin; #=number; dpl=days post lesion; n.s.=non-significant; Scale bar 50µm.

Overall, these results suggest a weaker phenotype of vhl^{hu2114} in axonal and glia regeneration, compared to the detrimental effect of $flt1^{ka604}$. To elucidate how $flt1$ exerts this severe effect, we decided to look more specifically into flt1 ligands; Plgf and Vegfb.

Flt1, apart from Vegfa, can also bind to other ligands such as Plgf and Vegfb. Overexpressing Plgf and/or Vegfb could compete Vegfa from binding to Flt1, thus more Vegfa would be available to bind to kdrl to induce angiogenesis. As Vegfa release is desired to be in close proximity to the ISVs, a muscle-specific promoter; *503unc* was used to make the *plgf* and *vegfb* GOF lines (Berger and Currie, 2013). To induce constitutive overexpression under the *503unc* promoter, *plgf* and *vegfb* were each individually cloned behind a GFP construct, connected through the self-cleaving peptide; p2A in order to preserve the protein's functionality. The plasmid was then injected alongside *tol2 transposase* mRNA at one-cell stage embryos. Both *plgf* and *vegfb* GOF models show an initial increase in the ISV diameter, with *plgf* GOF showing tertiary sprouts around the neural tube, similar to *flt1* full mutants. Contrary, the vessel diameter was thinner in *plgf* mutants ($plgf^{ka609}$), suggesting that *plgf* could be involved in the Vegfaa-Kdrl signalling (Alina Klems, unpublished).

Once more axonal regeneration was investigated using the Acetylated tubulin staining to stain the axonal connections in both $plgf^{ka609}$ mutants and *plgf* GOF scenarios. At 1dpl less axonal connections were observed in the *plgf* GOF scenarios, but $plgf^{ka609}$ seem to regenerate in a similar manner to WT (Figure 4.15k). This effect seemed to reverse at 2dpl, as regeneration significantly decreased at $plgf^{ka609}$ and increased in *plgf* GOF (Figure 4.15l). Despite, *plgf* GOF being an alternative *vegfaa* GOF model, regeneration was partially impaired, unlike in $flt1^{ka604}$ where axonal regeneration was almost completely absent (Figure 4.13). On the contrary, $plgf^{ka609}$ present a 'low-Vegfa' scenario, as the vessel diameter was thinner than WT or *vegfa* MO treated larvae (not shown). These results suggest that Vegfa bioavailability could be a key contributor in progressive or regressive neuroregeneration. To further investigate if this decrease or increase in *vegfa* levels, could also repair the functional recovery, the number of collaterals below the level of injury were also quantified (Figure 4.15g-j'). Even though collateral numbers were unaffected at 1dpl (Figure 4.15j), there was a significant

decrease in collateral formation in the *plgf* GOF scenario at 2dpl (Figure 4.15j'), similar to that observed in *flt1*^{ka604} (Figure 4.13j') and *vhl*^{hu2114} (Figure 4.14g'). Thus, *vegfa* overexpression could be important for initial but not functional recovery.

Additionally, after 1dpl, around 66% (4/6) of the WT larvae (Figure 4.15a-a'', k'), 100% in *plgf*^{ka609} mutants (6/6; Figure 4.15c-c'', k') and only 20% of the *plgf* GOF (2/10; Figure 4.15e-e'', k') had both axonal and glia processes. These further increased at 2dpl to 90% in WT (9/10; Figure 4.15b-b'', l'), halved in *plgf*^{ka609} mutants (7/13; Figure 4.15d-d'', l') and increased to 67% in *plgf* GOF (6/9; Figure 4.15f-f'', l'). This decrease in glia bridges could also attribute to the almost 2-fold decrease (from 82%; 9/11 to 50%; 9/18; Figure 4.15k,l) in axonal bridging in *plgf*^{ka609}. The reverse was observed in the *plgf* GOF, where this increase in glia bridges by 2dpl, boosted the axonal regeneration from 27% (4/15) at 1dpl to 91% (10/11) at 2dpl (Figure 4.15k,l). This is consistent with previous data suggesting that Vegfa is neuroprotective, as an enhanced regeneration is achieved when *vegfa* is overexpressed (*plgf* GOF scenario) and is decreased in 'low *vegfa*' levels (*plgf*^{ka609}).

Overall, these data suggest a delayed axonal regeneration in *plgf* GOF scenario, which is recapitulated by 2dpl. Axonal regeneration is thus delayed but not impaired. Instead, collaterals seem to be affected which might reflect the *vegfa* overexpression scenario, but is milder than the one observed in *flt1*^{ka604}. On the contrary, *plgf*^{ka609} exhibit a mild effect but not before 2dpl, significant only for axonal regeneration, as glia projections remain unaffected. These results could support the role of Vegfa as a bimodal neuroprotective factor.
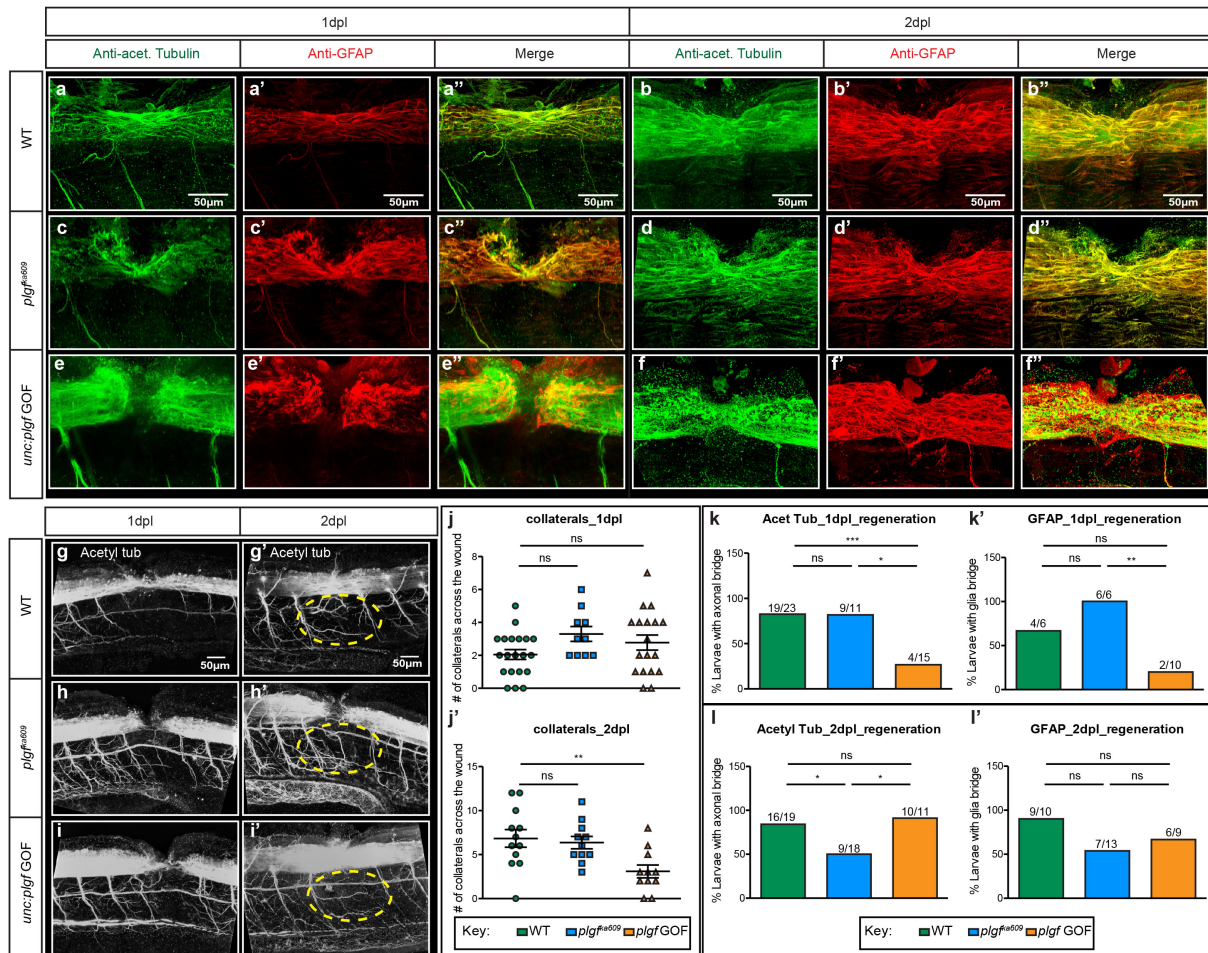
Figure 4. 15: *plgf* and *vegfa* levels need to be tightly regulated for functional recovery.

(a-f'') Double immunohistochemically stained larvae for Acetylated tubulin (mature axons in green) and GFAP (glia in red). Merged channels showing axonal and glia overlapping are indicated in yellow. **(a-b'')** WT injured larvae seem to regenerate their axonal and glia connections at 1dpl (a-a'') and 2dpl (b-b''). **(c-d'')** Similarly, *plgf*^*ka609*^ regenerate either their axonal or glia bridges at 1dpl (c-c'') and 2dpl (d-d''). **(e-f'')** However, contrary to *plgf*^*ka609*^, *plgf* GOF have a more delayed regeneration at 1dpl, which nonetheless increases by 2dpl. **(g-i')** Acetylated tubulin single stained (g-g') WT, (h-h') *plgf*^*ka609*^, **(i-i')** *plgf* GOF larvae at 1 and 2dpl. Collaterals are indicated by a yellow dotted circle. **(j-j')** Quantitative analysis of collaterals innervating the area below the spinal cord lesion at 1dpl (j) and 2dpl (j'). Kruskal-Wallis test ± s.e.m, n(WT_1dpl)=20; n(*plgf*^*ka609*^_1dpl)=10; n(*plgf* GOF_1dpl)=18; n(WT_2dpl)=12; n(*plgf*^*ka609*^_2dpl)=11; n(*plgf* GOF_2dpl)=11; n.s.=non-significant; **P<0.01. **(k-l')** Quantitative analysis shows the percentage of larvae with axonal (k,l) glia (k',l') bridges at 1dpl and 2dpl, respectively. Fisher's exact test; Fractions show how many larvae regenerated per sample group; n.s.=non-significant; *P<0.05; **P<0.01; ***P<0.001. WT=wild-type; Anti-acet. Tubulin= Anti-Acetylated tubulin; GOF=gain-of-function; #=number; dpl=days post lesion; n.s.=non-significant; Scale bar 50μm.

Even though Vegfb has been extensively studied in other models, little to no studies exist on the role of *vegfb* in zebrafish models. In zebrafish, *vegfb* exists in two variants; *vegfba* and *vegfbb.* Using the shared gene synteny analysis, scanning for common genes between the zebrafish and human *Vegfb*, revealed that *vegfba* shares a gene in their upstream region with the human Vegfb. On the other hand, no shared gene synteny was identified between the *vegfbb* and human Vegfb (Alina Klems, unpublished). Thus, for the purpose of this research, *vegfba* was used. Unlike, VEGF-A and PlGF, VEGF-B has very little effects on the vasculature and angiogenesis. It has however, been described to be neuroprotective, as it inhibits potential apoptosis via the VEGFR1 (Li *et al.*, 2008). VEGF-B further exerts its neuroprotective effect on MNs via VEGFR1 (Flt1), but not on astrocytes, despite that Flt1 is also present in glia cells. However, astrocytes may express VEGF-B post injury to maintain their survival (Poesen *et al.*, 2008).

In my work I have shown that the main pathway activating in *flt1* mutants to impair neuronal regeneration is the Vegfa/Kdrl pathway. Overexpression of Vegfb thus, should mimic the *flt1* mutant phenotype, because in this scenario, *vegfaa* is released from the decoy receptor; *flt1.* In *vegfba* mutants, instead, *vegfaa* levels should decrease and thus their neuroprotective role should be more evident.

Axonal regeneration was affected in a similar manner to the *plgf* loss and gain-of-function scenario. While axonal regeneration was unaffected at 1dpl both in *vegfba$^{-/-}$* and *vegfba* GOF scenarios (Figure 4.16g), this was altered at 2dpl. At 2dpl, axonal regeneration was decreased in *vegfba$^{-/-}$* (Figure 4.16h), similarly to the *plgf^{ka609}*(Figure 4.15l), while *vegfba* GOF led to an enhancement in regeneration rate, comparable to the one observed in *plgf* GOF scenario (Figure 4.15l). As Vegfb was shown to exert some neuroprotective effects via mFlt1 on MNs (Poesen *et al.*, 2008), this could be a possible explanation for the boosted regeneration rate at both 1dpl and 2dpl, as both Vegfb acting through Flt1 and Vegfa acting through Kdrl are able to exert their neuroprotective effects on MNs.

We then decided to investigate whether this increase in axonal regeneration was due to an enhanced glia bridging network. After 1dpl, around 44% (4/9) of the *vegfba⁻/⁻* (Figure 4.16c-c'',g') had both axonal and glia processes, which further decreased to 16% at 2dpl (2/14; Figure 4.16d-d'', h'). In the *vegfba* GOF glia bridges remained constant between 1dpl (27%; 4/15; Figure 4.16e-e'', g') to 2dpl (21%; 3/14; Figure 4.16f-f'',h'). For both *vegfba* loss and GOF scenarios glia bridges were significantly lower than the WT larvae (67% at 1dpl, 4/6; Figure 4.16a-a'', g' and 90% at 2dpl, 9/10; Figure 4.16b-b'', h'). This could suggest that *vegfba* could regulate glia formation post injury. Despite the low glia bridging, axonal connections were still able to form at 1dpl (55%, 5/6 in *vegfba⁻/⁻* and 60%, 9/15 in *vegfba* GOF; Figure 4,.16g).
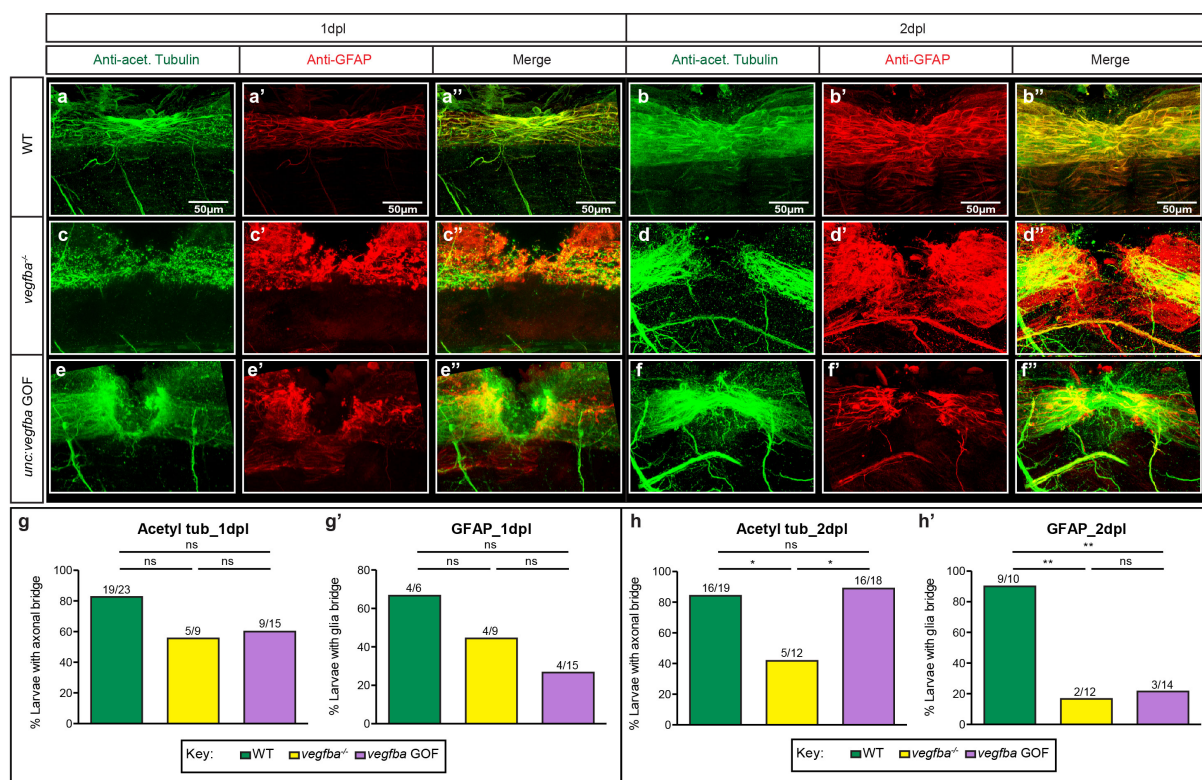
Figure 4. 16: *vegfba* is important in modulating glia bridging.

(a-f'') Double immunohistochemically stained larvae for Acetylated tubulin (mature axons in green) and GFAP (glia in red). Merged channels showing axonal and glia overlapping are indicated in yellow. **(a-b'')** WT injured larvae seem to regenerate their axonal and glia connections at 1dpl (a-a'') and 2dpl (b-b''). **(c-d'')** Similarly, *vegfba⁻/⁻* regenerate either their axonal and glia bridges at 1dpl (c-c''), however, these glia bridges seem to mostly retract by 2dpl (d-d''). **(e-f'')** In *vegfba* GOF axonal and some glia bridges form at 1dpl. These glia bridges then seem to retract by 2dpl, similarly to the *vegfba⁻/⁻*. **(g-h')** Quantitative analysis shows the percentage of larvae with axonal (g,h) glia (g',h') bridges at 1dpl and 2dpl, respectively. Fisher's exact test; Fractions show how many larvae regenerated per sample group;

n.s.=non-significant; *P<0.05; **P<0.01. WT=wild-type; Anti-acet. Tubulin= Anti-Acetylated tubulin; #=number; dpl=days post lesion; n.s.=non-significant; Scale bar 50μm.

This data further suggests that *vegfaa* levels are crucial for proper axonal regeneration and that axons are still able to bridge the gap independent of glia. To investigate another parameter aiding axonal bridging we decided to look at the effect of collagens in our *flt1^ka604^* mutants.

4.3.3 Collagens are slightly affected in *flt1^ka604^*

In mammals, collagen deposition post injury forms a dense inhibitory matrix, which prevents any axons from bridging across the wound (Goldshmit *et al.*, 2012). This is not the case in regenerating zebrafish, as the extracellular matrix (ECM) permits axons to cross over, suggesting that by controlling ECM could provide new insights into promoting regeneration processes. Indeed, some collagens were already identified to be involved in growth of developing motor axons and correct motor axon regeneration in zebrafish (Wehner *et al.*, 2017). In line with previous data (Figure 2.7), some axonal connections are made prior to any glia bridge formation. This could suggest that some axons can cross over independently of glia. An alternative 'path' for axonal bridges to grow over could be ECM components, in particular, collagens. We thus decided to investigate Collagen I (Col I); a major ECM component. This has previously been shown to be in close contact to regenerating axonal fascicles 1 day after a spinal cord injury, suggesting that axons could navigate through the non-neural lesion in close contact with ECM components. Furthermore, axonal re-connection, a process essential for functional recovery, depends on Wnt/β-catenin signalling. Indeed, Wnt/β-catenin signalling in fibroblast-like cells, which seem to be elevated within the lesion site, is a turning point for axonal regeneration and functional recovery. Wnt/β-catenin then induces Col XII (*col12a1a/b*) deposition through these fibroblast-like cells and thus promotes axonal regeneration (Wehner *et al.*, 2017). As there is no commercially available Col XII antibody in zebrafish models, we decided to check for this using qPCR analysis. The two collagen paralogs; *col12a1a* and *cola12a1b*, which were downregulated upon Wnt/β-catenin inhibition, and code for the essential α-chain of Col XII, were therefore used (Wehner *et al.*, 2017).

Double immunohistochemically staining was used to stain both neuronal (Acetylated tubulin staining) and Collagen I (Col I staining) processes in fixed lesioned larvae at 1 and 2dpl. Axonal branching (indicated by blue arrowhead) could grow along the Col I projections (yellow arrowhead) to form a stable axonal re-connection at both 1dpl (Figure 4.17a-b'') and 2dpl (Figure 4.17c-d''). Despite the fact that Col I (quantified using a *col1a1a* qPCR primer), was significantly downregulated in both unlesioned and 1dpl *flt1^{ka604}* mutants (Figure 4.17e-e', respectively), it was not severe enough to impair the Col I projections from forming. This could also explain why a small percentage of *flt1^{ka604}* are able to regenerate.

One step further, *col12a1a* and *col12a1b* were further quantified, as they were shown to play a key role in spinal cord regeneration. Both paralogues seemed to be unaffected in *flt1^{ka604}* under normal unlesioned conditions (Figure 4.17f,g). Interestingly, *col12a1a* was significantly decreased in *flt1^{ka604}* by 1dpl (Figure 4.17f'). This could be compensated by *col12a1b*, as that seemed to be unaffected in *flt1^{ka604}* when compared to WT controls at 1dpl (Figure 4.17g'). However, one should note that overexpression of only *col12a1a* was shown to be sufficient in inducing axonal bridging (Wehner *et al.*, 2017). Thus, *col12a1a* downregulation could be one alternative reasoning for *flt1^{ka604}* regeneration failure.
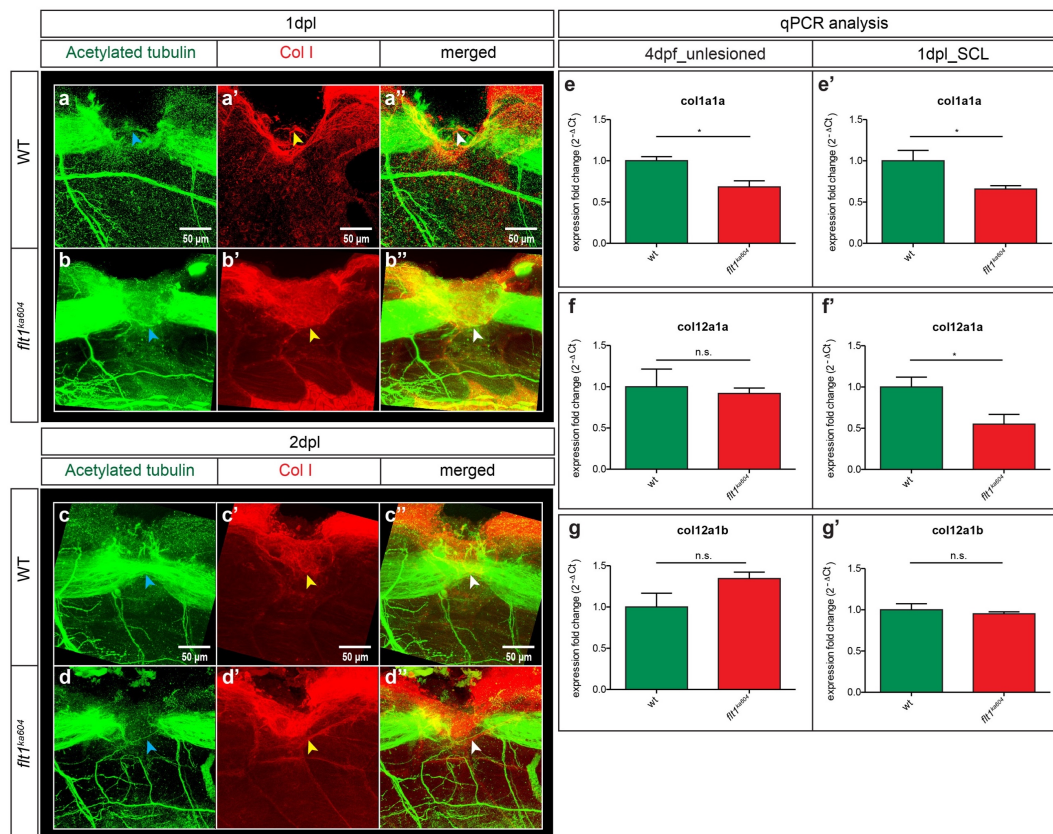
Figure 4. 17: Axonal bridging in *flt1^{ka604}* could be guided via Col I.

(a-d'') Double immunohistochemically stained larvae for Acetylated tubulin (mature axons in green) and Col I (Col I in red). Merged channels showing axonal and collagen overlapping are indicated in yellow. Blue arrowheads show axonal projections, yellow arrowheads show collagen projections and white arrowheads show axonal projections growing alongside collagen **(a-a'')** WT injured larvae axonal connections are guided through Col I projections at 1dpl. **(b-b'')** Likewise, axonal connections also grow across Col I projections in *flt1^{ka604}* at 1dpl. **(c-c'')** Axonal bridging keeps growing over Col I projections in WT larvae by 2dpl. **(d-d'')** Even though the axonal bridging is weak in *flt1^{ka604}*, the few axons that do grow across do so by traveling over Col I projections. **(e-g')** qPCR analysis of *col1a1a* (e-e'), *col12a1a* (f-f') and *col12a1b* (g-g') in unlesioned (e,f,g) and 1dpl (e',f',g') larvae. Unpaired t-test ± s.e.m, n(WT)=3; n(*flt1^{ka604}*)=4; n.s.=non-significant; *P<0.05. WT=wild-type; Anti-acet. Tubulin= Anti-Acetylated tubulin; Col I=Anti-Collagen I; dpf=days post fertilization; dpl=days post lesion; n.s.=non-significant; Scale bar 50µm.

Overall these data suggest that some axonal connections occur independently of glia projections. A possible alternative could be collagens as axons can also grow across a collagen matrix. Nonetheless, *vegfaa* overexpression seems to affect glia formation either at early (1dpl) or late (2dpl) regeneration stages. Compared to other *vegfa* GOF models, *flt1* mutants seem to have the most severe phenotype. As *flt1^{ka604}*, *vegfba^{-/-}*

and *vegfba* GOF scenarios experience the most severe glia impairment phenotypes it could suggest a novel interaction between *vegfb* and *sflt1*.

4.3.4 Macrophage migration is impaired in *vegfa* GOF scenarios

Similarly, to the collagens, a strong influx of innate immune responses post injury, contributes to the mammalian inhibitory environment, impeding axonal regeneration. This is due to the strong pro-inflammatory (M1) macrophage influx to the wound, which is neurotoxic, compared to the anti-inflammatory (M2) which aid in axonal regeneration (Kigerl *et al.*, 2009). This could thus suggest a dual function of macrophages in both promoting and impeding axonal regeneration. Unlike mammals, zebrafish are able to recapitulate their lost axonal connections. In adult zebrafish, microglia get activated post spinal cord injury, which could suggest a role of the innate immune system in axonal repair. As zebrafish larvae develop their adaptive immunity at juvenile stages, they are useful models to study the innate immunity during early embryonic stages (Tsarouchas *et al.*, 2018). This study will therefore focus on the role of macrophages in spinal cord regeneration, as neutrophils and microglia are not essential for axonal repair (Tsarouchas *et al.*, 2018).

Interestingly, VEGFR1 (Flt1) but not VEGFR2, was shown to be present on monocyte/macrophages (Sawano *et al.*, 2001). It is not then surprising that monocyte/macrophage migration is mediated via VEGF and PlGF interactions with the VEGFR-1 (Barleon *et al.*, 1996; Muramatsu *et al.*, 2010). This was further shown as VEGF- and PlGF- dependent macrophage migration was inhibited in Flt1 TK$^{-/-}$ (Muramatsu *et al.*, 2010). Therefore, this study will focus more on these ligands and receptors. Previous data showed that in *flt1* and *plgf* mutants, macrophages dispersed out of the areas which usually express *flt1* and *plgf* and moved towards the trunk and tail area instead (Krueger *et al.*, 2011; Alina Klems, unpublished). This was then further investigated in both *flt1^{ka604}, plgf^{ka609}* and *plgf* GOF scenarios

4.3.4.1 *flt1* LOF only impairs macrophage migration upon neuronal injury

Using the *flt1* LOF model, we identified that macrophage migration was solely affected upon neuronal injury (Appendix, Supplementary Figure 2). We thus went on to quantify the rate of macrophage migration to the wound after a spinal cord injury using the

macrophage transgenic line; *Tg(mpeg:EGFP)^{gl22}*. WT embryos were injected with a *flt1*-ATG MO to induce *flt1* loss of function scenario. To test that the morpholino was comparable to the *flt1^{ka604}* vascular phenotype, we used also used a vascular reporter line; *Tg(kdrl:*Hsa.HRAS-mCherry)^{s916} to observe the hypersprouting phenotype. As zebrafish apoptotic cells autofluorescence we decided to co-label macrophages using DAPI staining in order to stain the nuclei of macrophages and improve thus improve the accuracy of cell counting.

Macrophage migration was severely impaired in *flt1* loss of function scenario (Figure 4.18b-b'') in comparison to WT controls (Figure 4.18a-a''). This was further verified by quantitative analysis of the double labelled mpeg+/DAPI+ macrophages around the lesion site.
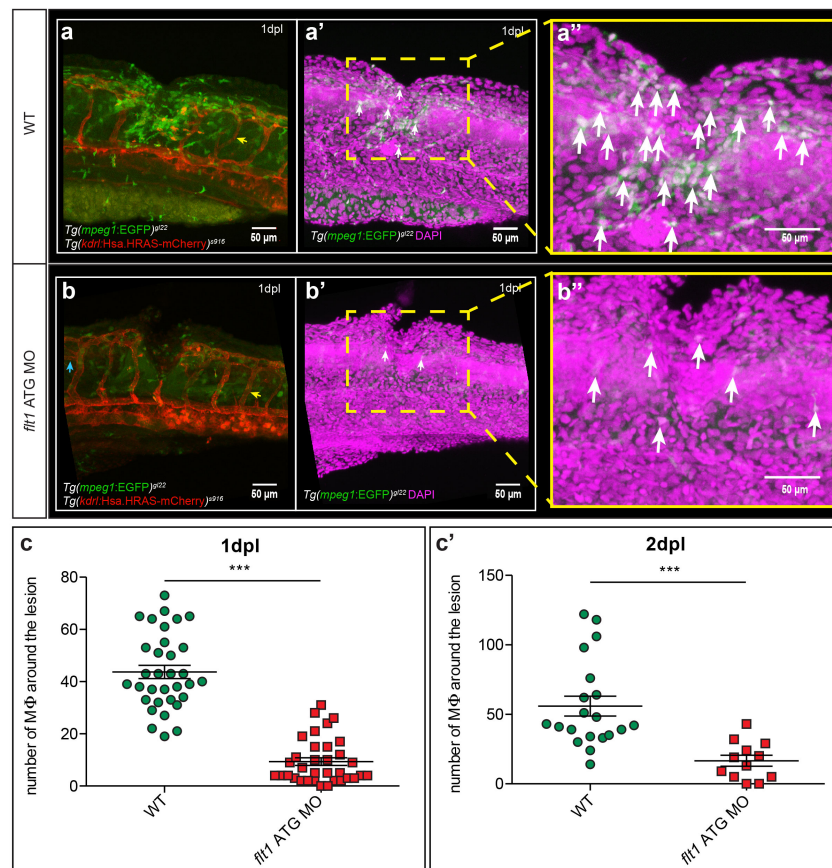
Figure 4. 18: *flt1* LOF impairs macrophage migration post neuronal injury.

(a,b) Double transgenic larvae (a) WT and (b) *flt1* LOF *Tg(mpeg1:EGFP)^{gl22}*;*Tg(kdrl:*Hsa.HRAS-mCherry)^{s916} were used to detect macrophages and vessels, post spinal cord injury. Macrophages are shown in green and vessels in red. The *flt1*-ATG MO was able to induce the *flt1^{ka604}* vascular phenotype, as hypersprouts are visible post injury (indicated by blue arrow). (a'-b'') DAPI staining (magenta) was used to stain the nuclei of the macrophages (green). Co-localization could thus be observed in white

(indicated by white arrows). The yellow dotted boxes in a' and b' are enlarged into the a'' and b'' panel for visualization purposes. **(c)** Quantitative analysis of the number of macrophages migrating to the wound at 1dpl. Mann-Whitney test ± s.e.m, n(WT_1dpl)=33; n(*flt1*-ATG MO _1dpl)=35; ***P<0.001. **(c')** Statistical analysis of the number of macrophages migrating to the wound at 2dpl. Mann-Whitney ± s.e.m, n(WT_2dpl)=20; n(*flt1*-ATG MO _2dpl)=12; ***P<0.001. dpl=days post lesion; MO=Morpholino; MΦ=Macrophages. Scale bar 50µm.

4.3.4.2 *plgf* is also important in macrophage migration post neuronal injury

Initial analysis thus indicated that *flt1* is important in macrophage migration post neuronal injury. To further investigate this*,* we compared the *flt1* LOF scenario, with the *plgf^ka609^* and *plgf* GOF scenarios upon spinal cord injury. If macrophage migration is also driven via PIGF, we would expect a similar decrease in macrophage migratory activity in the *plgf^ka609^*. As expected, *plgf^ka609^* displayed a macrophage migration deficiency at 1dpl (Figure 4.19b-b',d) compared to WT controls (Figure 4.19a-a',d). On the other hand, one would expect that overexpressing *plgf* should rescue this macrophage deficiency. However, a *plgf* overexpression also induces a *vegfa* GOF scenario, similar to the one observed in *flt1^ka604^*. Indeed, *plgf* GOF had reduced macrophage migration both at 1dpl (Figure 4.19c-c',d) and at 2dpl (Figure 4.19d-d'), in a similar manner to that observed in the *flt1* LOF scenario (Figure 4.18i-i'). As *vegfa* is constitutively overexpressed in *flt1^ka604^* and *plgf* GOF, this could also diminish the VEGF gradient, over which macrophage migration is guided.
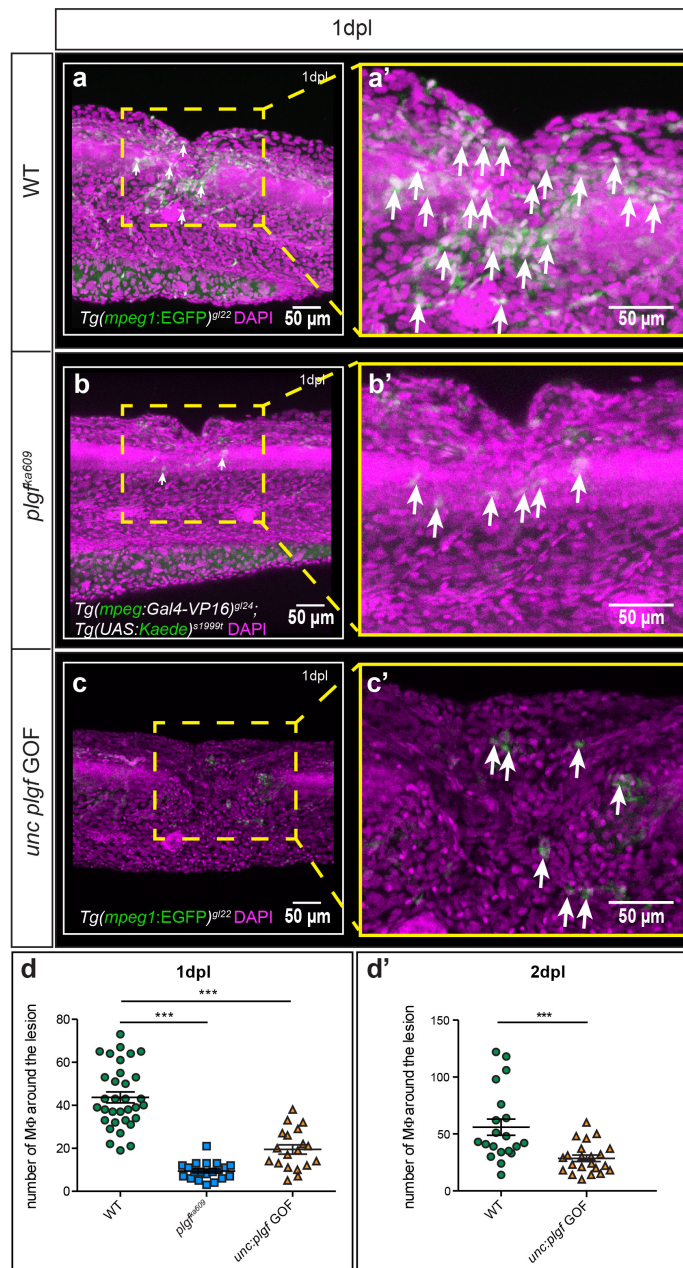
Figure 4. 19: *plgf^ka609* and *plgf* GOF impair macrophage migration post neuronal injury.

(a-c') Single transgenic larvae WT *Tg(mpeg:Gal4-VP16)^gl24; Tg(UAS:KAEDE)^s1999t* or *Tg(mpeg1:EGFP)^gl22* were used to detect macrophage migration post injury. DAPI staining (magenta) was used to stain the nuclei of the macrophages (green). Co-localization could thus be observed in white (indicated by white arrows). The yellow dotted boxes in a,b,c are enlarged into the a',b',c' panel for visualization purposes. **(d)** Quantitative analysis of the number of macrophages migrating to the wound at 1dpl. Kruskal-Wallis test ± s.e.m, n(WT_1dpl)=33; n(*plgf^ka609*_1dpl)=20; n(*plgf* GOF_1dpl)=19; ***P<0.001. **(d')** Statistical analysis of the number of macrophages migrating to the wound at 2dpl. Mann-Whitney ± s.e.m, n(WT_2dpl)=20; n(*plgf* GOF_2dpl)=22; ***P<0.001. dpl=days post lesion; GOF=gain-of-function; MΦ=Macrophages. Scale bar 50µm.

These results conclude that *vegfa* overexpression impairs the *vegfa* gradient over which macrophages can migrate across. Furthermore, *plgf* is also essential for macrophage migration as less macrophages were able to migrate to the wound in *plgf*^{ka609}.

4.3.4.3 Vegfa polarises M2 macrophages

One other important aspect of regeneration, apart from macrophage migration, is the type of macrophages that migrate to the wound. As previously mentioned, in zebrafish larvae, proper spinal cord regeneration is achieved with an early pro-inflammatory wave, which needs to be subsequently substituted by an anti-inflammatory wave in order to successfully resolve the wound (Tsarouchas *et al.*, 2018). To investigate these, two pro- (*il-1β* and *tnf-α*) and two anti- inflammatory (*tgf-β1a* and *tgf-β3*) cytokines were quantified using qPCR analysis at 18hpl (for early), and 24hpl and 48hpl (for late) spinal cord regeneration stages (Figure 4.20).
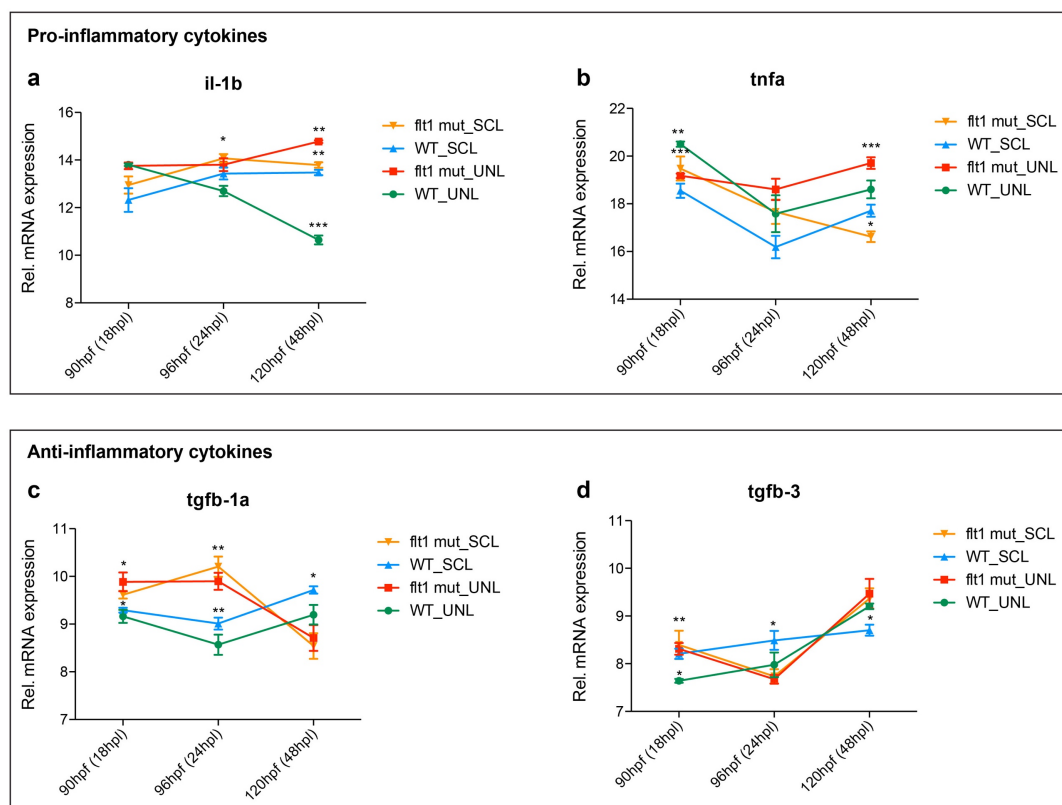
Figure 4. 20: Dual pro- and anti-inflammatory response during early regeneration *phase in flt1*^{ka604}.

(a-b) mRNA expression of pro-inflammatory cytokines; *il-1β* (a) and *tnf-α* (b) at different timepoints in unlesioned and lesioned larvae. **(c-d)** mRNA expression of anti-inflammatory cytokines; *tgf-β1a* (c) and

tgf-β3 (d) at different timepoints in unlesioned and lesioned larvae. Unpaired t-test ± s.e.m, n(WT)=4; n(*flt1^{ka604}*)=4; *P<0.05; **P<0.01; ***P<0.001. For detailed statistics look Supplementary table 1-4 in Appendix. hpf=hours post fertilization; hpl=hours post lesion.

In summary, *il-1β* seems to be upregulated in both WT and *flt1^{ka604}* at 2dpl, in comparison to unlesioned controls. Thus, *il-1β* does not seem be altered between WT and *flt1^{ka604}* prior and post injury. On the other hand, *tnf-α* levels seem to be significantly decreased post injury at 48hpl in *flt1^{ka604}* lesioned vs *flt1^{ka604}* unlesioned larvae. This could suggest that *tnf-α* expression is particularly altered post injury. However, post injury, even though slightly higher than in WT lesioned larvae, *tnf-α* levels in *flt1^{ka604}* lesioned larvae are still relatively lower at 48hpl than at 18hpl. This is consistent with Tsarouchas et al. suggesting a decreased pro-inflammatory response in later regeneration stages. The only data which could be mildly interesting is that *flt^{ka604}* exert a higher anti-inflammatory response at early and late regeneration stages in both lesioned and unlesioned scenarios. As this increase was not attributed by the lesion, we cannot link this change to the neuronal wound. This may rather be attributed to the VEGF overexpression, polarising M2 (anti-inflammatory) macrophages, as VEGF has been shown to induce the shift between M1 to M2 macrophages (Wheeler *et al.*, 2018). Therefore, these results seem inconclusive, providing us with no reliable estimate for further experiments on the macrophage polarity.

4.3.4.4 Boosting inflammation overwrites the effect of *flt1* LOF

As macrophage migration seems to be impaired in *vegfa* GOF models, we decided to boost the immune system in an attempt to enhance the axonal regenerative capacity. Bacterial lipopolysaccharides (LPS), were previously shown to enhance macrophage migration to the wound and also speed up the axonal regeneration (Tsarouchas *et al.*, 2018). To study this, *flt1*-ATG MO was injected at one-cell stage embryos, and LPS was added at 70hpf. While the larvae were still in LPS, spinal cord lesions were made 2 hours post treatment (72hpf). The larvae then stayed in LPS until the next morning (93hpf), when LPS was removed. The injured larvae were then fixed at 99hpf and stained with DAPI (not shown). A full outline of the treatment regime can be seen in Figure 4.21a. In publications, LPS is usually applied at 50ng-100ng/ml concentration (Gurevich *et al.*, 2018; Tsarouchas *et al.*, 2018). However, in our hands, these

concentrations were lethal for the larvae, thus two alternative concentrations were used; 25ng (Figure 4.21b',c') and 37.5ng (Figure 4.21b'',c''). In the inflammation scenario, axonal connections and macrophage migration become indistinguishable between WT and *flt1* LOF injured larvae (Figure 4.21 d-e). Thus, enhancing the immune system could aid in overwriting the effect of *vegfa* GOF/*flt1* LOF scenarios.
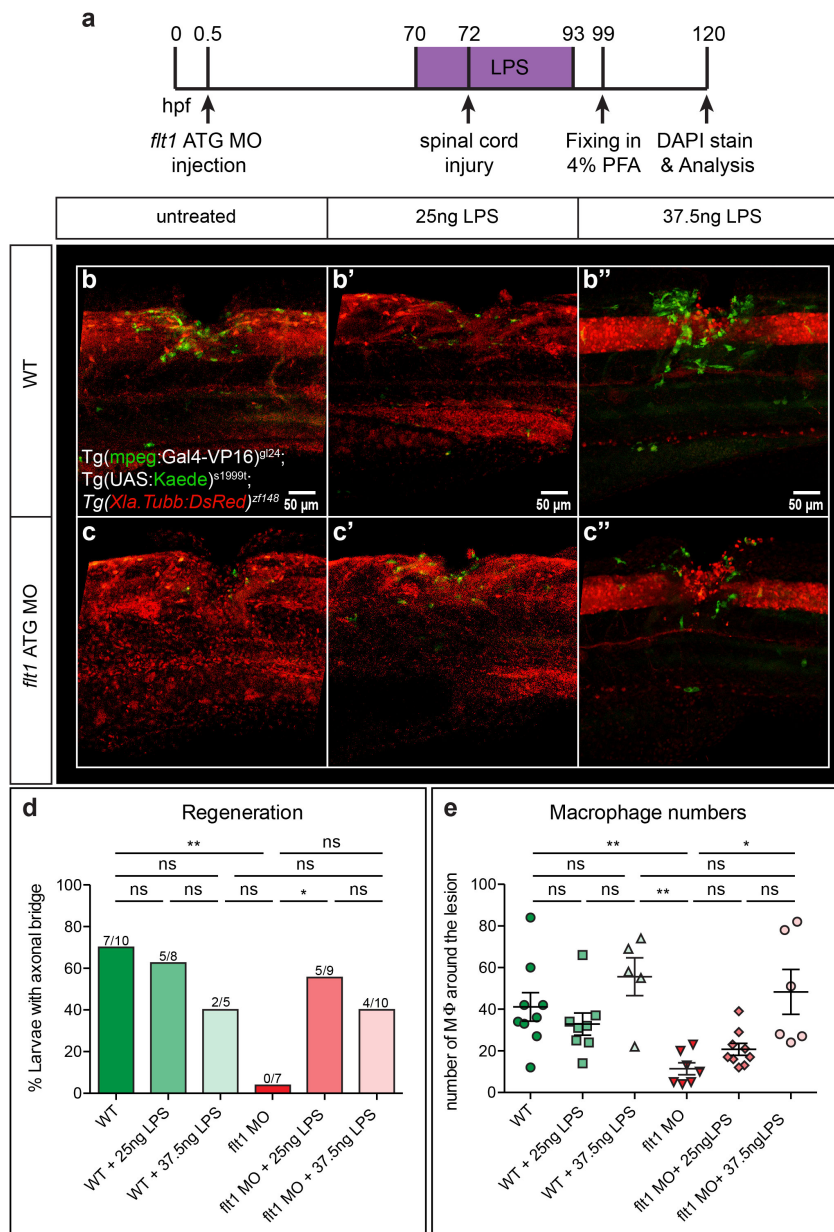

Figure 4. 21: Enhancing the immune systems boosts axonal regeneration.

(a) Timeline outlining LPS administration. **(b'-b'')** Lesioned WT *Tg(mpeg:Gal4-VP16)^{gl24}; Tg(UAS:KAEDE)^{s1999t} ; Tg(Xla.Tubb:DsRed)^{zf148}* larvae treated with LPS at two different concentrations; 25ng (b') and 37.5ng Neurons are shown in red and macrophages in green. (b''). **(c-c'')** Lesioned *flt1*-ATG MO injected *Tg(mpeg:Gal4-VP16)^{gl24}; Tg(UAS:KAEDE)^{s1999t} ; Tg(Xla.Tubb:DsRed)^{zf148}* larvae treated with LPS at two different concentrations; 25ng (c') and 37.5ng, (c''), are able to establish some

axonal connections. Neurons are shown in red and macrophages in green. **(d)** Quantitative analysis shows the percentage of larvae with axonal bridges at 99hpf. Fisher's exact test; Fractions show how many larvae regenerated per sample group; n.s.=non-significant; *P<0.05; **P<0.01. **(e)** Quantitative analysis of the number of macrophages migrating to the wound at 99hpf. Kruskal-Wallis test ± s.e.m, n(WT_untreated)=9; n(WT + 25ng LPS)=8; n(WT + 37.5ng LPS)=5; n(*flt1* MO_untreated)=7; n(*flt1* MO + 25ng LPS)=9; n(*flt1* MO + 37.5ng LPS)=6; n.s.=non-significant; *P<0.05; **P<0.01. WT=wild-type; MO=morpholino; hpf=hours post fertilization; LPS=bacterial lipopolysaccharides; MΦ=Macrophages; n.s.=non-significant; Scale bar 50μm.

These results highlight the complexity by which *vegfa* guides axonal regeneration. Vegfa signalling was previously proposed to act on astroglia activation and associated inflammatory responses (Boer *et al.*, 2008). Interestingly both macrophages and glia can express inducible NO synthase (iNOS)-derived Nitric oxide (NO) in response to inflammation and degeneration (de Almeida-Leite *et al.*, 2014). One possible explanation for the enhanced regeneration in LPS treated larvae could be the induction of NO and immune responses upon LPS treatment.

Another way of rescuing the inflammatory response is through bone marrow transplants from the WT larvae to the mutant. Unfortunately, zebrafish don't have a bone marrow for that to be feasible (Jingd and Zon, 2011). Cell transplantation is also not possible as the macrophage population is not as abundant as neuronal or EC populations (Wild *et al.*, 2017). To solve this, we decided to use parabiosis and fuse the WT with the *flt1*^ka604 mutants embryos (Hagedorn *et al.*, 2016). Macrophages should be therefore able to move through the shared vasculature from the WT larvae to the mutant and rescue the neuronal phenotype. Indeed, after multiple attempts, two larvae were successfully fused together. This fusion can be seen on Figure 2.22a-b, where the two larvae heads are fused. For the purpose of this experiment, a WT *Tg(mpeg:Gal4-VP16)*^gl24*; Tg(UAS:KAEDE)*^s1999t*; Tg(Xla.Tubb:DsRed)*^zf148 , was fused to a *flt1*^ka604 *Tg(Xla.Tubb:DsRed)*^zf148*; Tg(kdrl:EGFP)*^s843. A WT macrophage transgenic; *Tg(mpeg:Gal4-VP16)*^gl24*; Tg(UAS:KAEDE)*^s1999t, was used to visualize the WT-origin macrophages migration. As for the *flt1*^ka604 a neuronal transgenic; *Tg(Xla.Tubb:DsRed)*^zf148, was used to visualize mature neurons, and a vessel transgenic; *Tg(kdrl:EGFP)*^s843 to visualize the tertiary sprouts.

Spinal cord regeneration was successfully restored to almost WT levels, in the fused *flt1^{ka604}* mutants at both 1dpl (Figure 4.22c,g) and 2dpl (Figure 4.22d,g'). Interestingly, the number of tertiary sprouts also decreased both at 1dpl (Figure 4.22h) and 2dpl (Figure 4.22h'). This pioneer experiment raises some questions on whether, apart from macrophages, *sflt1* could also travel through the fused vasculature. If this is the case, then *sflt1* could be the key player in this rescue experiment. Last but not least, the number of WT macrophages traveling through to the *flt1^{ka604}* are not a lot, but perhaps in combination with the already present *flt1^{ka604}* (not visible in this experiment) be enough to boost regeneration.

Overall these results indicate an impaired macrophage migration in *vegfaa* overexpression scenario, as Vegfa overexpression might diminish the gradient over which macrophages can successfully travel across the wound. We also show that macrophages do not seem to be functionally affected, as boosting the inflammatory response, enhanced their migration and recapitulated axonal connections. Macrophages were previously suggested to influence glia progenitor proliferation, and boosting the immune system with LPS further enhanced their proliferation state (Wu *et al.*, 2010). One possible explanation could thus be a synergistic effect of both glia and macrophage processes in inducing neuroregeneration, both of which are regulated via the Vegfa and sFlt1.
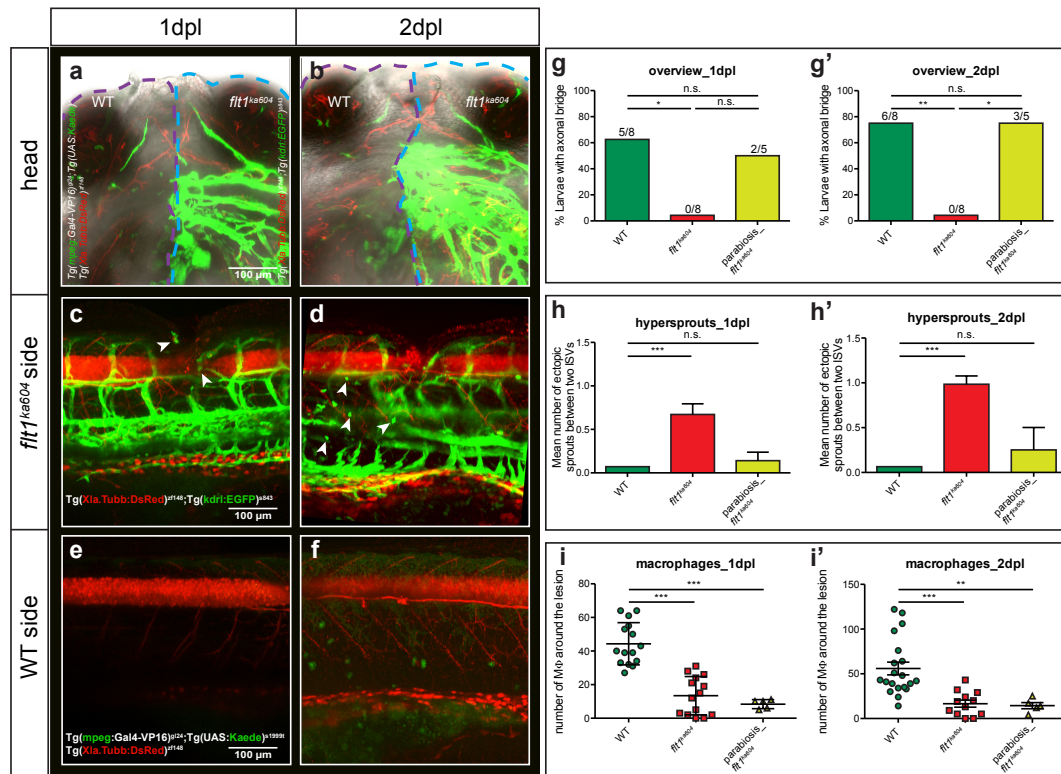
Figure 4. 22: Transplanting WT macrophages back into the *flt1^ka604* rescues the phenotype.

(a-a') Brightfield head images of WT *Tg(mpeg:Gal4-VP16)^gl24; Tg(UAS:KAEDE)^s1999t; Tg(Xla.Tubb:DsRed)^zf148*, fused to a *flt1^ka604 Tg(Xla.Tubb:DsRed)^zf148; Tg(kdrl:EGFP)^s843* at 1dpl (a) and 2dpl (b). The brightfield channel was merged with the transgenic channels to give an overview of the different transgenics in the fused heads. On the left-hand side, outlined with a purple dotted line, is the WT larvae (red neurons and green macrophages) and on the right-hand side, outlined with an orange dotted line, is the *flt1^ka604* (red neurons, green vessels). Note that some macrophages have already crossed over to the *flt1^ka604* side (visible in the eye regions) **(c-d)** Images of the lesioned *flt1^ka604 Tg(Xla.Tubb:DsRed)^zf148; Tg(kdrl:EGFP)^s843* side indicate axonal regeneration and a rescue of the vascular phenotype (less tertiary sprouts). White arrowheads indicate the migrating WT macrophages. **(e-f)** Images of the unlesioned WT *Tg(mpeg:Gal4-VP16)^gl24; Tg(UAS:KAEDE)^s1999t; Tg(Xla.Tubb:DsRed)^zf148* side **(g-g')** Quantitative analysis shows the percentage of larvae with axonal bridges at 1dpl (g) and 2dpl (g'). Fisher's exact test; Fractions show how many larvae regenerated per sample group; n.s.=non-significant; *P<0.05; **P<0.01. **(h-h')** Quantitative analysis of the average number of ectopic sprouts per two ISVs per larvae at 1dpl (h) and 2dpl (h'). Kruskal-Wallis test ± s.e.m, n(WT_1dpl)=10; n(*flt1^ka604*_1dpl)=7; n(parabiosis_*flt1^ka604*_1dpl)=5; n(WT_2dpl)=11; n(*flt1^ka604*_2dpl)=11; n(parabiosis_*flt1^ka604*_2dpl)=5; n.s.=non-significant; ***P < 0.001 **(i-i')** Quantitative analysis of the number of macrophages migrating to the wound at 1dpl (i) and 2dpl (i'). Kruskal-Wallis test ± s.e.m, n(WT_1dpl)=15; n(*flt1^ka604*_1dpl)=14; n(parabiosis_*flt1^ka604*_1dpl)=5; n(WT_2dpl)=20; n(*flt1^ka604*_2dpl)=12; n(parabiosis_*flt1^ka604*_2dpl)=5; **P<0.01; ***P < 0.001. WT=wild-type; dpl=days post lesion; MΦ=Macrophages; n.s.=non-significant; Scale bar 100μm.

5   Discussion

The nervous system is of vital importance to life, as it determines how we feel and perceive the world around us (Chambers, Sandoval and Seeley, 2013). One of its more crucial functions is its involvement in skeletal muscle contraction and body movement (Ng, Brack and Coote, 2001; P Ko, 2001; Hanna *et al.*, 2017). This is particularly evident in amyotrophic lateral sclerosis; ALS, Alzheimer's disease; AD and Parkinson disease; PD, where neuronal degeneration leads to paralysis and tremors (Dugger and Dickson, 2017). Studying the onset of neurodegeneration is fairly difficult in these diseases, thus other models, such external traumas, could be used instead to decipher how neuronal degeneration is initiated (Conforti, Gilley and Coleman, 2014). Despite the severity of neurodegenerative diseases and spinal cord injuries, our understanding of the nervous system is very limited, thus impeding our ability to decipher future therapeutic approaches.

Recent evidence suggests that development and branching of the neuronal and vascular system shares many similarities including the principle of directed guidance and common molecular cues. Molecules that share a function in both systems are termed angioneurins (Zacchigna, Lambrechts and Carmeliet, 2008). Interestingly, recent reports suggest that factors affecting vascular development have impact on the growth and survival of motor neurons in experimental models for ALS (Oosthuyse *et al.*, 2001). This led to the concept that such vascular growth factors may be used or targeted to improve neuronal regeneration and prevent regression.

VEGF-A, a pro-angiogenic factor, has been shown to be an important regulator in axonal guidance and neurogenesis (Zacchigna, Lambrechts and Carmeliet, 2008). It was also associated with ALS as low *Vegfa* levels lead to MN degeneration (Oosthuyse *et al.*, 2001; Lambrechts, Storkebaum, Morimoto, Del-Favero, *et al.*, 2003).

Vascular endothelial growth factor; VEGF, is the principle regulator of vascular development. In the vasculature Vegf levels have to be well titrated as loss and gain-of-function Vegf result in embryonic lethality due to aberrant vascular remodelling (Carmeliet *et al.*, 1996; Miquerol, Langille and Nagy, 2000; Oosthuyse *et al.*, 2001).

One way to achieve fine-tuning of local Vegf levels in the vasculature involves soluble Vegf receptor 1/Flt1. Flt1 is spliced in a membrane bound mFlt1 form with weak signalling properties and a soluble Flt1 (sFlt1) which lacks the transmembrane and intracellular domain of mFlt1. sFlt1 has a high affinity for Vegf and acts as a Vegf trap, thereby reducing Vegf bio-availability and signalling through Vegf receptor 2/Kdr(l). Neurons also express Vegf and sFlt1, and at the neurovascular interface the balance between these two factors regulates the onset and extent of, for example, spinal cord vascularization (Wild *et al.*, 2017).

One outstanding question in the field is whether Vegf can be safely used as therapeutic agent, as studies in the vascular system show that too much Vegf at the wrong place causes adverse conditions like hemangiomas and tumor like structures (Carmeliet, 2005). It is actually currently not known how Vegf levels need to be regulated in the nervous system in order to achieve proper growth and patterning. It is furthermore not clear which role Flt1 may play herein and whether this is solely due to Flt1's scavenging function, or whether it also involved a part regulated by mFlt1 signalling.

The zebrafish has the extraordinary capacity to regenerate organs like heart, brain, spinal cord and fins throughout life. As the developing zebrafish spinal cord expresses both Vegf and Flt1 we employed the spinal cord lesion model. To address the role of Flt1 and its ligands including Vegfa, Plgf and Vegfb, we generated Flt1 loss and gain-of-function models, and Flt1 ligand (Vegfa, Plgf, Vegfb) gain and loss-of-function models. Systematic analysis of these mutants and transgenics shows that Flt1 and Flt1 ligands are essential for mediating spinal cord regeneration in the zebrafish embryo. Our data suggest that spinal cord regeneration requires precise fine-tuning of Vegf/Kdr(l) signalling (not Nrp1 nor mFlt1) mediated by neuronal sFlt1. We show that sFlt1 exerts control over modulating glia bridging and macrophage invasion at the spinal cord lesion site. Targeting local Vegf levels with Flt1 may be beneficial to uncover the full therapeutic neuroprotective potency of Vegf.

5.1 The neuroprotective function of Flt1 depends on Vegfaa/Kdrl signalling

The CNS has very high energy demands and thus relies on a robust vasculature for its proper function (Paredes, Himmels and Ruiz de Almodovar, 2018). Wild et al. has

recently shown that *vegfaa* and neuronal *sflt1* coordinate the vascularization of the spinal cord (Wild *et al.*, 2017). In the present study, we asked whether similar signalling events might also coordinate nerve regrowth during spinal cord regeneration in an injury model.

To investigate this, we decided to first look how regeneration is affected in *flt1* LOF scenarios. In our setting, muscle and fin clip injuries in *flt1* LOF model had no impact on the overall tissue regeneration. However, upon spinal cord injury, we observed a defect in the neuron's ability to regenerate over the wound. This effect could either be attributed to the increased *vegfa* levels or due to mFlt1 signalling. To test if this regeneration defect is due to the tyrosine kinase signalling component, *mflt1* single mutants, where both the extracellular and intracellular component is missing, were used. Contradicting to previous publications (Poesen *et al.*, 2008), we observed no regeneration defects in our *mflt1* single mutants post spinal cord injury. This could suggest that the key contributor in spinal cord regeneration is the sFlt1. As the mFlt1 signalling component was excluded, we hypothesize that this phenotype is driven via the Vegf/Kdrl signalling.

Neuronal sFlt1 and Vegfaa have been already shown to induce the spinal cord vascularization (Wild *et al.*, 2017). Based on this finding, we decided to look if the defective neurogenesis is linked to neuronal Flt1. Indeed, ablation of the neuronal *flt1* showed a similar neuronal defective phenotype as the *flt1* mutant. In both neuronal *flt1* ablation and in *flt1* mutants, the neurons were unable to regenerate. Thus, in addition to being the key player in spinal cord vascularization (Wild *et al.*, 2017), neuronal *flt1* is also important for nerve regeneration. To specifically check if the neuronal sFlt1 is enough to recapitulate axonal connections, we used an inducible neuronal specific *sflt1* GOF line and showed that even slight overexpression of the neuronal sFlt1 was enough to rescue the *flt1* mutant defective phenotype. We thus conclude that the neuronal sFlt1/Vegfa relationship is important in both spinal cord vascularization and also during axonal regeneration.

Vegfa can induce axonal pathfinding through binding to either Kdr or Nrp1 receptor (Cariboni *et al.*, 2011; Erskine *et al.*, 2011, 2017; Ruiz de Almodovar *et al.*, 2011). To

decipher which pathway is important in our setting we modulated the Vegfa, Krdl and Nrp1 levels. First, to lower the *vegfa* levels in the *flt1* full mutants, we injected the larvae with a *vegfaa* MO. By lowering the *vegfa* levels we observed a complete rescue of the defective neuronal phenotype, suggesting that Vegfa needs to be tightly titrated for correct axonal regeneration. We thus wanted to test if the Vegfa acts through its Kdrl receptor. To do so, we then inhibited the VEGFR2/Kdrl in the *flt1* full mutant using a VEGFR2 inhibitor. Indeed, inhibition of the Kdrl receptor, offered a partial rescue of the axonal connections in the *flt1* mutant. To further test for Nrp1, we used both *nrp1a* and *nrp1b* single and double mutants, to exclude for any compensation between the two isoforms. Surprisingly, axonal regeneration was unaffected in either *nrp1a, nrp1b* single or double mutants, further verifying that the defective axonal phenotype is guided by neuronal sFlt1 expression acting on the Vegf/Kdrl signalling.

5.2   Neuronal regeneration is impaired in *flt1* mutants

Results so far indicate a reduced axonal regeneration post spinal cord injury in *flt1* mutants. As Flt1 was shown to be expressed in MNs, sensory neurons and most but not all astrocytes (most abundant glia cell type), we decided to investigate how these neuronal populations are affected in our *flt1* mutant (Mani *et al.*, 2005; Storkebaum *et al.*, 2005; Poesen *et al.*, 2008; Dhondt *et al.*, 2011; Selvaraj *et al.*, 2015; Wild *et al.*, 2017).

We first decided to look on the MN population, as they are the key neuronal population governing spinal cord regeneration. We first showed that MN regeneration is decreased in *flt1* mutant. To check if this decrease in MNs was due to cell death or due to decreased MN regeneration, we used the EdU and TUNEL assays. Even though the apoptotic rate was unaffected, less MNs seem to be able to regenerate post spinal cord lesion in *flt1* mutant. This suggests a defect in MN generation and not a decreased number due to apoptosis (Figure 5.2). We suggest that this decrease in MNs is attributed to the sFlt1, which contradicts recent data which show that VEGF-B acts as a MN neuroprotective factor via binding to mFlt1. In our setting we propose that sFlt1 is rather acting as a MN growth factor through the Vegf/Kdrl signalling (Poesen *et al.*, 2008).

A similar effect was also observed in HuC/D+ neurons (neuronal precursor cell population) suggesting that Flt1 affects both during early and late neuronal differentiation. This is also consistent with Krueger et al, where they showed that *flt1* LOF, decreased the number of HuC positive neurons (Krueger *et al.*, 2011).

Another aspect to investigate is the origin of these MN cells. After a spinal cord lesion adult zebrafish, there is an increase of slowly proliferating oligodendrocytes positive ependymo-radial glial cells (ERGs-self renewal properties) into MNs (Reimer *et al.*, 2008). A similar observation was also seen in zebrafish larvae, where within 2dpl, the progenitor MN domain switches into generating MNs at the expense of oligodendrocytes (Ohnmacht *et al.*, 2016). Interestingly, KDR was found in oligodendrocyte precursor cells and VEGF could promote their migration in a concentration-dependent manner (Hayakawa *et al.*, 2011). Therefore, it would be interesting to also check how oligodendrocytes are affected in *flt1* mutants and whether the proliferating MNs originate from oligodendrocytes (Figure 5.1).
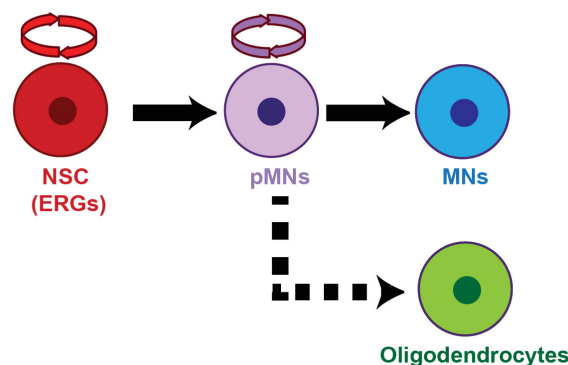
Figure 5. 1: ERGs and MN generation.

Upon spinal cord injury, the pMNs switch to MN generation at the expense of oligodendeocytes. ERGs=ependymo-radial glial cells; pMNs=progenitor motor neurons; MNs=motor neurons.

As functional recovery after spinal cord injury includes the regain of motility to the extremities and locomotion depends on both MN and the sensory neuron interactions, we decided to also look how this neuronal population is affected in the *flt1* mutants. Surprisingly, sensory neuron proliferation was unaffected after a spinal cord injury. However, a significant decrease in their apoptotic rate was observed in *flt1* mutants. This suggests a neuroprotective role for Flt1 in sensory neurons (Figure 5.2).

It has recently been published that partial elimination of sensory neurons led to MN defasciculating towards the limb, while MN elimination had minimal influence on sensory neuron patterning (Huettl *et al.*, 2011). As Flt1, is expressed in both MNs and sensory neurons, we hypothesize that a similar effect is observed in *flt1* mutants. MN and sensory neuron specific Flt1 loss of function lines could further verify if this inter-axonal signalling between MNs and sensory neurons is also induced via Flt1.

5.3   Glia bridges are impaired in *flt1* mutants

After a spinal cord injury, the regenerated axons need a scaffold or a platform over which they can 'bridge' across and re-connect with the axons on the opposite end of the lesion. To do so, they need to travel over a non-neural environment. Goldshmit et al. showed that glia, activated by FGF, grow across the wound, providing a path for the axons to grow across (Goldshmit *et al.*, 2012). Interestingly, in zebrafish, radial glia ablation, led to ectopic sprout formation around the neural tube. This effect was then attributed to the loss of sFlt1 (Matsuoka *et al.*, 2016). Indeed, glia coverage and bridges were significantly impaired in *flt1* mutants. This is consistent with other publications as inhibition of *flt1* led to a significant decrease of GFAP immunoreactivity (Mani *et al.*, 2005). Interestingly, mouse explants showed that *flt1,* but not *kdr,* is present in astrocytes (Mani *et al.*, 2005), which could suggest why the *flt1* mutants have a more severe phenotype than the other *vegfaa* GOF scenarios. Our study thus reveals that signalling via mFlt1 is not important, but instead regulating Vegfa levels by sFlt1 is the key player in both spinal cord vascularization and glia bridging.

As some axons, in WT larvae, were still able to grow across prior to any glia formation, we propose that this is due to the collagen scaffold which aids axonal regeneration across the wound in the absence of glia (Wehner *et al.*, 2017). However, as we did not find any significant changes in collagen bridging we suggest that glia is the main driver for axonal regeneration under our settings.
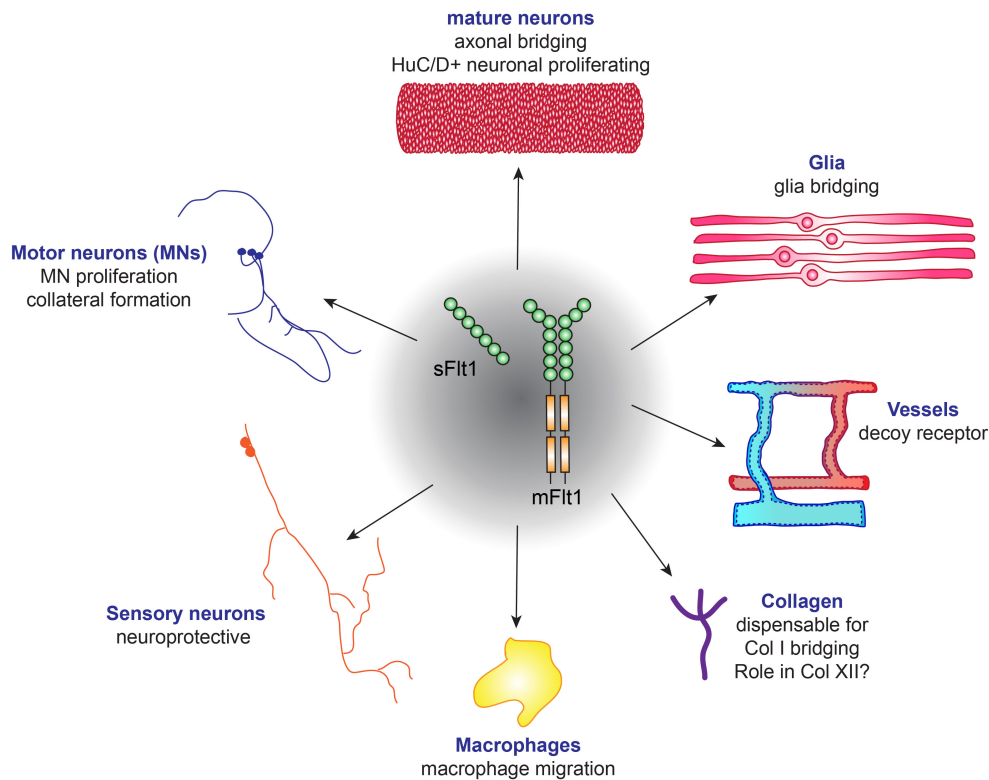
Figure 5. 2: Summary of Flt1 functions in different cell populations.

Schematic illustration of the pleiotropic actions of Flt1. Despite acting as a scavenger receptor in vessels, it is important for neuroregeneration and is neuroprotective in various neuronal populations. It is also involved in macrophage migration. Furthermore, it seems to be dispensable for collagen bridging.

5.4   Axonal bridging and collateral formation

The results so far demonstrate that the neuroprotective function of Flt1 is due to the regulation of Vegfa/Kdrl signalling. VEGF-A is an angioneurin, meaning that is not only a key contributor of angiogenesis but can also exert neuronal growth and neuroregenerative functions (Zacchigna, Lambrechts and Carmeliet, 2008). It has also been implicated in the axonal guidance and neurogenesis (Zacchigna, Lambrechts and Carmeliet, 2008). While some studies describe VEGF-A to be neuroprotective against MN degeneration (Oosthuyse *et al.*, 2001; Lambrechts, Storkebaum, Morimoto, Del-Favero, *et al.*, 2003), other studies show that VEGF-A/VEGFR2 need to be tightly titrated for proper dendritogenesis and axonal branching (Luck *et al.*, 2019). Thus VEGF-A/VEGFR2 could act as a bimodal regulator, similarly to Sema3A which has a positive effect on dendritogenesis and an inhibitory function on axonal growth (Luck *et al.*, 2019).

110

To investigate whether axonal impairment is conserved in other *vegfaa* GOF models, we decided to use the *vhl* mutant (Van Rooijen *et al.*, 2009), as it also presents hypersprouting around the spinal cord, yet is independent of Flt1. In this mutant, a hypoxia-induced *vegfaa* transcription is observed, similar to the one observed in the mouse models (Oosthuyse *et al.*, 2001; Pugh and Ratcliffe, 2003; Van Rooijen *et al.*, 2010). Axonal bridging across the wound was unaffected in *vhl* mutants, however collateral MN formation was impaired in a similar manner to the *flt1* mutants (Figure 5.3). This does not rule out that *vegfaa* could be neuroprotective, but it does raise some questions on its applicability in long term functional recovery. It is also likely that other angiogenic growth factors, apart from VEGF-A, such as angiopoietin-2, platelet-derived growth factor and CXC chemokine receptor 4, are also expressed in the *vhl* mutant which could further influence axonal bridging (Pugh and Ratcliffe, 2003; Van Rooijen *et al.*, 2010).
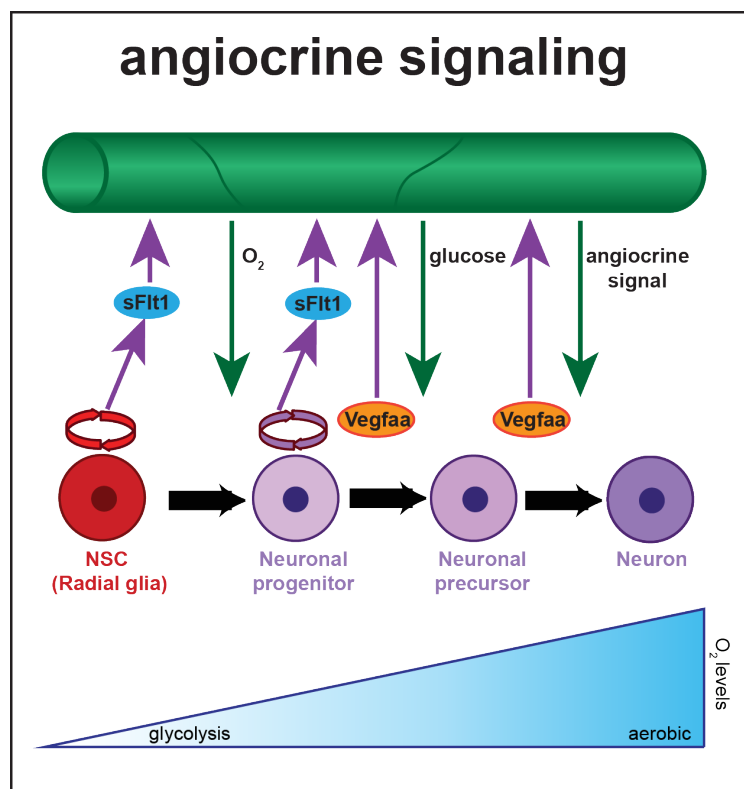
Figure 5. 3: sFlt1 functions acts in early neuronal cell populations under hypoxic conditions.

Schematic illustration of the angiocrine signalling between blood vessels (green tube) and neuronal development. sFlt1 seems to be important in radial glia and neuronal progenitor cell (NPC) proliferation under low oxygen levels, while acting as a decoy receptor in the vasculature. Vegfaa gets re-deployed at later stages in neuronal development to influence NPCs differentiation to neuronal precursors and neurons. Vegfaa elevation induces ectopic sprouting later on in development and in turn increases the oxygen availability. NSC=Neuronal stem cells; NPCs=Neuronal progenitor cells; O_2=oxygen.

Flt1, apart from binding to VEGF-A, can also bind to two other ligands; PlGF and VEGF-B (Autiero *et al.*, 2003; Olsson *et al.*, 2006). Overexpression of these two ligands, could also induce a *vegfaa* GOF scenario, as they compete Vegfa from binding to Flt1. Despite the fact that *plgf* GOF had no effect on the MN patterning under physiological conditions, we observed some degree of MN defects post injury. Even though axonal bridging was enhanced at 2dpl in *plgf* GOF (91%) compared to the *flt1* full mutant (15%), collateral MN formation was equally decreased.

plgf mutants had decreased axonal branching (50% at 2dpl), but no significant defect in collateral MN formation. These results could further verify that *vegfaa* levels are important for initial but not functional recovery and that Vegfa needs to be tightly regulated for correct axonal regeneration.

Similar to *plgf* GOF, *vegfba* GOF also had no effect on MN patterning under physiological conditions (Alina Klems, unpublished). Interestingly, upon spinal cord lesion, both *vegfba* loss and GOF scenarios show impaired glia bridges. These results could indicate a possible function of *vegfba* in regulating glia formation. Further tests need to be carried out to identify whether this function is through the Flt1 receptor as well. However, as *vegfa* MO injections and the VEGFR2 Kinase inhibitor; ki8751, rescued axonal bridging in the *flt1* mutant, the main pathway affecting regeneration seems to rather be the Vegfa/Kdrl signalling.
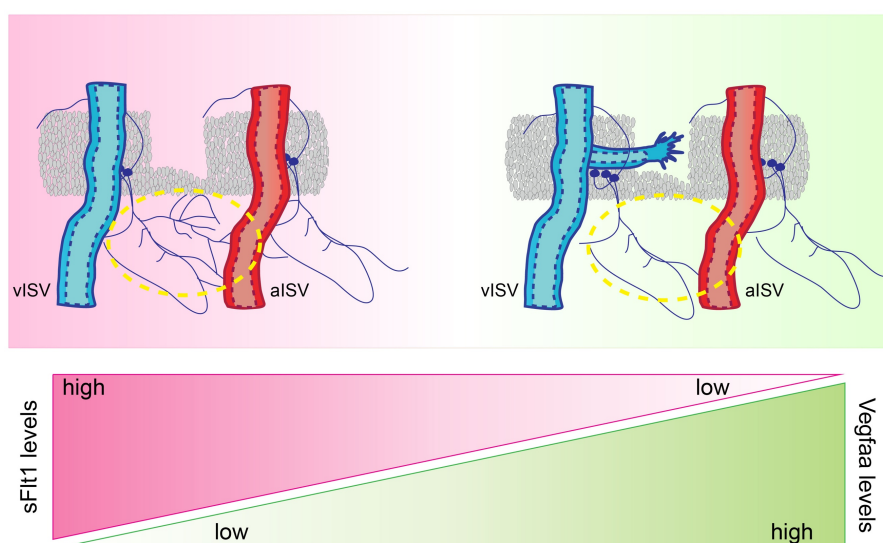
Figure 5. 4: Vegfaa/sFlt1 levels need to be tightly regulated for functional recovery.

Schematic illustration of the axonal connections (in grey) at high sFlt1/low Vegfaa levels (pink panel) versus low sFlt1/high Vegfaa levels (green panels). Low Vegfaa levels partially impairs axonal regeneration but not collateral formation (left panel), while high Vegfaa levels enhance axonal regeneration at the expense of collaterals (right panel). Yellow dotter circles indicate the collaterals under the spinal cord injury. vISV=venous intersegmental vessel; aISV=arterial intersegmental vessel.

Irrespective of the glia bridging impairment, *vegfba* GOF could still form axonal bridges similarly to the other *vegfaa* GOF scenarios; *plgf* GOF and *vhl* mutants, while *flt1* mutants exhibited the most severe phenotype, with no axonal bridging nor collateral MN formation. This could suggest a dual function of *flt1* both in inducing a *vegfaa* GOF scenario with also direct effects on glia formation. In order to test glia formation further, we decided to look on macrophages, as they were previously suggested to influence glia progenitor proliferation (Wu *et al.*, 2010).

5.5   Changes in macrophage behaviour

Macrophages are well known contributors in wound healing and recently in guiding axonal bridging post spinal cord injury in zebrafish larvae (Tsarouchas *et al.*, 2018). As fin clip and spinal cord injury data identified macrophages, but not neutrophils, as important modulators of wound repair, this study solely focuses on the role of macrophages (Petrie *et al.*, 2015; Tsarouchas *et al.*, 2018). Previously we identified that *flt1* LOF impairs neuronal but not tissue regeneration. To test if this is also linked with macrophage migration, the number of migrating macrophages post muscle, fin and spinal cord injury were also measured. In accordance with our previous findings, we identified no macrophage migration impairments in the muscle or fin clip injuries, but a significant decrease in migration upon neuronal injury.

VEGF-A and PlGF have both been implicated in inducing macrophage migration through the Flt1 receptor (Barleon *et al.*, 1996; Muramatsu *et al.*, 2010). We thus went on to investigate macrophage migration in both *plgf* mutants and *plgf* GOF scenarios. As expected, in *plgf* mutants, there was a decrease in macrophage migration post spinal cord injury. Surprisingly, overexpression of *plgf* had similar macrophage migration defects as the mutant phenotype. This could be attributed to the high *vegfaa* bioavailability in *plgf* GOF larvae, similar to the *flt1* LOF, impairing the *vegfaa* gradient over which macrophages are guided through.

We further wanted to identify if the 'wave' of macrophage migration to the wound is pro-/anti- inflammatory. Tsarouchas et al. showed that even though pro-inflammatory macrophages are important during initial stages of spinal cord regeneration, prolonged exposure impaired axonal regeneration (Tsarouchas *et al.*, 2018). To decipher this, we used two pro- and two anti-inflammatory cytokines to observed macrophage migration during early (18hpl) and late (48hpl) regeneration phase. While, pro-inflammatory cytokines showed a similar activity to the WT controls, one of the anti-inflammatory cytokines (*tgf-β1a*) was overexpressed during the early (18hpl) regeneration phase in both lesioned and unlesioned *flt1* mutants. This could be linked to the *vegfaa* constitutive overexpression in *flt1* mutants, as VEGF has been previously shown to induce the M1-M2 switch, favouring the M2 (anti-inflammatory) macrophages (Wheeler *et al.*, 2018).

To make sure that the sole malfunction of macrophages in *flt1* LOF scenario, is their migration capacity, we decided to use LPS to 'boost' the immune system in an attempt to induce a rescue. LPS was shown to enhance the immune system and to accelerate axonal regrowth in WT larvae (Gurevich *et al.*, 2018; Tsarouchas *et al.*, 2018). In our setting, LPS could recapitulate, to some extent, both macrophage migration to the wound and enhanced axonal regrowth in the *flt1* LOF scenario. This would verify that macrophages are not fundamentally impaired in *vegfaa* GOF scenarios, but rather their migratory activity is misguided or altered due to the high *vegfaa* bioavailability. Interestingly macrophages and glia were previously shown to express inducible NO synthase (iNOS)-derived Nitric oxide (NO) in response to inflammation and degeneration (de Almeida-Leite *et al.*, 2014). Therefore, this enhanced regeneration in LPS treated larvae could be the induction of NO and immune responses upon LPS treatment.

It would further be interesting to observe what would happen if we re-introduced WT macrophages back into the *flt1* mutants. As zebrafish don't have a bone marrow, a bone marrow transplant was not feasible (Jingd and Zon, 2011). Cell transplantation was also ruled out as the macrophage population is not as abundant as the neuronal or EC population (Wild *et al.*, 2017). For that purpose, we decided to deploy the parabiosis method, in order to fuse the WT and the *flt1* full mutante together (Hagedorn

et al., 2016). Interestingly, macrophages were able to move from the WT larvae all the way to the *flt1* mutant larvae in a fused pair, and repair axonal regeneration in the *flt1* mutant side. One should note that, the ectopic sprouts observed in the *flt1* mutant were also diminished upon fusion. This raises some questions on whether not only macrophages, but also *sflt1* can also pass through the circulation and into the *flt1* mutant. Further experiments are required to decipher if it is indeed the effect of macrophages, *sflt1* or a combination of both which leads to successful axonal recovery.

5.6   Differences in Vegf receptor expression exist between neurons and ECs

In this study we observe different regulatory properties of the VEGF-A and its two receptors; VEGFR1 (Flt1) and VEGFR2 (KDR/Kdrl) between angiogenesis and neurogenesis. In *vegfaa* GOF scenarios, *vegfaa* levels induce a hypersprouting phenotype in vessels, but are detrimental for collateral MN formation. On the contrary, low *vegfaa* levels induce thinner vessels, while decreasing the *vegfaa* levels in *flt1* mutants rescues the phenotype. What could be different in the receptor expression levels between vessels and neurons? What are the intracellular signalling pathways involved in angiogenesis versus neurogenesis?

In the vasculature, VEGF-A acts through the VEGFR2 receptor to induce angiogenesis (Wild *et al.*, 2017). Similarly, VEGF-A binding to VEGFR2 also serves as an axonal guidance cue (Ruiz de Almodovar *et al.*, 2011). Furthermore, VEGF-A could also guide axonal pathfinding through its NRP1 receptor (Erskine *et al.*, 2011), while in vessels NRP1 is essential for VEGF-A dependent arteriogenesis (Lanahan *et al.*, 2013).

Interestingly, *kdr/flk1* had no effect on astroglia growth and maturation, while inhibition of *flt1* decreases glia immunoreactivity. VEGF was shown to activate astrocytic *flt1,* and induce astrocyte proliferation, differentiation and maturation through the MAPK/PI-3 kinase downstream pathways (Mani *et al.*, 2005). On the contrary, combined action of VEGFR2 with the MAP kinase pathways are responsible for the maintenance of EC integrity (Zhong *et al.*, 2011). Furthermore, while VEGFR1 induces glia differentiation via binding to VEGF-A, through the MAPK/PI3K pathway, it could also induce EC differentiation through the PI3K/Akt pathway (Koch *et al.*, 2011). Additionally, EC

proliferation is controlled via VEGF-A/VEGFR2 binding, and downstream induction of the ERK (extracellular-signal-regulated kinase) pathway. While VEGFR1 (Flt1) acts as a negative regulator of angiogenesis, it has a positive effect in monocyte chemotaxis. This occurs through the VEGF-B and PlGF ligands, which induce downstream signalling pathways such as ERK, MAPK, PI3K/Akt and p38MAPK (Koch *et al.*, 2011). VEGF-A and PlGF can also induce macrophage migration by binding to VEGFR1 (Flt1) (Barleon *et al.*, 1996; Muramatsu *et al.*, 2010). EC motility, on the other hand, is modulated via VEGF-A/VEGFR2 binding, leading to the GAB1 recruitment and in turn PIP$_3$ (phosphatidylinositol 3,4,5-triphosphate) production, to activate Rac (Koch *et al.*, 2011).
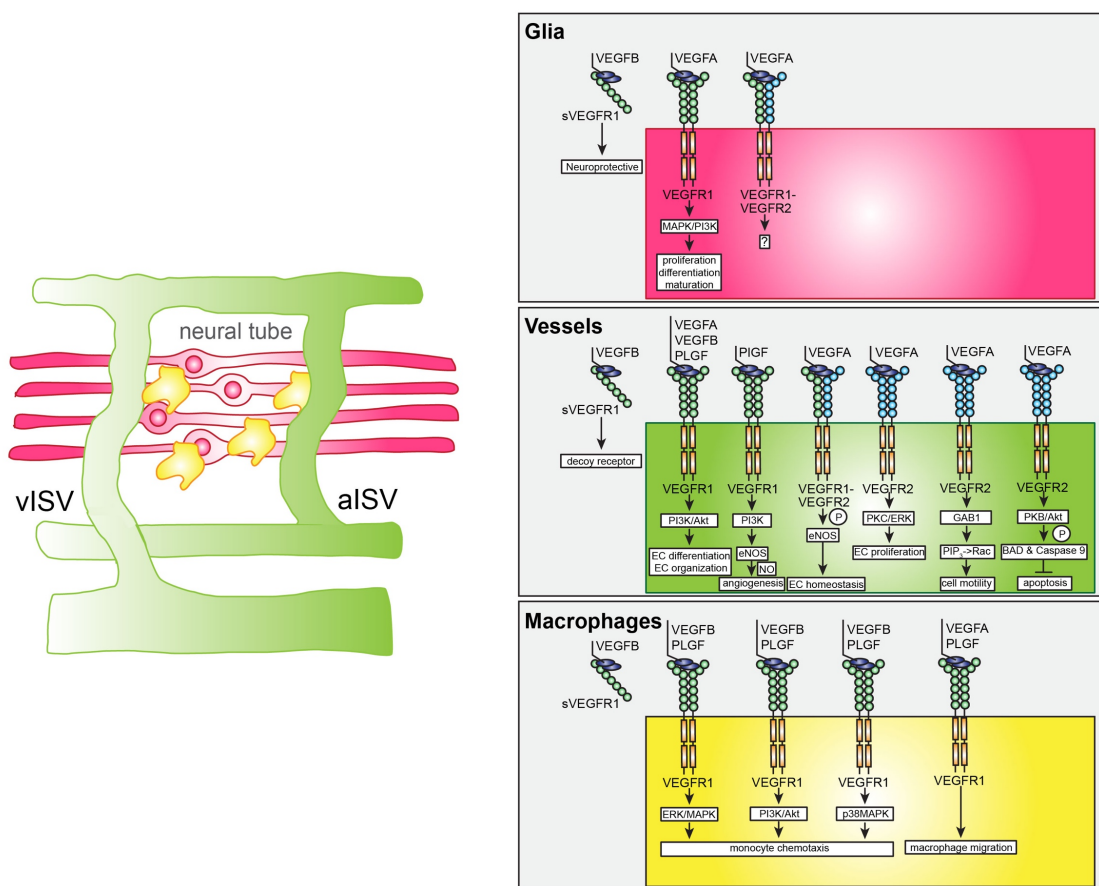
Figure 5. 5: Literature summary of all the intracellular signalling pathways in glia, vessel and macrophages.

Left panel: Schematic illustration of the glia (pink), vessels (green) and macrophages (yellow) at the neurovascular interface. Right panel: Downstream signalling pathways in respect to VEGFR-1/VEGFR-2 and their respective ligands in glia (pink), vessels (green) and macrophages (yellow). MAPK=mitogen-activated protein kinase; PI3K=phosphoinositide 3-kinase; ?=unknown function; Akt/PKB=protein kinase B; EC=Endothelial cell; eNOS=endothelial nitric oxide synthase; NO=nitric oxide;

P=phosphorylation; PKC=protein kinase C; ERK=extracellular signal-regulated kinases; GAB1=GRB2 (growth factor receptor-bound protein 2)-associated-binding protein 1; PIP$_3$=phosphatidylinositol (3,4,5)-trisphosphate; Rac= Ras-related C3 botulinum toxin substrate; BAD=Bcl-2-associated death promoter.

While cAMP signalling is important for determining axonal guidance in the olfactory bulb (Imai, Suzuki and Sakano, 2006; Schwartig and Henion, 2011), cAMP is detrimental for MNs post spinal cord injury (Cigliola, Becker and Poss, 2020). In fact, dopamine signalling activates the Hedgehog pathway, which is pivotal for MN regeneration, through inhibition of the cAMP/PKA activity (Reimer *et al.*, 2013). Future experiments will thus focus to decipher which other intracellular signalling pathways are affected in spinal cord lesions, and particularly in *vegfaa* GOF scenarios.

5.7   Clinical implications

Neurodegenerative diseases and neuronal injuries due to trauma lead to life-long paralysis and have a significant toll on the patient's quality of life (Oaklander and Horowitz, 2015; Dugger and Dickson, 2017). It thus raises the need for new personalized treatments in curing neuronal and neurodegenerative diseases. However, due to the lack of our basic understanding of the nervous systems, concepts such as neuronal plasticity and neuroregenerative capacities, impedes the design of rational therapeutic approaches, which could aid in these important medical areas. To improve the disease outcome in patients, one should first comprehend how neuronal degeneration can be prevented or reduced.

It is widely accepted that NSCs require a hypoxic (low oxygen) environment for their expansion. As spatio-temporal control of spinal cord vascularization is controlled by neuronal sFlt1-Vegfaa levels at the neurovascular interface (Wild *et al.*, 2017), we hypothesize that this will also affect neurogenesis. Indeed, high sFlt1 levels during the early stages of spinal cord development maintains a low vascular phenotype to permit stem cell functions, while later on, low sFlt1/ high Vegfaa levels attract blood vessels towards differentiating neurons (Figure 5.3). We hypothesize that radial glia, produce sFlt1 to prevent vascularization during the early stages of spinal cord development to ensure sufficient expansion of NSCs. Indeed, sFlt1 was shown to be essential for initiating glia projections post injury. We further showed that Flt1 is an important MN

and neuronal precursor cell growth factor, while exerting neuroprotective properties on sensory neurons. Therefore, sFlt1 seems to be important in neuronal development, stem cell numbers and neuronal regeneration.

Flt1 is a critical and essential regulator of regeneration. As Flt1 acts as a Vegfa trap, we decided to investigated the two Vegfa receptors linked to axonal pathfinding. We identify that Vegfa mainly acts through Kdrl and not via the Nrp1 receptor, as modulating either Vegfa levels (*vegfaa* MO) or pharmacologically inhibiting VEGFR2/Kdrl rescued the *flt1* mutant neuronal defective phenotype. While Vegfa has already been shown to exert neuroprotective effects on MNs, we show that the Vegfa levels need to be precisely well titrated for collateral MN formation and thus functional recovery.

We further suggest that sFlt1-Vegfa interactions exert their effect on both glia and macrophage populations upon spinal cord injury, as both cell populations were impaired in low sFlt1/high Vegfaa conditions. This further adds to the complexity by which Vegfa exerts its neuroprotective functions, suggesting a synergistic effect of both glia and macrophage processes in the process of neuroregeneration. Taken together, we propose that Vegfa regulation should be carefully re-evaluated in treating neurodegenerative diseases and spinal cord injuries.

6 Materials and Methods

6.1 Materials

Table 6. 1 Zebrafish transgenic reporter lines

Transgenic line	Fluorescent organs/cells	Publication
Tg(kdrl:GFP)[s843]	Green vascular reporter	(Jin *et al.*, 2005)
*Tg(kdrl:*Hsa.HRAS-mCherry)[s916]	Red vascular reporter	(Hogan *et al.*, 2009)
Tg(Xla.Tubb:DsRed)[zf148]	Red mature neuron reporter	(Peri and Nüsslein-Volhard, 2008)
TgBAC(gfap-GFP)[zf167]	Green glia reporter	(Chen, März and Strähle, 2009)
Tg(mnx1:mCherry)	Motor neuron reporter	(Panakova, unpublished)
Tg(-3.1ngn1:GFP)[sb2]	Sensory neuron reporter	(Blader, Plessy and Strähle, 2003)
Tg(huC:egfp)	Pan-neuronal reporter	(Park *et al.*, 2000)
Tg(mpeg1:GAL4-VP16)[gl24]; Tg(UAS-E1b:Kaede)[s1999t]	Macrophage reporter	(Ellett *et al.*, 2011)
Tg(mpeg1:EGFP)[gl22]	Macrophage reporter	(Ellett *et al.*, 2011)

Table 6. 2 Zebrafish mutant lines

Mutant line	Mutant allele	Publication
flt1[ka601]	flt1 exon3 -1nt	(Wild *et al.*, 2017)
flt1[ka604]	flt1 exon3 -14nt	(Wild *et al.*, 2017)
flt1[ka605] (mflt1)	mflt1exon 11b +28nt	(Wild *et al.*, 2017)
vhl[hu2117]	C->T	(Van Rooijen *et al.*, 2009)
plgf[ka609]	plgf -10nt	(Alina Klems, unpublished)
vegfba^{-/-}	vegfba -5nt	(Silvana Knapp, unpublished)

nrp1a[hu10012]	nrp1a -11nt	(De Bruin *et al.*, 2016)
nrp1b[bns221]	nrp1b -7nt	(Bettina Kirchmaier, unpublished)
nrp1a[hu10012]; nrp1b[bns221]	nrp1a -11nt; nrp1b -7nt	(Bettina Kirchmaier, unpublished)

Table 6. 3 Zebrafish GOF lines

Transgenic line	Publication
Tg(503unc:eGFP-p2A-plgf)[ka613]	(Alina Klems, unpublished)
Tg(503unc:eGFP-p2A-vegfb)[ka614]	(Alina Klems, unpublished)

Table 6. 4 Solutions

Solution	Composition
1x PBS	137.0mM NaCl, 2.7mM KCl, 6.5mM Na2HPO4, 1.5mM KH2PO4, pH 7.5
1x TAE EDTA	40.0mM Tris, 20mM sodium-acetate pH 8.3, 1.0mM
6x Orange G DNA Loading water	0.25% (w/v) Orange G, 40 % (w/v) sucrose distilled
DEPC-H_2O	1.0ml Diethylpyrocarbonate for 1L aqua bidest. Incubation overnight, inactivation of DEPC by autoclaving
Eggwater	7.5ml Salt Stock Solution (1.5 g/l), 2.5ml 0.1% methylenblue, fill up to 5L with millipore water
Permeabilization solution	1.0% (v/v) DMSO, 1.0% Triton in 1x PBS
PBT	0.1% (v/v) Tween® 20 in 1x PBS

PBTx	1.0% (v/v) Triton-X100, 0.1% Tween® 20 in 1x PBS
PFA 4%	4.0% Paraformaldehyde in 1x PBS
Phenol red solution	0.04 g phenol red in 1.13ml NaOH
PTU	500ml 10x PTU, 83.3ml 60x E3 Medium, fill up to 5L with DEPC water
RNase Buffer	0.1 M Hepes (pH 7.5), 0.15M NaCl, 0.1% (v/v) Tween®

Table 6. 5 Equipment

Equipment	Manufacturer
BD Microlance™ 3, 30 G x ½ "	Becton Dickinson GmbH, Heidelberg
Centrifuge 5415 R	Eppendorf AG, Hamburg
CFX Connect Real-Time System	BIO-RAD Laboratories, München
Colibri Microvolume	Berthold Detection Systems GmbH, Pforzheim
CSU-X1 Confocal Scanner Unit	Carl Zeiss AG, Oberkochen
Digital camera Regita Colour 12bit	QImaging, Surrey, Canada
Flexlid Mastercycler Nexus GX2	Eppendorf AG, Hamburg
Gel electrophoresis chamber	PEQLAV Biotechnology, Erlangen
Heraeus™ Biofuge fresco	ThermoFischer Scientific, Schwerta
IKA® T10 basic Ultra-TURRAX®	IKA Werke GmbH & Co. KG, Staufen
Incubator Avantgarde-Line BD/ED/FD	Binder GmbH, Tutlingen
KL 1500 LCD Optic Illuminator	Schott AG, Mainz
Maxisafe 2020	ThermoFischer Scientific, Schwerta
Multiphoton-Microscope TCS SP8	Leica, Wetzlar
MZ10F Fluorescence microscope	Leica, Wetzlar
MZFLIII microscope	Leica, Wetzlar
Power Supply 200	BIO-RAD Laboratories, München
Thermomixer compact	Eppendorf AG, Hamburg
Tweezers	Fine Science Tools GmbH, Heidelberg

Microlance Needles 30Gx1/2'' 0.3mmx13mm	VWR, Deutschland
Vortex-Genie 2	ThermoFischer Scientific, Schwerta
Water bath	GFL, Burgwedel
Water bath	Victor Recker, Berlin

Table 6. 6 Commercial kits

Product/Kit	Manufacturer
RNeasy Mini Kit	QIAGEN
Click-iT EdU Cell Proliferation Kit	Thermo Fisher
Click-iT Plus TUNEL Assay	Thermo Fisher

Table 6. 7 Inhibitors and chemicals

Product	Manufacturer
Ki8751 (VEGFR-2 inhibitor)	Sigma-Aldrich
Lipopolysaccharides from *E.coli* O111:B4 (LPS)	Sigma-Aldrich

Table 6. 8 Plasmids

Plasmid	Manufacturer or provider
pME_gal4ERt2	pME-geta4 was a gift from Strähle U, KIT, Germany
p5E_3.2elavl	p5E_-3.2HuC was a gift from Strähle U, KIT, Germany
pME_Cas9-T2A-GFP	pME-Cas9-T2A-GFP was a gift from Leonard Zon (Addgene plasmid #63155)
pME_GFP-p2A_SmaI	Cloned from Tol2Kit plasmid #455 (Wild *et al.*, 2017)
pME_GFP-p2A-sFlt1	Cloned from pME_GFP-p2A_SmaI (Wild *et al.*, 2017)

pDestTol2CG2-U6:gRNA	pDestTol2CG2-U6:gRNA was a gift from Leonard Zon (Addgene plasmid #63156)
pDestTol2CG2-U6:flt1E3	Cloned from pDestTol2CG2-U6:gRNA (Wild *et al.*, 2017)
pDestTol2CG2-U6:flt1E3_Cas9-T2A-GFP	Cloned by gateway cloning using pME_Cas9-T2A-GFP and pDestTol2CG2-U6:flt1E3 (Wild *et al.*, 2017)
pCG2_elavl3.2_gal4ERt2	Cloned by gateway cloning using pME_gal4ERt2 and p5E_elavl3.2 (Wild *et al.*, 2017)
pCG2_UAS_GFP-p2A-sFlt1	Clones by gateway cloning using pME_GFP-p2A-sFlt1 and p5E_UAS (tol2kit) (Wild *et al.*, 2017)

Table 6. 9 Morpholino sequences

Target gene	MO sequence	Injection amount	MO type
flt1	5'ATATCGAACATTCTCTTGGTCTTGC-3'	3ng	ATG-MO
vegfaa	5'-GTATCAAATAAACAACCAAGTTCAT-3'	0.8ng	ATG-MO
Ctrl MO	5'-CTCTTACCTCAGTTACAATTTATA-3'	10ng	

Table 6. 10 qPCR primer sequences

gene	Forward primer	Reverse primer
β-actin	5'-CACTGAGGCTCCCCTGAATCCC-3'	5'-CGTACAGAGAGAGCACAGCCTGG-3'
elavl	5'-ACTGAGGAGTGGTATCGCTCAAA-3'	5'-AGACCCACGGAGAGATTCCA-3'
il-1β	5'-ATGGCGAACGTCATCCAAGA-3'	5'-GAGACCCGCTGATCTCCTTG-3'
tnf-α	5'-TCACGCTCCATAAGACCCAG-3'	5'-GATGTGCAAAGACACCTGGC-3'

tgf-β1a	5'-GCTGTATGCGCAAGCTTTACA-3'	5'-GGACAATTGCTCCACCTTGTG-3'
tgf-β3	5'-AAAACGCCAGCAACCTGTTC-3'	5'-CCTCAACGTCCATCCCTCTG-3'

Table 6. 11 Primers for sequencing

primer name	primer sequence
Flt1_E3_gDNA_f	5'-CAGCTCAACACACACAGTATTGTTTTA-3'
Flt1_E3_gDNA_r	5'-ACACCTGAAGCATCTTACCTGTGA-3'
Flt1E11A2386576F	5'-ATTCCCAAGAGACCTGAAATCGGAA-3'
Flt1E11A2386151R	5'-GCTTGATTGCAGTTATCTTGAGGCA-3'
gDNA-vhl_fw	5'-AGTCACGTACACAGTCTTTCTCTCC-3'
gDNA-vhl_rev	5'-AACGCGTAGATAGCAATTTCACCAA-3'
plgf_E3_gDNA_fw	5'-TGTGTGTTCATGTGTGTGTTTCTCTCTC-3'
plgf_E3_gDNA_rev	5'-CCGGCTCATGACAGACTTAAATAGGGC-3'
Vegfba_Exon1_fw #620	5'-TGGACGTTGGACCTGGTGTATTATT-3'
Vegfba_Exon1_rev #621	5'-TACAGCCACATCTTTAAAAGCAGCA-3'
nrp1a_Tal46_F3	5'-GTGCCAATTTGTTTTATGGACA-3'
nrp1a_Tal46_R3	5'-GCGCTGTTAGGGTTAGGACA-3'
nrp1b fw	5'-TTTCTGTGTACTACTGCTGGGA-3'
nrp1b rev2	5'-TCCAGTCCTCTCCGTTTGAG-3'

Table 6. 12 Online tools

Online tool	Description	Website
NCBI	Genome browser	http://www.ncbi.nlm.nih.gov
UCSC	Genome browser	https://genome.ucsc.edu
Ensembl	Genome browser	http://www.ensembl.org
Primer Blast	Primer design	https://www.ncbi.nlm.nih.gov/tools/primer-blast/
Eurofins Genomics	Primer orders	https://www.eurofinsgenomics.eu/

Table 6. 13 Software

Online tool	Source
Adobe Illustrator CS6	Adobe Systems Inc., San Jose, USA
Adobe Photoshop CS3	Adobe Systems Inc., San Jose, USA
CFX Maestro™ Software	BIO-RAD Laboratories, München
Image J	Free Software
GraphPad Prism 6	GraphPad Software Inc, La Jolla, USA
Openlab 5.5.0	Openlab, Heidelberg

6.2   Methods

6.2.1 Zebrafish methods

6.2.1.1 Zebrafish maintenance – ethics statement

Zebrafish husbandry, maintenance and experimental procedures were performed in accordance to the German animal protection standards and were approved by the Government of Baden-Württemberg, Regierungspräsidium Karlsruhe, Germany (Akz.: 35-9185.81/G-93/15).

6.2.1.2 Maintenance of embryos and prevention of melanisation

For most imaging and staining experiments, pigmentation was undesirable and thus embryos were treated in 1x E3 medium (60x E3 medium: 34.8g NaCl; 1.6g KCl; 5.8g $CaCl_2 \cdot 2H_2O$; 9.78g $MgCl_2 \cdot 6H_2O$; in 2l H_2O) with 0.2mM 1-phenyl 2-thiourea (PTU) at 24hpf. PTU is a tyrosinase inhibitor which prevents melanin formation. Embryonic chorions were then removed, whenever necessary, either manually (using forceps) or enzymatically (incubating in 1mg/ml pronase diluted in eggwater).

6.2.1.3 Microinjections

Zebrafish were mated in fish breeding tanks and their embryos were collected for injection. Within the first half hour post fertilization, and while the embryos were still at one-cell stage, embryos were placed in a mould containing 2% liquid agarose in eggwater. Microinjection needles were generated by pulling 1mm capillary tubes with filaments (World Precision Instruments) using a needle puller (Sutter Instrument Co.). For morpholino injections, embryos were injected into the yolk, while for plasmid/Tol2 injections embryos were injected into the oocyte using a micromanipulator (World Precision Instruments) and applying enough pressure to inject 1-2nl volume per embryo (FemtoJet Mircoinjector, Eppendorf). For Tol2 injections, to induce the tissue specific loss and gain-of-function constructs, a co-injection of 25ng/μl *tol2 transposase* mRNA and 25ng/μl of each plasmid DNA were used.

126

6.2.1.4 Zebrafish embryo treatments

Stock solutions of the VEGFR2 inhibitor (ki8751) and LPS (Sigma-Aldrich) were prepared in pure DMSO and PBS (1x PBS: 137.0mM NaCl, 2.7mM KCl, 6.5mM Na_2HPO_4, 1.5mM KH_2PO_4, pH 7.5) respectively. VEGFR2 inhibitor was used at a 0.125μM, while LPS was used at 25ng and 37.5ng in a total of 8ml. Control embryos were treated in equal volume of eggwater. In order to induce the *sflt1* GOF (Gal4-ERT2 construct), endoxifen (Sigma-Aldrich) was dissolved in DMSO and added at a 0.5μM end-concentration to the embryos. They were then incubated in the dark until further experimental procedures and imaging.

6.2.1.5 Lesion methods

To investigate regeneration, three different regeneration regimes were carried out. For muscle injury, 3dpf larvae were injured using a 30G microlance needle, by inducing a tiny incision at the skin above the spinal cord. This lesion led to muscle, tissue and blood vessel damage but left the spinal cord intact. This is a modification of the muscle injury model, as their injury, as published, was more severe and could have also induced neuronal damage, even though this was not investigated in the publication (Gurevich *et al.*, 2018). In order to be consistent with our other lesion models, fin clips were also implicated at 3dpf. The tissue surrounding the tail, but not the notochord, blood vessels or neurons, was removed by slight touching of the tail with a 30G microlance needle (Lisse, Brochu and Rieger, 2015). Muscle and fin clip lesions were carried out on top of a 4% agarose gel. Water was removed as much as possible prior to injury. Spinal cord lesions were carried out above the yolk extension at 3dpf larvae using a 30G microlance needle (Wehner *et al.*, 2017). Importantly, the lesion was deep enough to cut out the whole neural tube but not to the extent that the notochord was also impaired, as this leads to reduced regeneration in WT larvae. Larvae with cut notochord or incomplete lesions were excluded from the study.
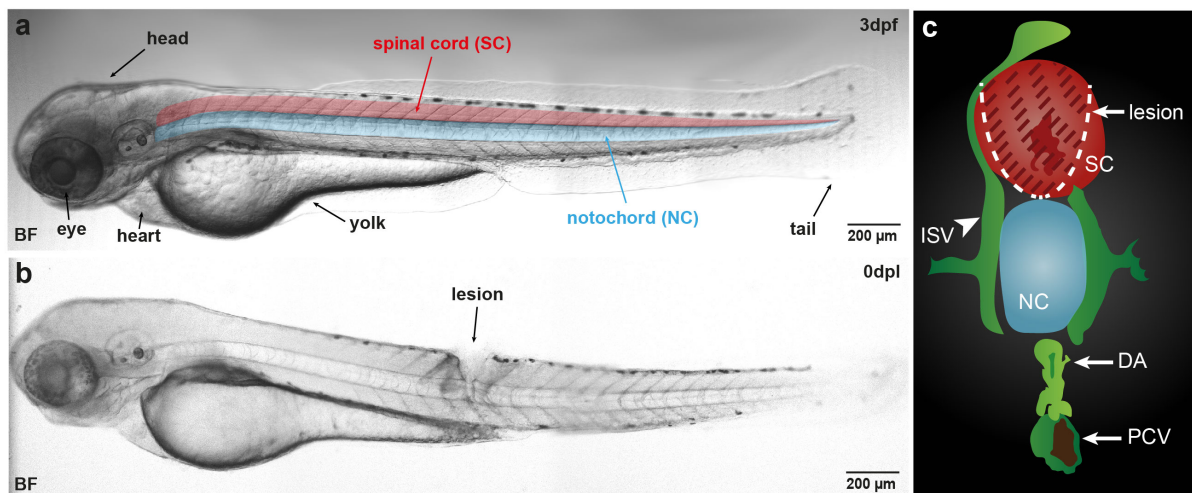
Figure 6. 1: Zebrafish larvae with spinal cord lesion.

(a) Brightfield image of a zebrafish larvae at 3dpf prior to spinal cord lesion. Spinal cord is highlighted in red and the notochord in blue. The eye, heart, head, yolk and tail are annotated by black arrows. **(b)** Brightfield image of a zebrafish larvae at 3dpf post spinal cord injury. The lesion is indicated by black arrows. **(c)** Cross section of the zebrafish larvae, indicating the spinal cord (SC) in red, notochord (NC) in blue and the vessels in green. Dotted white curved line indicates the lesioned area, and the shaded red area is the area impaired by the lesion. BF=brightfield; SC=spinal cord; NC=notochord; ISV=intersegmental vessel; DA=dorsal aorta; PCV= posterior cardinal vein. Scale bar, 200μm.

All lesioned larvae, apart from the ones used for qPCR, were treated with PTU to decrease melanocyte production.

6.2.2 Staining methods

6.2.2.1 Immunohistochemical (IHC) staining

Larvae were lesioned at 3dpf and fixed in 4%PFA-PBS at 1dpl and 2dpl for one hour at room temperature. The larvae were then dehydrated in ascending MetOH-PBS concentrations and were finally kept overnight at -20°C in 100% MetOH. The head and tail were removed, the next day, to increase permeability and embryos were kept in 100% MetOH for another day. Samples were then rehydrated in descending MetOH-PBS concentrations and finally washed in PBT (0.1% Tween in PBS). They were washed twice in distilled water and transferred to pre-chilled aceton in -20°C for 10 minutes. Aceton was then washed out by distilled water and repeated PBT washes. The larvae were then digested in 10μg/ml proteinase K and subsequently washed

twice in PBT. A 15-minute further PFA fixation was carried out and then washed out using 1% PBTx (1%Triton-X100 in PBS). The larvae were then blocked in 4% BSA (in PBTx) blocking buffer for 2 hours and incubated in 1° antibody (1:300 dilution) over the next 3 days. The 1° antibody was washed out using repeated 1% PBTx washes and the 2° antibody was added for 2 more days. Finally, unbound 2° antibody was removed in repeated 1% PBTx washes. Samples were stored at 4°C until imaging.

Table 6. 14 Antibodies for IHC

1° Antibody	Manufacturer	Dilution	2° Antibody	Manufacturer	Dilution
Anti-Tubulin, acetylated (clone 6-11B-1)	Sigma-Aldrich, Steinheim (Cat. # T6793-2ML)	1:300	Goat anti-mouse IgG (H+L) Alexa Fluor 488	Invitrogen (Cat. # A-11029)	1:300
Anti-Glial Fibrillary Acidic Protein	Dako, Santa Clara, USA (Cat. # Z033429-2)	1:300	Goat, anti-rabbit IgG (H+L) Alexa Fluor 633	Invitrogen (Cat. # A-21070)	1:300

6.2.2.2 EdU – proliferation assay

Lesioned larvae were placed in 200uM of EdU in PTU and incubated for 24 hours. The larvae were then fixed in 4%PFA-PBS overnight at 4°C.

For *Tg(-3.1ngn1:GFP)^sb2*, the larvae were rinsed in PBT and used directly for the EdU staining (see below). Larvae in *Tg(mnx1:mCherry)* and *Tg(huC:egfp)* background were dehydrated in ascending MetOH-PBS concentrations and kept overnight at -20°C in 100% MetOH. They were stained as mentioned in Section 6.2.2.1 using the following Antibodies.

Table 6. 15 Click-iT reaction cocktails

1° Antibody	Manufacturer	Dilution	2° Antibody	Manufacturer	Dilution
Living Colors® DsRed Polyclonal Antibody	Takarabio (Cat. # 632496)	1:300	Goat, anti-rabbit IgG (H+L) Alexa Fluor 633	Invitrogen (Cat. # A-21070)	1:300
HuC/HuD Monoclonal Antibody	Invitrogen (Cat. # A-21271)	1:300	Goat anti-mouse IgG (H+L) Alexa Fluor 488	Invitrogen (Cat. # A-11029)	1:300

The next day, larvae were washed in distilled water and placed in pre-chilled aceton at -20°C for 7 minutes. Distilled water was used to wash off the aceton and the larvae were subsequently permeabilised for 1 hour in PBS/1% DMSO/1% Triton at room temperature. The Click-iT reaction cocktail was then prepared, according to the Click-iT EdU Cell Proliferation Kit (Invitrogen), shortly before application to the samples.

Table 6. 16 Click-iT reaction cocktails

Reaction components	Amount used per sample
1x Click-iT reaction buffer	430μl
$CuSO_4$ (100mM aqueous solution)	20μl
Alexa Fluor azide (Alexa 594)	1.2μl
Reaction buffer additive	50μl
Total volume	500μl

The embryos were then treated in the Click-iT reaction cocktail and left to incubate for an hour in the dark at room temperature. The reaction cocktail was then washed out in repeated PBS rinses. Larvae were left in PBS at 4°C until imaging.

6.2.2.3 TUNEL – apoptotic assay

Lesioned larvae were fixed at 1dpl in 4% PFA-PBS overnight at 4°C. For *Tg(-3.1ngn1:GFP)^{sb2}*, the larvae were rinsed in PBT and used directly for the TUNEL staining (see below). Larvae in *Tg(mnx1:mCherry)* and *Tg(huC:egfp)* background were dehydrated in ascending MetOH-PBS concentrations and were kept overnight at -20°C in 100% MetOH. They were stained in a similar manner to Section 6.2.2.1 using the antibodies as outlined in Table 6.12.

The Click-iT Plus TUNEL Assay (Invitrogen) was then used according to manufacturer's instructions, using the cell fixation and permeabilization protocol. Modifications include treating the larvae with 1x proteinase K (25x Solution in the kit; dissolved 1:25 in PBS) for one hour and subsequently washing them in PBS. Some larvae were used as a positive controls as advised in the protocol. The TdT Reaction Buffer was then applied and the TdT Reaction mixture, prepared according to manufacturer's instructions, was subsequently applied to the samples for one hour at 37°C. The larvae were then washed twice in 3% BSA in PBS and immediately treated with the Click-iT Plus TUNEL reaction cocktail, prepared as outlined in the company's protocol. The larvae were incubated in the Click-iT Plus TUNEL reaction cocktail for half an hour at 37°C and finally washed in 3% BSA in PBS. Finally, the larvae were stored in PBS at 4°C until imaging.

6.2.2.4 DAPI staining – nuclei

In order to distinguish between auto-fluorescent apoptotic cells and macrophages, DAPI staining was used to stain the nuclei. Thus, double fluorescent mpeg+/DAPI+ cells were counted instead. Lesioned larvae were fixed at 1dpl and 2dpl in 4% PFA-PBS overnight at 4°C. The next day, the larvae were washed in PBT and subsequently permeabilized in PBTx (1%Triton in PBS) for 20 minutes at room temperature. Three additional washes with PBT were applied before adding the DAPI stain (1:1000; diluted in PBT), incubating the larvae for 20 minutes at 4°C in the dark. DAPI was then washed out using PBT. Larvae were stored in PBT at 4°C until imaging.

6.2.3 Molecular biology methods

6.2.3.1 RNA extraction – using the RNeasy Mini Kit (Qiagen)

Lesioned and unlesioned larvae were fixed in liquid Nitrogen at the desired developmental stages to be used for qPCR analysis. A total of 15 larvae were used per RNA sample. Larvae were lysed in Trizol using the homogenisator (Ultra-Turrax) until the tissue was sufficiently disrupted. The lyzed larvae were then treated with 140μl Chloroform and centrifuged to separate the mixture into a lower red phenol-chloroform phase and a colourless upper aqueous phase. The upper phase was then transferred into new Eppendorf tubes and ethanol was added to the mixture. The mixture was then transferred to a spin column and was briefly centrifuged.

In order to digest the DNA, RW1 Buffer was added to the column and re-centrifuged for a couple of seconds. Then DNase I, diluted in the RDD Buffer, was added to the column and left to stand at room temperature for 15 minutes. RW1 Buffer was twice more added to the column and centrifuged. Lastly, RPE buffer was added to the column and re-centrifuged. The column was then transferred to a new reaction tube and the RNA was eluted in 30μl of RNAse-free water. The RNA efficacy was checked on a 1% Agarose gel using 2μl of the extracted RNA, 3μl of 100% Formamide (denatures RNA) and 1μl Orange G to visualize the ribosomal RNA. The concentration of the RNA was photometrically determined using a nanodrop (Berthold Detection Systems GmbH, Pforzheim). RNA was stored at -80°C for long-term storage.

6.2.3.2 cDNA synthesis for qPCR

150ng of RNA were used for the cDNA synthesis reaction.

Table 6. 17 cDNA synthesis – Step 1

Components	Volume
150ng RNA	Dependent on the RNA's concentration
Random hexamer primer (0.5µg/µl)	0.25µl
Oligo(dT) primer (0.5µg/µl)	0.25µl
H_2O	to 10µl

To exclude DNA contaminations, a negative control was used per condition. The mixture was then incubated at 70°C for 5 minutes, followed by a cool down period to 4°C.

The whole mixture was then combined with the following mix. Note that for the negative samples no MMLV-RT (enzyme) was added.

Table 6. 18 cDNA synthesis – Step 2

Components	Volume
Mixture obtained from Step 1 (Table 6.13)	10µl
MMLV-Buffer (5x)	4µl
dNTPs (10mM)	0.5µl
MMLV-RT	0.5µl
H_2O	to 20µl

The PCR program was then set for 5 minutes at 25°C, followed by 60 minutes at 42°C and ending with 15 minutes at 72°C. The obtained cDNA was then diluted 1:10 in RNase free water and stored at -20°C until further use.

6.2.3.4 cDNA check prior to qPCR

Prior to running the qPCR reaction, a normal PCR reaction was performed using the housekeeping gene β-actin, to check the validity of the cDNA. PCR reaction was carried out using the GoTaq DNA-Polymerase and a Green GoTaq Buffer for visualization purposes. The annealing temperature used was 60°C. Samples were then run on a 1% agarose gel for visualizing the cDNA.

6.2.3.5 Quantitative polymerase chain reaction (qPCR)

qPCR reaction was run on an RNase free area. The following reaction was used:

Table 6. 19 qPCR reaction

Components	Volume
cDNA (1:10 diluted)	3.75μl
SYBR Green Mix (Thermo Scientific)	7.50μl
Forward primer	0.75μl
Reverse primer	0.75μl
H_2O	to 15μl

Samples we used in duplicate to test for any pipetting errors. Two negative controls were used; NC (without the enzyme) and NTC (water instead of cDNA). qPCR was run and the threshold cycles (C_t) were used for the statistical analysis.

6.2.4 Genotyping of mutants

The genomic DNA was extracted from fin clips of adult or larvae zebrafish via the HotSHOT (Hot Sodium Hydroxide Tris) method (Truett *et al.*, 2000). The extracted genomic DNA was then used as PCR template. Mutations were then identified either by genotyping or through running them on a 2% agarose gel.

Table 6. 20 Genotyping

Mutant line	Mutation	Forward Primer	Reverse Primer	Analysis
flt1[ka601]	flt1 exon3 - 1nt	Flt1_E3_gDNA_f	Flt1_E3_gDNA_r	Seq.
flt1[ka604]	flt1 exon3 - 14nt	Flt1_E3_gDNA_f	Flt1_E3_gDNA_r	Seq.
flt1[ka605] (mflt1)	mflt1exon 11b +28nt	Flt1E11A2386576F	Flt1E11A2386151R	Gel
vhl[hu2117]	C->T	gDNA-vhl_fw	gDNA-vhl_rev	Seq.
plgf[ka609]	plgf -10nt	plgf_E3_gDNA_fw	plgf_E3_gDNA_rev	Seq.
vegfba^{-/-}	vegfba -5nt	Vegfba_Exon1_fw #620	Vegfba_Exon1_rev #621	Seq.
nrp1a[hu10012]	nrp1a -11nt	nrp1a_Tal46_F3	nrp1a_Tal46_R3	Seq.
nrp1b[bns221]	nrp1b -7nt	nrp1b fw	nrp1b rev2	Seq.
nrp1a[hu10012]; nrp1b[bns221]	nrp1a -11nt; nrp1b -7nt	nrp1a_Tal46_F3 nrp1b fw	nrp1a_Tal46_R3 nrp1b rev2	Seq.

6.2.5 Parabiosis

Parabiosis was performed as published (Hagedorn *et al.*, 2016). Modifications of the protocol included the use of pronase (Roche, Basel, Switzerland) at 1mg/ml to dechorionated the embryos. The dechorionated embryos (256-cell-stage) were then washed in 500ml of E3-Medium until all the chorions were removed. The embryos were then placed in agarose coated plates and selected using a glass pipette. The pair which would be used for parabiosis was placed in methylcellulose and joined by 'stitching' the cells together using an injection needle. The embryos were left in methylcellulose in the incubator until the next day. Successfully fused larvae were then lesioned and imaged accordingly.

6.2.6 Imaging

Live larvae were initially anesthetized with 25x Tricaine (Sigma-Aldrich) in E3 and embedded in microscopy dishes (MatTek) in 0.7x (w/v) low-melting NuSieve GTG

Agarose (Lonza) in E3 medium. Once the agarose hardened, it was additionally covered in 0.7x Tricaine in PTU to keep the larvae anaesthetized for the duration of imaging. Fixed larvae, were also embedded in microscopy dishes (MatTek) in 0.7x (w/v) low-melting NuSieve GTG Agarose (Lonza) in E3 medium. Water or PBS was added at the top of the hardened agarose to keep it from drying out during imaging. Images were taken using the Leica TCS SP8 Confocal inverted microscope using the 20x and 40x objectives. Time lapse imaging was performed at 28.5°C.

6.2.7 Computational methods

6.2.7.1 SnapGene

Gene sequences were obtained via UCSC and Ensembl. Primers were designed using the online tool Primer Blast and ordered via Eurofins genomics. SnapGene software was used to check for sequences.

6.2.7.2 Image processing

ImageJ/Fiji was used for image processing and analysis. For the majority of images, the maximum intensity z projection was merged or separated in multicolour channels. For the macrophage, proliferation and apoptotic data, a pre-determined square was used to annotate the area of lesion and the cells were counted throughout the stack using the cell counter option.

6.2.8 Statistical analysis

6.2.8.1 Neuronal cell counts

For the proliferation and apoptotic assays, a pre-determined rectangle was used to measure only the proliferating or apoptotic neuronal positive cells at the level of the spinal cord. The number was then presented per 100μm rostral and caudal to the spinal cord to be comparable to recent publications (Ohnmacht *et al.*, 2016).

6.2.8.2 %Area coverage

To measure that GFAP+ neurons were in generally affected in $flt1^{ka601}$, the whole area was used to measure the cell coverage measuring the pixel coverage as %Area.

6.2.8.3 Collateral bridging

To identify the number of bridging collaterals, a pre-set slanted vertical line was added at the centre of the injury. The number of axonal connection points intersecting this line were then measured.

6.2.8.4 Macrophage migration

Macrophage migration was measured along the whole z-stack in fin clip larvae. For muscle and spinal cord injuries, a pre-determined square was used around the area of the lesion to measure only the macrophages which migrate to the wound. The macrophages were then counted along the whole z-stack.

6.2.8.5 Ectopic sprouts and branch points

Ectopic sprouts/hypersprouts and branch points were measured per 2 ISVs. A total of 3-4 pair of measurements were done per larvae and the numbers obtained per two ISVs were averaged. The averages were then compared in between different larvae.

6.2.8.6 Statistical quantification and analysis

Statistics were analysed using GraphPad Prism 6. Results are indicated as mean ± standard error of the mean (s.e.m.). The statistical analysis used were as follows:

Table 6. 21 Statistical analysis

Statistical test	Gaussian distribution	Test parameter
Mann-Whitney test	No	Means
Unpaired t-test	Yes	Means
Fisher's exact test	-	Contingency (% regeneration)
Kruskal-Wallis test	No	Multiple comparisons

Significance was annotated by asterisk rating to summarize the p-values: n.s. (non-significant), * $P<0.05$; **$P<0.01$; ***$P<0.001$.

7 Bibliography

Abel, E. I. (2007) 'Football increases the risk for Lou Gehrig's disease, amyotrophic lateral sclerosis', *Perceptual and Motor Skills*, 104, pp. 1251–1254. doi: 10.1055/s-0038-1635141.

Ablain, J. *et al.* (2016) 'A CRISPR/Cas9 vector system for tissue-specific gene disruption in zebrafish', *Physiology & behavior*, 176(1), pp. 139–148. doi: 10.1016/j.physbeh.2017.03.040.

Adams, R. H. and Alitalo, K. (2007) 'Molecular regulation of angiogenesis and lymphangiogenesis', *Nature Reviews Molecular Cell Biology*, 8(6), pp. 464–478. doi: 10.1038/nrm2183.

Adams, R. H. and Eichmann, A. (2010) 'Axon guidance molecules in vascular patterning.', *Cold Spring Harbor perspectives in biology*, 2(5), pp. 1–19. doi: 10.1101/cshperspect.a001875.

Ahmad, S. *et al.* (2006) 'Direct evidence for endothelial vascular endothelial growth factor receptor-1 function in nitric oxide-mediated angiogenesis', *Circulation Research*, 99(7), pp. 715–722. doi: 10.1161/01.RES.0000243989.46006.b9.

Ahuja, C. S. *et al.* (2017) 'Traumatic spinal cord injury - Repair and regeneration', *Clinical Neurosurgery*, 80(3), pp. S22–S90. doi: 10.1093/neuros/nyw080.

de Almeida-Leite, C. M. *et al.* (2014) 'Sympathetic glial cells and macrophages develop different responses to Trypanosoma cruzi infection or lipopolysaccharide stimulation', *Memorias do Instituto Oswaldo Cruz*, 109(4), pp. 459–465. doi: 10.1590/0074-0276130492.

De Almodovar, C. R. *et al.* (2009) 'Role and therapeutic potential of VEGF in the nervous system', *Physiological Reviews*, 89(2), pp. 607–648. doi: 10.1152/physrev.00031.2008.

Alves, G. S. *et al.* (2015) 'Integrating retrogenesis theory to alzheimer's disease pathology: Insight from DTI-TBSS investigation of the white matter microstructural integrity', *BioMed Research International*, 291658. doi: 10.1155/2015/291658.

Artegiani, B. and Calegari, F. (2012) 'Age-related cognitive decline: Can neural stem cells help us?', *Aging*, 4(3), pp. 176–186. doi: 10.18632/aging.100446.

Autiero, M. *et al.* (2003) 'Role of PlGF in the intra- and intermolecular cross talk

between the VEGF receptors Flt1 and Flk1', *Nature Medicine*, 9(7), pp. 936–943. doi: 10.1038/nm884.

Baddar, N. W. A. H., Clithrala, A. and Voss, S. R. (2019) 'Amputation-Induced ROS Signaling is Required for Axolotl Tail Regeneration', *Dev Dyn*, 248(2), pp. 189–196. doi: 10.1016/j.physbeh.2017.03.040.

Banerjee, S. *et al.* (2008) 'VEGF-A165 induces human aortic smooth muscle cell migration by activating neuropilin-1-VEGFR1-PI3K axis', *Biochemistry*, 47(11), pp. 3345–3351. doi: 10.1021/bi8000352.

Bareyre, F. M. and Schwab, M. E. (2003) 'Inflammation, degeneration and regeneration in the injured spinal cord: Insights from DNA microarrays', *Trends in Neurosciences*, 26(10), pp. 555–563. doi: 10.1016/j.tins.2003.08.004.

Barleon, B. *et al.* (1996) 'Migration of human monocytes in response to vascular endothelial growth factor (VEGF) is mediated via the VEGF receptor flt-1', *Blood*, 87(8), pp. 3336–3343. doi: 10.1182/blood.v87.8.3336.bloodjournal8783336.

Basso, L. *et al.* (2019) 'Peripheral neurons: Master regulators of skin and mucosal immune response', *European Journal of Immunology*, 49(11), pp. 1984–1997. doi: 10.1002/eji.201848027.

Beck, K. D. *et al.* (2010) 'Quantitative analysis of cellular inflammation after traumatic spinal cord injury: Evidence for a multiphasic inflammatory response in the acute to chronic environment', *Brain*, 133(2), pp. 433–447. doi: 10.1093/brain/awp322.

Becker, C. G. and Becker, T. (2015) 'Neuronal Regeneration from Ependymo-Radial Glial Cells: Cook, Little Pot, Cook!', *Developmental Cell*. Elsevier Inc., 32(4), pp. 516–527. doi: 10.1016/j.devcel.2015.01.001.

Behfar, A. *et al.* (2014) 'Cell therapy for cardiac repair-lessons from clinical trials', *Nature Reviews Cardiology*. Nature Publishing Group, 11(4), pp. 232–246. doi: 10.1038/nrcardio.2014.9.

Beirowski, B. *et al.* (2005) 'The progressive nature of Wallerian degeneration in wild-type and slow Wallerian degeneration (WldS) nerves', *BMC Neuroscience*, 6, pp. 1–27. doi: 10.1186/1471-2202-6-6.

Berger, J. and Currie, P. D. (2013) '503Unc, a Small and Muscle-Specific Zebrafish Promoter', *Genesis*, 51(6), pp. 443–447. doi: 10.1002/dvg.22385.

Blader, P., Plessy, C. and Strähle, U. (2003) 'Multiple regulatory elements with spatially and temporally distinct activities control neurogenin1 expression in

primary neurons of the zebrafish embryo Patrick', *Mechanisms of Development*, 120, pp. 211–218. doi: 10.1016/S0.

Blum, D. *et al.* (2001) 'Molecular pathways involved in the neurotoxicity of 6-OHDA, dopamine and MPTP: Contribution to the apoptotic theory in Parkinson's disease', *Progress in Neurobiology*, 65(2), pp. 135–172. doi: 10.1016/S0301-0082(01)00003-X.

Boeckel, J. N. *et al.* (2011) 'Jumonji domain-containing protein 6 (Jmjd6) is required for angiogenic sprouting and regulates splicing of VEGF-receptor 1', *Proceedings of the National Academy of Sciences of the United States of America*, 108(8), pp. 3276–3281. doi: 10.1073/pnas.1008098108.

Boer, K. *et al.* (2008) 'Cellular distribution of vascular endothelial growth factor A (VEGFA) and B (VEGFB) and VEGF receptors 1 and 2 in focal cortical dysplasia type IIB', *Acta Neuropathologica*, 115(6), pp. 683–696. doi: 10.1007/s00401-008-0354-6.

Boos, N. and Aebi, M. (2008) *Spinal Disorders: Fundamentals of Diagnosis and Treatment.* Available at: https://books.google.de/books?id=kFhZGjFwjVYC&pg=PA29&lpg=PA29&dq=hippocrates+table+for+spinal+cord+lesions&source=bl&ots=C84uRDuGa_&sig=ACfU3U0MsAhUeDVYwa6caMDdyZQ0geinfQ&hl=en&sa=X&ved=2ahUKEwilyJnsoYnpAhUpsaQKHa6pBQsQ6AEwAHoECAoQAQ#v=onepage&q&f=false (Accessed: 27 April 2020).

Bovenkamp, D. E. *et al.* (2004) 'Expression and mapping of duplicate neuropili-1 and neuropilin-2 genes in developing zebrafish', *Gene Expression Patterns*, 4(4), pp. 361–370. doi: 10.1016/j.modgep.2004.01.014.

Le Bras, B. *et al.* (2006) 'VEGF-C is a trophic factor for neural progenitors in the vertebrate embryonic brain', *Nature Neuroscience*, 9(3), pp. 340–348. doi: 10.1038/nn1646.

Britto, D. D. *et al.* (2018) 'Macrophages enhance Vegfa-driven angiogenesis in an embryonic zebrafish tumour xenograft model', *Disease Models and Mechanisms*, 11, pp. 1–14. doi: 10.1242/dmm.035998.

De Bruin, A. *et al.* (2016) 'Genome-wide analysis reveals NRP1 as a direct HIF1α-E2F7 target in the regulation of motorneuron guidance in vivo', *Nucleic Acids Research*, 44(8), pp. 3549–3566. doi: 10.1093/nar/gkv1471.

Brunet, I. *et al.* (2014) 'Netrin-1 controls sympathetic arterial innervation', *Journal of Clinical Investigation*, 124(7), pp. 3230–3240. doi: 10.1172/JCI75181.

Burnside, E. R. and Bradbury, E. J. (2014) 'Review: Manipulating the extracellular matrix and its role in brain and spinal cord plasticity and repair', *Neuropathology and Applied Neurobiology*, 40(1), pp. 26–59. doi: 10.1111/nan.12114.

Cakir, B. *et al.* (2019) 'Engineering of human brain organoids with a functional vascular-like system', *Nature Methods*. Springer US, 16(11), pp. 1169–1175. doi: 10.1038/s41592-019-0586-5.

Calvi, L. M. *et al.* (2003) 'Osteoblastic cells regulate the haematopoietic stem cell niche.', *Nature*, 425(6960), pp. 841–846. doi: 10.1038/nature02041.

Cardozo, M. J. *et al.* (2017) 'Reduce, reuse, recycle – Developmental signals in spinal cord regeneration', *Developmental Biology*. Elsevier Inc., 432(1), pp. 53–62. doi: 10.1016/j.ydbio.2017.05.011.

Cariboni, A. *et al.* (2011) 'VEGF signalling controls GnRH neuron survival via NRP1 independently of KDR and blood vessels', *Development*, 138(17), pp. 3723–3733. doi: 10.1242/dev.063362.

Carmeliet, P. *et al.* (1996) 'Abnormal blood vessel development and lethality in embryos lacking a single VEGF allele Peter', *Nature*, 380, pp. 435–439.

Carmeliet, P. (2005) 'VEGF as a key mediator of angiogenesis in cancer', *Oncology*, 69(SUPPL. 3), pp. 4–10. doi: 10.1159/000088478.

Carmeliet, P. and De Almodovar, C. R. (2013) 'VEGF ligands and receptors: Implications in neurodevelopment and neurodegeneration', *Cellular and Molecular Life Sciences*, 70(10), pp. 1763–1778. doi: 10.1007/s00018-013-1283-7.

Carmeliet, P. and Tessier-Lavigne, M. (2005) 'Common mechanisms of nerve and blood vessel wiring', *Nature*, 436(7048), pp. 193–200. doi: 10.1038/nature03875.

Chambers, A. P., Sandoval, D. A. and Seeley, R. J. (2013) 'Integration of satiety signals by the central nervous system', *Current Biology*, 23(9). doi: 10.1016/j.cub.2013.03.020.

Chappell, J. C. *et al.* (2016) 'Flt-1 (VEGFR-1) coordinates discrete stages of blood vessel formation', *Cardiovascular Research*, 111(1), pp. 84–93. doi: 10.1093/cvr/cvw091.

Chen, S. L., März, M. and Strähle, U. (2009) 'Gfap and Nestin Reporter Lines Reveal

Characteristics of Neural Progenitors in the Adult Zebrafish Brain', *Developmental Dynamics*, 238(2), pp. 475–486. doi: 10.1002/dvdy.21853.

Cheng, H. C. and Burke, R. E. (2010) 'The WldS mutation delays anterograde, but not retrograde, axonal degeneration of the dopaminergic nigro-striatal pathway in vivo', *Journal of Neurochemistry*, 113(3), pp. 683–691. doi: 10.1111/j.1471-4159.2010.06632.x.

Cigliola, V., Becker, C. J. and Poss, K. D. (2020) 'Building bridges , not walls : spinal cord regeneration in zebrafish', *Disease Models & Mechanisms*, 13. doi: 10.1242/dmm.044131.

Cleveland, D. W. and Rothstein, J. D. (2001) 'From charcot to lou gehrig: deciphering selective motor neuron death in als', *Nature Reviews Neuroscience*, 2(11), pp. 806–819. doi: 10.1038/35097565.

Clevers, H. (2016) 'Modeling Development and Disease with Organoids', *Cell*. Elsevier Inc., 165(7), pp. 1586–1597. doi: 10.1016/j.cell.2016.05.082.

Cohn, J. N., Ferrari, R. and Sharpe, N. (2000) 'Cardiac remodeling-concepts and clinical implications: A consensus paper from an International Forum on Cardiac Remodeling', *Journal of the American College of Cardiology*. Elsevier Masson SAS, 35(3), pp. 569–582. doi: 10.1016/S0735-1097(99)00630-0.

Coleman, M. P. and Perry, V. H. (2002) 'Axon pathology in neurological disease: A neglected therapeutic target', *Trends in Neurosciences*, 25(10), pp. 532–537. doi: 10.1016/S0166-2236(02)02255-5.

Conforti, L., Gilley, J. and Coleman, M. P. (2014) 'Wallerian degeneration: An emerging axon death pathway linking injury and disease', *Nature Reviews Neuroscience*. Nature Publishing Group, 15(6), pp. 394–409. doi: 10.1038/nrn3680.

Covassin, L. D. *et al.* (2009) 'A genetic screen for vascular mutants in zebrafish reveals dynamic roles for Vegf/Plcg1 signaling during artery development', *Developmental Biology*, 329(2), pp. 1-212–226. doi: 10.1038/jid.2014.371.

Crouch, E. E. *et al.* (2015) 'Regional and stage-specific effects of prospectively purified vascular cells on the adult V-SVZ neural stem cell lineage', *Journal of Neuroscience*, 35(11), pp. 4528–4539. doi: 10.1523/JNEUROSCI.1188-14.2015.

Cudmore, M. J. *et al.* (2012) 'The role of heterodimerization between VEGFR-1 and VEGFR-2 in the regulation of endothelial cell homeostasis', *Nature*

Communications. Nature Publishing Group, 3. doi: 10.1038/ncomms1977.

Cui, X. *et al.* (2015) 'Venous Endothelial Marker COUP-TFII Regulates the Distinct Pathologic Potentials of Adult Arteries and Veins', *Scientific Reports*. Nature Publishing Group, 5(June), pp. 1–15. doi: 10.1038/srep16193.

Dewerchin, M. and Carmeliet, P. (2012) 'PlGF: A multitasking cytokine with disease-restricted activity', *Cold Spring Harbor Perspectives in Medicine*, 2(8), pp. 1–24. doi: 10.1101/cshperspect.a011056.

Dhondt, J. *et al.* (2011) 'Neuronal FLT1 receptor and its selective ligand VEGF-B protect against retrograde degeneration of sensory neurons', *The FASEB Journal*, 25(5), pp. 1461–1473. doi: 10.1096/fj.10-170944.

Doetsch, F. *et al.* (1999) 'Subventricular Zone Astrocytes Are Neural Stem Cells in the Adult Mammalian Brain', 97, pp. 703–716. doi: 10.1016/s0092-8674(00)80783-7.

Dovi, J. V, He, L. and Dipietro, L. A. (2002) 'Accelerated wound closure in neutrophil-depleted mice Abstract : The infiltration of neutrophils into in- jured tissue is known to protect wounds from in- repair process . To investigate the role of neutro-'. doi: 10.1189/jlb.0802406.

Le Dréau, G. and Martí, E. (2012) 'Dorsal-ventral patterning of the neural tube: A tale of three signals', *Developmental Neurobiology*, 72(12), pp. 1471–1481. doi: 10.1002/dneu.22015.

Dugger, B. N. and Dickson, D. W. (2017) 'Pathology of neurodegenerative diseases', *Cold Spring Harbor Perspectives in Biology*, 9(7), pp. 1–22. doi: 10.1101/cshperspect.a028035.

Eilken, H. M. *et al.* (2017) 'Pericytes regulate VEGF-induced endothelial sprouting through VEGFR1', *Nature Communications*. Springer US, 8(1). doi: 10.1038/s41467-017-01738-3.

Ellett, F. *et al.* (2011) 'mpeg1 promoter transgenes direct macrophage-lineage expression in zebrafis', *Blood*, 117(4), pp. e49–e56. doi: 10.1182/blood-2010-10-314120.The.

Erskine, L. *et al.* (2011) 'VEGF Signaling through Neuropilin 1 Guides Commissural Axon Crossing at the Optic Chiasm', *Neuron*. Elsevier Inc., 70(5), pp. 951–965. doi: 10.1016/j.neuron.2011.02.052.

Erskine, L. *et al.* (2017) 'VEGF-A and neuropilin 1 (NRP1) shape axon projections in

the developing CNS via dual roles in neurons and blood vessels', *Development (Cambridge)*, 144(13), pp. 2504–2516. doi: 10.1242/dev.151621.

F. O. Kok *et al.* (2015) 'Reverse genetic screening reveals poor correlation between Morpholino-induced and mutant phenotypes in zebrafish', *Developmental cell*, 32(1), pp. 97–108. doi: 10.1530/ERC-14-0411.Persistent.

Fantin, A. *et al.* (2010) 'Tissue macrophages act as cellular chaperones for vascular anastomosis downstream of VEGF-mediated endothelial tip cell induction', *Blood*, 116(5), pp. 829–840. doi: 10.1182/blood-2009-12-257832.

Fawcett, J. W. *et al.* (2012) 'Defeating inhibition of regeneration by scar and myelin components', *Handbook of Clinical Neurology*, 109, pp. 503–522. doi: 10.1016/B978-0-444-52137-8.00031-0.

Ferraro, F. and Lo Celso, C. (2010) 'Adult Stem Cells and their Niches', *Advances in Experimental Medicine and Biology*, 695, pp. 1–222. doi: 10.1007/978-1-4419-7037-4.

Ferri, A. *et al.* (2003) 'Inhibiting Axon Degeneration and Synapse Loss Attenuates Apoptosis and Disease Progression in a Mouse Model of Motoneuron Disease', *Current Biology*, 13, pp. 669–673. doi: 10.1016/S0960-9822(03)00206-9.

Fischer, L. R. *et al.* (2005) 'The WldS gene modestly prolongs survival in the SOD1 G93A fALS mouse', *Neurobiology of Disease*, 19(1–2), pp. 293–300. doi: 10.1016/j.nbd.2005.01.008.

Fong, G. H. *et al.* (1995) 'Role of the Flt-1 receptor tyrosine kinase in regulating the assembly of vascular endothelium', *Nature*, 376, pp. 66–70. doi: 10.1038/376066a0.

Fong, G. H. *et al.* (1999) 'Increased hemangioblast commitment, not vascular disorganization, is the primary defect in flt-1 knock-out mice', *Development*, 126, pp. 3015–3025.

Furutani-Seiki, M. and Wittbrodt, J. (2004) 'Medaka and zebrafish, an evolutionary twin study', *Mechanisms of Development*, 121(7–8), pp. 629–637. doi: 10.1016/j.mod.2004.05.010.

Gale, N. W. *et al.* (2004) 'Haploinsufficiency of delta-like 4 ligand results in embryonic lethality due to major defects in arterial and vascular development', *Proceedings of the National Academy of Sciences of the United States of America,* 101(45), pp. 15949–15954. doi: 10.1073/pnas.0407290101.

Gallico, G. G. *et al.* (1984) 'Permanent Coverage of Large Burn Wounds with Autologous Cultured Human Epithelium', *New England Journal of Medicine*, 311(7), pp. 448–451. doi: 10.1056/NEJM198408163110706.

Gaspar-Maia, A. *et al.* (2011) 'Open chromatin in pluripotency and reprogramming', *Nature Reviews Molecular Cell Biology*, 12(1), pp. 36–47. doi: 10.1038/nrm3036.

Gensel, J. C. *et al.* (2009) 'Macrophages promote axon regeneration with concurrent neurotoxicity', *Journal of Neuroscience*, 29(12), pp. 3956–3968. doi: 10.1523/JNEUROSCI.3992-08.2009.

Gerhardt, H. *et al.* (2003) 'VEGF guides angiogenic sprouting utilizing endothelial tip cell filopodia', *Journal of Cell Biology*, 161(6), pp. 1163–1177. doi: 10.1083/jcb.200302047.

Glasauer, S. M. K. and Neuhauss, S. C. F. (2014) 'Whole-genome duplication in teleost fishes and its evolutionary consequences', *Molecular Genetics and Genomics*, 289(6), pp. 1045–1060. doi: 10.1007/s00438-014-0889-2.

Gogiraju, R., Bochenek, M. L. and Schäfer, K. (2019) 'Angiogenic Endothelial Cell Signaling in Cardiac Hypertrophy and Heart Failure', *Frontiers in Cardiovascular Medicine*, 6(March). doi: 10.3389/fcvm.2019.00020.

Goldshmit, Y. *et al.* (2012) 'Fgf-dependent glial cell bridges facilitate spinal cord regeneration in Zebrafish', *Journal of Neuroscience*, 32(22), pp. 7477–7492. doi: 10.1523/JNEUROSCI.0758-12.2012.

Gouti, M., Metzis, V. and Briscoe, J. (2015) 'The route to spinal cord cell types: A tale of signals and switches', *Trends in Genetics*. Elsevier Ltd, 31(6), pp. 282–289. doi: 10.1016/j.tig.2015.03.001.

Grebenyuk, S. and Ranga, A. (2019) 'Engineering organoid vascularization', *Frontiers in Bioengineering and Biotechnology*, 7(MAR), pp. 1–12. doi: 10.3389/fbioe.2019.00039.

Gurevich, D. B. *et al.* (2018) 'Live imaging of wound angiogenesis reveals macrophage orchestrated vessel sprouting and regression', *The EMBO Journal*, 37(13), pp. 1–23. doi: 10.15252/embj.201797786.

Gustavsson, P. *et al.* (2007) 'Galectin-3 inhibits Schwann cell proliferation in cultured sciatic nerve', *NeuroReport*, 18(7), pp. 669–673. doi: 10.1097/WNR.0b013e3280bef97b.

Hagedorn, E. J. *et al.* (2016) 'Generation of parabiotic zebrafish embryos by surgical

fusion of developing blastulae', *Journal of Visualized Experiments*, 2016(112), pp. 1–11. doi: 10.3791/54168.

Hagg, T. (2006) 'Collateral sprouting as a target for improved function after spinal cord injury', *Journal of Neurotrauma*, 23(3–4), pp. 281–294. doi: 10.1089/neu.2006.23.281.

Hanna, P. *et al.* (2017) 'Cardiac neuroanatomy - Imaging nerves to define functional control', *Autonomic Neuroscience: Basic and Clinical*, 207, pp. 48–58. doi: 10.1016/j.autneu.2017.07.008.

Harde, E. *et al.* (2019) 'EphrinB2 regulates VEGFR2 during dendritogenesis and hippocampal circuitry development', *eLife*, 8, pp. 1–24. doi: 10.7554/eLife.49819.

Harkey, H. L. *et al.* (2003) 'A clinician's view of spinal cord injury', *Anatomical Record - Part B New Anatomist*, 271(1), pp. 41–48. doi: 10.1002/ar.b.10012.

Hasbani, D. M. and O'Malley, K. L. (2006) 'WldS mice are protected against the Parkinsonian mimetic MPTP', *Experimental Neurology*, 202(1), pp. 93–99. doi: 10.1016/j.expneurol.2006.05.017.

Hashimoto, H., Olson, E. N. and Bassel-Duby, R. (2018) 'Therapeutic approaches for cardiac regeneration and repair', *Nature Reviews Cardiology*, 15(10), pp. 585–600. doi: 10.1038/s41569-018-0036-6.

Hausmann, O. N. (2003) 'Post-traumatic inflammation following spinal cord injury', *Spinal Cord*, 41(7), pp. 369–378. doi: 10.1038/sj.sc.3101483.

Hayakawa, K. *et al.* (2011) 'Vascular endothelial growth factor regulates the migration of oligodendrocyte precursor cells', *Journal of Neuroscience*, 31(29), pp. 10666–10670. doi: 10.1523/JNEUROSCI.1944-11.2011.

He, Z. and Koprivica, V. (2004) 'the Nogo Signaling Pathway for Regeneration Block', *Annual Review of Neuroscience*, 27(1), pp. 341–368. doi: 10.1146/annurev.neuro.27.070203.144340.

Henry, C. J., Marusyk, A. and DeGregori, J. (2011) 'Aging-associated changes in hematopoiesis and leukemogenesis: What's the connection?', *Aging*, 3(6), pp. 643–656. doi: 10.18632/aging.100351.

Herbert, S. P. and Stainier, D. Y. R. (2011) 'Molecular control of endothelial cell behaviour during blood vessel morphogenesis', *Nature Reviews Molecular Cell Biology*, 12(9), pp. 551–564. doi: 10.1038/nrm3176.Molecular.

Herbomel, P., Thisse, B. and Thisse, C. (1999) 'Ontogeny and behaviour of early

macrophages in the zebrafish embryo', *Development*, 126(17), pp. 3735–3745.

Ho, V. C. *et al.* (2012) 'Elevated VEGF Receptor-2 Abundance Contributes to Increased Angiogenesis in VEGF Receptor-1 Deficient Mice', *Circulation*, 126(6), pp. 741–752. doi: 10.1038/jid.2014.371.

Hogan, B. M. *et al.* (2009) 'Vegfc/Flt4 signalling is suppressed by Dll4 in developing zebrafish intersegmental arteries', *Development*, 136(23), pp. 4001–4009. doi: 10.1242/dev.039990.

Holtzman, D. M., Morris, J. C. and Goate, A. M. (2011) 'Alzheimer's disease: The challenge of the second century', *Science Translational Medicine*, 3(77), pp. 1–35. doi: 10.1126/scitranslmed.3002369.

Huang, W. C. *et al.* (2013) 'Treatment of Glucocorticoids Inhibited Early Immune Responses and Impaired Cardiac Repair in Adult Zebrafish', *PLoS ONE*, 8(6), pp. 1–11. doi: 10.1371/journal.pone.0066613.

Huettl, R. E. *et al.* (2011) 'Npn-1 contributes to axon-axon interactions that differentially control sensory and motor innervation of the limb', *PLoS Biology*, 9(2). doi: 10.1371/journal.pbio.1001020.

Ikeda, T. *et al.* (2011) 'Hypoxia down-regulates sFlt-1 (sVEGFR-1) expression in human microvascular endothelial cells by a mechanism involving mRNA alternative processing', *Biochemical Journal*, 436(2), pp. 399–407. doi: 10.1042/BJ20101490.

Imai, T., Suzuki, M. and Sakano, H. (2006) 'Odorant Receptor–Derived cAMP Signals Direct Axonal Targeting', *Science*, 314, pp. 657–662. doi: 10.7551/mitpress/8876.003.0036.

Isogai, S., Horiguchi, M. and Weinstein, B. M. (2001) 'The vascular anatomy of the developing zebrafish: An atlas of embryonic and early larval development', *Developmental Biology*, 230(2), pp. 278–301. doi: 10.1006/dbio.2000.9995.

Ito, K. *et al.* (2014) 'Differential reparative phenotypes between zebrafish and medaka after cardiac injury', *Developmental Dynamics*, 243(9), pp. 1106–1115. doi: 10.1002/dvdy.24154.

Jakobsson, L. *et al.* (2010) 'Endothelial cells dynamically compete for the tip cell position during angiogenic sprouting', *Nature Cell Biology*. Nature Publishing Group, 12(10), pp. 943–953. doi: 10.1038/ncb2103.

Jensen, L. D. *et al.* (2012) 'Opposing Effects of Circadian Clock Genes Bmal1 and

Period2 in Regulation of VEGF-Dependent Angiogenesis in Developing Zebrafish', *Cell Reports*, 2(2), pp. 231–241. doi: 10.1016/j.celrep.2012.07.005.

Jensen, L. D. *et al.* (2015) 'VEGF-B-Neuropilin-1 signaling is spatiotemporally indispensable for vascular and neuronal development in zebrafish', *Proceedings of the National Academy of Sciences*, 112(44), pp. E5944–E5953. doi: 10.1073/pnas.1510245112.

Jessberger, S. (2016) 'Neural repair in the adult brain', *F1000Research*, 5((F1000 Faculty Rev): 169), pp. 1–8. doi: 10.12688/f1000research.7459.1.

Jin, S. W. *et al.* (2005) 'Cellular and molecular analyses of vascular tube and lumen formation in zebrafish', *Development*, 132(23), pp. 5199–5209. doi: 10.1242/dev.02087.

Jingd, L. and Zon, L. I. (2011) 'Zebrafish as a model for normal and malignant hematopoiesis', *DMM Disease Models and Mechanisms*, 4(4), pp. 433–438. doi: 10.1242/dmm.006791.

de Jong, Y. *et al.* (2020) 'A systematic review and external validation of stroke prediction models demonstrates poor performance in dialysis patients', *Journal of Clinical Epidemiology*. Elsevier Inc. doi: 10.1016/j.jclinepi.2020.03.015.

Kanaan, N. M. *et al.* (2013) 'Axonal degeneration in Alzheimer's disease: When signaling abnormalities meet the axonal transport system', *Experimental Neurology*, (246), pp. 44–53. doi: 10.1016/j.expneurol.2012.06.003.Axonal.

Karakatsani, A., Shah, B. and Ruiz de Almodovar, C. (2019) 'Blood vessels as regulators of neural stem cell properties', *Frontiers in Molecular Neuroscience*, 12(April), pp. 1–11. doi: 10.3389/fnmol.2019.00085.

Kearney, J. B. *et al.* (2004) 'The VEGF receptor flt-1 (VEGFR-1) is a positive modulator of vascular sprout formation and branching morphogenesis', *Blood*, 103(12), pp. 4527–4535. doi: 10.1182/blood-2003-07-2315.

Kigerl, K. A. *et al.* (2009) 'Identification of two distinct macrophage subsets with divergent effects causing either neurotoxicity or regeneration in the injured mouse spinal cord', *Journal of Neuroscience*, 29(43), pp. 13435–13444. doi: 10.1523/JNEUROSCI.3257-09.2009.

Kikuchi, K. and Poss, K. D. (2012) 'Cardiac Regenerative Capacity and Mechanisms', *Annual Review of Cell and Developmental Biology*, 28(1), pp. 719–741. doi: 10.1146/annurev-cellbio-101011-155739.

Kim, C. H. *et al.* (1996) 'Zebrafish elav/HuC homologue as a very early neuronal marker', *Neuroscience Letters*, 216(2), pp. 109–112. doi: 10.1016/0304-3940(96)13021-4.

Kirshblum, S. C. *et al.* (2011) 'International Standards for Neurological Classification of Spinal Cord Injury (Revised 2011)', *Journal of Spinal Cord Medicine*, 34(6), pp. 535–546. doi: 10.1179/107902611X13186000420242.

Koch, S. *et al.* (2011) 'Signal transduction by vascular endothelial growth factor receptors', *Biochemical Journal*, 437(2), pp. 169–183. doi: 10.1042/BJ20110301.

Krueger, J. *et al.* (2011) 'Flt1 acts as a negative regulator of tip cell formation and branching morphogenesis in the zebrafish embryo', *Development*, 138(10), pp. 2111–2120. doi: 10.1242/dev.063933.

Kudoh, T., Wilson, S. W. and Dawid, I. B. (2002) 'Distinct roles for Fgf, Wnt and retinoic acid in posteriorizing the neural ectoderm', *Development*, 129(18), pp. 4335–4346.

Lai, S. L. *et al.* (2017) 'Reciprocal analyses in zebrafish and medaka reveal that harnessing the immune response promotes cardiac regeneration', *eLife*, 6, pp. 1–20. doi: 10.7554/eLife.25605.

Lambrechts, D., Storkebaum, E., Morimoto, M., Del-favero, J., *et al.* (2003) 'VEGF is a modifier of amyotrophic lateral sclerosis in mice and humans and protects motoneurons against ischemic death', 34(4), pp. 383–394.

Lambrechts, D., Storkebaum, E., Morimoto, M., Del-Favero, J., *et al.* (2003) 'VEGF is a modifier of amyotrophic lateral sclerosis in mice and humans and protects motoneurons against ischemic death', *Nature Genetics*, 34(4), pp. 383–394. doi: 10.1038/ng1211.

Lanahan, A. *et al.* (2013) 'The Neuropilin 1 Cytoplasmic Domain Is Required for VEGF-A-Dependent Arteriogenesis', *Developmental Cell*. Elsevier Inc., 25(2), pp. 156–168. doi: 10.1016/j.devcel.2013.03.019.

Lancaster, J. J. *et al.* (2019) 'Human Induced Pluripotent Stem Cell–Derived Cardiomyocyte Patch in Rats With Heart Failure', *Annals of Thoracic Surgery*. The Society of Thoracic Surgeons, 108(4), pp. 1169–1177. doi: 10.1016/j.athoracsur.2019.03.099.

Lange, C. *et al.* (2016) 'Vascular endothelial growth factor: A neurovascular target in neurological diseases', *Nature Reviews Neurology*. Nature Publishing Group,

12(8), pp. 439–454. doi: 10.1038/nrneurol.2016.88.

Lavine, K. J. *et al.* (2014) 'Distinct macrophage lineages contribute to disparate patterns of cardiac recovery and remodeling in the neonatal and adult heart', *Proceedings of the National Academy of Sciences of the United States of America*, 111(45), pp. 16029–16034. doi: 10.1073/pnas.1406508111.

Lawson, N. D. and Weinstein, B. M. (2002) 'In vivo imaging of embryonic vascular development using transgenic zebrafish', *Developmental Biology*, 248(2), pp. 307–318. doi: 10.1006/dbio.2002.0711.

Leppänen, V. M. *et al.* (2013) 'Structural and mechanistic insights into VEGF receptor 3 ligand binding and activation', *Proceedings of the National Academy of Sciences of the United States of America*, 110(32), pp. 12960–12965. doi: 10.1073/pnas.1301415110.

Li, Y. *et al.* (2008) 'VEGF-B inhibits apoptosis via VEGFR-1– mediated suppression of the expression of BH3-only protein genes in mice and rats', *The Journal of Clinical Investigation*, 118(3), pp. 913–923. doi: 10.1172/JCI33673.deficient.

Lindberg, K. *et al.* (1993) 'In vitro propagation of human ocular surface epithelial cells for transplantation', *Investigative Ophthalmology and Visual Science*, 34(9), pp. 2672–2679.

Lisse, T. S., Brochu, E. A. and Rieger, S. (2015) 'Capturing Tissue Repair in Zebrafish Larvae with Time-lapse Brightfield Stereomicroscopy', *Journal of Visualized Experiments*, (95), pp. 1–9. doi: 10.3791/52654.

Living with Attendant Care: Spinal Cord injury : Understanding spinal cord injury (no date). Available at: http://www.living-with-attendant-care.info/Content/Spinal_Cord_Injury_c_Understanding_spinal_cord_injury.html (Accessed: 28 April 2020).

Lohia, A. and McKenzie, J. (2019) *Neuroanatomy, Pyramidal Tract Lesions*, *StatPearls*. StatPearls Publishing. Available at: http://www.ncbi.nlm.nih.gov/pubmed/31082020 (Accessed: 13 April 2020).

Lowery, L. A. and Vactor, D. Van (2009) 'The trip of the tip: Understanding the growth cone machinery', *Nature Reviews Molecular Cell Biology*, 10(5), pp. 332–343. doi: 10.1038/nrm2679.

Luck, R. *et al.* (2019) 'VEGF/VEGFR2 signaling regulates hippocampal axon branching during development', *eLife*, 8, pp. 1–24. doi: 10.7554/eLife.49818.

Mack, T. G. A. *et al.* (2001) 'Wallerian degeneration of injured axons and synapses is delayed by a Ube4b/Nmnat chimeric gene', *Nature Neuroscience*, 4(12), pp. 1199–1206. doi: 10.1038/nn770.

Mani, N. *et al.* (2005) 'Astrocyte growth effects of vascular endothelial growth factor (VEGF) application to perinatal neocortical explants: Receptor mediation and signal transduction pathways', *Experimental Neurology*, 192(2), pp. 394–406. doi: 10.1016/j.expneurol.2004.12.022.

Martyn, U. and Schulfe-Merker, S. (2004) 'Zebrafish neuropilins are differentially expressed and interact with vascular endothelial growth factor during embryonic vascular development', *Developmental Dynamics*, 231(1), pp. 33–42. doi: 10.1002/dvdy.20048.

Matsuoka, R. L. *et al.* (2016) 'Radial glia regulate vascular patterning around the developing spinal cord', *eLife*, 5(NOVEMBER2016), pp. 1–24. doi: 10.7554/eLife.20253.

Mckee, A. C. *et al.* (2010) 'TDP-43 Proteinopathy and Motor Neuron Disease in CTE', *Journal of Neuropathology & Experimental Neurology*, 69(9), pp. 918–929. doi: 10.1097/NEN.0b013e3181ee7d85.TDP-43.

Mietto, B. S. *et al.* (2013) 'Lack of galectin-3 speeds Wallerian degeneration by altering TLR and pro-inflammatory cytokine expressions in injured sciatic nerve', *European Journal of Neuroscience*, 37(10), pp. 1682–1690. doi: 10.1111/ejn.12161.

Mietto, B. S., Mostacada, K. and Martinez, A. M. B. (2015) 'Neurotrauma and inflammation: CNS and PNS responses', *Mediators of Inflammation*, 2015. doi: 10.1155/2015/251204.

Miquerol, L., Langille, B. L. and Nagy, A. (2000) 'Embryonic development is disrupted by modest increases in vascular endothelial growth factor gene expression', *Development*, 127(18), pp. 3941–3946.

Mukouyama, Y. S. *et al.* (2002) 'Sensory Nerves Determine the Pattern of Arterial Differentiation and Blood Vessel Branching in the Skin', *Cell*, 109, pp. 639–705. doi: 10.1016/S0092-8674(02)00757-2.

Muramatsu, M. *et al.* (2010) 'Vascular endothelial growth factor receptor-1 signaling promotes mobilization of macrophage lineage cells from bone marrow and stimulates solid tumor growth', *Cancer Research*, 70(20), pp. 8211–8221. doi:

10.1158/0008-5472.CAN-10-0202.

Narciso, M. S. *et al.* (2009) 'Sciatic nerve regeneration is accelerated in galectin-3 knockout mice', *Experimental Neurology*. Elsevier Inc., 217(1), pp. 7–15. doi: 10.1016/j.expneurol.2009.01.008.

Nasevicius, A., Larson, J. and Ekker, S. C. (2000) ' Distinct Requirements for Zebrafish Angiogenesis Revealed by a VEGF-A Morphant ', *Yeast*, 1(4), pp. 294–301. doi: 10.1002/1097-0061(200012)17:4<294::aid-yea54>3.0.co;2-5.

Ng, G. A., Brack, K. E. and Coote, J. H. (2001) 'Effects of direct sympathetic and vagus nerve stimulation on the physiology of the whole heart - A novel model of isolated Langendorff perfused rabbit heart with intact dual autonomic innervation', *Experimental Physiology*, 86(3), pp. 319–329. doi: 10.1113/eph8602146.

Niethammer, P. *et al.* (2009) 'A tissue-scale gradient of hydrogen peroxide mediates rapid wound detection in zebrafish', *Nature*. Nature Publishing Group, 459(7249), pp. 996–999. doi: 10.1038/nature08119.

Nishijima, K. *et al.* (2007) 'Vascular endothelial growth factor-A is a survival factor for retinal neurons and a critical neuroprotectant during the adaptive response to ischemic injury', *American Journal of Pathology*, 171(1), pp. 53–67. doi: 10.2353/ajpath.2007.061237.

Nussbaum, J. M. *et al.* (2012) 'Prion-Like Behavior and Tau-dependent Cytotoxicity of Pyroglutamylated β-Amyloid Justin', *Nature*, 485(7400), pp. 651–655. doi: 10.1038/nature11060.

Oaklander, A. L. and Horowitz, S. H. (2015) *The complex regional pain syndrome*. 1st edn, *Handbook of Clinical Neurology*. 1st edn. Elsevier B.V. doi: 10.1016/B978-0-444-62627-1.00026-3.

Ohnmacht, J. *et al.* (2016) 'Spinal motor neurons are regenerated after mechanical lesion and genetic ablation in larval zebrafish', *Development (Cambridge)*, 143(9), pp. 1464–1474. doi: 10.1242/dev.129155.

Olsson, A. K. *et al.* (2006) 'VEGF receptor signalling - In control of vascular function', *Nature Reviews Molecular Cell Biology*, 7(5), pp. 359–371. doi: 10.1038/nrm1911.

Oosthuyse, B. *et al.* (2001) 'Deletion of the hypoxia-response element in the vascular endothelial growth factor promoter causes motor neuron degeneration', *Nature Genetics*, 28(2), pp. 131–138. doi: 10.1038/88842.

P Ko, C. (2001) 'Neuromuscular system', *International Encyclopedia of the Social & Behavioral Sciences*, pp. 10595–10600. doi: 10.1016/B0-12-370870-2/00138-4.

Palmer, T. D., Takahashi, J. and Gage, F. H. (1997) 'The adult rat hippocampus contains primordial neural stem cells', *Molecular and Cellular Neurosciences*, 8(6), pp. 389–404. doi: 10.1006/mcne.1996.0595.

Pan, Q. *et al.* (2007) 'Blocking Neuropilin-1 Function Has an Additive Effect with Anti-VEGF to Inhibit Tumor Growth', *Cancer Cell*, 11(1), pp. 53–67. doi: 10.1016/j.ccr.2006.10.018.

Paredes, I., Himmels, P. and Ruiz de Almodovar, C. (2018) 'Review Neurovascular Communication during CNS Development', *Developmental Cell*, 45(1), pp. 10–32.

Park, H. C. *et al.* (2000) 'Analysis of upstream elements in the HuC promoter leads to the establishment of transgenic Zebrafish with fluorescent neurons', *Developmental Biology*, 227, pp. 279–293. doi: 10.1006/dbio.2000.9898.

Patton, E. E. and Zon, L. I. (2001) 'The art and design of genetic screens: zebrafish', *Nature Reviews Genetics*, 2, pp. 956–966. doi: 10.1038/nrg2364.

Payne, E. and Look, T. (2009) 'Zebrafish modelling of leukaemias', *British Journal of Haematology*, 146(3), pp. 247–256. doi: 10.1111/j.1365-2141.2009.07705.x.

Pennings, S., Liu, K. J. and Qian, H. (2018) 'The stem cell niche: Interactions between stem cells and their environment', *Stem Cells International*, 2018, pp. 10–13. doi: 10.1155/2018/4879379.

Peri, F. and Nüsslein-Volhard, C. (2008) 'Live Imaging of Neuronal Degradation by Microglia Reveals a Role for v0-ATPase a1 in Phagosomal Fusion In Vivo', *Cell*, 133(5), pp. 916–927. doi: 10.1016/j.cell.2008.04.037.

Péron, S. and Berninger, B. (2015) 'Reawakening the sleeping beauty in the adult brain: Neurogenesis from parenchymal glia', *Current Opinion in Genetics and Development*, 34, pp. 46–53. doi: 10.1016/j.gde.2015.07.004.

Petrie, T. A. *et al.* (2015) 'Macrophages modulate adult zebrafish tail fin regeneration', *Development*, 142(2), pp. 406–406. doi: 10.1242/dev.120642.

Pfefferli, C. and Jaźwińska, A. (2015) 'The art of fin regeneration in zebrafish', *Regeneration*, 2(2), pp. 72–83. doi: 10.1002/reg2.33.

Pocock, R. and Hobert, O. (2008) 'Oxygen levels affect axon guidance and neuronal migration in Caenorhabditis elegans', *Nature Neuroscience*, 11(8), pp. 894–900.

doi: 10.1038/nn.2152.

Poesen, K. *et al.* (2008) 'Novel role for vascular endothelial growth factor (VEGF) receptor-1 and its ligand VEGF-B in motor neuron degeneration', *Journal of Neuroscience*, 28(42), pp. 10451–10459. doi: 10.1523/JNEUROSCI.1092-08.2008.

Poliak, S. *et al.* (2015) 'Synergistic integration of netrin and ephrin axon guidance signals by spinal motor neurons', *eLife*, 4(DECEMBER2015), pp. 1–26. doi: 10.7554/eLife.10841.

Pugh, C. W. and Ratcliffe, P. J. (2003) 'Regulation of angiogenesis by hypoxia: role of the HIF system', *Nature Medicine*, 9(6), pp. 677–684. Available at: https://www.nature.com/nm/journal/v9/n6/pdf/nm0603-677.pdf.

Quaegebeur, A., Lange, C. and Carmeliet, P. (2011) 'The neurovascular link in health and disease: Molecular mechanisms and therapeutic implications', *Neuron*. Elsevier Inc., 71(3), pp. 406–424. doi: 10.1016/j.neuron.2011.07.013.

Rafii, S., Butler, J. M. and Ding, B.-S. (2016) 'Angiocrine functions of organ-specific endothelial cells', *Nature*, 529(7586), pp. 316–325. doi: 10.1016/j.physbeh.2017.03.040.

Rama, P. *et al.* (2010) 'Limbal stem-cell therapy and long-term corneal regeneration', *New England Journal of Medicine*, 363(2), pp. 147–155. doi: 10.1056/NEJMoa0905955.

Ran, F. A. *et al.* (2013) 'Genome engineering using the CRISPR-Cas9 system', *Nature Protocols*, 8(11), pp. 2281–2308. doi: 10.1038/nprot.2013.143.

Rasmussen, J. P. and Sagasti, A. (2017) 'Learning to swim, again: Axon regeneration in fish', *Experimental Neurology*. Elsevier B.V., 287, pp. 318–330. doi: 10.1016/j.expneurol.2016.02.022.

Raveh-Amit, H. *et al.* (2013) 'Tissue resident stem cells: Till death do us part', *Biogerontology*, 14(6), pp. 573–590. doi: 10.1007/s10522-013-9469-9.

Rehman, J. (2013) 'Bone Marrow Tinctures for Cardiovascular Disease: Lost in Translation', *Circulation*, 127(19), pp. 1–7. doi: 10.1038/jid.2014.371.

Reimer, M. M. *et al.* (2008) 'Motor neuron regeneration in adult zebrafish', *Journal of Neuroscience*, 28(34), pp. 8510–8516. doi: 10.1523/JNEUROSCI.1189-08.2008.

Reimer, M. M. *et al.* (2013) 'Dopamine from the Brain Promotes Spinal Motor Neuron Generation during Development and Adult Regeneration', *Developmental Cell*.

Elsevier Inc., 25(5), pp. 478–491. doi: 10.1016/j.devcel.2013.04.012.

Des Rieux, A. *et al.* (2014) 'Vascular endothelial growth factor-loaded injectable hydrogel enhances plasticity in the injured spinal cord', *Journal of Biomedical Materials Research - Part A*, 102(7), pp. 2345–2355. doi: 10.1002/jbm.a.34915.

Risau, W. and Flamme, I. (1995) 'Vasculogenesis', *Annual review of cell and developmental biology*, 11, pp. 73–91.

Rolls, E. T. (2015) 'Limbic systems for emotion and for memory, but no single limbic system', *Cortex*. Elsevier Ltd, 62, pp. 119–157. doi: 10.1016/j.cortex.2013.12.005.

Van Rooijen, E. *et al.* (2009) 'Zebrafish mutants in the von Hippel-Lindau tumor suppressor display a hypoxic response and recapitulate key aspects of Chuvash polycythemia', *Blood*, 113(25), pp. 6449–6460. doi: 10.1182/blood-2008-07-167890.

Van Rooijen, E. *et al.* (2010) 'Von Hippel-Lindau tumor suppressor mutants faithfully model pathological hypoxia-driven angiogenesis and vascular retinopathies in zebrafish', *DMM Disease Models and Mechanisms*, 3(5–6), pp. 343–353. doi: 10.1242/dmm.004036.

Rossi, A. *et al.* (2016) 'Regulation of Vegf signaling by natural and synthetic ligands', *Blood*, 128(19), pp. 2359–2366. doi: 10.1182/blood-2016-04-711192.

Roth, G. A. *et al.* (2017) 'Global, Regional, and National Burden of Cardiovascular Diseases for 10 Causes, 1990 to 2015', *Journal of the American College of Cardiology*, 70(1), pp. 1–25. doi: 10.1016/j.jacc.2017.04.052.

Rottbauer, W. *et al.* (2005) 'VEGF-PLCγ1 pathway controls cardiac contractility in the embryonic heart', *Genes and Development*, 19(13), pp. 1624–1634. doi: 10.1101/gad.1319405.

Ruiz de Almodovar, C. *et al.* (2011) 'VEGF Mediates Commissural Axon Chemoattraction through Its Receptor Flk1', *Neuron*. Elsevier Inc., 70(5), pp. 966–978. doi: 10.1016/j.neuron.2011.04.014.

Sajadi, A., Schneider, B. L. and Aebischer, P. (2004) 'Wld s -Mediated Protection of Dopaminergic Fibers in an Animal Model of Parkinson Disease Wld s mice express a fusion protein linking the nicotin- amide mononucleotide adenylyl transferase enzyme with the terminal portion of the ubiquitination factor E4b', *Current Biology*, 14, pp. 326–330. doi: 10.1016//j.cub.2004.01.053.

Sawano, A. *et al.* (2001) 'Flt-1, vascular endothelial growth factor receptor 1, is a novel cell surface marker for the lineage of monocyte-macrophages in humans', *Blood*, 97(3), pp. 785–791. doi: 10.1182/blood.V97.3.785.

Schwartig, G. A. and Henion, T. R. (2011) 'Regulation and Function of Axon Guidance and Adhesion Molecules During Olfactory Map Formation Gerald', *J Cell Biochem*, 112(10). doi: 10.1038/jid.2014.371.

Segura, I. *et al.* (2009) 'The neurovascular link in health and disease: an update', *Trends in Molecular Medicine*, 15(10), pp. 439–451. doi: 10.1016/j.molmed.2009.08.005.

Seifert, A. W. and Voss, S. R. (2013) 'Revisiting the relationship between regenerative ability and aging', *BMC Biology*, 11, pp. 2–5. doi: 10.1186/1741-7007-11-2.

Selvaraj, D. *et al.* (2015) 'A Functional Role for VEGFR1 Expressed in Peripheral Sensory Neurons in Cancer Pain', *Cancer Cell*, 27(6), pp. 780–796. doi: 10.1016/j.ccell.2015.04.017.

Shalaby, F., Janet, R., *et al.* (1995) 'Failure of blood-island formation and vasculogenesis in Flk-1-deficient mice', *Nature*, pp. 62–66. doi: 10.1038/376062a0.

Shalaby, F., Rossant, J., *et al.* (1995) 'Failure of blood-island formation and vasculogenesis in Flk-1 deficient mice', *Nature*, 376, pp. 62–66. Available at: https://www.nature.com/articles/376062a0.pdf.

Shen, Q. *et al.* (2004) 'Endothelial cells stimulate self-renewal and expand neurogenesis of neural stem cells', *Science*, 304(5675), pp. 1338–1340. doi: 10.1126/science.1095505.

Shibuya, M. *et al.* (1990) 'Nucleotide sequence and expression of a novel human receptor-type tyrosine kinase gene (flt) closely relatd to the fms family', *Oncogene*, 5(4), pp. 519–524.

Shyh-Chang, N. and Ng, H. H. (2017) 'The metabolic programming of stem cells', *Genes and Development*, 31(4), pp. 336–346. doi: 10.1101/gad.293167.116.

Siekmann, A. F. and Lawson, N. D. (2007) 'Notch signalling limits angiogenic cell behaviour in developing zebrafish arteries', *Nature*, 445(7129), pp. 781–784. doi: 10.1038/nature05577.

Simkin, J., Gawriluk, T. R., *et al.* (2017) 'Macrophages are necessary for epimorphic regeneration in African spiny mice', *eLife*, 6, pp. 1–26. doi: 10.7554/eLife.24623.

Simkin, J., Sammarco, M. C., *et al.* (2017) 'Macrophages are required to coordinate mouse digit tip regeneration', *Development (Cambridge)*, 144(21), pp. 3907–3916. doi: 10.1242/dev.150086.

Sipkins, D. A. *et al.* (2005) 'In vivo imaging of specialized bone marrow endothelial microdomains for tumour engraftment', *Nature*, 435(7044), pp. 969–973. doi: 10.1038/nature03703.

Snuderl, M. *et al.* (2013) 'Targeting placental growth factor/neuropilin 1 pathway inhibits growth and spread of medulloblastoma', *Cell*, 152(5), pp. 1065–1076. doi: 10.1016/j.cell.2013.01.036.Targeting.

Sondell, M., Lundborg, G. and Kanje, M. (1999) 'Vascular endothelial growth factor has neurotrophic activity and stimulates axonal outgrowth, enhancing cell survival and Schwann cell proliferation in the peripheral nervous system', *Journal of Neuroscience*, 19(14), pp. 5731–5740. doi: 10.1523/jneurosci.19-14-05731.1999.

Stainier, D. Y. R. *et al.* (1996) 'Mutations affecting the formation and function of the cardiovascular system in the zebrafish embryo', *Development*, 123, pp. 285–292. doi: 10.5167/uzh-237.

Stefater III, J. A. *et al.* (2011) 'Regulation of angiogenesis by a non-canonical Wnt-Flt1 pathway in myeloid cells', *Nature*, 474(7352), pp. 511–515. doi: 10.1038/nature10085.Regulation.

Stoeckli, E. T. (2018) 'Understanding axon guidance: Are we nearly there yet?', *Development (Cambridge)*, 145(10). doi: 10.1242/dev.151415.

Storkebaum, E. *et al.* (2005) 'Treatment of motoneuron degeneration by intracerebroventricular delivery of VEGF in a rat model of ALS', *Nature Neuroscience*, 8(1), pp. 85–92. doi: 10.1038/nn1360.

Sweeney, M. D. *et al.* (2018) 'The role of brain vasculature in neurodegenerative disorders', *Nature Neuroscience*, 21(10), pp. 1318–1331. doi: 10.1016/j.physbeh.2017.03.040.

Tata, M. *et al.* (2016) 'Regulation of embryonic neurogenesis by germinal zone vasculature', *Proceedings of the National Academy of Sciences of the United States of America*, 113(47), pp. 13414–13419. doi: 10.1073/pnas.1613113113.

Tata, M. and Ruhrberg, C. (2018) 'Cross-talk between blood vessels and neural progenitors in the developing brain', *Neuronal Signaling*, 2(1), pp. 1–13. doi:

10.1042/ns20170139.

Thobois, S., Delamarre-Damier, F. and Derkinderen, P. (2005) 'Treatment of motor dysfunction in Parkinson's disease: An overview', *Clinical Neurology and Neurosurgery*, 107(4), pp. 269–281. doi: 10.1016/j.clineuro.2005.02.002.

Torres-Vázquez, J. *et al.* (2004) 'Semaphorin-plexin signaling guides patterning of the developing vasculature', *Developmental Cell*, 7(1), pp. 117–123. doi: 10.1016/j.devcel.2004.06.008.

Truett, G. E. *et al.* (2000) 'Preparation of PCR-quality mouse genomic dna with hot sodium hydroxide and tris (HotSHOT)', *BioTechniques*, 29(1), pp. 52–54. doi: 10.2144/00291bm09.

Tsarouchas, T. M. *et al.* (2018) 'Dynamic control of proinflammatory cytokines Il-1β and Tnf-α by macrophages in zebrafish spinal cord regeneration', *Nature Communications*, 9(1). doi: 10.1038/s41467-018-07036-w.

Vargas, M. E. and Barres, B. A. (2007) 'Why Is Wallerian Degeneration in the CNS So Slow?', *Annual Review of Neuroscience*, 30(1), pp. 153–179. doi: 10.1146/annurev.neuro.30.051606.094354.

Velde, C. Vande *et al.* (2004) 'The Neuroprotective Factor Wlds Does Not Attenuate Mutant SOD1-Mediated Motor Neuron Disease', *Neuromolecular Medicine*, 5, pp. 193–203.

Vergara, M. N., Arsenijevic, Y. and Del Rio-Tsonis, K. (2005) 'CNS regeneration: A morphogen's tale', *Journal of Neurobiology*, 64(4), pp. 491–507. doi: 10.1002/neu.20158.

Villefranc, J. A. *et al.* (2013) 'A truncation allele in vascular endothelial growth factor c reveals distinct modes of signaling during lymphatic and vascular development', *Development (Cambridge)*, 140(7), pp. 1497–1506. doi: 10.1242/dev.084152.

Vivien, C. J., Hudson, J. E. and Porrello, E. R. (2016) 'Evolution, comparative biology and ontogeny of vertebrate heart regeneration', *npj Regenerative Medicine*. The Author(s), 1(1), pp. 1–14. doi: 10.1038/npjregenmed.2016.12.

Wagner, R. and Myers, R. R. (1996) 'Schwann cells produce tumor necrosis factor alpha: Expression in injured and non-injured nerves', *Neuroscience*, 73(3), pp. 625–629. doi: 10.1016/0306-4522(96)00127-3.

Wälchli, T. *et al.* (2015) 'Wiring the Vascular Network with Neural Cues: A CNS Perspective', *Neuron*, 87(2), pp. 271–296. doi: 10.1016/j.neuron.2015.06.038.

Waller, A. (1850) 'Experiments on the section of the glossopharyngeal and hypoglossal nerves of the frog, and observations of the alterations produced thereby in the structure of their primitive fibres', *Philos. Trans. R. Soc. London*, 140, pp. 423–429. doi: 10.1098/rstl.1850.0021.

Webby, C. J. *et al.* (2009) 'Jmjd6 Catalyses Lysyl-Hydroxylation of U2AF65, a Protein Associated with RNA Splicing Celia', *Science (New York, N.Y.)*, 325(5936), pp. 90–94.

Wehner, D. *et al.* (2014) 'Wnt/β-catenin signaling defines organizing centers that orchestrate growth and differentiation of the regenerating zebrafish caudal fin', *Cell Reports*, 6(3), pp. 467–481. doi: 10.1016/j.celrep.2013.12.036.

Wehner, D. *et al.* (2017) 'Wnt signaling controls pro-regenerative Collagen XII in functional spinal cord regeneration in zebrafish', *Nature Communications*. Springer US, 8(1), pp. 1–16. doi: 10.1038/s41467-017-00143-0.

Wheeler, K. C. *et al.* (2018) 'VEGF may contribute to macrophage recruitment and M2 polarization in the decidua', *PLoS ONE*, 13(1), pp. 1–18. doi: 10.1371/journal.pone.0191040.

Widenfalk, J. *et al.* (2003) 'Vascular endothelial growth factor improves functional outcome and decreases secondary degeneration in experimental spinal cord contusion injury', *Neuroscience*, 120(4), pp. 951–960. doi: 10.1016/S0306-4522(03)00399-3.

Wild, R. *et al.* (2017) 'Neuronal sFlt1 and Vegfaa determine venous sprouting and spinal cord vascularization', *Nature Communications*, 8(May 2016). doi: 10.1038/ncomms13991.

Wimmer, R. A. *et al.* (2019) 'Human blood vessel organoids as a model of diabetic vasculopathy', *Nature*. Springer US, 565(7740), pp. 505–510. doi: 10.1038/s41586-018-0858-8.

Wright, A. K. *et al.* (2010) 'Synaptic protection in the brain of WldS mice occurs independently of age but is sensitive to gene-dose', *PLoS ONE*, 5(11). doi: 10.1371/journal.pone.0015108.

Wu, J. *et al.* (2010) 'Interaction of NG2+ glial progenitors and microglia/macrophages from the injured spinal cord', *Glia*, 58(4), pp. 410–422. doi: 10.1002/glia.20932.

Wurmser, A. E., Palmer, T. D. and Gage, F. H. (2004) 'Cellular interactions in the stem cell niche', *Science*, 304(5675), pp. 1253–1255. doi: 10.1126/science.1099344.

Wynn, T. A. and Vannella, K. M. (2016) 'Macrophages in tissue repair, regeneration, and fibrosis', *Immunity*, 44(3), pp. 450–462. doi: 10.1016/j.physbeh.2017.03.040.

Yeager, S. and Miller, C. (2014) 'Acute Nontraumatic Weakness', *AACN Advanced Critical Care*, 25(3), pp. 251–265. doi: 10.4037/nci.0000000000000037.

Yeung, E. *et al.* (2019) 'Cardiac regeneration using human-induced pluripotent stem cell-derived biomaterial-free 3D-bioprinted cardiac patch in vivo', *Journal of Tissue Engineering and Regenerative Medicine*, 13(11), pp. 2031–2039. doi: 10.1002/term.2954.

Yu, S. *et al.* (2016) 'Angiogenic microspheres promote neural regeneration and motor function recovery after spinal cord injury in rats', *Scientific Reports*. Nature Publishing Group, 6(August), pp. 1–13. doi: 10.1038/srep33428.

Zacchigna, S., Lambrechts, D. and Carmeliet, P. (2008) 'Neurovascular signalling defects in neurodegeneration', *Nature Reviews Neuroscience*, 9(3), pp. 169–181. doi: 10.1038/nrn2336.

Zhang, F. *et al.* (2018) 'Lacteal junction zippering protects against diet-induced obesity', *Science*, 361(6402), pp. 599–603. doi: 10.1126/science.aap9331.

Zhong, H. *et al.* (2011) 'Combinatory action of VEGFR2 and MAP kinase pathways maintains endothelial-cell integrity', *Cell Research*. Nature Publishing Group, 21(7), pp. 1080–1087. doi: 10.1038/cr.2011.41.

Zlokovic, B. V. (2014) 'Neurovascular pathways to neurodegeneration in Alzheimer's disease and other disorders Berislav', *Nature Reviews Neuroscience*, 12(12), pp. 723–738. doi: 10.1038/nrn3114.

8   Abbreviations

6-OHDA	6-hydroxydopamine
Aβ	Amyloid peptide β
AD	Alzheimer's disease
aISVs	arterial Intersegmental Vessels
ALS	Amyotrophic lateral schlerosis
AP	anterior-posterior
AS-ODNs	antisense-oligonucleotides
aSCs	adult Stem Cells
BAD	Bcl-2-associated death promoter
BBB	Blood brain barrier
BM-MNCs	bone marrow mononuclear cells
BMP	bone morphogenic protein
cAMP	Cyclic adenosine monophosphate
CNS	Central Nervous System
Col I	Collagen I
Col XII	Collagen XII
CRISPR	clustered regularly interspaced shirt palindromic repeats
DA	dorsal aorta
DAPI	4', 6'-diamidino-2-phenylindole
DCC	deleted in colorectal carcinoma
DLAV	dorsal longitudinal anastomotic vessel
Dll4	delta-like 4 ligand
dpf	days post fertilization
dpl	days post lesion
DV	dorsal-ventral
ECM	extracellular matrix
ECs	Endothelial cells
Elavl	elav-like protein
eNOS	endothelial nitric oxide synthase
EphB2	Ephrin receptor 2

ERGs	ependymo-radial glia
ERK	extracellular-signal-regulated kinase
ERt2	oestrogen receptor
ES	embryonic Stem Cells
ETV2	ETS variant 2
FC	fin clip
FGF	fibroblast growth factor
Flt1	Fms Related Receptor Tyrosine Kinase 1
FLT4	Fms-related tyrosine kinase 4
FP	floor plate
GAB1	GRB2 (growth factor receptor-bound protein 2)-associated-binding protein 1
Gal-3	galectin-3
GFAP	Glial fibrillary acidic protein
GOF	gain-of-function
hAOSMCs	human aortic smooth muscle cells
hCOs	human cortical organoids
Hh	Hedgehog
HIF-1α	hypoxia-induced transcription factor α
HIF-1β	hypoxia-induced transcription factor β
HIFs	hypoxia-inducible transcription factors
hiPSC-CMs	Human induced pluripotent stem cell-derived cardiomyocytes
HMVECs	human microvascular endothelial cells
hpf	hours post fertilization
hpl	hours post lesion
HREs	hypoxia responsive elements
HUVECs	human umbilical vein ECs
il-1β	inteleukin β
Inh	inhibitor
iNOS	inducible NO synthase
iPS	induced pluripotent stem cells
ISVs	intersegmental vessels
jmjd6	Jumonji domain-containing protein 6

KDR/FLK	kinase insert domain receptor
kdrl	kdr-like receptor
l-plastin	leucocyte-specific plastin
LMN	lower motor neuron
LOF	loss-of-function
LPS	bacterial lipopolysaccharides
MΦ	Macrophages
MAPK	mitogen-activated protein kinase
mFlt1	membrane-bound Flt1
MI	myocardial infarction
MN	motor neuron
MO	morpholino
MPTP	1-methyl-4-phenyl-1,2,3,6-tetrahydropyridine
n.s.	non-significant
NGF	nerve growth factor
Nmnat1	nicotinamide mononucleotide adenyltransferase 1
NO	nitric oxide
NPCs	Neuronal progenitors
NRP1	Neuropilin 1
NRP2	Neuropilin 2
NRPs	Neuropilins
NSCs	neural stem cells
PCV	posterior cardinal vein
PD	Parkinson's disease
PHDs	prolyl hydroxylases
PI3K	phosphoinositide 3-kinase
PIP_3	phosphatidylinositol (3,4,5)-trisphosphate
PKA	Protein kinase A
PKB/Akt	Protein Kinase B
PKC	Protein kinase C
PLCγ	phospholipase C
PLGF-	placental growth factor
PLGF-1	placental growth factor 1

PLGF-2	placental growth factor 2
pmn	progressive motor neuropathy
PNS	Peripheral nervous system
PSCs	Pluripotent stem cells
RA	retinoic acid
Rac	Ras-related C3 botulinum toxin substrate
ROS	Reactive oxygen species
RP	roof plate
RTKs	receptor tyrosine kinases
SCL	spinal cord lesion
Sema3	semaphorin 3
sFlt1	soluble Flt1
SGZ	subgranular zone
Shh	Sonic hedgehog
SOD1	superoxide dismutase
Sox2	SRY (sex determining region Y)-box 2
SVZ	subventricular zone
TALENs	Transcription activator-like effector nucleases
tgf-β1a	transforming growth factor-beta 1a
tgf-β3	transforming growth factor-beta 3
tnfa/tnf-α	Tumour necrosis factor alpha
U2AF65	U2 small nuclear ribonucleoprotein auxiliary factor 65-kilodalton subunit
Ube4b	ubiquitination factor E4B
UMN	upper motor neuron
Unc5b	Unc-5 Netrin Receptor B
VE-	vascular endothelial
VEGF	Vascular Endothelial Growth Factor
VEGF-B	Vascular Endothelial Growth Factor B
VEGF-C	Vascular Endothelial Growth Factor C
VEGF-D	Vascular Endothelial Growth Factor D
VEGF-E	Vascular Endothelial Growth Factor E
VEGF/VEGF-A	Vascular Endothelial Growth Factor A

VEGFR1	Vascular Endothelial Growth Factor Receptor 1
VEGFR2	Vascular Endothelial Growth Factor Receptor 1
VEGFR3	Vascular Endothelial Growth Factor Receptor 3
VHL	von Hippel-Lindau
vISVs	venous intersegmental vessels
vSMCs	vascular smooth muscle cells
VZ	ventricular zone
WD	Wallerian degeneration
WLD	Wallerian-like degeneration
WT	wild type

9 List of figures

# 10   List of tables

11 List of publications

Wehner, D, Tsarouchas, T.M, **Michael, A**, Hasse, C, Weidinger, G, Reimer, M.M, Becker, T, and Becker, C.G, 2017. Wnt signaling controls pro-regenerative Collagen XII in functional spinal cord regeneration. **Nature Communications** 8, 126. DOI: 10.1038/s41467-017-00143-0.

12   Appendix
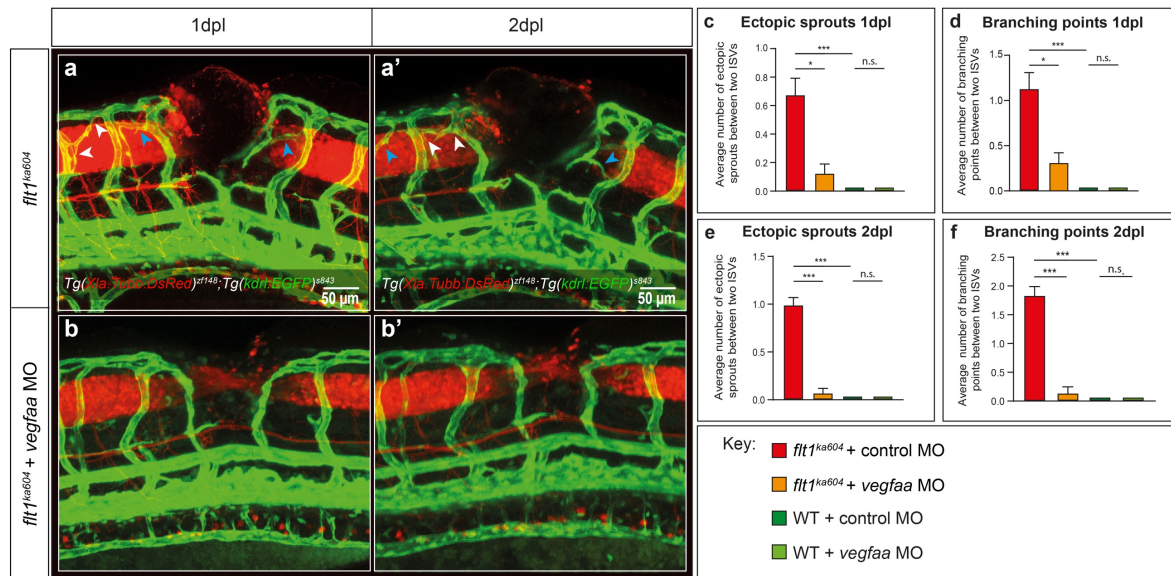
Supplementary Figure 1: *vegfaa* MO rescues the hypersprouting phenotype

(a-a') *flt1^{ka604} Tg(Xla.Tubb:DsRed)^{zf148}; Tg(kdrl:EGFP)^{s843}* mutants injected with the control morpholino show impaired axonal bridging at both 1dpl (c) and 2dpl (c'). Neurons are shown in red and vessels in green. Blue arrowheads indicate the ectopic sprouts and white arrowheads the branching points. **(b-b')** *flt1^{ka604} Tg(Xla.Tubb:DsRed)^{zf148}; Tg(kdrl:EGFP)^{s843}* mutants injected with *vegfaa* MO impair the ectopic sprout formation and enhances their regenerative capacity at both 1dpl (d) and 2dpl (d'). **(c-d)** Quantitative analysis of the average number of ectopic sprouts (c) and branching points (d) per two ISVs per larvae at 1dpl. Mann-Whitney test ± s.e.m, n(WT + control MO)=10; n(*flt1^{ka604}* + control MO)=7; n(WT + *vegfaa* MO)=6; n(*flt1^{ka604}* + *vegfaa* MO)=4; n.s.=non-significant; *P<0.05; ***P < 0.001 **(e-f)** Quantitative analysis of the average number of ectopic sprouts (e) and branching points (f) per two ISVs per larvae at 2dpl. Mann-Whitney test ± s.e.m, n(WT + control MO)=11; n(*flt1^{ka604}* + control MO)=11; n(WT + *vegfaa* MO)=11; n(*flt1^{ka604}* + *vegfaa* MO)=4; n.s.=non-significant; ***P < 0.001. WT=wild-type; MO=morpholino; ISVs=Intersegmental vessels; dpl=days post lesion; n.s.=non-significant; Scale bar 50µm.
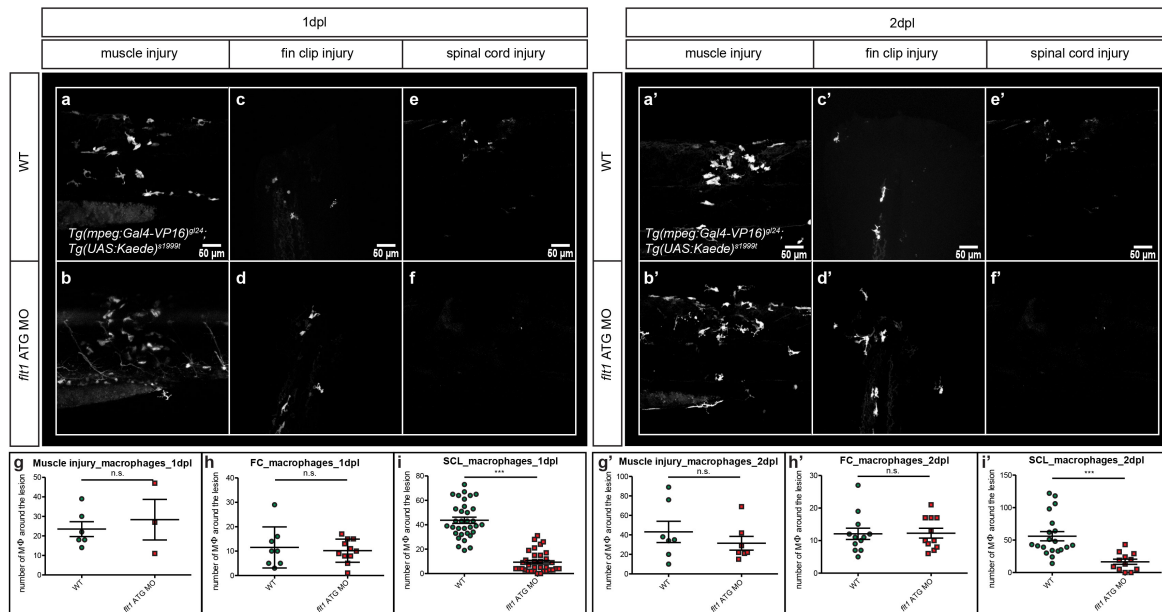
Supplementary Figure 2: *flt1* LOF impairs macrophage migration post neuronal injury.

(a-f') Single transgenic larvae WT *Tg(mpeg:Gal4-VP16)^{gl24}; Tg(UAS:KAEDE)^{s1999t}* were used to detect macrophage migration post injury. **(a, a', b, b')** WT larvae at 1day (a) and 2day (a') and *flt1*-ATG MO injected larvae at 1day (b) and 2day (b') post muscle injury show no difference in macrophage migration. **(c, c', d, d')** WT larvae at 1day (c) and 2day (c') and *flt1*-ATG MO injected larvae at 1day (d) and 2day (d') post fin clip injury show similar macrophage migration. **(e, e', f, f')** WT at 1day (e) and 2day (e') post spinal cord (neuronal) injury, show macrophage migration to the wound. Contrary *flt1*-ATG MO injected larvae exhibit a macrophage migration deficiency at both 1dpl (f) and 2dpl (f'). **(g-i)** Statistical analysis of the number of macrophages migrating to the wound at 1dpl. (g) Mann-Whitney ± s.e.m, n(WT)=6, n(*flt1*-ATG MO)=3; n.s.=non-significant. (h) Unpaired t-test ± s.e.m, n(WT)=8, n(*flt1*-ATG MO)=11; n.s.=non-significant. (i) Mann-Whitney ± s.e.m, n(WT)=33, n(*flt1*-ATG MO)=34; ***P<0.001. **(g'-i')** Statistical analysis of the number of macrophages migrating to the wound at 2dpl. (g') Mann-Whitney ± s.e.m, n(WT)=6, n(*flt1*-ATG MO)=6; n.s.=non-significant. (h) Mann-Whitney ± s.e.m, n(WT)=12, n(*flt1*-ATG MO)=11; n.s.=non-significant. (i) Mann-Whitney ± s.e.m, n(WT)=20, n(*flt1*-ATG MO)=12; ***P<0.001. WT=wild-type; MO=Morpholino; FC=Fin clip; SCL=Spinal cord lesion; MΦ=Macrophages; dpl=days post lesion; n.s.= non-significant. Scale bar 50µm.

Supplementary Table 1

Pro-inflammatory_ *il-1β*				
Timepoint	Comparison			Significance
24hpl	WT UNL	Vs	flt1^{ka604} UNL	*
48hpl	WT UNL		flt1^{ka604} UNL	**
	WT UNL		flt1^{ka604} SCL	***
	flt1^{ka604} UNL		flt1^{ka604} SCL	**

Supplementary Table 2

Pro-inflammatory_ *tnf-α*				
Timepoint	Comparison			Significance
18hpl	WT UNL	Vs	flt1^{ka604} UNL	***
	WT UNL		WT SCL	**
48hpl	flt1^{ka604} UNL		flt1^{ka604} SCL	***
	WT SCL		flt1^{ka604} SCL	*

Supplementary Table 3

Anti-inflammatory_ *tgf-β1a*				
Timepoint	Comparison			Significance
18hpl	WT UNL	Vs	flt1^{ka604} UNL	*
	WT SCL		flt1^{ka604} SCL	*
24hpl	WT UNL		flt1^{ka604} UNL	**
	WT SCL		flt1^{ka604} SCL	**
48hpl	WT SCL		flt1^{ka604} SCL	*

Supplementary Table 4

Anti-inflammatory_ *tgf-β3*				
Timepoint	Comparison			Significance
18hpl	WT UNL	Vs	flt1^{ka604} UNL	*
	WT UNL		WT SCL	**
24hpl	WT SCL		flt1^{ka604} SCL	*
48hpl	WT UNL		WT SCL	*